Springer Protocols

Methods in Molecular Biology 582

DNA Topoisomerases

Methods and Protocols

Edited by
Duncan J. Clarke

Humana Press

METHODS IN MOLECULAR BIOLOGY™

Series Editor
John M. Walker
School of Life Sciences
University of Hertfordshire
Hatfield, Hertfordshire, AL10 9AB, UK

For other titles published in this series, go to
www.springer.com/series/7651

DNA Topoisomerases

Methods and Protocols

Edited by

Duncan J. Clarke

University of Minnesota Medical School, Minneapolis, MN, USA

Humana Press

Editor
Duncan J. Clarke
Department of Genetics, Cell Biology &
Development
University of Minnesota Medical School
Minneapolis, MN 55455
USA
clark140@umn.edu

ISSN 1064-3745 e-ISSN 1940-6029
ISBN 978-1-60761-339-8 e-ISBN 978-1-60761-340-4
DOI 10.1007/978-1-60761-340-4

Library of Congress Control Number: 2009933621

Printed on acid-free paper

springer.com

Preface

Enzymes that alter the topology of DNA, collectively DNA topoisomerases and gyrases, arose early in the evolution of the DNA-based cells of archaea, bacteria, and eukaryotes. Together, they perform essential functions that are required for the basic processes of cell division: DNA replication, transcription, recombination, chromosome condensation, and chromosome segregation. Previous volumes in the *Methods in Molecular Biology* series have covered in great depth the methodologies needed to study topoisomerases from a biochemical perspective, including the topoisomerase–drug interactions relevant to clinical applications, and have provided indispensable protocols to topoisomerase researchers that cover almost every aspect of topoisomerase enzymology. However, the past decade has seen an expansion in topoisomerase research at the molecular and cellular levels, and this activity will doubtless continue to increase. With a greater understanding of the cellular functions performed by topoisomerases, there now is a clear need for a compendium of protocols that extends into the new areas of research that have been recently uncovered. Thus, this volume is not an updated republication of methods, nor does it aim to be all-inclusive, but rather the methods provided here add new approaches to the study of topoisomerase functions that are relevant in what is a rapidly changing field of research.

First in this volume is a series of chapters that describe methods to analyze DNA topologies and the interaction of topoisomerases with DNA as tools to measure topoisomerase functions (Chapters 2, 3, 4, 5, 6, and 7). Although the topoisomerase reactions performed by different topoisomerases have been defined, little is understood about their regulation by co-factors or post-translational modifications. These assays will be useful in assessing factors that influence topoisomerase activity. A novel example of a DNA topological change performed by a topoisomerase has recently become known. Holliday junction *dissolution* functions to allow the repair of recombination intermediates without sister chromatid exchange. An assay to monitor this reaction is presented in Chapter 8.

Chapters 9, 10, and 11 pertain to the binding of topoisomerases to specific sites in the genomes of eukaryotes, including origins of DNA replication. The interaction of topoisomerases with DNA can now be measured by ChIP-on-chip analyses, revealing their specific locations within whole chromosomes and within the cell cycle context. Chapter 9 describes methods to detect topoisomerase binding sites across the genome, and Chapters 10 and 11 explain how the binding of topoisomerases to DNA at specific sites can be measured, even to single-nucleotide resolution. Using these methods, the association of topoisomerases with functional units such as replication origins can be determined.

The molecular approaches described above are followed by a series of chapters that delve into the consequences of perturbed topoisomerase function. It has long been known that DNA topology must be fashioned to allow the dramatic changes in chromatin packing that take place during mitosis, but methods for assessing the effects

of topoisomerase inhibition in vivo on chromosome structure have not been compiled in a single volume. Methods to examine chromosome structural aberrations and measure DNA damage after topoisomerase inhibition are included in Chapters 12 and 15. Because DNA replication produces catenated sister chromatids, topoisomerases have key functions in the segregation of the genome. Perturbed topoisomerase II function delays progression into and through mitosis to prevent failed attempts to segregate the genome. Methods of measuring cell cycle progression into mitosis and the associated changes in MPF and Plk1 kinase activity are described in Chapter 13. These methods provide reliable ways to assay the integrity of the G2 topoisomerase II checkpoint. Chapter 14 contains protocols that can be used to analyze similar topoisomerase II checkpoints in yeast cells, which offer the advantage of being genetically tractable.

Finally, the last series of chapters in this volume include methods specific to the study of topoisomerase II and its regulation in vivo (Chapters 16, 17, 18, and 19). Recent studies have begun to reveal the importance of the post-translational modifications that befall topoisomerases, such as sumoylation, which can affect the localization of topoisomerases in cells. Cell biology methods are also needed to put into context the modifications with the cell cycle. The dynamics of topoisomerases in live cells can also now be measured. Thus, methods designed to study sumo modification (Chapters 16 and 17) as well as the dynamics of topoisomerase II in the nucleus (Chapter 18) are included, which ought to aid further research in this important area.

With the expanded study of topoisomerases in relation to cell cycle position, there has been a need to devise and optimize protocols that achieve depletion of topoisomerases from mammalian cells, as well as methods that combine depletion with cell cycle synchrony. This volume concludes with Chapter 19 that discusses the different approaches that can be employed to deplete topoisomerase II from mammalian cells.

In all, this collection of protocols describes the methodology needed to study topoisomerases in the molecular and cellular context, reflecting an expanded understanding of the functions of these essential enzymes. The studies described above provide evidence that research on the functions of topoisomerases is in a growth phase and that key discoveries will be made in the coming years. It is the hope that the methods provided here will aid in those discoveries.

Duncan J. Clarke

Contents

Contributors

Yoshiaki Azuma • *Department of Molecular Biosciences, University of Kansas, Lawrence, KS*

Jeffrey Bachant • *Department of Cell Biology and Neuroscience, University of California at Riverside, Riverside, CA*

Csanád Z. Bachrati • *Weatherall Institute of Molecular Medicine, University of Oxford, Oxford, United Kingdom*

Melissa Baldwin • *Department of Cell Biology and Neuroscience, University of California at Riverside, Riverside, CA*

Omari J. Bandele • *Department of Biochemistry, Vanderbilt University School of Medicine, Nashville, TN*

Rodrigo Bermejo • *Fondazione Italiana per la Ricerca sul Cancro, Institute of Molecular Oncology Foundation, Milan, Italy*

Nynke H. Dekker • *Kavli Institute of NanoScience, Delft University of Technology, Delft, The Netherlands*

James J. Champoux • *Department of Microbiology, University of Washington, Seattle, WA*

Duncan J. Clarke • *Department of Genetics, Cell Biology & Development, University of Minnesota, Minneapolis, MN*

Tammy R.L. Collins • *Department of Biochemistry, Duke University, Durham, NC*

Zbigniew Darzynkiewicz • *Brander Cancer Research Institute, New York Medical College, Valhalla, NY*

John R. Daum • *Oklahoma Medical Research Foundation, Oklahoma City, OK*

Arturo Falaschi • *International Centre for Genetic Engineering and Biotechnology, Trieste, Italy; Scuola Normale Superiore, Pisa, Italy; Istituto di Fisiologia Clinica, CNR, Pisa, Italy*

Marco Foiani • *Fondazione Italiana per la Ricerca sul Cancro, Institute of Molecular Oncology Foundation, Milan, Italy; DSBB-Università degli Studi di Milano, Milan, Italy*

Katherine Furniss • *Department of Genetics, Cell Biology & Development, University of Minnesota, Minneapolis, MN*

Juan F. Giménez-Abián • *Reproducción Celular y Animal, CIB, CSIC, Madrid, Spain*

Gary J. Gorbsky • *Oklahoma Medical Research Foundation, Oklahoma City, OK*

Susanne Hage • *Kavli Institute of NanoScience, Delft University of Technology, Delft, The Netherlands*

H. Dorota Halicka • *Brander Cancer Research Institute, New York Medical College, Valhalla, NY*

Ian D. Hickson • *Weatherall Institute of Molecular Medicine, University of Oxford, Oxford, United Kingdom*

Tao-shih Hsieh • *Department of Biochemistry, Duke University, Durham, NC*

Yuki-Mori Katou • *Laboratory of Genome Structure and Function, Division for Gene Research, Center for Biological Resources and Informatics, Tokyo Institute of Technology, Yokohama City, Kanagawa, Japan*

William K. Kaufmann • *Department of Pathology and Laboratory Medicine, University of North Carolina at Chapel Hill, Chapel Hill, NC*

Daniel Koster • *Kavli Institute of NanoScience, Delft University of Technology, Delft, The Netherlands; Departments of Physics of Complex Systems and Molecular Cell Biology, Weizmann Institute of Science, Rehovot, Israel*

Andrew Lane • *Department of Genetics, Cell Biology & Development, University of Minnesota, Minneapolis, MN*

Stephen D. Levene • *Department of Molecular and Cell Biology, The University of Texas at Dallas, Richardson, TX*

Jan Lipfert • *Kavli Institute of NanoScience, Delft University of Technology, Delft, The Netherlands*

Yin Yuan Mo • *Department of Medical Microbiology, Immunology and Cell Biology, Southern Illinois University School of Medicine, Springfield, IL*

Neil Osheroff • *Department of Biochemistry and Medicine, Vanderbilt University School of Medicine, Nashville, TN*

Andrew C.G. Porter • *Department of Haematology, Imperial College Faculty of Medicine, London, United Kingdom*

Joaquim Roca • *IBMB-CSIC, Barcelona, Spain*

Katsuhiko Shirahige • *Laboratory of Genome Structure and Function, Division for Gene Research, Center for Biological Resources and Informatics, Tokyo Institute of Technology, Yokohama City, Kanagawa, Japan*

Toshiki Tanaka • *Brander Cancer Research Institute and Pathology Department, New York Medical College, Valhalla, NY; First Department of Surgery, Yamaguchi University School of Medicine, Yamaguchi, Japan*

Amit C.J. Vas • *Department of Genetics, Cell Biology & Development, University of Minnesota, Minneapolis, MN*

Igor D. Vilfan • *Kavli Institute of NanoScience, Delft University of Technology, Delft, The Netherlands*

Tariq Warsi • *Department of Cell Biology and Neuroscience, University of California at Riverside, Riverside, CA*

Zheng Yang • *Department of Microbiology, University of Washington, Seattle, WA*

Chapter 1

Introduction: Emerging Themes in DNA Topoisomerase Research

Duncan J. Clarke and Andrew Lane

Abstract

DNA topoisomerases are enzymes that alter the topology of DNA. They have important functions in DNA replication, transcription, Holliday junction dissolution, chromosome condensation, and sister chromatid separation. Deficiencies in these enzymes are associated with diseases that result from genome instability. The last 10–15 years has seen a great deal of exciting research in the field of topoisomerase. Here we discuss a selection of the new themes that have been recently introduced into the already large body of topoisomerase research.

Key words: DNA topoisomerase, checkpoint, catenation, Holliday junction, sumo.

1. The Topological States of DNA

Double-stranded DNA is a duplex of two single strands that coil around each other as they base-pair, an elegant arrangement that confers upon it great structural stability. However, this entanglement is not conducive to neatly separating the strands for replicative polymerase access, particularly when replication is being initiated at hundreds or thousands of sites across the chromosome. From each origin, a replication fork moves against these coils through what progressively becomes a highly twisted length of new and old DNA, turning upon itself to relieve the buildup of tension ahead of each of the converging replication forks. The result is two fully replicated sister chromatids that are necessarily physically associated (1). This entanglement is often viewed as being a topological problem because it requires that the sister

D.J. Clarke (ed.), *DNA Topoisomerases*, Methods in Molecular Biology 582,
DOI 10.1007/978-1-60761-340-4_1,

DNA molecules undergo resolution, or decatenation, so that they can be separated during cell division. However, chromosomal catenation also serves as a way of ensuring that sister chromatids remain paired following DNA replication until they are segregated during mitosis. By keeping sister chromatids together until mitosis, the cell ensures that each of the paired chromatids is attached to opposite poles of the mitotic spindle apparatus so that they can be segregated appropriately between the daughter cells.

Clearly, however, there is a step missing in this description: At some point the sister chromatids must be decatenated so that they can segregate unencumbered. This function is fulfilled by a DNA topoisomerase and is just a single (albeit important) example of the importance of topoisomerases in controlling DNA topology; many processes, for example, transcription and DNA repair, bring forth topological challenges that are met by one or more members of the topoisomerase family. It becomes immediately apparent that management of chromosome topology is dependent on these enzymes and that their introduction must have coincided with the origin of the double helix itself.

DNA can assume a number of distinct topological states. In a relaxed state under physiological conditions, there are approximately 10 base pairs per turn of the double helix in linear DNA, but in vivo local overwinding and underwinding occur, resulting in more or fewer base pairs per turn of the DNA helix. These changes in the pitch of the helix cause even linear chromosomes to adopt supercoiled topological states, wherein two regions of double helix coil around each other, either resulting from overwinding of the helix (positive supercoiling) or underwinding (negative supercoiling). The local environments of chromatin within linear chromosomes also allow DNA helices to become knotted and catenated.

2. DNA Topoisomerase Enzyme Activity

DNA topoisomerases alter the topology of DNA by transiently breaking single- or double-stranded DNA molecules and then religating them after rotation of the helix or passage of one DNA through another (2–4). Upon strand breakage, a covalent bond is formed between the active site tyrosine of the enzyme and the newly cleaved DNA end. In some circumstances, the free double-stranded ends may become ligated to other DNA ends, but, in general, the topoisomerases act to break the DNA and to keep hold of the DNA ends so that they can be religated. Type II topoisomerases can achieve this by acting as multimers which bind covalently to the DNA ends. ATP is essential for type II topoisomerase function, though its hydrolysis drives conformational changes

within the multimeric enzyme structure rather than initiating DNA breakage or religation. The topology modifications performed by topoisomerases are varied and in turn they are required to carry out diverse functions. Thus, a number of DNA topoisomerase subfamilies have evolved. These can be generally categorized based on whether they break one or both strands of the DNA helix and on the nature of the protein–DNA covalent interaction (*see* **Table 1.1**).

Table 1.1
The major topoisomerase activities in selected organisms

Organism	Type	Enzyme	Function/notes	References
Bacteria/ archaea	IA	Topoisomerase I	Control of DNA supercoiling; chromosomal segregation. Present in bacteria and archaea	(25–27) (28; for general biochemical data)
	IA	Topoisomerase III	Involved in regulation of recombination. Present in bacteria and archaea	(29, 30)
	IA	Reverse gyrase	Introduces positive supercoils; protects DNA at high temperatures. Present only in bacterial and archaean hyperthermophiles	(31)
	IB	Topoisomerase V	Functions in DNA repair. Found only in *Methanopyrus kandleri*	(32, 33)
	IIA	DNA gyrase	Introduces negative supercoiling or removes positive supercoiling on a single DNA duplex	(34, 35)
	IIA	Bacterial topoisomerase IV	Removal of linkage between two DNA duplexes. Involved in chromosome cohesion	(36, 37)
	IIB	Topoisomerase VI	Involved in recombination. Present in archaea and some bacteria (but not *E. coli*). Shares sequence similarity with eukaryotic Spo11. Formed as a heterotetramer ($\alpha 2\beta 2$)	(38)
S. cerevisiae	IA	Topoisomerase III (Top3)	Relaxes single-stranded negatively coiled DNA. Mutants exhibit elevated recombination rates	(39, 40)
	IB	Topoisomerase Iα (Top1)	Relaxes positive and negative supercoiling by nicking double-stranded DNA	(41, 42)

(continued)

Table 1.1 (continued)

Organism	Type	Enzyme	Function/notes	References
	IIA	Topoisomerase II (Top2)	Relaxes positive and negative supercoiling. Required for chromosome condensation and segregation	(43)
Mammalian	IA	Topoisomerase IIIα	Relaxes supercoiling in highly negatively supercoiled DNA. Expressed tissue specifically, with altered pattern between Topo IIIα and Topo IIIβ	(44, 45)
	IA	Topoisomerase IIIβ	See notes for Topo IIIα	(45)
	IB	Topoisomerase I	Relaxes positive and negative supercoiling by nicking double-stranded DNA	(25, 29)
	IIA	Topoisomerase IIα	Relaxes positive and negative supercoiling. Required for chromosome condensation and segregation. Alpha and beta isozymes have differing tissue and cell-cycle-stage specific expression	(46, 47)
	IIA	Topoisomerase IIβ	See notes for Topo IIα	(48)

3. Cellular Functions of DNA Topoisomerases

The basic need for topoisomerase activities in cells has been appreciated for many years, and much has been learned about the enzymatic cycles of the major topoisomerase classes. However, more recent studies have begun to dissect specific cellular processes that require topoisomerases and have determined how topoisomerase activity, or the lack thereof, integrates into the cell division cycle. Topoisomerases have been found to have significant importance in the clinic, particularly in the context of cancer biology. Not only are the topoisomerases major targets of chemotherapeutic drugs, but it is now known that the normal cellular responses to perturbed topoisomerase function are often defective or lacking in tumor cells. These cellular controls are also absent from mammalian stem cells.

A recent area of excitement has been the discovery that eukaryotic DNA topoisomerase IIIα along with the RecQ helicase (implicated in Bloom's syndrome) functions in the dissolution of double-Holliday junctions. This DNA topology arises as an

intermediate of homologous recombination, which occurs during meiosis as well as during the repair of double-stranded DNA breaks. In meiosis, cross-over recombination provides genetic variation because Holliday junction *resolution* can result in the exchange of DNA between the homologs. In contrast, Holliday junction *dissolution* functions to allow repair of the recombination intermediate without exchange.

In front of DNA replication forks, the double helix must undergo swivel to counteract overwinding that occurs as the two strands are separated and replicated. This can be achieved by either single- or double-stranded incisions. Recent data have indicated that in the yeast system, the lack of this activity might cause the accumulation of overwound, nicked DNA at sites of failed replication termination (5). Transcription has similar requirements for topoisomerases to act as swivelases, relaxing overwound DNA in front of the transcription machinery. It has become important to be able to analyze the association of topoisomerases with functional units such as replication origins and promoter elements of genes, and recent studies have developed such abilities.

In very small chromosomes, for example, in the budding yeast genome, DNA catenations that arise during DNA replication appear to be resolved quickly, before mitosis. In the larger chromosomes and in metazoans, however, catenations persist at least until the onset of anaphase of mitosis and some appear to be maintained until late anaphase. Topoisomerases therefore have key functions in the segregation of the genome. When topoisomerase II is perturbed, progression into and through mitosis is inhibited, presumably to prevent attempts at segregating the genome before sister chromatid catenations have been resolved. This is becoming a complicated field of research because it now seems that different cell cycle checkpoints are activated depending on the manner in which topoisomerase II is compromised. In mammalian cells, topoisomerase II poisons such as etoposide form a ternary complex with the broken DNA and the enzyme. This activates DNA damage checkpoint controls that arrest the cells in G2-phase of the cell cycle. Other topoisomerase II inhibitors, such as the bisdioxopiperazines (e.g., ICRF-193), lock topoisomerase II onto the DNA but without directly generating DNA breaks. These inhibitors activate what have been described as topoisomerase II checkpoints to distinguish this mode of cell cycle regulation from the responses that are mounted in response to DNA breakage. Mammalian topoisomerase II checkpoints can arrest cells in G2 and, albeit rather transiently, in metaphase of mitosis (6, 7). Moreover, the G2 topoisomerase II checkpoint seems to be clinically relevant since this cell cycle response is absent in some tumor cells and also in some stem cells (8–10). In yeast, topoisomerase II checkpoints also function to delay mitotic progression in the absence of topoisomerase II activity (Top2 in yeast) (6, 11). The

yeast cell cycle is organized differently from that of other eukaryotes in that there is little distinction between G2 and the early stages of mitosis. Within about 10 min following the completion of DNA replication, chromosomes have already achieved biorientation on an assembled mitotic spindle and are poised for anaphase chromosome segregation. It may be for this reason that perturbing topoisomerase II in yeast activates a topoisomerase II checkpoint similar to the mammalian topoisomerase II checkpoint acting in metaphase. The mammalian metaphase topoisomerase II checkpoint and the yeast topoisomerase II checkpoint use a different signaling mechanism (from the G2 checkpoint) that depends on components of the spindle assembly checkpoint such as Mad2 (11). Further analysis in the yeast system revealed that the spindle checkpoint target, Pds1/securin, is not required for the preanaphase arrest when topoisomerase II is perturbed. This defined the yeast topoisomerase II checkpoint as being at least partially separate from the spindle checkpoint. These studies also defined a topoisomerase II checkpoint for the first time in a single-celled organism that can be easily manipulated genetically, and thus paved the way for a detailed analysis.

In mammalian cells, removal of DNA catenations not only allows chromosomes to segregate but is essential in early mitosis for the structural changes that drive chromosome compaction (12–15). There are two main cytological observations when topoisomerase II is perturbed shortly before mitosis or during early prophase that presumably are a result of persistent catenation between the sister DNA molecules: a lack of sister chromatid resolution and a lack of chromosome arm shortening (16). A third consequence is the persistence of interchromosome and intrachromatid catenations that presumably arise because topoisomerase II does not distinguish catenation from decatenation. In other words, some catenations are inevitably introduced between chromosomes and within chromatids that ought not to have been generated. These are thought to be resolved in prophase as chromosomes become individualized and chromatids condense, but they persist when topoisomerase II is perturbed (16).

A recent finding has been that topoisomerase II is modified by sumoylation in eukaryotes, and this has been studied in yeast, Xenopus eggs, and mammalian cells (17–22). Surprisingly, little is known about how topoisomerase II is regulated by posttranslational modifications, and it has been widely supposed that the topological DNA modifications carried out by topoisomerase II occur in a largely unregulated manner. The studies of topoisomerase II sumoylation have implicated this modification in centric chromatin structure as well as the localization of topoisomerase II to centromeres (18, 20, 21). In mice, it has been reported that a lack of sumo modification of topoisomerase II correlates with a high incidence of tumors (23).

Because topoisomerase II was found to be an important target of chemotherapeutic drugs, a series of such drugs has been available for many years and for this reason studies of the function of topoisomerase II have relied heavily on the inhibitors. However, it is clear that there are limitations to the use of the inhibitors for experimental studies. The drugs affect topoisomerase activity in different ways and cause potentially nonphysiological situations to arise or can have side effects resulting from the formation of DNA double-stranded breaks. Also of concern is that the drugs typically do not distinguish the alpha and beta topoisomerase II isoforms, so specific functions of each one of these differentially regulated and localized enzymes cannot be dissected. While studies using the inhibitors have been extremely valuable, conditions where topoisomerase II is cleanly depleted from cells would provide a much needed research tool to the field. Successful attempts to achieve this goal have recently been made (24).

This volume describes the state of the art in methods used by active topoisomerase researchers in their own laboratories. The contributors have supplied tested protocols used to assay DNA topology, biochemistry and structure as well as DNA–topoisomerase interactions and methods for downstream cell-level functional assays. It is hoped that the chapters will better inform on these methods and aid in the expansion of topoisomerase research.

References

1. Cook, P. R. (1991) The nucleoskeleton and the topology of replication. *Cell* **66**, 627–35.
2. Champoux, J. J. (1978) Proteins that affect DNA conformation. *Annu Rev Biochem* **47**, 449–79.
3. Liu, L. F., Liu, C. C. and Alberts, B. M. (1979) T4 DNA topoisomerase: a new ATP-dependent enzyme essential for initiation of T4 bacteriophage DNA replication. *Nature* **281**, 456–61.
4. Brown, P. O. and Cozzarelli, N. R. (1979) A sign inversion mechanism for enzymatic supercoiling of DNA. *Science* **206**, 1081–3.
5. Baxter, J. and Diffley, J. F. (2008) Topoisomerase II inactivation prevents the completion of DNA replication in budding yeast. *Mol Cell* **30**, 790–802.
6. Clarke, D. J., Vas, A. C., Andrews, C. A., Diaz-Martinez, L. A. and Gimenez-Abian, J. F. (2006) Topoisomerase II checkpoints: universal mechanisms that regulate mitosis. *Cell Cycle* **5**, 1925–8.
7. Skoufias, D. A., Lacroix, F. B., Andreassen, P. R., Wilson, L. and Margolis, R. L. (2004) Inhibition of DNA decatenation, but not DNA damage, arrests cells at metaphase. *Mol Cell* **15**, 977–90.
8. Damelin, M., Sun, Y. E., Sodja, V. B. and Bestor, T. H. (2005) Decatenation checkpoint deficiency in stem and progenitor cells. *Cancer Cell* **8**, 479–84.
9. Doherty, S. C., McKeown, S. R., McKelvey-Martin, V., Downes, C. S., Atala, A., Yoo, J. J., Simpson, D. A. and Kaufmann, W. K. (2003) Cell cycle checkpoint function in bladder cancer. *J Natl Cancer Inst* **95**, 1859–68.
10. Nakagawa, T., Hayashita, Y., Maeno, K., Masuda, A., Sugito, N., Osada, H., Yanagisawa, K., Ebi, H., Shimokata, K. and Takahashi, T. (2004) Identification of decatenation G2 checkpoint impairment independently of DNA damage G2 checkpoint in human lung cancer cell lines. *Cancer Res* **64**, 4826–32.
11. Andrews, C. A., Vas, A. C., Meier, B., Gimenez-Abian, J. F., Diaz-Martinez, L. A., Green, J., Erickson, S. L., Vanderwaal, K. E., Hsu, W. S. and Clarke, D. J. (2006) A mitotic topoisomerase II checkpoint in budding yeast is required for genome stability

but acts independently of Pds1/securing. *Genes Dev* **20**, 1162–74.

12. Newport, J. and Spann, T. (1987) Disassembly of the nucleus in mitotic extracts: membrane vesicularization, lamin disassembly, and chromosome condensation are independent processes. *Cell* **48**, 219–30.
13. Uemura, T., Ohkura, H., Adachi, Y., Morino, K., Shiozaki, K. and Yanagida, M. (1987) DNA topoisomerase II is required for condensation and separation of mitotic chromosomes in *S. pombe*. *Cell* **50**, 917–25.
14. Wood, E. R. and Earnshaw, W. C. (1990) Mitotic chromatin condensation in vitro using somatic cell extracts and nuclei with variable levels of endogenous topoisomerase II. *J Cell Biol* **111**, 2839–50.
15. Adachi, Y., Luke, M. and Laemmli, U. K. (1991) Chromosome assembly in vitro: topoisomerase II is required for condensation. *Cell* **64**, 137–48.
16. Giménez-Abián, J. F., Clarke, D. J., Devlin, J., Giménez-Abián, M., De la Torre, C., Johnson, R. T., Mullinger, A. M. and Downes, C. S. (2000) Premitotic chromosome individualization in mammalian cells depends on topoisomerase II activity. *Chromosoma* **109**, 235–44.
17. Agostinho, M., Santos, V., Ferreira, F., Costa, R., Cardoso, J., Pinheiro, I., Rino, J., Jaffray, E., Hay, R. T. and Ferreira, J. (2008) Conjugation of human topoisomerase 2 alpha with small ubiquitin-like modifiers 2/3 in response to topoisomerase inhibitors: cell cycle stage and chromosome domain specificity. *Cancer Res* **68**, 2409–18.
18. Azuma, Y., Arnaoutov, A., Anan, T. and Dasso, M. (2005) PIASy mediates SUMO-2 conjugation of Topoisomerase-II on mitotic chromosomes. *EMBO J* **24**, 2172–82.
19. Azuma, Y., Arnaoutov, A. and Dasso, M. (2003) SUMO-2/3 regulates topoisomerase II in mitosis. *J Cell Biol* **163**, 477–87.
20. Bachant, J., Alcasabas, A., Blat, Y., Kleckner, N. and Elledge, S. J. (2002) The SUMO-1 isopeptidase Smt4 is linked to centromeric cohesion through SUMO-1 modification of DNA topoisomerase II. *Mol Cell* **9**, 1169–82.
21. Diaz-Martinez, L. A., Gimenez-Abian, J. F., Azuma, Y., Guacci, V., Gimenez-Martin, G., Lanier, L. M. and Clarke, D. J. (2006) PIASgamma is required for faithful chromosome segregation in human cells. *PLoS ONE* **1**, e53.
22. Takahashi, Y., Yong-Gonzalez, V., Kikuchi, Y. and Strunnikov, A. (2006) SIZ1/SIZ2 control of chromosome transmission fidelity is mediated by the sumoylation of topoisomerase II. *Genetics* **172**, 783–94.
23. Dawlaty, M. M., Malureanu, L., Jeganathan, K. B., Kao, E., Sustmann, C., Tahk, S., Shuai, K., Grosschedl, R. and van Deursen, J. M. (2008) Resolution of sister centromeres requires RanBP2-mediated SUMOylation of topoisomerase IIalpha. *Cell* **133**, 103–15.
24. Carpenter, A. J. and Porter, A. C. (2004) Construction, characterization, and complementation of a conditional-lethal DNA topoisomerase IIalpha mutant human cell line. *Mol Biol Cell* **15**, 5700–11.
25. Wang, J. C. (2002) Cellular roles of DNA topoisomerases: a molecular perspective. *Nat Rev Mol Cell Biol* **3**, 430–40.
26. Zhu, Q., Pongpech, P. and DiGate, R. J. (2001) Type I topoisomerase activity is required for proper chromosomal segregation in *Escherichia coli*. *Proc Natl Acad Sci USA* **98**, 9766–71.
27. Masse, E. and Drolet, M. (1999) Relaxation of transcription-induced negative supercoiling is an essential function of *Escherichia coli* DNA topoisomerase I. *J Biol Chem* **274**, 16654–8.
28. Kirkegaard, K. and Wang, J. C. (1985) Bacterial DNA topoisomerase I can relax positively supercoiled DNA containing a single-stranded loop. *J Mol Biol* **185**, 625–37.
29. Champoux, J. J. (2001) DNA topoisomerases: structure, function, and mechanism. *Annu Rev Biochem* **70**, 369–413.
30. Lopez, C. R., Yang, S., Deibler, R. W., Ray, S. A., Pennington, J. M., Digate, R. J., Hastings, P. J., Rosenberg, S. M. and Zechiedrich, E. L. (2005) A role for topoisomerase III in a recombination pathway alternative to RuvABC. *Mol Microbiol* **58**, 80–101.
31. del Toro Duany, Y., Jungblut, S. P., Schmidt, A. S. and Klostermeier, D. (2008) The reverse gyrase helicase-like domain is a nucleotide-dependent switch that is attenuated by the topoisomerase domain. *Nucleic Acids Res* **36**, 5882–95.
32. Taneja, B., Schnurr, B., Slesarev, A., Marko, J. F. and Mondragon, A. (2007) Topoisomerase V relaxes supercoiled DNA by a constrained swiveling mechanism. *Proc Natl Acad Sci USA* **104**, 14670–5.
33. Belova, G. I., Prasad, R., Kozyavkin, S. A., Lake, J. A., Wilson, S. H. and Slesarev, A. I. (2001) A type IB topoisomerase with DNA

repair activities. *Proc Natl Acad Sci USA* **98**, 6015–20.

34. Snoep, J. L., van der Weijden, C. C., Andersen, H. W., Westerhoff, H. V. and Jensen, P. R. (2002) DNA supercoiling in *Escherichia coli* is under tight and subtle homeostatic control, involving gene-expression and metabolic regulation of both topoisomerase I and DNA gyrase. *Eur J Biochem* **269**, 1662–9.
35. Menzel, R. and Gellert, M. (1983) Regulation of the genes for *E. coli* DNA gyrase: homeostatic control of DNA supercoiling. *Cell* **34**, 105–13.
36. Wang, X., Reyes-Lamothe, R. and Sherratt, D. J. (2008) Modulation of *Escherichia coli* sister chromosome cohesion by topoisomerase IV. *Genes Dev* **22**, 2426–33.
37. Zechiedrich, E. L., Khodursky, A. B. and Cozzarelli, N. R. (1997) Topoisomerase IV, not gyrase, decatenates products of site-specific recombination in *Escherichia coli*. *Genes Dev* **11**, 2580–92.
38. Nichols, M. D., DeAngelis, K., Keck, J. L. and Berger, J. M. (1999) Structure and function of an archaeal topoisomerase VI subunit with homology to the meiotic recombination factor Spo11. *Embo J* **18**, 6177–88.
39. Wallis, J. W., Chrebet, G., Brodsky, G., Rolfe, M. and Rothstein, R. (1989) A hyper-recombination mutation in *S. cerevisiae* identifies a novel eukaryotic topoisomerase. *Cell* **58**, 409–19.
40. Kim, R. A. and Wang, J. C. (1992) Identification of the yeast TOP3 gene product as a single strand-specific DNA topoisomerase. *J Biol Chem* **267**, 17178–85.
41. Megonigal, M. D., Fertala, J. and Bjornsti, M. A. (1997) Alterations in the catalytic activity of yeast DNA topoisomerase I result in cell cycle arrest and cell death. *J Biol Chem* **272**, 12801–8.
42. Garinther, W. I. and Schultz, M. C. (1997) Topoisomerase function during replication-independent chromatin assembly in yeast. *Mol Cell Biol* **17**, 3520–6.
43. DiNardo, S., Voelkel, K. and Sternglanz, R. (1984) DNA topoisomerase II mutant of *Saccharomyces cerevisiae*: topoisomerase II is required for segregation of daughter molecules at the termination of DNA replication. *Proc Natl Acad Sci USA* **81**, 2616–20.
44. Hanai, R., Caron, P. R. and Wang, J. C. (1996) Human TOP3: a single-copy gene encoding DNA topoisomerase III. *Proc Natl Acad Sci USA* **93**, 3653–7.
45. Ng, S. W., Liu, Y., Hasselblatt, K. T., Mok, S. C. and Berkowitz, R. S. (1999) A new human topoisomerase III that interacts with SGS1 protein. *Nucleic Acids Res* **27**, 993–1000.
46. Gimenez-Abian, J. F., Clarke, D. J., Gimenez-Martin, G., Weingartner, M., Gimenez-Abian, M. I., Carballo, J. A., Diaz, D., Bogre, L. and De, L. (2002) DNA catenations that link sister chromatids until the onset of anaphase are maintained by a checkpoint mechanism. *Eur J Cell Biol* **81**, 9–16.
47. Warburton, P. E. and Earnshaw, W. C. (1997) Untangling the role of DNA topoisomerase II in mitotic chromosome structure and function. *Bioessays* **19**, 97–9.
48. Bauman, M. E., Holden, J. A., Brown, K. A., Harker, W. G. and Perkins, S. L. (1997) Differential immunohistochemical staining for DNA topoisomerase II alpha and beta in human tissues and for DNA topoisomerase II beta in non-Hodgkin's lymphomas. *Mod Pathol* **10**, 168–75.

Chapter 2

Analysis of DNA Topoisomers, Knots, and Catenanes by Agarose Gel Electrophoresis

Stephen D. Levene

Abstract

Agarose gel electrophoresis is by far the most widely used method for characterizing the topological state of DNA molecules. Although this technique has been used for more than 30 years, the physical mechanism underlying the resolution of topological states remains poorly understood. However, electrophoretic methods remain the most robust and precise techniques for determining the local unwinding of DNA induced by the binding of proteins and small-molecule ligands, analyzing conformational transitions in duplex DNA, measuring changes in helical repeat that accompany shifts in environmental conditions, and characterizing knotting and linking in duplex DNA.

Key words: Topoisomers, electrophoresis, catenanes, linking number, DNA knots.

1. Introduction

Linking-number topoisomers, knots, and catenanes (linked circles) are topological forms of circular DNA that have distinct three-dimensional conformational properties.[1] The analysis of DNA topology has played a major role in molecular biology, yielding essential insights into the mechanisms of topoisomerases and related proteins such as site-specific recombinases. The mechanistic feature common to all of these systems is that they

[1] We follow typical usage here, in which the term "topoisomer" refers specifically to unknotted or unlinked DNA circles with distinct linking-number values. However, molecules that differ in knot and catenane type are also properly regarded as topoisomers because these forms are identical apart from differences in their respective topological states.

D.J. Clarke (ed.), *DNA Topoisomerases*, Methods in Molecular Biology 582,
DOI 10.1007/978-1-60761-340-4_2,

pass DNA strands through one another; however, there is extraordinary variation in the details of strand exchange. The resulting distributions of product topologies provide strong mechanistic clues that illuminate the biochemical details of DNA reorganization during the reaction pathway (1–3). For example, **Fig. 2.1** shows a mechanistic model for members of the tyrosine-recombinase superfamily, which includes λ int, Cre, and Flp. The mechanism consists of protein binding to a circular DNA molecule, cutting of the DNA at two specific sites, and subsequent exchange and rejoining of the cleaved ends, producing a specific knot (**Fig. 2.1A**) or catenane (**Fig. 2.1B**). In systems that act on recombination-target sites having sequence asymmetry, only one juxtaposition of sites leads to productive recombination. Thus, in the example shown in **Fig. 2.1A**, recombination of an unknotted supercoiled plasmid bearing inversely oriented sites leads to a knotted product, whereas recombination of directly oriented sites on a similar superhelical DNA in **Fig. 2.1B** generates a catenane.

On a circular DNA molecule, the pair of target sites bound by the topoisomerase or recombinase during site synapsis divides the DNA contour into two distinct domains. For a particular conformation of the synaptic complex, the number of DNA crossings in the product is a function of the number of interdomainal windings. In the case of an intramolecular tyrosine-recombinase reaction taking place on an unknotted circular DNA, the number of irreducible crossings in the products is proportional to the number of superhelical turns that are trapped between the sites (**Fig. 2.1**). The knot or catenane types that are generated in a particular enzymatic reaction are a signature for a specific enzymatic mechanism. This is generally posed as an inverse problem, in which one deduces the enzymatic mechanism from a particular distribution of superhelical, knotted, or catenated products (2, 3). Solution of the inverse problem is not as difficult as it may appear; although the space of possible knots grows exponentially with the number of irreducible crossings (there are 1,388,705 prime knots with 16 or fewer crossings), only a limited subset of knots is generated by an enzyme system (**Fig. 2.2**).

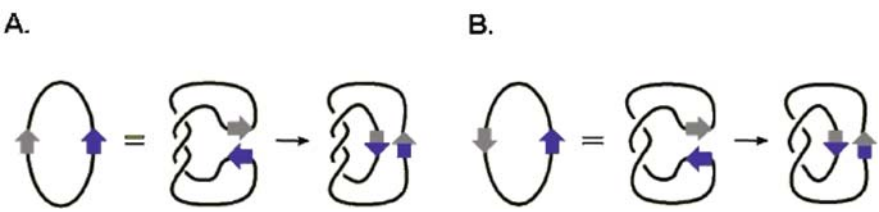

Fig. 2.1. **Tyrosine recombinases can knot and link circular DNA molecules. (A)** Knotting of DNA by recombination of inversely repeated sites. **(B)** Linking of product DNA circles by recombination of directly repeated sites.

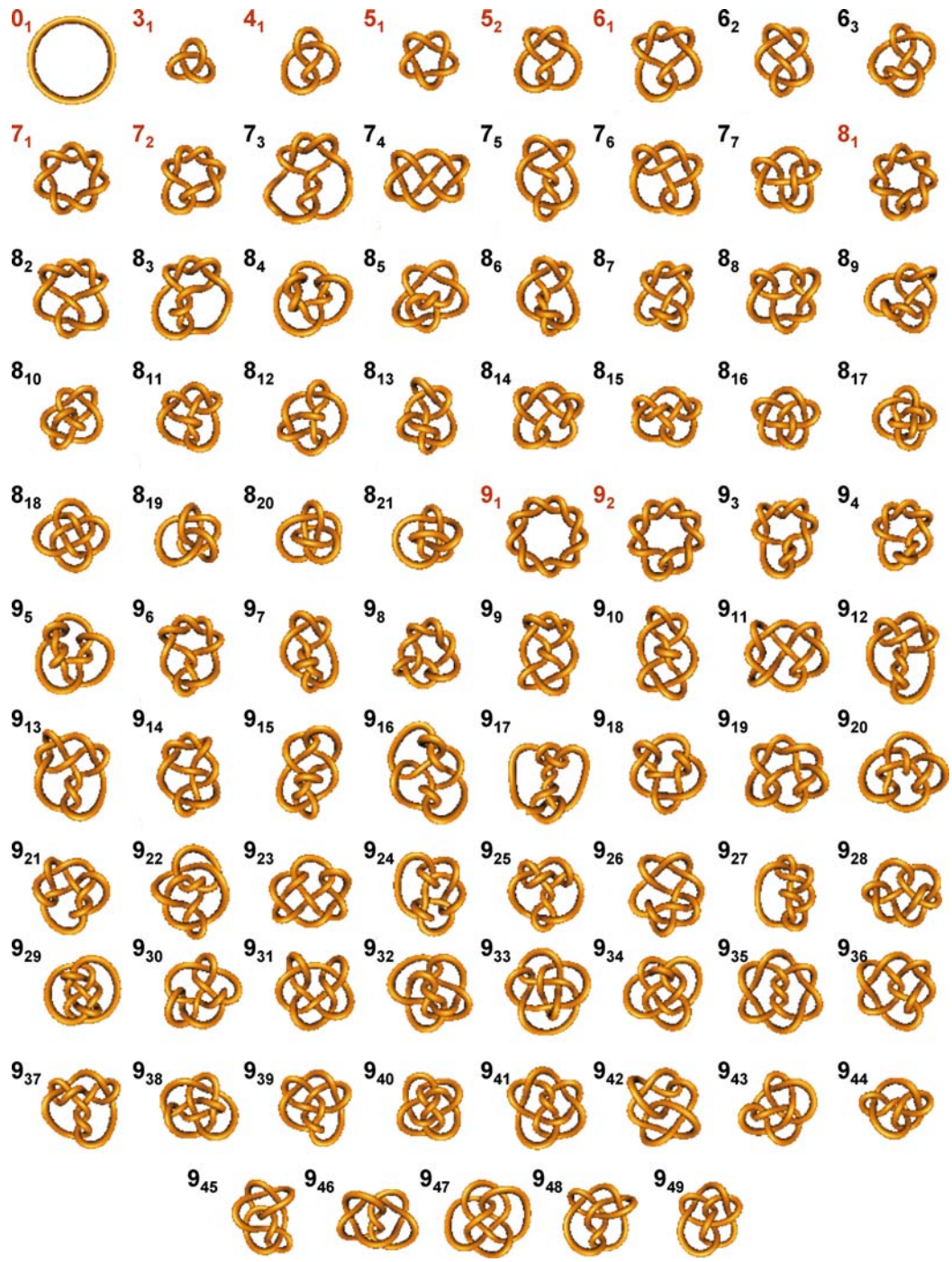

Fig. 2.2. **Prime knots.** Minimal diagrams of all prime knots containing up to nine irreducible crossings generated with the program *KnotPlot* (4). Each knot is labeled according to the notation of Alexander-Briggs. Knots that are commonly observed as topoisomerase and recombinase products are indicated by *gray* labels.

1.1. Gel Electrophoretic Analysis of Linking-Number Topoisomers

Supercoiling is parameterized in terms of the linking number of duplex strands, *Lk*, which is a topologically invariant quantity for closed-circular DNA molecules (5). The *Lk* value trapped by cyclization, ligation at a nick, or topoisomerase activity is an integer equal to the sum of two geometric variables, twist, *Tw*, and writhe, *Wr*, which fluctuate at thermal equilibrium. For plasmid-sized DNAs, covalent closure in vitro generates a Gaussian distribution of species typically composed of several *Lk* topoisomers. Topoisomers can be analyzed by gel electrophoresis using one-dimensional (1-d) and two-dimensional (2-d) agarose gels (6–9). Although the physical basis for the electrophoretic separation of topoisomers is poorly understood, it has been proposed that gel mobility is largely a function of the average DNA writhe, $<Wr>$ (6–14). The actual value of *Lk* is rarely of interest; instead, changes in this parameter are measured by comparing *Lk* distributions obtained under different conditions, for example, in the presence and absence of a perturbing ligand. Both 1-d and 2-d methods offer particular advantages in different experimental contexts.

1.1.1. One-Dimensional Agarose Gel Analysis of Topoisomers

The 1-d gels offer a straightforward approach for quantitating differences in DNA helical repeat and are less technically challenging than the 2-d methods. The experiment outlined in **Fig. 2.3** shows an example of 1-d gel analysis of the helical-repeat change induced in duplex DNA by formation of a RecA strand-exchange complex (15, 16). Under appropriate conditions, *Escherichia coli* RecA protein forms a stable complex with the duplex and a single-stranded DNA complimentary to one of the duplex strands; in this complex, the duplex is strongly unwound. Unwinding is detected by a shift in the center of the plasmid/strand-exchange complex *Lk* distribution, $<Lk>$, relative to that in the absence of the complex, after relaxation with topoisomerase I.

1.1.2. Two-Dimensional Agarose Gel Analysis of Topoisomers

The 2-d gels are a method of choice for characterizing supercoiling-dependent localized changes in helical structure such as cruciform extrusion, formation of Z-DNA, and local denaturation (7). Unlike 1-d gels, which are capable of resolving topoisomers only over a narrow ΔLk interval (typically a maximum of ten species), 2-d gels can resolve more than 20 individual topoisomers (**Fig. 2.4**). Moreover, under appropriate conditions, topoisomers of similar $|\Delta Lk|$, but opposing sign are well resolved on 2-d gels; these species comigrate in 1-d electrophoresis. The 2-d methods exploit the strong dependence of topoisomer mobility on electrophoresis conditions usually by running the gel without an intercalating agent such as chloroquine or ethidium in the first dimension, but including an intercalator in the gel and running buffer in the second dimension.

The example shown in **Fig. 2.4** illustrates the analysis of supercoiling-dependent DNA structure using 2-d agarose gel electrophoresis. Here, the discontinuity in the arc-like pattern of

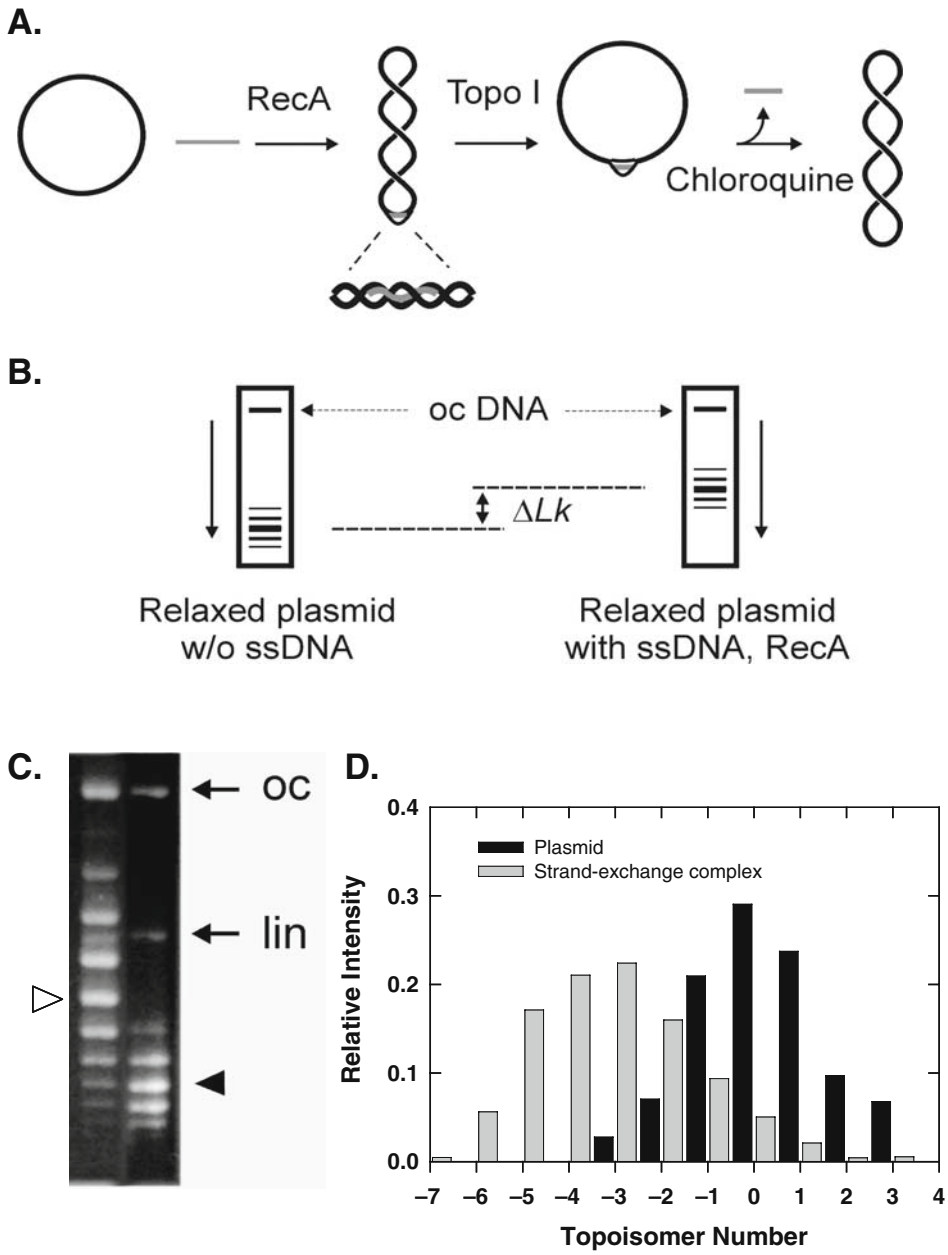

Fig. 2.3. **One-dimensional analysis of topoisomers**. **(A)** Incubation of relaxed plasmid DNA with an ssDNA-containing RecA filament results in the formation of a paranemic ssDNA–dsDNA complex bound to RecA. Relaxation with topoisomerase I removes extraneous supercoils from the locally underwound paranemic complex. The change in DNA twist accompanying formation of the complex is revealed by agarose gel electrophoresis in the presence of the intercalator chloroquine, which also disrupts the complex through positive supercoiling. **(B)** Measurement of the linking difference, ΔLk, by agarose gel electrophoresis. The distribution of topoisomers is quantitated from digital images of gel lanes containing native plasmid DNA and plasmid relaxed under conditions in which the complex is formed. The values of Lk used in computing ΔLk are those corresponding to the most probable topoisomer in each distribution. **(C)** The 1-d agarose gel analysis of topoisomer distributions for the native plasmid (*right lane*) and strand-exchange complex (*left lane*). Positions of the most probable topoisomers are given by the filled and open arrowheads. **(D)** Equilibrium distributions of topoisomers in the relaxed plasmid and the strand-exchange complex. (Adapted with permission from Ref. 16. Copyright 2005 American Chemical Society.)

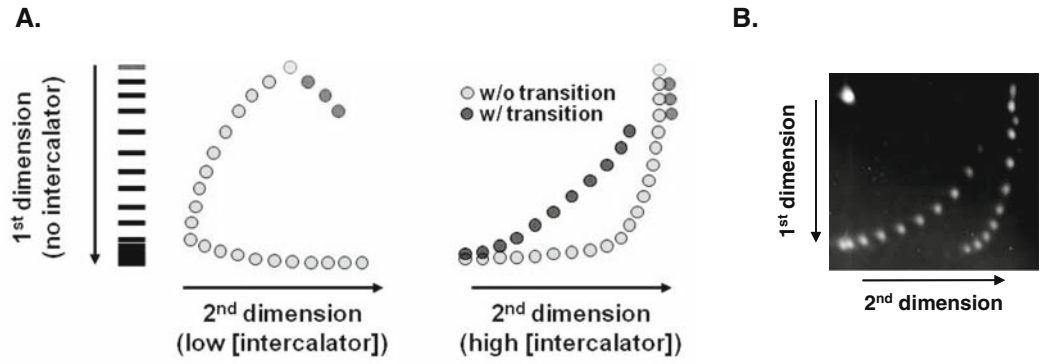

Fig. 2.4. **Two-dimensional analysis of topoisomers**. (**A**) Principle of 2-d gel electrophoresis. Topoisomer separation achieved by a typical 1-d gel in the absence of an intercalating agent is shown on the far left. After equilibrating the gel with running buffer containing an intercalator, subsequent electrophoresis in the orthogonal direction allows resolution of bands that comigrate in the first dimension. If sufficient intercalator is present to drive all of the topoisomers into a (+) supercoiled state (high [intercalator]), a concave arc-like pattern of topoisomer bands is observed. The expected behavior for a plasmid undergoing a structural transition is indicated by the *dark gray* bands in the high [intercalator] example, which follows a discontinuous arc pattern. (**B**) The 2-d agarose gel analysis of pUC8S1F2, which contains a 60-bp inverted-repeat sequence shown to undergo a cruciform transition (5). Electrophoresis was carried out without intercalator in the first dimension and in 3.0 μg/ml chloroquine in the second dimension. Note the discontinuity in the 2-d gel pattern at $\Delta Lk = -10$. (Reproduced from Ref. 5.)

topoisomers seen in **Fig. 2.4B** is characteristic of the formation of an extrahelical DNA structure at a critical level of (–) supercoiling, in this case, a cruciform structure (5). Extrusion of the cruciform sharply increases ΔLk, which abruptly shifts the pattern of topoisomers toward the origin of the first dimension. This behavior is not normally detected in 1-d gels because of the overlap between shifted and unshifted topoisomer bands.

1.2. Gel Electrophoretic Analysis of DNA Knots and Catenanes

Because of the great sensitivity of gel mobility to supercoiling, knotted and catenated circular DNA must be nicked prior to electrophoresis to obtain readily interpretable gel patterns. Otherwise, separations of knotted and catenated circular DNAs take place in much the same way as 1-d gel electrophoresis of *Lk* topoisomers (*see* **Section 1.1.1**), apart from the use of intercalating agents, which do not affect the relative mobilities of nicked knots and catenanes. At sufficiently low field strengths, spacing between successive knot and catenane bands is nearly constant with the mobility of a particular species effectively proportional to the number of irreducible crossings (**Fig. 2.5**). There is very little compression of knot or catenane ladders at high crossing number, although small differences in mobility can be detected for distinct knot types having the same number of irreducible crossings at low crossing number (17). Separations of distinct knot types with identical crossing number can be acheived using 2-d gel- electrophoresis methods (18).

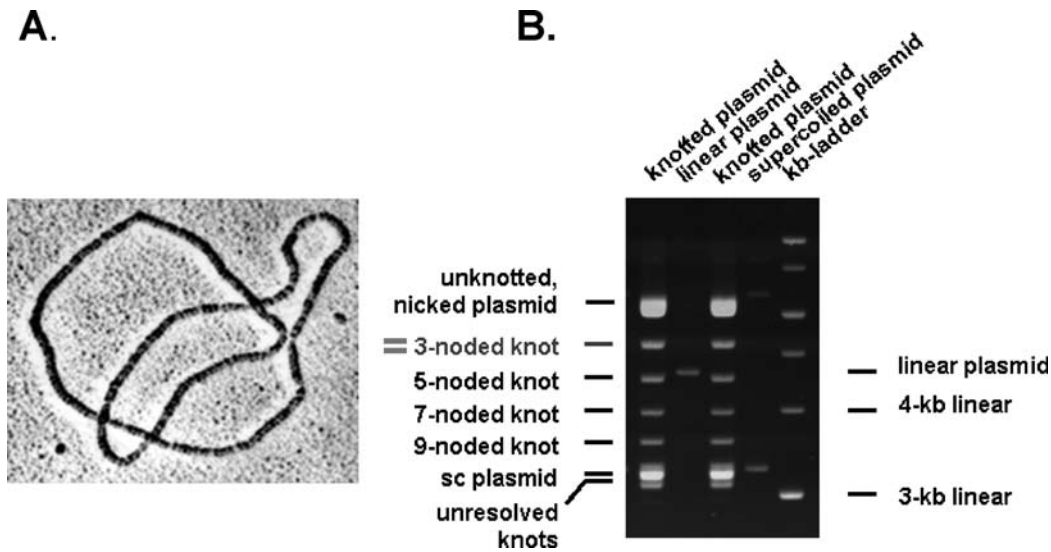

Fig. 2.5. **Physical characterization of knotted DNAs**. **(A)** Electron micrograph of a three-noded DNA knot visualized after coating with *E. coli* RecA protein and rotary shadowing. **(B)** Separation of DNA torus knots by agarose gel electrophoresis. Gel electrophoresis can separate knots (and catenanes) by their minimal crossing numbers, but is otherwise relatively insensitive to knot type. Samples such as in **(A)** are obtained by isolating DNA molecules from specific bands in the gel (Micrograph reproduced with permission from Krasnow et al. (1983) *Nature* 304, 559–560. Copyright 1983 Nature Publishing Group).

Despite the high resolution of gel techniques, the quantitative relationship between knot/catenane mobility and DNA topology remains poorly understood. Thus, additional experiments are generally needed to definitively establish the DNA topology that corresponds to a particular gel band (e.g., the four-noded knot and four-noded torus catenane have similar mobilities). The most reliable (though by no means foolproof) technique for identifying knot topology is electron microscopy of RecA-coated DNA (*see* **Fig. 2.5A**) (19). Although potentially error-prone, it is more typical for bands to be assigned by running samples in parallel with a ladder of known knots or catenanes generated by recombination or topoisomerase activity (2).

2. Materials

2.1. Plasmid DNA

Most of the plasmids used in our laboratory are derived from the pGEM series of cloning vehicles available from Promega, Inc. These pGEM derivatives have a very high copy number, yielding in the range of 4–10 mg of plasmid per liter of culture. The inventory of constructs we have developed for use as substrates

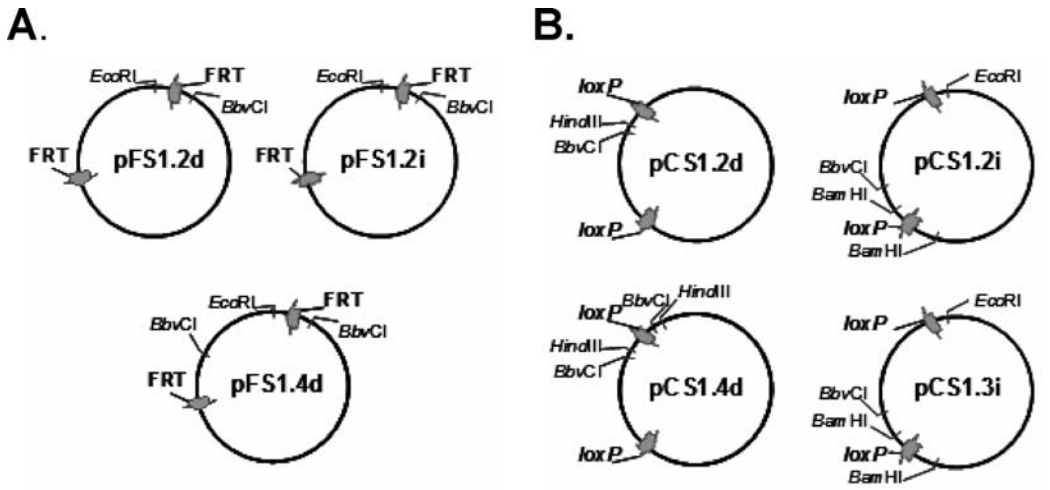

Fig. 2.6. **Plasmid DNAs**. Examples of plasmid DNAs used as Flp-recombination **(A)** and Cre-recombination **(B)** substrates. Plasmids pFS1.2d and pFS1.2i are identical 3759-bp DNAs containing directly and inversely oriented minimal FRT sites, respectively. Plasmid pFS1.4d (3763 bp) is identical to pFS1.2d except for the presence of a second *Bbv*CI recognition site in the small plasmid domain between the FRTs. Plasmid pCS1.4d (3657 bp) is identical to pFS1.2d (3625 bp), except for the presence of a second *Bbv*CI recognition site in the large plasmid domain between the loxP sites. Locations of *Bbv*CI and unique *Eco* RI or *Hind* III sites in both plasmids are as indicated. (Reproduced from Ref. 22.)

in site-specific recombination is too large to describe here, however, maps of several examples are shown in **Fig. 2.6**. Aside from the presence of loxP or FRT sites, the most notable feature is the strategic placement of *Bbv* CI restriction sites, which function as site-specific nicking sites when the plasmid is incubated with either of the mutant enzymes Nt.*Bbv* CI or Nb.*Bbv* CI (20). *Bbv* CI is a heterodimer; in these mutant enzymes, one of the two subunits is present in a catalytically inactive form. Thus, the mutant endonucleases recognize the cleavage site normally, but act on only one of the strands to generate a site-specific nick. The yield of nicked DNA in a digest containing excess nicking enzyme is generally 90–95%, with near-negligible contamination from linear DNA. Therefore, this method is much preferred to more traditional methods relying on limited nicking by DNaseI in the presence of ethidium bromide.

Note that DNA substrates containing direct repeats of recombination-target sites generate unlinked circles or catenanes as recombination products (**Fig. 2.1**). Depending on the information that is needed, site-specific nicking sites can be introduced into the plasmid domains corresponding to either of the product circles. If only one nicking site is present on a direct-repeat substrate, then the product after nicking will be a hemi-nicked catenane, which will complicate the electrophoretic analysis relative to that for a fully nicked catenane.

2.2. Recombination Proteins and Topoisomerases

Proteins can be obtained from a number of different sources, and we have been successful in isolating and purifying many of these proteins in our laboratory according to published procedures (21, 22); however, we have also relied on commercial preparations in some cases. Wheat-germ topoisomerase I, human topoisomerase II, Cre, Nb.*Bbv* CI, and Nt.*Bbv* CI are all available commercially from various suppliers (*see* **Note 1**).

2.3. Solutions (see Note 2)

1. Int-recombination buffer ($+Mg^{2+}$): 20 mM Tris–HCl, 50 mM NaCl, 20 mM KCl, 10 mM $MgCl_2$, pH 7.6.
2. Int-recombination buffer ($-Mg^{2+}$): 10 mM Tris–HCl, 50 mM NaCl, 5 mM spermidine, 1 mM Na_2EDTA, pH 7.5.
3. Flp reaction buffer: 25 mM HEPES, 100 mM NaCl, 1 mM Na_2EDTA, 25% (w/v) ethylene glycol, pH 7.5.
4. Cre reaction buffer: 10 mM Tris–HCl, 50 mM NaCl, 10 mM $MgCl_2$, 1 mM dithiothreitol, pH 7.9.
5. Topoisomerase I buffer: 50 mM Tris–HCl, 50 mM NaCl, 1 mM Na_2EDTA, 1 mM DTT, 0.1 mg/ml bovine serum albumin, pH 7.5.
6. TE buffer: 10 mM Tris–HCl, 1 mM Na_2EDTA, pH 8.0.
7. TBE electrophoresis buffer: 50 mM Tris–borate, 1 mM Na_2EDTA, pH 8.5. The conductivity of each batch of electrophoresis buffer is monitored to ensure reproducibility; typical values are in the range 8.0–9.0 mS/cm.
8. Agarose: 0.7–1.0% agarose gels are prepared from SeaKem® LE agarose in TBE buffer. Small quantities of low-melting agarose, such as SeaPlaque GTG, are used as an adhesive in 2-d gels. Both can be obtained from the Lonza Group, Ltd.
9. Chloroquine phosphate stock solution: 10 mg/ml.
10. Ethidium bromide stock solution: 5 mg/ml.
11. 3 M sodium acetate, pH 5.2.
12. TE-saturated phenol.
13. TE-saturated butanol.
14. Chloroform–isoamyl alcohol (24:1).

3. Methods

3.1. Plasmid Purification

1. Isolate plasmid DNA from *E. coli* strain DH5α by using the alkaline lysis method followed by polyethylene-glycol precipitation (23).

2. Resuspend the DNA pellets in TE buffer and distribute into aliquots containing 100–250 μg DNA.
3. Add 3 volumes of absolute ethanol. (These DNA slurries can be stored in screw-capped microcentrifuge tubes at –20°C until use.)
4. Recover the plasmid DNA from the slurry by pelleting at 15,000*g* for 20 min.
5. Resuspend the pelleted DNA at a concentration of 1 mg/ml in TE buffer.
6. Determine the relative proportion of nicked to superhelical plasmid DNA by electrophoresis in a 0.8% agarose minigel. (If the proportion of nicked DNA is greater than 20%, then the plasmid should be repurified by banding on a 3-ml ethidium bromide CsCl gradient. After extraction of the ethidium bromide with TE/CsCl-saturated butanol, the CsCl should be removed by extensive microdialysis against TE buffer.)

3.2. Preparation of Lk*-Topoisomer Ladders*

1. Resuspend 1–10 μg of plasmid DNA, along with ethidium bromide or chloroquine phosphate from appropriate stock solutions, if required, in topoisomerase I buffer.
2. Add wheat-germ or yeast topoisomerase I at 5–10 U/μg of DNA (*see* **Note 3**).
3. Incubate for 30–60 min at constant temperature (*see* **Note 4**).
4. Add 0.1 volume of 10% SDS.
5. Add 0.1 volume of 3 M sodium acetate, pH 5.2, and extract twice with phenol, once with phenol:chloroform (50:50), and once with chloroform. Extract at least twice with TE-saturated butanol to remove traces of the intercalator.
6. Precipitate the DNA with 3 volumes of absolute ethanol.
7. Analyze the topoisomers using 1-d agarose gel electrophoresis (*see* **Section 3.5** and **Note 5**).

Equilibrium distributions of topoisomers are Gaussian, about an average value of ΔLk determined by the concentration of chloroquine. To generate a quasiuniform distribution of ΔLk values for 2-d gel electrophoresis, individual topoisomer distributions are pooled after 1-d analysis (step 7).

3.3. Preparation of Torus-Knot and Torus-Catenane Ladders by Phage-λ Integrative Recombination

1. Incubate 2 μg of (–) supercoiled DNA, 200 ng of Int, and 240 ng of IHF in 20 μl of Int-reaction buffer at 22°C for 30 min.
2. Quench the reaction by incubating it at 65°C for 5 min.
3. If using $+Mg^{2+}$ conditions, add 5 U of Nb.*Bbv*CI or Nt.*Bbv*CI to the reaction mixture and incubate at 37°C for

1 h. If using $-Mg^{2+}$ conditions, supplement the reaction to 10 mM $MgCl_2$, add 10 U of Nt.*Bbv*CI or Nt.*Bbv*CI and incubate at 37°C for 1 h.

4. Extract twice with phenol, once with chloroform–isoamyl alcohol, and once with chloroform.
5. Recover the DNA by precipitation with 3 volumes of absolute ethanol and resuspend in 20 µl of TE buffer.

3.4. Preparation of Twist-Knot Ladders Using Type-II Topoisomerases (see Note 6)

1. Preincubate 2 µg of plasmid DNA in 20 µl of Int-recombination ($+Mg^{2+}$) buffer at 37°C for 10 min.
2. Add 4.5 µg of T2 topoisomerase and incubate for an additional 15 min at the same temperature.
3. Quench the reaction by heating to 65°C for 10 min.
4. Add 5 U of Nb.*Bbv*CI or Nt.*Bbv*CI to the reaction mixture and incubate at 37°C for 1 h.
5. Extract twice with phenol, once with chloroform–isoamyl alcohol, and once with chloroform.
6. Recover the DNA by precipitation with 3 volumes of absolute ethanol and resuspend in 20 µl of TE buffer.

3.5. One-Dimensional Gel Electrophoresis (see Note 7)

1. Prepare a 0.8% agarose–TBE gel by suspending 0.8 g of low-EEO agarose per 100 ml in TBE buffer. Weigh the agarose plus buffer (including the flask) prior to heating the suspension in a microwave.
2. Heat the suspension to just short of the boiling point (make certain that the suspension does not boil over). Repeat until the agarose dissolves.
3. Place the agarose solution in a 65°C water bath for at least 10 min.
4. Prepare a casting tray and comb. For optimum resolution, use the thinnest possible comb and ensure that the comb clears the tray by at least 1–1.5 mm.
5. Reweigh the flask containing the agarose solution and add back any water driven off during heating. Add ethidium or chloroquine from stock solution, if required, to the agarose prior to casting the gel. Avoid bubbles when pouring the agarose and cover the tray with plastic wrap to minimize dust contamination. Allow the gel to set at room temperature for at least 1 h.
6. Transfer the solidified gel to an electrophoresis tank and fill with TBE buffer to just cover the gel (approximately 1 l). If the gel contains an intercalator, add an identical concentration of the intercalator to the buffer. Load 5–10 µl samples plus a 1 kbp ladder lane.

7. Run the gel at 2–2.5 V/cm for 30–60 min *without* buffer circulation to electrophorese the DNA into the gel. If an intercalating agent is used, stop the electrophoresis and lay a thin glass plate over the gel to secure the gel to the casting tray. Initiate buffer circulation by turning on the magnetic stirrer and resume electrophoresis.
8. Run the gel for 20–24 h, circulating the buffer and shielding the apparatus from light if an intercalator is present.
9. If the gel does not contain an intercalator, continue to step 10. Otherwise, remove the intercalator by soaking the gel twice in 0.5 M NaCl for 1 h with agitation. Pour off the NaCl and soak the gel twice in ddH_2O.
10. Stain the gel with ethidium bromide (0.5 μg/ml in ddH_2O) for 20 min or with SYBR Green/Gold per manufacturer's instructions. Destain the gel with ddH_2O for 20–30 min.

3.6. Two-Dimensional Gel Electrophoresis of Lk *Topoisomers*

1. Prepare a 20-cm-long 0.8% agarose–TBE gel without an intercalating agent according to steps 1–6 described in **Section 3.4**.
2. Apply a minimum of 1.5 μg of pooled topoisomers (*see* **Section 3.2**) to each of two lanes on a 1-d gel. Include at least one empty gel lane between the samples.
3. Run the 1-d gel under the conditions described in **Section 3.4**.
4. Prepare a 20 × 20 cm slab gel without wells.
5. Divide the first-dimension gel along one edge of a lane containing the topoisomers. Stain the gel with ethidium or SYBR dyes as described above and visualize the topoisomer bands with a transilluminator. If the bands are well resolved in the first dimension, excise the parallel to poisomer lane from the unstained portion of the gel and trim to the minimum dimensions of the gel pattern, if desired.
6. Prepare 10–20 ml of low-melting agarose and cool to 50°C in a water bath. Rotating the excised gel lane 90 degrees along its long axis, fix the first-dimension topoisomer lane to one edge of the 20 × 20 cm gel using the low-melting agarose. Cool for at least 30 min, and then transfer the composite gel to an electrophoresis tank.
7. Run the gel at 2–2.5 V/cm with buffer recirculation for 24–48 h in TBE buffer containing chloroquine. Protect the apparatus from light. If running for more than 24 h, replace the buffer at least once during this period.
8. Stain and destain the gel according to steps 9 and 10 in **Section 3.5**.

3.7. Gel Analysis and Quantitation

Quantitation of the DNA should be performed using a cooled CCD camera. We perform routine quantitation using an Alta U32 cooled-CCD camera (2148 × 1472 6.8 μm pixels, Apogee Instruments). The camera operates in 16-bit mode (1:65,536 dynamic range), although the practical dynamic range is between 13 and 14 bits (1:8192–1:16,384). We quantitate individual bands by analyzing the digital image using ImageQuant software (GE Healthcare). For ethidium-stained gels, we use a FirstLight UV transilluminator (UVP), which has highly uniform illumination across the full filter area. For gels stained with SYBR dyes, we visualize the DNA using the Dark Reader visible light transilluminator (Clare Chemical). High-quality interference bandpass filters centered at each dye's emission wavelength (Andover Corp.) are mounted to the CCD camera's objective lens (Schneider Optics).

4. Notes

1. Wheat-germ topoisomerase I is available from Promega, human topoisomerase II from USB Corporation, and Cre, Nb.*Bbv*CI, and Nt.*Bbv*CI from New England Biolabs.
2. All aqueous reagents should be 0.22-μm filtered. Tris buffers should be standardized according to their pH values at 22°C.
3. Topoisomerase I should be assayed periodically to confirm unit activity. The standard unit definition is the amount of enzyme required to relax 1 μg of plasmid in 1 h at 37°C. Use of high-specific activity topoisomerase I preparations is essential to avoid perturbation of the linking-number distribution by inactive enzyme molecules that may bind to DNA.
4. Relaxation with wheat-germ topoisomerase I can be carried out at any temperature from 15°C to approximately 40°C.
5. A common problem is that the topoisomer distributions do not overlap enough to give a quasiuniform distribution of topoisomers when mixed. This is why it is important to analyze the individual equilibrium distributions before pooling the reactions. If there is insufficient overlap, additional reactions containing intermediate concentrations of intercalator should be prepared.
6. This protocol was originally developed using T2 topoisomerase, but should also apply to other type-II enzymes, including those from human cells.

7. Although any horizontal gel electrophoresis apparatus can be used, we prefer the Onephorall electrophoresis units from IBI-Shelton Scientific. These electrophoresis tanks are designed to recirculate buffer with the use of a magnetic stirrer and are therefore well suited for analyzing DNA topology.

Acknowledgment

This work was supported by grants from the NSF-DMS/NIGMS Joint Initiative in Mathematical Biology.

References

1. Stark, W. M. and Boocock, M. R. (1994) The linkage change of a knotting reaction catalysed by Tn3 resolvase. *J Mol Biol* **239**, 25–36.
2. Wasserman, S. A. and Cozzarelli, N. R. (1986) Biochemical topology: applications to DNA recombination and replication. *Science* **232**, 951–960.
3. Cozzarelli, N. R., Krasnow, M. A., Gerrard, S. P. and White, J. H. (1984) A topological treatment of recombination and topoisomerases. *Cold Spring Harb Symp Quant Biol* **49**, 383–400.
4. Scharein, R. G. (1998) Interactive Topological Drawing. Ph.D. dissertation. University of British Columbia, Vancouver, BC.
5. Tsen, H. and Levene, S.D. (2004) Analysis of chemical and enzymatic cleavage frequencies in supercoiled DNA. *J Mol Biol* **336**, 1087–1102.
6. Bauer, W. R., Crick, F. H. and White, J. H. (1980) Supercoiled DNA. *Scientific American* **243**, 100–113.
7. Bowater, R., Aboul-Ela, F. and Lilley, D. M. (1992) Two-dimensional gel electrophoresis of circular DNA topoisomers. *Methods Enzymol* **212**, 105–120.
8. Zimm, B. H. and Levene, S. D. (1992) Problems and prospects in the theory of gel electrophoresis of DNA. *Q Rev Biophys* **25**, 171–204.
9. Zivanovic, Y., Goulet, I. and Prunell, A. (1986) Properties of supercoiled DNA in gel electrophoresis. The V-like dependence of mobility on topological constraint. DNA-matrix interactions. *J Mol Biol* **192**, 645–660.
10. Wang, J. C. (1979) Helical repeat of DNA in solution. *Proc Natl Acad Sci USA* **76**, 200–203.
11. Wang, J. C. (1979) DNA: bihelical structure, supercoiling, and relaxation. *Cold Spring Harb Symp Quant Biol* **43**, Pt 1:29–33.
12. Peck, L. J. and Wang, J. C. (1981) Sequence dependence of the helical repeat of DNA in solution. *Nature* **292**, 375–378.
13. Peck, L. J. and Wang, J. C. (1983) Energetics of B-to-Z transition in DNA. *Proc Natl Acad Sci USA* **80**, 6206–6210.
14. Richardson, S. M., Boles, T. C. and Cozzarelli, N. R. (1988) The helical repeat of underwound DNA in solution. *Nucleic Acids Res* **16**, 6607–6616.
15. Kiianitsa, K. and Stasiak, A. (1997) Helical repeat of DNA in the region of homologous pairing. *Proc Natl Acad Sci USA* **94**, 7837–7840.
16. Zein, S. S. and Levene, S. D. (2005) Structural aspects of RecA-dependent homologous strand exchange involving human telomeric DNA. *Biochemistry* **44**, 4817–4828.
17. Stasiak, A., Katritch, V., Bednar, J., Michoud, D. and Dubochet, J. (1996) Electrophoretic mobility of DNA knots. *Nature* **384**, 122.
18. Trigueros, S., Arsuaga, J., Vazquez, M. E., Sumners, D. W. and Roca, J. (2001) Novel display of knotted DNA molecules by two-dimensional gel electrophoresis. *Nucleic Acids Res* **29**, E67.
19. Zechiedrich, E. L. and Crisona, N. J. (1999) Coating DNA with RecA protein to

distinguish DNA path by electron microscopy. *Methods Mol Biol* **94**, 99–107.

20. Heiter, D. F., Lunnen, K. D. and Wilson, G. G. (2005) Site-specific DNA-nicking mutants of the heterodimeric restriction endonuclease R.BbvCI. *J Mol Biol* **348**, 631–640.
21. Levene, S. D. and Tsen, H. (1999) Analysis of DNA knots and catenanes by agarose-gel electrophoresis. *Methods Mol Biol* **94**, 75–85.
22. Vetcher, A. A., Lushnikov, A. Y., Navarra-Madsen, J., Scharein, R. G., Lyubchenko, Y. L., Darcy, I. K. and Levene, S. D. (2006) DNA topology and geometry in Flp and Cre recombination. *J Mol Biol* **357**, 1089–1104.
23. Sambrook, J., Fritsch, E. F. and Maniatis, T. (1989) Molecular cloning: a laboratory manual. Cold Spring Harbor Laboratory Press, Cold Spring Harbor.

Chapter 3

Two-Dimensional Agarose Gel Electrophoresis of DNA Topoisomers

Joaquim Roca

Abstract

The electrophoretic velocity of a duplex DNA ring is mainly determined by its overall shape. Consequently, DNA topoisomers of opposite supercoiling handedness can have identical gel velocity, and topoisomers highly supercoiled cannot be separated beyond some point. These problems are overcome by two-dimensional agarose gel electrophoresis, which involves two successive electrophoresis steps in one gel slab. The first and second electrophoresis steps are conducted in orthogonal directions with different concentrations of DNA intercalating agents. These compounds alter the overall shape of the DNA and, thereby, change the relative mobility of individual DNA topoisomers.

Key words: DNA supercoiling, DNA linking number, DNA twist, DNA writhe, chloroquine, Z-DNA.

1. Introduction

Identification of different conformers of a double-stranded DNA molecule is not always possible by gel electrophoresis in one dimension. Many linking-number topoisomers of DNA (supercoiled or knotted forms) can have similar velocity during electrophoresis. Moreover, nicked DNA rings and linear DNA molecules can overlap with topoisomers of covalently closed DNA circles. These problems are resolved by two-dimensional (2-D) agarose gel electrophoresis, which involves two successive electrophoresis steps carried out in orthogonal directions in one gel slab.

This chapter focuses on the resolution of supercoiled topoisomers of DNA. For this case, the need for two electrophoretic dimensions becomes acute as the spectrum of linking number to

D.J. Clarke (ed.), *DNA Topoisomerases*, Methods in Molecular Biology 582,
DOI 10.1007/978-1-60761-340-4_3,

be examined becomes broad. Since the electrophoretic mobility of a duplex DNA ring is mainly determined by its overall shape, DNA topoisomers with similar overall dimensions have similar electrophoretic velocities. This problem can be overcome by using compounds (e.g., DNA intercalating agents) that alter the shape of the DNA and, thereby, change the relative mobility of individual topoisomers during the first and second electrophoresis.

Topoisomer separation in two dimensions was first reported by Lee et al. in 1981 (1). In their study of the effects of dehydration on the helical pitch of DNA, positively and negatively supercoiled topoisomers were separated by the presence of a low concentration of ethidium bromide in the electrophoresis buffer for the second dimension. This technique soon became useful in the thermodynamic characterization of the B–Z transition by Peck and Wang (2) and was particularly instrumental in the discovery of the H-form of the DNA by Frank-Kamenetskii and associates (3). Since then, 2-D electrophoresis using intercalating agents had been routinely employed to study supercoiled topoisomers of DNA. Other 2-D techniques exist to resolve other DNA conformers, for example, DNA replication intermediates (4) and knotted DNA molecules (5). Those techniques, which do not involve the use of DNA intercalators, are beyond the scope of this chapter.

1.1. Separation of Supercoiled Topoisomers by 2-D Electrophoresis

The electrophoretic mobility of a DNA ring is determined by its overall dimension. As the molecule becomes supercoiled, it compacts and migrates faster. In mathematical terms, this phenomenon is related to the observation $Wr = 0.73\Delta Lk$ (6), where Wr is the writhe of the DNA (the spatial turns made by the axis of the duplex) and ΔLk is the difference of the duplex linking number from that of the relaxed state. The linking-number difference then results in a change in the writhe, which translates into a difference in the electrophoretic velocity. This principle, however, has two limitations. One is that ΔLk does not make a discernible difference in velocity beyond some point. This happens when a supercoiled DNA ring adopts a tight plectonemic fold, such that the overall shape of the molecule becomes insensitive to the change of Wr. This applies to most bacterial plasmids, which have a typical superhelical density about –0.06 (linking-number deficit of 6%), and to DNA circles isolated from *Saccharomyces cerevisiae* and other eukaryotes, which have a typical superhelical density about –0.05 (linking-number deficit of 5%). Under standard electrophoretic conditions, DNA molecules in such a range of superhelical density have similar gel velocity and individual topoisomers are not resolved. The other limitation is that the electrophoretic velocity cannot reflect the sign of Wr, i.e., the handedness of the DNA coils. The above problems can be overcome by 2-D electrophoresis.

Because of the relation $Wr = Lk - Tw$ (6), the overall shape of a covalently closed DNA ring can be altered by modifying Tw. In the case of negatively supercoiled plasmids, reduction of Tw (untwisting of the duplex) will result in a smaller $|Wr|$, thereby bringing individual topoisomers into a range where their differences in Lk are effectively reflected in differences of electrophoretic velocity. The twist of DNA can be reduced by the addition of intercalator molecules, which insert themselves between stacked base pairs and untwist the duplex. For instance, an intercalated ethidium molecule untwists its neighboring base pairs by 26° (7). The appropriate concentration of an intercalator during electrophoresis will, therefore, tune the gel velocity of supercoiled topoisomers of DNA.

Although intercalators allow most topoisomers of a DNA sample to be resolved in one gel dimension, the distribution of Lk values may be often too wide to be fit in the same sign range of Wr: Topoisomers of both supercoiling handedness may overlap and the order of Lk cannot be determined. By performing a second electrophoresis in an orthogonal direction with a higher concentration of intercalator, those topoisomer populations of similar velocity in the first dimension are separated from each other in the second. As a result, individual topoisomers distribute along an arch similar to that illustrated in **Fig. 3.1.** The apex I topoisomer

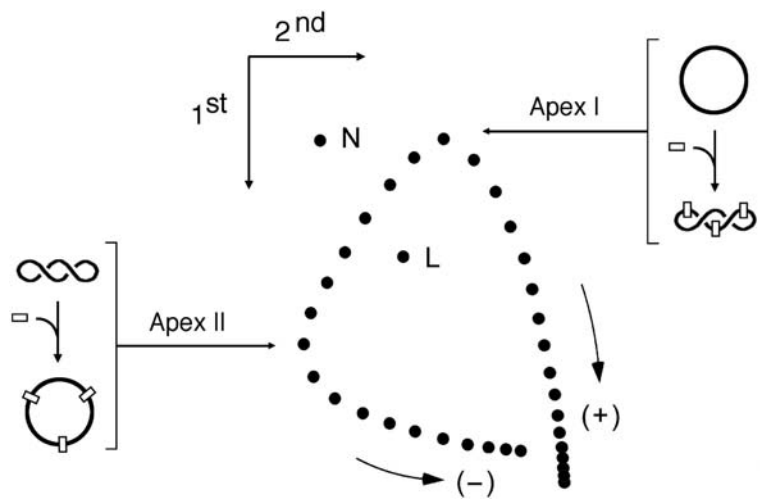

Fig. 3.1. **Separation of supercoiled topoisomers by 2-D gel electrophoresis.** In the scheme, topoisomers, represented by *dots*, were electrophoresed without an intercalator during the first dimension and with an intercalator during the second dimension. Apex I indicates the topoisomer that had the smallest writhe, and hence the smallest velocity, during the first dimension. Binding of intercalator, represented by *open rectangles*, changed the overall dimension of this topoisomer such that it migrated faster in the second dimension. Apex II points to an originally negatively supercoiled topoisomer that became the most slowly migrating species in the second dimension because binding of the intercalator changes its writhe to near zero. N, nicked DNA circles. L, linear DNA.

had about zero writhe during the first electrophoresis and assumed some writhe in the second. The apex II topoisomer had some negative writhe during the first electrophoresis, becoming about zero in the second. Since intercalation has no effect on the writhe of a nicked DNA ring, which is near zero, the nicked circle has low velocity in both gel dimensions and falls out of the topoisomer arch.

While in most biological systems DNA is negatively supercoiled, circular DNA molecules may become positively supercoiled during experimentation (e.g., with topoisomerase mutants). Topoisomers with high-positive writhe can have similar overall shape and, therefore, no discernible difference in electrophoretic velocity beyond some point. In this case, an increase of *Tw* is needed to reduce *Wr* into a range where the differences in *Lk* are reflected by gel velocity. The twist of DNA can be increased to some extent by running the first electrophoresis at low temperature (4°C) and in the presence of divalent metal ions (8).

1.2. DNA Structural Conversion During 2-D Electrophoresis

Some DNA sequences can locally absorb negative superhelical tension by adopting a conformation different from the standard B-form, such as Z-, H-, and cruciform-forms (Ref. 9 and

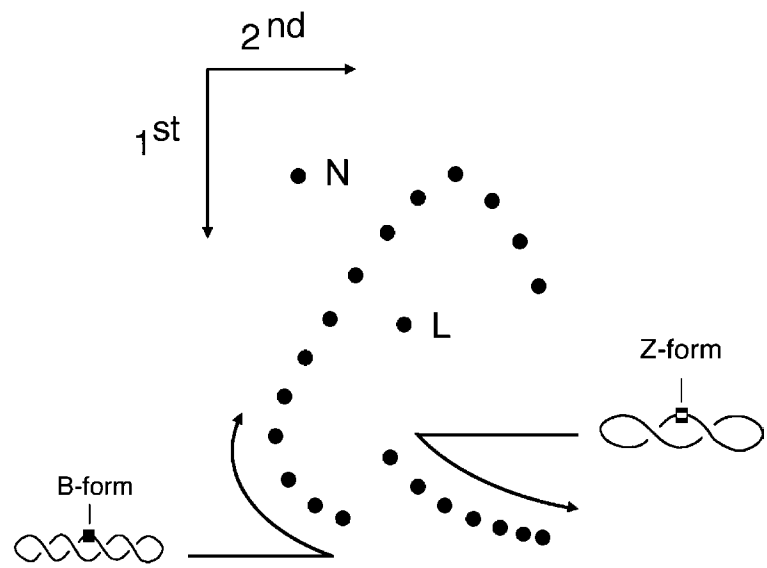

Fig. 3.2. **DNA structural conversions during electrophoresis.** Electrophoretic pattern of a plasmid containing a segment that can flip to the left-handed Z-form. At the threshold level of negative supercoiling tension, the transition to Z-form occurs and reduces the electrophoretic mobility of the DNA topoisomers. Consequently, in the first dimension, topoisomers with the segment in Z-form (all beyond the threshold) overlap topoisomers with the segment in B-form (with tension below the threshold). By the second electrophoresis, these overlapping populations are separated because intercalation reduces negative supercoiling tension and the Z-form segment assumes the B-form.

references therein). Such structural conversions require a threshold-negative superhelical tension to occur. At the threshold, a DNA segment containing such a sequence flips abruptly. Since the conversion reduces *Tw* in such molecules, their electrophoretic mobilities decrease. This transition can be visualized in 2-D electrophoresis as a break of the topoisomer arch similar to that illustrated in **Fig. 3.2**. In the first dimension, a plasmid containing a segment that underwent a B–Z transition presents a discontinuity of velocity between the topoisomers around the threshold tension. During the second dimension, this discontinuity is corrected because the presence of an intercalator reduces negative helical tension and the flipped segment takes on the normal B-form.

2. Materials

2.1. Plasmid DNA

1. *Escherichia coli* plasmid DNA: This can be prepared either by the alkali mini-prep method or commercially available spin-columns have enough quality to be analyzed by 2-D gel electrophoresis.
2. *S. cerevisiae* plasmid DNA: This can be prepared by the procedures described in **Sections 3.1** and **3.2** (*see* **Note 1**).
3. Toluene solution: 20 mM Tris–HCl, pH 8.0, 95% ethanol, 3% toluene, 10 mM EDTA, chilled to –20°C (*see* **Note 2**).
4. TE: 10 mM Tris–HCl, pH 8.0, 1 mM EDTA.
5. RNase A (Sigma): DNase-free RNase A powder. Store at –20°C.
6. Spheroplasting solution: 1 M sorbitol, 100 mM Tris–HCl, pH 8.8, 20 mM EDTA, 0.1% β-mercaptoethanol, 1 mg/ml yeast lytic enzyme (ICN) (*see* **Note 3**).
7. 10% SDS.
8. 5 M potassium acetate.
9. Glass beads 425–600 μm (Sigma).
10. 5 M ammonium acetate.

2.2. DNA Topoisomerase Protein

Type-IB topoisomerases are the most convenient and commonly used to manipulate the linking number of a plasmid. Topoisomerase I from different sources (Vaccinia virus, yeasts, plants, mammals) are commercially available.

2.3. Electrophoresis Apparatus

Any horizontal gel electrophoresis apparatus can be used, provided that the gel can be securely submerged in the running buffer in either orientation. A square glass plate taped at

the edges can be used to cast a gel slab. For good resolution of topoisomers, samples should be loaded into holes of about 2 mm in size. It is convenient to have a specialized set of apparatus if 2-D gel electrophoresis is conducted routinely (*see* **Note 4**). One such set used in our laboratory consists of the following:

1. A 20-cm square gel-casting tray, otherwise regularly shaped. A gel volume of 250 ml on this tray makes the gel slab thick enough to be handled with ease.
2. A tank 35-cm long such that the 20-cm tray fits in.
3. A comb made of 1.5-mm thick acrylic that has 2-mm-wide teeth spaced 8 mm in between.

2.4. Electrophoresis Solutions

1. Electrophoresis buffer (10X TBE): 0.9 M Tris–borate, 20 mM EDTA (*see* **Note 5**).
2. Choloroquine diphosphate stock solution: 10 mg/ml choloroquine diphosphate dissolved in distilled water. Store in the dark at 4°C.
3. Sample loading buffer (5X): 0.25% bromophenol blue, 0.25% xylene cyanole, 30% glycerol.
4. Ethidium bromide stock solution: 10 mg/ml ethidium bromide dissolved in distilled water. Store in the dark at 4°C (*see* **Note 6**).

3. Methods

3.1. Preparation of S. cerevisiae Plasmid DNA from Spheroplasts

1. Pellet approximately 10^8 yeast cells. When the topological state of the DNA needs to be fixed at the time of cell harvesting, 1 volume of cold toluene solution is added to the culture. Fixed cells can be stored in suspension at 4°C or at –20°C and pelleted at the time of plasmid preparation.
2. Wash the cells with TE and resuspend them in 1 ml of spheroplasting solution. Transfer the suspension to a microcentrifuge tube.
3. Incubate at 37°C for 15 min. Gently spin down the spheroplasted cells in a microcentrifuge at 2000*g* for 5 min (*see* **Note 7**). Pipette out and discard the supernatant, which may be cloudy.
4. Resuspend the spheroplasts in 300 µl of TE. Add 30 µl of 10% SDS. Gently mix the suspension to lyse the cells. Allow to stand for 5 min at room temperature.

5. Add 200 µl of 5 M potassium acetate to the lysate and mix well. Spin the mixture in a microcentrifuge at 16,000*g* for 5 min. Transfer the supernatant to a new microcentrifuge tube.
6. Add 1.2 ml of ethanol and mix well. Allow to stand at room temperature or at –20°C for 10 min, and spin at 16,000*g* for 10 min. A white pellet, mostly nucleic acids, should be visible. Carefully discard the liquid and wash the pellet with 70% ethanol.
7. Dissolve the pellet in 100 µl of TE plus 1 mg/ml DNase-free RNaseA. Allow to stand for 20–30 min at room temperature. Precipitate the DNA with 2.5 volumes of absolute ethanol and pellet it by centrifugation at 14,000*g* for 5 min in a microcentrifuge.
8. Dissolve the DNA pellet in 25 µl of TE.

3.2. Preparation of S. cerevisiae Plasmid DNA by Cell Disruption with Glass Beads

1. Pellet approximately 10^8 yeast cells. When the topological state of the DNA needs to be frozen at the time of cell harvesting, an equal volume of cold toluene solution is added to the culture. Fixed cells can be stored in suspension at 4°C or at –20°C and pelleted at the time of plasmid preparation.
2. Resuspend the cells in 0.4 ml of TE solution. Transfer the suspension to a microcentrifuge tube. Add 0.4 ml of glass beads and 0.4 ml of phenol.
3. Shake the mixture by using a Fast Prep® apparatus at the power setting 5 for 10 s at 4°C (*see* **Note 8**).
4. Spin the cell lysate in a microcentrifuge at 16,000*g* for 5 min. Transfer the aqueous phase to a new microcentrifuge tube.
5. Add 100 µl of 5 M ammonium acetate to the lysate and mix. Add 1.2 ml of absolute ethanol and mix. Allow to stand at room temperature or at –20°C for 10 min, and centrifuge at 14,000*g* for 10 min in a microcentrifuge. Carefully discard the liquid, and wash the pellet with 70% ethanol.
6. Dissolve the pellet in 100 µl of TE plus 1 mg/ml DNase-free RNaseA. Allow to stand for 20–30 min at room temperature.
7. Precipitate the DNA with 2.5 volumes of absolute ethanol and centrifuge at 14,000*g* for 10 min in a microcentrifuge.
8. Dissolve the DNA pellet in 25 µl of TE.

3.3. Generation of Topoisomers of Desired Linking Numbers

A distribution of topoisomers with a desired range of linking numbers can be prepared by relaxing the DNA using a type-IB topoisomerase in the presence of ethidium bromide. The right amount of ethidium has to be empirically determined, although the tight binding of the compound to DNA results in an almost

stoichiometric linking-number deficit. A deficit of approximately –1% is attained per 1% (w/w) ethidium bromide added to DNA. Termination of the relaxation reaction by phenol extraction and further extractions with butanol ensure a complete removal of ethidium from DNA. **Fig. 3.3** depicts a 2-D electrophoresis of a plasmid, which was prepared from different sources to obtain different linking-number distributions.

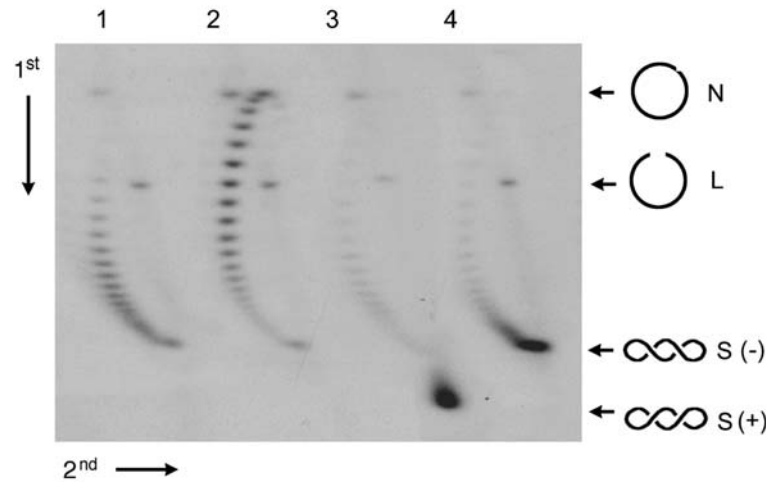

Fig. 3.3. **Two-dimensional gel electrophoresis of a 5-kbp DNA plasmid obtained from different sources.** Lane 1, the plasmid was extracted from *E. coli* by the alkali mini-prep method. Lane 2, the plasmid was extracted from *S. cerevisiae* by cell disruption with glass beads. Lane 3, the plasmid was extracted from *S. cerevisiae* (*dtop1, top2-ts, pGPD:TopA*), in which positive supercoils were accumulated into DNA upon thermal inactivation of topoisomerase II. Lane 4, the plasmid was incubated with 20% ethidium bromide (w/w) and then relaxed with type-IB topoisomerase. Electrophoresis was done in a 0.7% agarose gel slab at room temperature. The first dimension was in TBE containing 0.6 mg/ml chloroquine (1.2 V/cm $\times$ 20 h). The second dimension was in TBE containing 3 mg/ml chloroquine (2 V/cm $\times$ 4 h). N, nicked DNA circles. L, linear DNA. S(+) and S(–), positively and negatively supercoiled circles.

3.4. Electrophoresis

For 2-D agarose gel electrophoresis of supercoiled DNA topoisomers, only regular care, as required for 1-D gels, needs to be taken. If a more rigorous purpose, such as thermodynamic analyses of structure conversion, is sought, then the temperature and the buffer conditions have to be controlled. In such cases, the buffer needs to be circulated between the cathode and the anode chamber.

1. Cast an agarose gel in 0.5X TBE containing the intercalator (*see* **Note 9**). The gel concentration of agarose is chosen according to the size of the DNA of interest, for example, 1% for 3-kbp, 0.8% for 4-kbp, 0.7% for 6-kbp, and 0.6% for 8-kbp rings. The concentration of the intercalator is chosen according to the linking number range of interest. **Table 3.1** should serve as a guideline.

Table 3.1
Guideline conditions for 2-D agarose gel electrophoresis of supercoiled DNA

Superhelical density	First gel dimension	Second gel dimension
–0.04 to + 0.04	TBE+5 mM Mg acetate	TBE
	Run at 4°C	Run at RT
	1.2 V/cm × 40 h	2 V/cm × 4–8 h
–0.06 to + 0.02	TBE	TBE + 2 mg/ml chloroquine
	Run at RT	Run at RT
	1.2 V/cm × 20 h	2 V/cm × 4–8 h
–0.08 to 0	TBE + 0.6 mg/ml chloroquine	TBE + 3 mg/ml chloroquine
	Run at RT	Run at RT
	1.2 V/cm × 20 h	2 V/cm × 4–8 h
–0.12 to –0.02	TBE + 3 mg/ml chloroquine	TBE + 15 mg/ml chloroquine
	Run at RT	Run at RT
	1.2 V/cm × 20 h	2 V/cm × 4–8 h

2. Mix load samples with gel loading solution (*see* **Note 10**).
3. Carry out the first electrophoresis. The field strength should not exceed 1.5 V/cm to attain good resolution. **Table 3.1** should serve as a guideline.
4. Soak the gel in the second electrophoresis buffer with gentle shaking for 1 h.
5. Perform the second electrophoresis. A higher field strength than that for the first dimension can be applied. The electrophoresis time for the second dimension depends on the required resolution of the particular experiment. **Table 3.1** should serve as a guideline.

4. Notes

1. Both spheroplasting and mechanical disruption with glass beads yield comparable amounts of yeast DNA rings, which can be detected by hybridization of a 2-D gel blot after transfer to a membrane. Spheroplasting is preferred to mechanical lysis when contamination with chromosomal

DNA needs to be minimized. Chromosomal DNA fragments can give a strong diagonal signal even with blot hybridization using a specific probe.

2. To avoid precipitation due to low temperature, EDTA is added immediately prior to use.
3. The last two components are to be added immediately before use.
4. The tray, tank, and combs used for 2-D electrophoresis should be washed well to avoid residual intercalator (e.g., chloroquine or ethidium) used in previous experiments.
5. TAE buffers are also appropriate for 2-D agarose gel electrophoresis (10X TAE: 0.4 M Tris–acetate, 10 mM EDTA).
6. To stain an agarose gel, consider fluorescent probes (e.g., SYBR® Green) that are more sensitive and safe than ethidium for detecting nucleic acids.
7. Too strong a centrifugal force will lyse the spheroplasts. This must be avoided at this stage.
8. Other commercially available devices can be used to break yeast cells with glass beads. A standard laboratory vortex fitted with a microfuge tube holder is a cheap option. Care should be taken to avoid overheating the sample. Cell disruption can be examined by phase contrast microscopy. Cells will appear phase-dark or fragmented when disrupted.
9. Agarose can be melted in the intercalator containing buffer. Ethidium and chloroquine are apparently stable under heating by microwave.
10. Any gel-loading solution containing xylene cyanole and/or bromophenol blue can be used to give density to DNA samples. In a 2-D 1% agarose gel, xylene cyanole has roughly the velocity of 3-kbp DNA rings.

References

1. Lee, C.-H., Mizusawa, H. and Kakefuda, T. (1981) Unwinding of double-stranded DNA helix by dehydration. *Proc Natl Acad Sci USA* **78**, 2838–2842.
2. Peck, L. J. and Wang, J. C. (1983) Energetics of B-to-Z transition in DNA. *Proc Natl Acad Sci USA* **80**, 6206–6210.
3. Lyamichev, V. I., Mirkin, S. M. and Frank-Kamenetskii, M. D. (1985) A pH-dependent structural transition in the homopurine-homopyrimidine tract in superhelical DNA. *J Biomol Struct Dyn* **3**, 327–338.
4. Trigueros, S., Arsuaga, J., Vazquez, M. E., Sumners, D. W. and Roca, J. (2001) Novel display of knotted DNA molecules by two-dimensional gel electrophoresis. *Nucleic Acids Res* **29**, 13–e67.
5. Friedman, K. L. and Brewer, B. J. (1995) Analysis of replication intermediates by two-dimensional agarose gel electrophoresis. *Methods Enzymol* **262**, 613–627.
6. Cozzarelli, N. R., Boles, T. C. and White, J. H. (1990) Primer on the topology and geometry of DNA supercoiling. In *DNA Topology and Its Biological Effects*, (eds) Cozzarelli, N. R. and Wang, J. C. (Cold Spring Harbor Laboratory Press, New York), pp. 139–184.

7. Wang, J. C. (1974) The degree of unwinding of the DNA helix by ethidium. I. Titration of twisted PM2 DNA molecules in alkaline cesium chloride density gradient. *J Mol Biol* **89**, 783–801.
8. Salceda, J., Fernández, X. and Roca, J. (2006) Topoisomerase II, not topoisomerase I, is the proficient relaxase of nucleosomal DNA. *EMBO J* **25**, 2575–2583.
9. Frank-Kamenetskii, M. D. (1990) DNA supercoiling and unusual structures. In *DNA Topology and Its Biological Effects*, (eds) Cozzarelli, N. R. and Wang, J. C. (Cold Spring Harbor Laboratory Press, New York), pp. 185–215.

Chapter 4

Cleavage of Plasmid DNA by Eukaryotic Topoisomerase II

Omari J. Bandele and Neil Osheroff

Abstract

Topoisomerase II is an essential enzyme that is required for a number of critical nuclear processes. All of the catalytic functions of topoisomerase II require the enzyme to generate a transient double-stranded break in the backbone of the double helix. To maintain genomic integrity during the cleavage event, topoisomerase II forms covalent bonds between active site tyrosyl residues and the newly generated 5′-DNA termini. In addition to the critical cellular functions of the type II enzyme, several important anticancer drugs kill cells by increasing levels of covalent topoisomerase II–DNA cleavage complexes. Due to the physiological importance of topoisomerase II and its role in cancer chemotherapy, several methods have been developed to monitor the in vitro DNA cleavage activity of the type II enzyme. The plasmid-based system described in this chapter quantifies enzyme-mediated double-stranded DNA cleavage by monitoring the conversion of covalently closed supercoiled DNA to linear molecules. The assay is simple, straightforward, and does not require the use of radiolabeled substrates.

Key words: Topoisomerase II, plasmid DNA, supercoiled DNA, DNA cleavage, agarose gel electrophoresis, topoisomerase II-targeted agents.

1. Introduction

Topoisomerase II is a ubiquitous enzyme that removes knots and tangles from the genetic material and is required for a number of critical nuclear processes (1–3). The enzyme modulates the topological state of DNA by generating transient double-stranded breaks in the backbone of the genetic material (1–3). The points of cleavage on the opposite strands of the double helix are staggered by four bases, such that scission results in 5′-overhanging cohesive ends (1–3). To maintain genomic integrity during the cleavage event, topoisomerase II forms covalent bonds between active site tyrosyl residues (one on each subunit of the

D.J. Clarke (ed.), *DNA Topoisomerases*, Methods in Molecular Biology 582,
DOI 10.1007/978-1-60761-340-4_4,

homodimeric enzyme) and the 5′-terminal phosphates created by scission of the DNA (1–3). These covalent topoisomerase II-cleaved DNA intermediates are known as *cleavage complexes.*

Under normal conditions, topoisomerase II-cleaved DNA complexes are fleeting intermediates in the catalytic cycle of the enzyme and are tolerated by the cell (2, 4, 5). However, conditions that significantly increase the concentration of cleavage complexes generate permanent DNA strand breaks that trigger illegitimate recombination, chromosomal aberrations, sister chromatid exchange, and cell death pathways (2, 5–7).

A variety of important anticancer drugs, such as etoposide and doxorubicin, kill cells by increasing levels of topoisomerase II–DNA cleavage complexes (2, 5, 8). Since the DNA cleavage/ligation equilibrium of topoisomerase II was found to be the primary target for these drugs (9), there has been intense interest in the DNA cleavage activity of the type II enzyme.

All of the essential catalytic functions of topoisomerase II require the enzyme to generate a transient double-stranded break in the backbone of DNA (1–3, 5). Therefore, several methods have been developed to monitor the in vitro DNA cleavage activity of the type II enzyme. They all take advantage of the fact that cleavage complexes can be trapped by rapidly denaturing the complexed enzyme with SDS. The plasmid-based system was first utilized by Sander and Hsieh (10) and Liu et al. (11). The assay described in this chapter is based on the method of Osheroff and Zechiedrich (12). Although the method discussed below has been optimized for human topoisomerase IIα, it can be adapted for virtually any type II topoisomerase.

The plasmid-based assay quantifies enzyme-mediated double-stranded DNA cleavage by monitoring the conversion of covalently closed supercoiled DNA to linear molecules. It also can quantify topoisomerase II-generated single-stranded breaks by monitoring the production of nicked plasmids. The assay is simple, straightforward, and does not require the use of radiolabeled substrates. However, it requires relatively high concentrations of topoisomerase II and is not as sensitive as methods that utilize radiolabeled DNA.

2. Materials

2.1. Assay Components

1. Human topoisomerase IIα (*see* **Note 1**).
2. 5X assay buffer stock: 50 mM Tris–HCl, pH 7.9, 500 mM KCl, 0.5mM Na_2EDTA, 25mM $MgCl_2$, 12.5% glycerol (stored at 4°C) (*see* **Note 2**).

3. Stock solution of 20 mM ATP or a nonhydrolyzable ATP analog such as adenyl-5′-yl imidodiphosphate [APP(NH)P] (optional) (stored at –20°C).
4. Supercoiled plasmid DNA such as pBR322 (*see* **Notes 3** and **4**).
5. Stock solution of 5% (w/v) SDS (stored at room temperature).
6. Stock solution of 250 mM Na_2EDTA (stored at 4°C).
7. Stock solution of 0.8 mg/ml proteinase K in 50 mM Tris–HCl, pH 7.9, 1 mM $CaCl_2$ (stored at 4°C).

2.2. Gel Electrophoresis

1. Agarose gel loading buffer: 10 mM Tris–HCl, pH 7.9, 60% w/v sucrose, 0.5% (w/v) bromophenol blue, 0.5% (w/v) xylene cyanole FF (stored at room temperature).
2. Stock solution of 10 mg/ml ethidium bromide in H_2O (stored in the dark at 4°C).
3. 50X TAE electrophoresis running buffer: 2 M Tris, 5.4% (v/v) glacial acetic acid, 100 mM Na_2EDTA (stored at 4°C).
4. Agarose (SeaKem LE agarose, FMC BioProducts, or equivalent).
5. Agarose gel electrophoresis apparatus.
6. Microwave oven.
7. 50°C water bath.
8. Digital imaging system with medium wave (~300 nm) ultraviolet light box.

3. Methods

1. Prepare samples on ice for 20 µl reactions as follows: Mix 4 µl of 5X assay buffer, 1 µl of ATP or APP(NH)P if desired (*see* **Notes 5** and **6**), supercoiled plasmid DNA to a final concentration of 5–10 nM (this is equivalent to ~20–40 µM base pairs when pBR322 plasmid DNA is used), and H_2O to a final volume that will result in a 20 µl reaction after the addition of topoisomerase II.
2. Initiate the reaction by the addition of topoisomerase IIα to a final concentration of 200 nM (*see* **Note 7**) and incubate the sample at 37°C for 6 min (*see* **Note 8**). Terminate the reaction by the addition of 2 µl of 5% SDS (*see* **Note 9**).
3. Add 1 µl of 250 mM Na_2EDTA followed by 2 µl of 0.8 mg/ml proteinase K, and incubate the samples at 45°C for 30 min to digest topoisomerase IIα.

4. Prepare the agarose gel by making a 1% agarose solution (w/v) in 1X TAE buffer containing 0.5 μg/ml ethidium bromide (*see* **Note 10**). Melt the agarose by heating the solution in a microwave oven (~2 min) and allow to cool to ~50°C in a water bath. Pour the gel and allow it to solidify (this should take 15–30 min).
5. Add 2 μl of agarose gel loading buffer to assay samples and heat at 45°C for 2 min immediately prior to electrophoresis.
6. Load the samples on the agarose gel and resolve reaction products by electrophoresis in 1X TAE buffer at ~5 V/cm for ~3 h (until the bromophenol blue has run approximately to the end of the gel and the xylene cyanole FF has run approximately half as far) (*see* **Note 11**).
7. The gel may be destained in H_2O for 30–60 min, but generally it is not necessary.
8. Visualize DNA reaction products by transillumination with medium wave (~300 nm) ultraviolet light. DNA cleavage products may be quantified by digital imaging based on the fluorescence of DNA-bound ethidium bromide.
9. Topoisomerase II-mediated double-stranded or single-stranded DNA cleavage results in the conversion of covalently closed supercoiled plasmids (form I DNA, FI) to linear (form III, FIII) or nicked (form II, FII) molecules, respectively (**Fig. 4.1**).

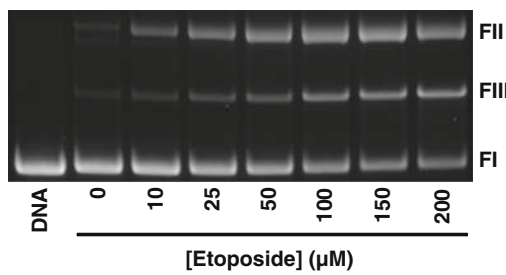

Fig. 4.1. **DNA cleavage mediated by human topoisomerase IIα.** The effects of the anticancer drug etoposide on enzyme-mediated DNA cleavage are shown. Double-stranded DNA cleavage by topoisomerase II converts negatively supercoiled plasmid (form I, FI) to linear DNA (form III, FIII) and single-stranded cleavage converts it to nicked circular DNA (form II, FII).

4. Notes

1. Reaction conditions described have been optimized for human topoisomerase IIα. However, enzyme and DNA concentrations as well as the specific buffer components, reaction

volume, assay temperature, and reaction time can be altered to optimize individual systems. Topoisomerase II from a variety of species can be obtained from commercial sources. However, these enzymes generally are diluted for use in DNA relaxation/catenation/decatenation assays and are sold as activity "units." Consequently, commercial enzymes are often too dilute (or prohibitively expensive) to use routinely for DNA cleavage assays. If an extensive number of DNA cleavage assays are required, it is recommended that the type II enzyme be prepared "in house." Systems for the overexpression and purification of recombinant human topoisomerase IIα and β, as well as yeast, *Drosophila*, and *Chlorella* virus topoisomerase II have been described (13–16).

2. In addition to Mg^{2+}, the divalent cation requirement of topoisomerase IIα may be fulfilled in DNA cleavage assays by Ca^{2+}, Co^{2+}, or Mn^{2+} (12, 17). Although these alternative divalent metal ions do not support the ATPase activity of the enzyme, and hence the DNA strand passage activity of topoisomerase II (12, 17, 18), they promote higher levels of pre-strand passage DNA cleavage (*see* **Note 5**) than Mg^{2+} and do not significantly alter the site specificity of the type II enzyme.
3. Negatively supercoiled plasmid DNA can be prepared from bacteria by a number of protocols. The Plasmid Mega Kit by Qiagen routinely works well.
4. The affinity of topoisomerase II for its DNA substrate varies with sequence (19). Therefore, the cleavage activity of the enzyme may depend on the plasmid utilized. Levels of cleavage also depend on the topological state of the plasmid, with negatively supercoiled substrates being preferred over positively supercoiled, relaxed, nicked, or linear molecules (20, 21).
5. Topoisomerase II establishes two distinct DNA cleavage/ligation equilibria: one prior to its double-stranded DNA passage event (which corresponds to the ATP-free form of the enzyme) and another following its DNA passage event (which corresponds to the ATP-bound form) (1–3, 22). Hence, assays carried out in the absence of a nucleotide triphosphate monitor pre-strand passage DNA cleavage, those in the presence of a nonhydrolyzable ATP analog monitor post-strand passage DNA cleavage, and those in the presence of ATP monitor a mixture of the two. Levels of DNA cleavage observed following strand passage generally are higher than those observed prior to strand passage (22).
6. Due to the high concentration of topoisomerase II employed in cleavage assays, DNA catentation may be observed in the presence of ATP or nonhydrolyzable ATP

analogs (23). If uncleaved (i.e., nonlinear) plasmid molecules become part of catenated networks, they remain at the origin in agarose gels (23).

7. The DNA cleavage/ligation equilibrium of topoisomerase II greatly favors the ligation event. Therefore, at any given time, only a small proportion (<1%) of the topoisomerase II–DNA complex exists with DNA in the cleaved state. Consequently, to visualize DNA cleavage products, the topoisomerase II:plasmid ratio is generally in excess of 10:1.
8. In the absence of cleavage-enhancing drugs, topoisomerase II establishes its DNA cleavage/ligation equilibrium rapidly (within 5–10 s) (24). In contrast, equilibrium is often reached more slowly in the presence of drugs (several minutes may be required to reach maximal levels of cleavage) (24).
9. It is critical to terminate DNA cleavage reactions with SDS prior to the addition of EDTA, as chelation of the Mg^{2+} in the assay buffer inhibits topoisomerase II-mediated DNA scission and leads to the rapid loss of cleavage complexes (10, 12). The ability of SDS to trap cleavage complexes diminishes considerably when the final concentration of the detergent drops below ~0.5%.
10. The inclusion of ethidium bromide in the gel and running buffer alters the electrophoretic mobility of all covalently closed plasmid molecules and causes them to comigrate with the supercoiled band. Since the relative electrophoretic mobilities of nicked and linear DNA molecules (in TAE buffer) are not affected by the presence of ethidium bromide, the presence of the intercalating dye ensures that cleaved DNA bands are separated from any relaxed plasmid topoisomers (generated in the presence of ATP or nonhydrolyzable ATP analogs). If a nucleotide triphosphate is not included in assays, gels can be stained with ethidium bromide following electrophoresis. In this case, the gel can be stained in 1 μg/ml ethidium bromide (in H_2O or 1X TAE buffer) for ~30 min with continuous agitation.
11. The mobility of linear DNA molecules in agarose gels changes relative to those of nicked and supercoiled circular plasmids depending on the running buffer that is used. In TAE buffer, linear pBR322 molecules migrate intermediate to nicked and supercoiled DNA (supercoiled molecules have the fastest electrophoretic mobility; *see* **Fig. 4.1**). However, in TBE (Tris–borate–EDTA) buffers, the mobility of linear DNA is often greater than that of supercoiled plasmid. The optimal concentration of agarose and the running buffer may have to be determined if plasmids other than pBR322 are employed.

12. Since topoisomerase II-mediated DNA cleavage is the target reaction for a number of important chemotherapeutic agents, the plasmid-based assay represents a straightforward technique for analyzing the effects of drugs on the enzyme. An example of such a drug-induced DNA cleavage titration is shown in **Fig. 4.1**.
13. While most topoisomerase II-targeted drugs interact with the enzyme in a noncovalent manner (2, 5, 25), compounds such as 1,4-benzoquinone (a major metabolite of benzene) and (–)-epigallocatechin gallate (EGCG; the most abundant and biologically active polyphenol in green tea) require redox cycling and interact covalently with topoisomerase II (5, 26, 27). The most straightforward method for distinguishing between "traditional" enzyme-targeted agents and "redox-dependent" agents is to incubate the compound with a reducing agent such as dithiothreitol (DTT) prior to its addition to DNA cleavage assay mixtures. The activity of redox-dependent agents will be greatly diminished following exposure to the reducing agent (*see* **Fig. 4.2**).

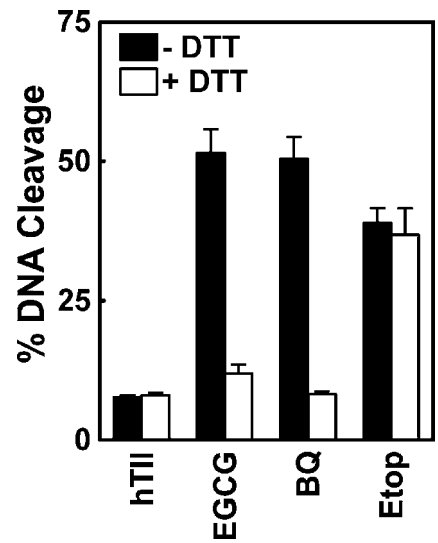

Fig. 4.2. **Effects of a reducing agent (DTT) on the ability of traditional and redox-dependent topoisomerase II-targeted agents to enhance DNA cleavage mediated by human topoisomerase IIα.** EGCG (500 μM), 1,4-benzoquinone (BQ) (25 μM), or etoposide (Etop) (50 μM) was incubated without DTT (–DTT; *closed bars*) or with 1 mM DTT (+DTT; *open bars*) prior to its addition to topoisomerase IIα–DNA complexes. Control reactions contained DNA and enzyme in the absence of compounds (hTII). *Error bars* represent standard deviations for three independent experiments.

14. Dimethyl sulfoxide, which is used often as a solvent for drugs, alters the DNA cleavage/ligation equilibrium of topoisomerase II and tends to increase the levels of cleavage. Therefore, care must be taken to minimize the final concentration of dimethyl sulfoxide in reaction mixtures.

Acknowledgments

This protocol was developed in part under the auspices of Grant GM33944 from the National Institutes of Health. O.J.B. was a trainee under grant 5 T32 CA09582 from the National Institutes of Health and was supported in part by Ruth L. Kirschstein National Research Service Award Predoctoral Fellowship F31 GM78744 from the National Institutes of Health. We are grateful to Amanda C. Gentry for critical reading of the manuscript.

References

1. Wang, J.C. (1996) DNA Topoisomerases. *Annu Rev Biochem* **65**, 635–692.
2. Fortune, J.M. and Osheroff, N. (2000) Topoisomerase II as a target for anticancer drugs: When enzymes stop being nice. *Prog Nucleic Acid Res Mol Biol* **64**, 221–253.
3. Champoux, J.J. (2001) DNA topoisomerases: Structure, function, and mechanism. *Annu Rev Biochem* **70**, 369–413.
4. Wang, J.C. (2002) Cellular roles of DNA topoisomerases: A molecular perspective. *Nat Rev Mol Cell Biol* **3**, 430–440.
5. McClendon, A.K. and Osheroff, N. (2007) DNA topoisomerase II, genotoxicity, and cancer. *Mutat Res* **623**, 83–97.
6. Baguley, B.C. and Ferguson, L.R. (1998) Mutagenic properties of topoisomerase-targeted drugs. *Biochim Biophys Acta* **1400**, 213–222.
7. Kaufmann, S.H. (1998) Cell death induced by topoisomerase-targeted drugs: More questions than answers. *Biochim Biophys Acta* **1400**, 195–211.
8. Walker, J.V. and Nitiss, J.L. (2002) DNA topoisomerase II as a target for cancer chemotherapy. *Cancer Invest* **20**, 570–589.
9. Nelson, E.M., Tewey, K.M. and Liu, L.F. (1984) Mechanism of antitumor drug action: Poisoning of mammalian DNA topoisomerase II on DNA by 4′-(9-acridinylamino)-methanesulfon-*m*-anisidide. *Proc Natl Acad Sci USA* **81**, 1361–1365.
10. Sander, M. and Hsieh, T. (1983) Double strand DNA cleavage by type II DNA topoisomerase from *Drosophila melanogaster*. *J Biol Chem* **258**, 8421–8428.
11. Liu, L.F., Rowe, T.C., Yang, L., Tewey, K.M. and Chen, G.L. (1983) Cleavage of DNA by mammalian DNA topoisomerase II. *J Biol Chem* **258**, 15365–15370.
12. Osheroff, N. and Zechiedrich, E.L. (1987) Calcium-promoted DNA cleavage by eukaryotic topoisomerase II: Trapping the covalent enzyme-DNA complex in an active form. *Biochemistry* **26**, 4303–4309.
13. Worland, S.T. and Wang, J.C. (1989) Inducible overexpression, purification, and active site mapping of DNA topoisomerase II from the yeast *Saccharomyces cerevisiae*. *J Biol Chem* **264**, 4412–4416.
14. Kingma, P.S., Greider, C.A. and Osheroff, N. (1997) Spontaneous DNA lesions poison human topoisomerase IIα and stimulate cleavage proximal to leukemic 11q23 chromosomal breakpoints. *Biochemistry* **36**, 5934–5939.
15. Hu, T., Chang, S. and Hsieh, T. (1998) Identifying Lys359 as a critical residue for the ATP-dependent reactions of *Drosophila* DNA topoisomerase II. *J Biol Chem* **273**, 9586–9592.
16. Lavrukhin, O.V., Fortune, J.M., Wood, T.G., Burbank, D.E., Van Etten, J.L., Osheroff, N. and Lloyd, R.S. (2000)

Topoisomerase II from *Chlorella* virus PBCV-1. Characterization of the smallest known type II topoisomerase. *J Biol Chem* **275**, 6915–6921.

17. Baldwin, E.L., Byl, J.A. and Osheroff, N. (2004) Cobalt enhances DNA cleavage mediated by human topoisomerase IIα in vitro and in cultured cells. *Biochemistry* **43**, 728–735.
18. Osheroff, N. (1987) Role of the divalent cation in topoisomerase II mediated reactions. *Biochemistry* **26**, 6402–6406.
19. Osheroff, N., Shelton, E.R. and Brutlag, D.L. (1983) DNA topoisomerase II from *Drosophila melanogaster*. Relaxation of supercoiled DNA. *J Biol Chem* **258**, 9536–9543.
20. Zechiedrich, E.L. and Osheroff, N. (1990) Eukaryotic topoisomerases recognize nucleic acid topology by preferentially interacting with DNA crossovers. *EMBO J* **9**, 4555–4562.
21. McClendon, A.K. and Osheroff, N. (2006) The geometry of DNA supercoils modulates topoisomerase-mediated DNA cleavage and enzyme response to anticancer drugs. *Biochemistry* **45**, 3040–3050.
22. Osheroff, N. (1986) Eukaryotic topoisomerase II. Characterization of enzyme turnover. *J Biol Chem* **261**, 9944–9950.
23. Corbett, A.H., Zechiedrich, E.L., Lloyd, R.S. and Osheroff, N. (1991) Inhibition of eukaryotic topoisomerase II by ultraviolet-induced cyclobutane pyrimidine dimers. *J Biol Chem* **266**, 19666–19671.
24. Froelich-Ammon, S.J., Burden, D.A., Patchan, M.W., Elsea, S.H., Thompson, R.B. and Osheroff, N. (1995) Increased drug affinity as the mechanistic basis for drug hypersensitivity of a mutant type II topoisomerase. *J Biol Chem* **270**, 28018–28021.
25. Pommier, Y. and Marchand, C. (2005) Interfacial inhibitors of protein-nucleic acid interactions. *Curr Med Chem Anticancer Agents* **5**, 421–429.
26. Lindsey, R.H., Jr., Bromberg, K.D., Felix, C.A. and Osheroff, N. (2004) 1,4-Benzoquinone is a topoisomerase II poison. *Biochemistry* **43**, 7563–7574.
27. Bandele, O.J. and Osheroff, N. (2008) (–)-Epigallocatechin gallate, a major constituent of green tea, poisons human type II topoisomerases. *Chem Res Toxicol* **21**, 936–943.

Chapter 5

Assays for the Preferential Binding of Human Topoisomerase I to Supercoiled DNA

Zheng Yang and James J. Champoux

Abstract

To assay the preferential binding of eukaryotic type IB topoisomerases to supercoiled DNA, two methods are described that make use of a catalytically inactive mutant form of the enzyme. In the gel shift assay, the preference for binding to supercoiled plasmid DNA is detected in the presence of linear and nicked forms of the same DNA by a reduction in the mobility of the supercoiled plasmid during electrophoresis in agarose. The more quantitative filter binding assay compares the ability of nicked and supercoiled forms of the circular DNA to compete for the binding of a ^{3}H-labeled nicked DNA to the topoisomerase where the enzyme–DNA complexes are quantitated by the retention of the labeled DNA on a nitrocellulose membrane.

Key words: Topoisomerases, supercoiled DNA, plasmid DNA, nicked DNA, gel shift assay, filter binding assay, nitrocellulose filters.

1. Introduction

Type I DNA topoisomerases release the torsional strain that builds up in DNA during essential biological processes such as DNA replication and transcription by introducing a transient single-strand break into the DNA [for review, *see* (1)]. During the lifetime of the break, the enzyme is covalently attached to one end of the DNA through a phosphodiester bond to a tyrosine side chain. The type I topoisomerases are further classified into two subfamilies based on the polarity of the covalent linkage. For the type IA subfamily, the linkage is to the 5′ end of the DNA at the site of the break; this subfamily includes the prototypical bacterial topoisomerase I. The eukaryotic topoisomerases I belong to the

D.J. Clarke (ed.), *DNA Topoisomerases*, Methods in Molecular Biology 582,
DOI 10.1007/978-1-60761-340-4_5,

type IB subfamily since the linkage in this case is to the 3′ end of the DNA. In the nicked state for the type IB enzymes, supercoils are relaxed by rotation of the free 5′ end of the broken strand around the intact strand of the DNA (2). The eukaryotic type I topoisomerases are able to relax both negative and positive supercoils.

Human topoisomerase I has been shown to preferentially bind supercoiled DNA over relaxed DNA (3–5), providing a likely explanation for how the enzyme is targeted to torsionally strained regions of the chromosomal DNA in the cell. An early method for detecting this preferential binding relied on measuring the amount of nicked topoisomerase I–DNA covalent complex formed after incubation of supercoiled or relaxed plasmid DNAs with the topoisomerase (3), but this method is complicated by the relaxation of the supercoiled DNA during the course of the analysis. A second method that suffers from the same weakness and is also laborious involves electron microscopic visualization of enzyme bound to DNA nodes in supercoiled DNA (4). Here, we describe in detail two methods for measuring the preferential binding of topoisomerase I to supercoiled DNAs that circumvent the problem of DNA relaxation during the assay by utilizing a mutant form of the enzyme in which the active site tyrosine in the human topoisomerase I has been replaced with phenylalanine (Y723F mutation herein referred to as Y/F). In the gel shift assay, topoisomerase I binding to the DNAs in an equimolar mixture of supercoiled circles, nicked circles, and linear molecules with increasing protein concentration is detected by a reduction in the mobility of the DNA during electrophoresis in agarose (**Fig. 5.1**). A similar assay has been described for the preferential binding of the p53 protein and HMG proteins to supercoiled DNA (6–10). The

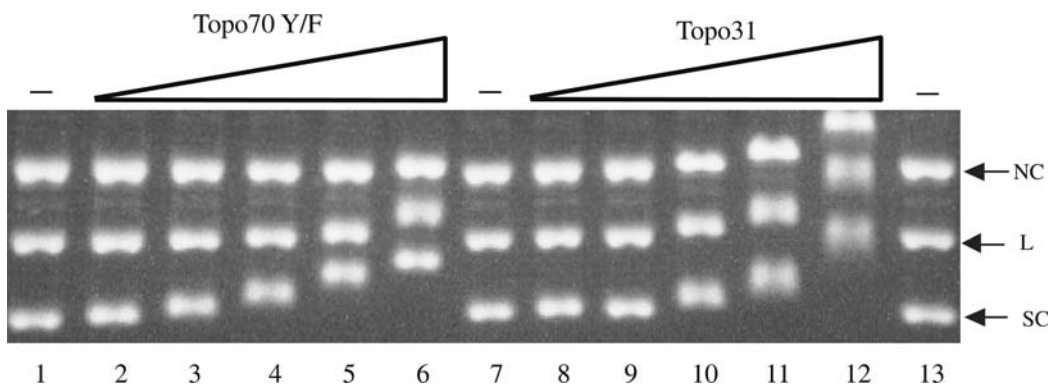

Fig. 5.1. **Gel shift assay with topo70 Y/F and topo31**. Equal amounts of supercoiled circles (SC), linears (L), and nicked circles (NC) of pKSII+ plasmid DNA (0.08 pmol each) were incubated with increasing amounts of the indicated proteins in 20 μl of DNA binding buffer and analyzed by agarose gel electrophoresis as described in the text. Lanes 1, 7, and 13 contained no protein to mark the mobilities of the unbound DNAs. Lanes 2–6 contained 0.88, 1.75, 3.5, 7, and 15 pmol of topo70 Y/F protein, respectively. Lanes 8–12 contained 1.75, 3.5, 7, 15, and 30 pmol of topo31, respectively.

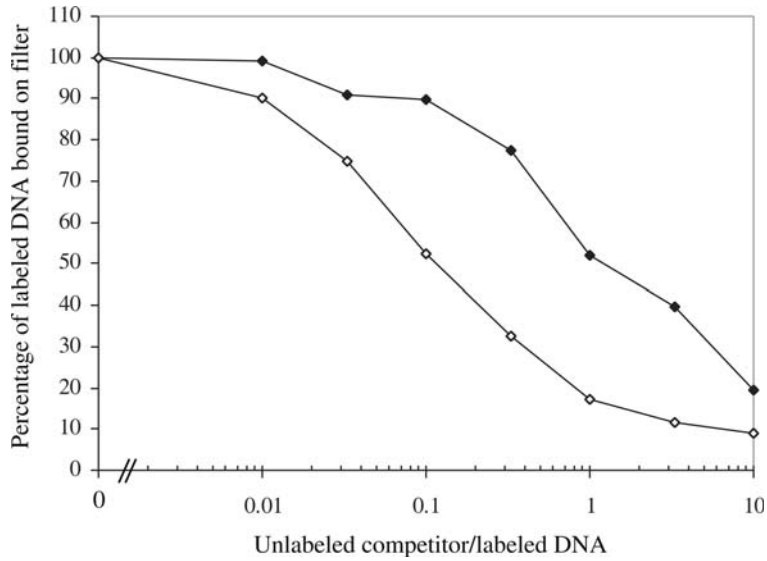

Fig. 5.2. **Filter binding assay**. ^{3}H-labeled nicked SV40 DNA (80 fmol) was incubated with topo70 Y/F and then challenged with increasing amounts of unlabeled nicked competitor (*filled diamonds*) or unlabeled supercoiled competitor (*open diamonds*) as described in the text. The percentage of ^{3}H-labeled nicked SV40 DNA retained on the filter is plotted against the ratio of the unlabeled competitor to labeled DNA.

second more quantitative filter binding assay measures DNA binding by capturing labeled DNA–topoisomerase I complexes on a nitrocellulose filter (**Fig. 5.2**) (11). The relative ability of unlabeled competitor DNAs (supercoiled versus nicked) to reduce the binding of a labeled nicked DNA to the enzyme as measured by retention of the radioactive label on the filter provides a direct measure of the preference for supercoiled DNA.

2. Materials

2.1. Topoisomerase I Protein

1. Topo70 Y/F protein: An N-terminally truncated (topo70, missing amino acids 1–174) and catalytically inactive Y/F mutant form of human topoisomerase I. This can be purified from recombinant baculovirus-infected insect SF9 cells, as has been described (12) (*see* **Note 1**).
2. Topo31: A fragment containing residues 175–433 of human topoisomerase I. This can be purified as described elsewhere (13).

2.2. Gel Shift Assay

1. Restriction endonucleases (New England Biolabs): *EcoR* I (20 units/μl) and *BamH* I (20 units/μl).

2. The pKSII+plasmid DNA (Stratagene) (*see* **Note 2**).
3. 10X TBE: 0.89 M Tris–borate, 20 mM EDTA, pH 8.0.
4. TE: 10 mM Tris–HCl, pH 7.5, 1 mM EDTA.
5. 3X agarose gel loading buffer: 30 mM EDTA, 1.5% SDS, 15% Ficol-400, 0.03% bromophenol blue.
6. 10X DNA binding buffer: 100 mM Tris–HCl, pH 7.5, 500 mM KCl, 10 mM EDTA, and 10 mM DTT.
7. *EcoR* I reaction buffer (New England Biolabs): 50 mM NaCl, 100 mM Tris–HCl, pH 7.5, 10 mM $MgCl_2$, 0.025% Triton X-100.
8. *BamH* I reaction buffer (New England Biolabs): 150 mM NaCl, 10 mM Tris–HCl, pH 7.9, 10 mM $MgCl_2$, 1 mM DTT, 100 μg/ml BSA.

2.3. Filter Binding Assay

1. Unlabeled and ^{3}H-labeled (2–4 $\times$ 10^4 cpm/μg) supercoiled SV40 DNAs: These can be isolated from SV40-infected-CV-1 cells using the Hirt procedure (14) and purified by CsCl–ethidium bromide equilibrium centrifugation (5) (*see* **Note 3**).
2. Nitrocellulose filters of 13 mm (mixed cellulose ester): These should have a 0.45-μm pore size and can be purchased from Advantec MFS Inc., Dublin, CA.
3. Suction filter apparatus: This needs to accommodate the 13-mm filters, and the vacuum must be adjusted to achieve a filtration rate of 3–4 ml/min (*see* **Note 4**).
4. Toluene/Ominifluor (4 g/l) scintillation fluid.

3. Methods

3.1. Preparation of Nicked Circular DNA for Both Assays

The nicked DNA is prepared from the supercoiled DNA (pKSII+ plasmid DNA for the gel shift assay and ^{3}H-labeled SV40 DNA for the filter binding assay), as described by Shortle et al. (15), as follows:

1. Digest 500 μg of supercoiled SV40 DNA or pKSII+ DNA with 200 units of *EcoR* I (*see* **Note 5**) in 0.5 ml *EcoR* I reaction buffer in the presence of ethidium bromide (15 μg/ml) for 5 h at 37°C.
2. Extract the sample with an equal volume of phenol–chloroform and precipitate the DNA with an equal volume of isopropanol.
3. Centrifuge the sample at 16,000*g* for 15 min and wash the pellet with ice-cold 70% ethanol.

4. Resuspend the DNA in TE buffer and determine the DNA concentration from the absorbance at 260 nm.
5. Add a one-half volume of 3X agarose gel loading buffer to a small sample of the DNA (~0.6 μg) and subject the sample to electrophoresis in a 1% agarose gel in 1X TBE buffer to verify that the conversion to nicked circles was complete without any substantial production of linear molecules (*see* **Note 6**).

3.2. Gel Shift Assay

The gel shift assay for DNA binding by topoisomerase I depends on the observation that bound protein will reduce the mobility of a DNA during gel electrophoresis. Under the conditions described below, when the catalytically inactive form of human topoisomerase I (topo70 Y/F) is combined with a mixture of supercoiled, linear, and nicked circular DNAs, any selectivity of the protein for one or more of the topological forms of the DNA will result in a preferential reduction in the mobility of that DNA in the gel. This gel shift procedure provides the basis for a semiquantitative assay to detect the preferential binding of human topoisomerase I to supercoiled DNA.

3.2.1. Preparation of Linear Plasmid DNA

1. Digest 500 μg of pKSII+ DNA with 200 units of *BamH* I in *BamH* I buffer for 1 h at 37°C.
2. Purify and characterize the linearized DNA as described in steps 2–5 of **Section 3.1**.

3.2.2. Sample Preparation

1. Prepare a master mix containing equimolar concentrations of supercoiled, nicked, and linear pKSII+ DNAs in 1X DNA binding buffer in which the concentration of each DNA is 8 fmol/μl.
2. Prepare two-fold serial dilutions of topo70 Y/F (or other protein of interest) in 1X DNA binding buffer where the amount of protein typically ranges from 1.5 to 0.088 pmol/μl, and 10 μl aliquots of each dilution are added into a reaction tube on ice.
3. Initiate the reaction by mixing 10 μl of the DNA substrate mix with the serially diluted samples of topo70 Y/F and incubate at room temperature for 20 min.

3.2.3. Agarose Gel Electrophoresis

1. Add 5 μl of 50% glycerol to the reaction and load the sample onto a 1% agarose gel cast in 0.5X TBE. Include control samples containing no protein to mark the mobilities of the three DNA forms.
2. Run the gel in 0.5X TBE at 1.2 V/cm at 4°C for 20 h.
3. Stain the gel in 0.15 μg/ml ethidium bromide for 30 min and visualize the DNA bands photographically.

A typical analysis is shown in **Fig. 5.1** comparing the binding properties of topo70 Y/F with topo31, which is a C-terminally truncated form of topo70 that displays no preference for supercoils (Z. Yang and J. J. Champoux, unpublished). As can be seen in lanes 2–4 of **Fig. 5.1**, the binding of topo 70 at the lower protein concentrations retards the mobility of the supercoiled DNA (SC) without noticeably affecting the mobility of either the linears (L) or the nicked circles (NC). With higher protein concentrations, the mobilities of all three forms of the DNA are affected. This observation is in sharp contrast to the results with topo31, where the protein binds and shifts the mobility of all three forms of the DNA equally at all ratios of protein to DNA (**Fig. 5.1**, lanes 10–12, note that higher protein concentrations were required for topo31, owing to its lower affinity for DNA).

3.3. Filter Binding Assay

In the filter binding assay, ^{3}H-labeled nicked DNA is first incubated with the catalytically inactive form of human topoisomerase I (topo70 Y/F) (or mutant forms of the protein), followed by the addition of an unlabeled competitor DNA (either nicked or supercoiled). After an additional incubation, the fraction of labeled DNA containing bound protein is assessed by collecting the complexes on a nitrocellulose membrane. By varying the molar ratios of the unlabeled competitors to the labeled DNA, competition profiles are generated that permit one to compare the binding properties of the supercoiled and nicked DNAs for the protein of interest.

3.3.1. Sample Preparation

1. Incubate ^{3}H-labeled nicked SV40 DNA (80 fmol per reaction) with 320 fmol of topo70 Y/F in 10 µl of 1X DNA binding buffer at room temperature for 20 min.
2. Prepare a series of 10 µl samples containing the following amounts of the unlabeled nicked DNA in 1X DNA binding buffer to serve as the "like" competitor: 800, 240, 80, 24, 8, 2.4, and 0.8 fmol. These amounts cover the range from 10 times to 0.01 times the amount of labeled nicked DNA in the reactions. Likewise, prepare a series of 10 µl samples containing the same amounts of the supercoiled competitor DNA.
3. Initiate the competition reactions by mixing the 10 µl samples containing the unlabeled competitor DNAs with the 10 µl reactions that contain the ^{3}H-labeled nicked SV40 DNA with bound topo 70 Y/F, and incubate the reactions at 23°C for 30 min.

3.3.2. Filtration and Determination of Bound Radioactivity

1. During the incubation, soak the 13-mm, 0.45-µm pore size nitrocellulose membranes in distilled water (*see* **Note 7**).

2. After the incubation, position a prewetted 13-mm nitrocellulose filter on a suction apparatus set for a filtration rate of 3–4 ml/min, and apply the 20 µl reaction directly to the filter.
3. Immediately wash the filter with 0.8 ml of 1X DNA binding buffer (*see* **Note 8**).
4. Air dry the filters and count the samples in 5 ml of toluene/Ominifluor (4 g/l) scintillation fluid (*see* **Note 9**) in a scintillation counter.

A typical experiment is shown in **Fig. 5.2** where the percentage of labeled DNA bound on the filter is plotted as a function of the ratio of unlabeled competitor to labeled DNA. With the "like" nicked competitor, half-maximal binding of the labeled DNA occurs at a ratio of 1.0 as expected (*closed symbols*). However, with the unlabeled supercoiled competitor, it can be seen that approximately 10-fold less competitor DNA is required to compete the labeled DNA to the level of half-maximal binding (*open symbols*). We have previously suggested that this difference reflects the existence of ~10 times more binding sites for the enzyme on supercoiled DNA as compared with nicked or relaxed DNA (5).

4. Notes

1. Although we describe the methods and show data for the N-terminally truncated form of human topoisomerase I (topo70), similar results are obtained for the full-length protein.
2. Any circular plasmid DNA in the size range from 2.5 to 3.5 kb is suitable for the analysis. However, since the magnitude of the gel shift is inversely related to the size of the DNA, it is recommended that larger plasmids not be used. The plasmid DNA should be purified from *Escherichia coli* using the Qiagen plasmid purification kit (Qiagen Corp.). The purified DNA must be free of contaminating protein and needs to be primarily composed of negatively supercoiled DNA molecules with nicked circles representing no more than 20% of the total DNA.
3. We find it convenient to prepare ^{3}H-labeled SV40 DNA as described, but the nature and source of the supercoiled circular DNA are not important as long as the specific activity is at least 2×10^{4} cpm/µg.
4. A suction filter holder appropriate for this use is available from Millipore Corp.

5. Other single-cut restriction enzymes can be used for this purpose, but the reaction conditions must be adjusted as described by Shortle et al. (15).
6. If the nicked DNA preparation contains an unsatisfactory level of linear molecules, the ethidium bromide concentration in the restriction enzyme reaction should be empirically titrated upward to the point where nicking is complete without the generation of linears.
7. If complete wetting of the filter does not occur as judged by the presence of a uniform gray color, the filter should be discarded.
8. Care should be taken to avoid drying the filter prior to the wash step. For this reason, we recommend carrying out the filtrations one at a time.
9. Any scintillation fluid suitable for nonaqueous samples is satisfactory for this purpose.

Acknowledgment

This work was supported by the National Institutes of Health Grant GM49156.

References

1. Champoux, J. J. (2001) DNA topoisomerases: structure, function, and mechanism. *Annu Rev Biochem* **70**, 369–413.
2. Koster, D. A., Croquette, V., Dekker, C., Shuman, S. and Dekker, N. H. (2005) Friction and torque govern the relaxation of DNA supercoils by eukaryotic topoisomerase Iβ. *Nature* **434**, 671–674.
3. Muller, M. T. (1985) Quantitation of eukaryotic topoisomerase I reactivity with DNA. Preferential cleavage of supercoiled DNA. *Biochim Biophys Acta* **824**, 263–267.
4. Zechiedrich, E. L. and Osheroff, N. (1990) Eukaryotic topoisomerases recognize nucleic acid topology by preferentially interacting with DNA crossovers. *EMBO J* **9**, 4555–4562.
5. Madden, K. R., Stewart, L. and Champoux, J. J. (1995) Preferential binding of human topoisomerase I to superhelical DNA. *EMBO J* **14**, 5399–5409.
6. Stros, M. and Muselikova, E. (2000) A role of basic residues and the putative intercalating phenylalanine of the HMG-1 box B in DNA supercoiling and binding to four-way DNA junctions. *J Biol Chem* **275**, 35699–35707.
7. Grasser, K. D., Teo, S. H., Lee, K. B., Broadhurst, R. W., Rees, C., Hardman, C. H. and Thomas, J. O. (1998) DNA-binding properties of the tandem HMG boxes of high-mobility-group protein 1 (HMG1). *Eur J Biochem* **253**, 787–795.
8. Payet, D. and Travers, A. (1997) The acidic tail of the high mobility group protein HMG-D modulates the structural selectivity of DNA binding. *J Mol Biol* **266**, 66–75.
9. Palecek, E., Brazdova, M., Brazda, V., Palecek, J., Billova, S., Subramaniam, V. and Jovin, T. M. (2001) Binding of p53 and its core domain to supercoiled DNA. *Eur J Biochem* **268**, 573–581.
10. Mazur, S. J., Sakaguchi, K., Appella, E., Wang, X. W., Harris, C. C. and Bohr, V. A. (1999) Preferential binding of tumor suppressor p53 to positively or negatively

supercoiled DNA involves the C-terminal domain. *J Mol Biol* **292**, 241–249.

11. Hinkle, D. C. and Chamberlin, M. J. (1972) Studies of the binding of *Escherichia coli* RNA polymerase to DNA. I. The role of sigma subunit in site selection. *J Mol Biol* **70**, 157–185.
12. Stewart, L. and Champoux, J. J. (1996) Purification of baculovirus expressed human DNA topoisomerase I. In DNA Topoisomerase Protocols, Volume 1: DNA Topology and Enzymes (Bjornsti, M.-A. and Osheroff, N., eds.), Vol. 94, pp. 223–234. Humana Press, Totowa, NJ.
13. Yang, Z. and Champoux, J. J. (2002) Reconstitution of enzymatic activity by the association of the cap and catalytic domains of human topoisomerase I. *J Biol Chem* **277**, 30815–30823.
14. Hirt, B. (1967) Selective extraction of polyoma DNA from infected mouse cell cultures. *J Mol Biol* **26**, 365–369.
15. Shortle, D., Grisafi, P., Benkovic, S. J. and Botstein, D. (1982) Gap misrepair mutagenesis: efficient site-directed induction of transition, transversion, and frameshift mutations in vitro. *Proc Natl Acad Sci USA* **79**, 1588–1592.

Chapter 6

Monitoring the Topoisomerase II DNA Gate Conformational Change with Fluorescence Resonance Energy Transfer

Tammy R.L. Collins and Tao-shih Hsieh

Abstract

Type II DNA topoisomerases are essential, ubiquitous enzymes responsible for performing vital functions in chromosome condensation and segregation and in regulating intracellular DNA supercoiling. Topoisomerase II (topo II) performs these DNA transactions by passing one segment of DNA through the other using a reversible, enzyme-bridged double-stranded DNA break. This cleavage/religation of the DNA backbone is coupled to the opening and closing of the DNA gate, a critical step for strand passage during the catalytic cycle. To monitor the opening and closing of the DNA gate, we designed an oligonucleotide substrate with a pair of fluorophores flanking the topoisomerase II cleavage site, such that the fluorophores undergo efficient fluorescence resonance energy transfer (FRET) in the intact DNA substrate, but the FRET efficiency decreases as topo II opens the DNA gate. Here we present a method for creating the DNA substrate and using it as a tool to monitor the conformational changes at the topo II DNA gate. We detail how to collect and process fluorescence spectra to determine the FRET efficiency of the DNA substrate.

Key words: Topoisomerase II, fluorescence resonance energy transfer, $ratio_A$, cleavage, religation.

1. Introduction

During various processes involving DNA, topological entanglements including supercoiling, knotting, and catenation can arise, which are removed by DNA topoisomerases (1–3). Type II topoisomerases, the focus of this chapter, remove such topological complexities in DNA using two active site tyrosines that each carry out a nucleophilic attack to form a covalent adduct with a DNA backbone phosphate, thus generating a transient, reversible double-stranded break through which another segment of DNA can pass. This large-scale movement of DNA is fueled in part by

D.J. Clarke (ed.), *DNA Topoisomerases*, Methods in Molecular Biology 582,
DOI 10.1007/978-1-60761-340-4_6,

ATP binding and hydrolysis, which triggers capture of a DNA segment by the N-terminal clamp, and coordinates strand passage with DNA cleavage/religation (4, 5).

The reversible cleavage/religation of DNA is a key step in the topoisomerase II (topo II) reaction cycle, and a number of clinically important anticancer drugs target this step, exploiting the fact that topo II creates breaks in DNA (6, 7). These topoisomerase-mediated DNA breaks can be monitored by entrapping the DNA cleavage complex with a potent denaturant such as alkali or detergent, but addition of a protein denaturant may perturb the cleavage/religation equilibrium. To address this issue, we developed a FRET-based assay to monitor the topo II DNA gate, which eliminates the need for a denaturant. Since the optical method obviates the need for the use of a denaturant, it affords an opportunity to monitor the DNA gate conformation in real time.

In this chapter, we present a protocol to prepare an oligonucleotide substrate labeled with Alexa Fluor 488 and Alexa Fluor 555, fluorophores constituting a FRET pair and situated to straddle a known topo II cleavage site (8). The fluorophores undergo efficient energy transfer in the intact DNA substrate, because the calculated distance between the FRET pair is ~54 Å, and the distance for 50% FRET (R_o) is 70 Å. Topo II-mediated opening of the DNA gate physically separates the fluorophores ~21 Å causing less efficient energy transfer between the FRET pair (9). As a result, the fluorescent DNA substrate provides a unique means to monitor the gate movement of topo II.

To examine topo II gate movement with FRET, preparation of a double-stranded fluorescent substrate is facilitated by commercial availability of fluorescent oligonucleotides labeled with Alexa Fluor 488 and Alexa Fluor 555. The FRET efficiency between this pair can be determined with fluorescence spectroscopy. Fluorescence spectra are collected to measure the enhanced emission of the acceptor when exciting the donor using the $ratio_A$ method (10). This technique allows measurement of the effect of various cofactors, anticancer drugs, and temperature on the conformational change at the topo II DNA gate.

2. Materials

2.1. Oligonucleotides

1. Lyophilized oligonucleotides: The nucleotide sequence and location of fluorophores are shown in **Fig. 6.1**. Alexa Fluor 488 is attached to the top oligonucleotide strand (Top 488) and Alexa Fluor 555 is attached to the bottom strand (Bot 555). Both fluorophores are conjugated to the thymidine ring at the C5 position. Top 488 and Bot 555 can be obtained

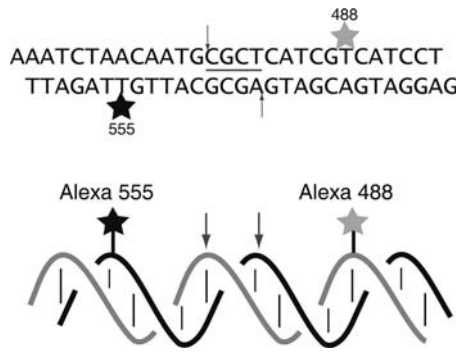

Fig. 6.1. **Design of the DNA substrate with a FRET pair**. A 28-bp oligonucleotide-based DNA substrate was synthesized with a known *Drosophila melanogaster* topo II cleavage site (indicated with *arrows*) flanked by the FRET pair Alexa Fluor 488 (*gray star*) and Alexa Fluor 555 (*black star*). The fluorophores are separated by ~1.5 helical turns on complementary strands.

from Integrated DNA Technologies (Caralville, IA), while nonfluorescent oligonucleotides of the same sequence can be obtained from MWG-Biotech (Ebersberg, Germany).

2. Dissolved oligonucleotides: Dissolve the lyophilized oligonucleotides in TE buffer (10 mM Tris–HCl, pH 7.9, 0.1 mM EDTA) upon receipt. Store oligonucleotides at a concentration of 0.075 nmol/μl in the dark at –20°C.
3. 40% (w/v) sucrose: Prepare sucrose in water and store at 4°C (EMD Pharmaceuticals, Gibbstown, NJ).

2.2. Polyacrylamide Gel Electrophoresis (PAGE) of Oligonucleotides

1. Running buffer and gel preparation buffer (10X TBE): 0.89 M Tris, 0.89 M boric acid, 20 mM EDTA, pH 8.4.
2. 40% acrylamide/bis solution (19:1) (Bio-Rad, Hercules, CA): Store at 4°C, avoid exposure because this is neurotoxic when unpolymerized.
3. TEMED: *N*, *N*, *N*, *N*′-tetramethyl-ethylenediamine (Bio-Rad, Hercules, CA).
4. 10% (w/v) ammonium persulfate: Prepare in water and store at 4°C (Bio-Rad, Hercules, CA).
5. 6X loading dye: 0.25% bromophenol blue, 0.25% xylene cyanol FF, 40% (w/v) sucrose in water, store at 4°C.
6. 0.5 M ammonium acetate.

2.3. NAP-5 Gel Filtration of Oligonucleotides

1. NAP-5 gel filtration column: Sephadex G-25 DNA Grade, containing 0.15% Kathon CG preservative (Amersham Biosciences, Uppsala, Sweden).
2. TE: 10 mM Tris–HCl, pH 7.9, 0.1 mM EDTA.
3. Bovine serum albumin (BSA): 1 mg/ml in TE buffer (BSA from Research Organics, Cleveland, OH).

2.4. Fluorescence Spectroscopy

1. Quartz fluorometer cell: 50 µl volume, 10 mm path length (Starna Cells, Atascadero, CA).
2. Reaction buffer: 10 mM Tris–HCl, pH 7.9, 50 mM NaCl, 0.1 mM EDTA.
3. DNA: 100 pmol annealed fluorescent oligonucleotides.
4. Enzyme: 300 pmol *Drosophila melanogaster* topoisomerase II (*see* **Note 1**).
5. 1 M $MgCl_2$.
6. Adenosine triphosphate (ATP): 86 mM adenosine 5′-triphosphate (USB, Cleveland, OH) in 10 mM sodium phosphate, pH 7.0.
7. AMPPNP: 20 mM adenosine 5′-(β,γ-imido)triphosphate, tetralithium salt (Calbiochem, La Jolla, CA) in 10 mM sodium phosphate, pH 7.0.
8. 5 M NaCl.
9. 0.5 M EDTA, pH 8.

3. Methods

Fluorescence spectra of DNA substrates bound with either only the donor or the acceptor demonstrate that the excitation/emission spectra of Alexa Fluor 488 and Alexa Fluor 555 have extensive spectral overlap near 520 nm and can serve as a donor–acceptor pair in FRET experiments (**Fig. 6.2**). FRET between this pair is efficient in the intact 28-bp DNA substrate because Alexa Fluor 488 and Alexa Fluor 555 are positioned ~54 Å apart, and the distance for 50% FRET (R_o) is 70 Å. Because the fluorophores are positioned to flank a topo II cleavage site, topo II-mediated opening of the DNA physically separates the fluorophores resulting in a FRET decrease. To accurately interpret these FRET changes, it is important to obtain a pure substrate by annealing the fluorescent DNA strands and carefully removing any single-stranded fluorescent DNA. Removal of single-stranded DNA is accomplished by PAGE purification of the double-stranded substrate, followed by gel filtration using a NAP-5 column.

Once a pure substrate is obtained, two fluorescence emission spectra are collected for each tested condition to determine the FRET efficiency between Alexa Fluor 488 and Alexa Fluor 555. In one spectrum, the donor is excited at its excitation maximum, and emission from the acceptor can be seen as a result of FRET. In the second spectrum, the acceptor is directly excited (no FRET). Next, a donor-only spectrum is

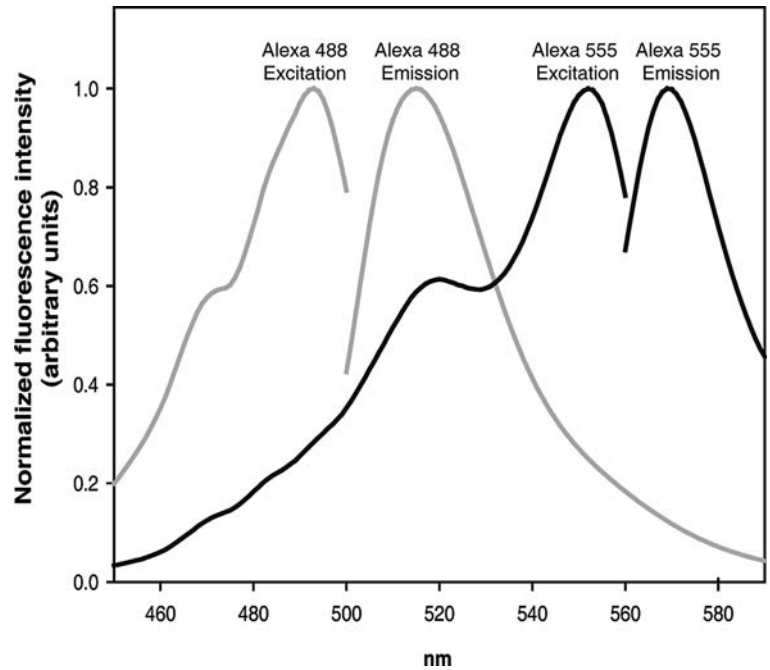

Fig. 6.2. **Fluorescence excitation and emission spectra of DNA bound with either Alexa Fluor 488 or Alexa Fluor 555**. Extensive spectral overlap occurs between the emission of Alexa Fluor 488 and the excitation of Alexa Fluor 555.

subtracted from the FRET spectrum to remove donor spillover fluorescence from acceptor emission. As a result, we can compare (1) the measured acceptor emission as a result of energy transfer with (2) the measured acceptor emission upon direct excitation. Measurement of acceptor emission upon direct excitation indicates how Alexa Fluor 555 emits in the case of 100% energy transfer. From these spectra, we can obtain the ratio_A, and use it to calculate the energy transfer efficiency between the donor and acceptor pair (10). Decreases in FRET are indicative of a larger population of topo II being in the open-gate state. With this technique, it is possible to measure the conformational changes at the topo II DNA gate in response to various conditions, such as the presence of different divalent cations, cofactors, anticancer drugs, etc.

3.1. Annealing Oligonucleotides

1. Protection from exposure to light: While both fluorophores are relatively stable to ambient light, apply precaution wherever possible to protect samples from light exposure (*see* **Note 2**).
2. Prepare eight 45 μl samples containing equimolar amounts (~0.5 nmol) of Top 488 and Bot 555 in TE buffer, and place these samples in PCR tubes.

3. Anneal the Top 488 and Bot 555 oligonucleotides with an Applied Biosystems GeneAmp PCR 2400 or other thermocycling machine: Heat the oligonucleotides to 80°C and hold this temperature for 7 min, and cool the oligonucleotides 1°C every 90 s until 23°C is reached.
4. When annealing is complete, pool the eight reactions and add 40% sucrose to a final concentration of 6% sucrose.
5. For a donor-only and acceptor-only spectrum, repeat steps 2–4 to anneal Top 488 with a nonfluorescent bottom strand and to anneal Bot 555 with a nonfluorescent top strand.

3.2. PAGE Purification of Oligonucleotides

1. We used a homemade vertical slab gel system to purify the annealed oligonucleotides, but commercial gel systems (such as a dual vertical slab gel system; CBS Scientific, Korea) can easily be substituted. Our homemade system includes glass plates ~16.5 × 26.5 cm. The dimensions of the six wells are 1.5 × 1.5 cm; the thickness of the plate separators is ~1 mm.
2. Prepare the glass plates and separators by cleaning with a detergent and rinsing extensively with distilled water, followed by wiping with ethanol. Place one of the glass plates on a horizontal surface and slightly tilt the bottom of the plate downward. Place the separators on the side and bottom edges of the plate, using a small amount of petroleum jelly on the ends of the separators to hold them in place when positioning the second plate on top. Tape the edges of the plates together or use a sealing strip to prevent gel leakage, and clamp the edges of the plates together.
3. Prepare a 1 mm thick, 15% gel by mixing 28 ml of acrylamide/bis solution with 7.5 ml of 10X TBE buffer and 39 ml of water. Filter and degas for 5 min, then add 400 µl of ammonium persulfate and 40 µl of TEMED. Swirl the flask, carefully avoiding bubble formation.
4. Slowly pour the gel between the glass plates, filling the plates to the top (*see* **Note 3**). Insert the comb and place clamps over the comb sandwiched between the plates. The plates will become warm once polymerization has begun, and the gel should completely polymerize in approximately 30 min.
5. Prepare the running buffer in a graduated cylinder by diluting 75 ml of 10X TBE with deionized water to a final volume of 750 ml and mix thoroughly.
6. Once the gel has polymerized, carefully remove the comb and tape (or sealing strips). Also, remove the clamps and separator from the bottom of the gel, while keeping those on the sides in place.

7. Fill the lower chamber of the gel system with running buffer and place the gel in the assembly unit, using a syringe fitted with a needle to remove any bubbles that may accumulate near the bottom of the gel. Secure the gel in place with rubber bands. To prevent leakage, seal the area between the glass plate and top chamber with 1% agarose. Once the gel is in place, fill the top chamber with running buffer and rinse the wells using the same syringe and needle.
8. Pipet annealed oligonucleotides into two central wells. Dilute 17 μl of 6X loading dye with TE buffer to a final volume of 100 μl and load in an adjacent well.
9. Connect the gel system to a power supply. Run the gel at 500 V (*see* **Note 4**) until the lowest dye front (bromophenol blue) has migrated three quarters of the way down the gel, ~1.5–2 h. The oligonucleotides are visible as a pink band migrating at a distance similar to the xylene cyanol dye.
10. Disassemble the gel system and remove the separators. Use a wedge to pry the plates apart, removing the top plate. Place saran wrap on top of the gel, and flip over. Use the wedge to remove the gel from the glass plate so that the gel is now positioned on the saran wrap. Place the gel (saran-wrap side down) on a cardboard-type backing and cover with another layer of saran wrap, so that the gel is now sandwiched between two strips of saran wrap.
11. Use a clean razor blade to cut out the annealed oligonucleotide bands and combine all of the slices in a single eppendorf tube. Use a clean pipet tip to crush the gel into smaller pieces, and soak overnight in the dark in 500 μl of 0.5 M ammonium acetate, ensuring that all of the pieces are submerged.
12. Repeat steps 1–11 for donor-only and acceptor-only labeled substrates.

3.3. NAP-5 Gel Filtration of Annealed Oligonucleotides

1. Remove the top cap from the NAP-5 column, pour off the liquid, and then remove the bottom cap. Secure the column on a ring stand and place a waste container underneath the column.
2. Wash the column successively with 5 ml of TE, 5 ml of 1 mg/ml BSA, and 20 ml of TE.
3. Prepare the annealed oligonucleotides to be loaded onto the NAP-5 column. To this end, use a pipet to remove as much liquid as possible from the crushed gel. The liquid should appear pink (except for the donor-only labeled substrate), indicating that the solution contains the fluorescent DNA substrate. To collect the remaining liquid, pierce the bottom and side of the eppendorf tube with a needle and place a capless collection tube under the eppendorf. Centrifuge to remove the excess liquid from the gel.

4. Add enough TE to the annealed oligonucleotides to increase the sample volume to 500 µl. Load the sample onto the NAP-5 column, allowing it to enter the column completely while collecting the flow-through. Except in the case of the donor-only substrate, the NAP-5 column should appear pink.
5. Elute the DNA with 1 ml of TE. Collect the first few drops in a separate eppendorf, and when the eluate acquires a pink color, collect a single fraction of nearly 500 µL. In the case of the donor-only labeled substrate, a hand-held long-wavelength UV lamp may be required to visualize the DNA eluting from the NAP-5 column.
6. Calculate the concentration of the DNA by measuring the absorption spectrum in the 200–700 nm range, specifically determining the absorbance at 260, 492, and 555 nm. Each fluorophore contributes a small amount to the A_{260}, which must be corrected for. The correction factor for Alexa Fluor 488 is 0.3 and that for Alexa Fluor 555 is 0.04. Multiply each of the correction factors by A_{492} and A_{555}, respectively, and subtract this value from A_{260} to obtain the absorbance of the DNA. For the substrates labeled with either Alexa Fluor 488 or Alexa Fluor 555, A_{260} is corrected for the fluorophore that is present. Once the corrected A_{260} is calculated, use Beer's law to determine DNA concentration with an extinction coefficient of 50 µg/ml per A_{260}.

3.4. Fluorescence Spectroscopy of DNA Substrate

1. Obtain fluorescence measurements with an SLM 8100 fluorometer (Jobin Yvon, Inc.) or a comparable instrument. When operating a fluorometer (1) ensure the shutters to all the photomultiplier tube (PMT) detectors are closed before placing the sample in the holder, (2) simultaneously measure a reference spectrum to ensure the lamp intensity does not fluctuate, (3) adjust the PMT voltage to the minimum required to detect signal from the fluorophores, and (4) control the temperature of the sample chamber by flushing with 30°C water.
2. Pipet 100 pmol of annealed oligonucleotides into the cuvette (*see* **Note 5**) in the indicated reaction buffer, and adjust the settings on the fluorometer to the desired excitation and emission wavelengths. Two spectra are collected; for the first spectrum, excite Alexa Fluor 488 at 492 nm and collect the spectrum in the range of 510–590 nm. Subsequently, excite Alexa Fluor 555 at 555 nm and collect the spectrum in the range of 560–590 nm (*see* **Note 6**). Alexa Fluor 555 is directly excited at its excitation maximum to observe the theoretical acceptor emission intensity if there were 100% FRET. Ensure that the PMT voltage remains constant for both measurements.

3. After collecting data from the annealed oligonucleotides, remove the sample from the cuvette and place into an eppendorf tube. Add 300 pmol of topo II and mix by gentle pipetting (*see* **Note 7**). Place the sample into the cuvette and incubate for 2 min at 30°C before collecting two emission spectra as described above (*see* **Note 8**).
4. Repeat the steps outlined in **Section 3.4** for successive addition of Mg^{2+} to a final concentration of 10 mM, and ATP or AMPPNP to final concentrations of 1 mM. To reverse the cleavage of DNA, add EDTA to a final concentration of 12 mM and NaCl to a final concentration of 0.5 M, and incubate for 10 min at 30°C before collecting the two emission spectra as described in **Section 3.4**, step 3 (*see* **Note 9**).
5. For calculation of FRET efficiency, collect a spectrum of a DNA substrate in which only the donor, Alexa Fluor 488, is present. Excite Alexa Fluor 488 at 492 nm and collect a spectrum in the range 510–590 nm. Also, collect an excitation spectrum for a substrate with only Alexa Fluor 555 present by monitoring the emission intensity at 565 nm upon excitation of Alexa Fluor 555 across the range 450–560 nm.

3.5. Processing of Fluorescence Spectra to Determine FRET Efficiency

1. Use the ratio_A method (equation [1]) to determine the efficiency, *E*, of energy transfer between Alexa Fluor 488 and Alexa Fluor 555 (10) (*see* **Note 10**):

$$\text{ratio}_A = E.d^{+}.\frac{\varepsilon^{D}_{492\text{nm}}}{\varepsilon^{A}_{555\text{nm}}} + \frac{\varepsilon^{A}_{492\text{nm}}}{\varepsilon^{A}_{555\text{nm}}} \qquad [1]$$

2. We used a value of unity for the term d^{+}, which is the donor labeling efficiency. The factor $\varepsilon^{D}_{492\,\text{nm}}/\varepsilon^{A}_{555\,\text{nm}}$ is the ratio of the extinction coefficients of the donor at 492 nm and the acceptor at 555 nm, for which we used a value of 0.41, based on information provided by the manufacturer. The factor $\varepsilon^{A}_{492\,\text{nm}}/\varepsilon^{A}_{555\,\text{nm}}$ accounts for the fact that the acceptor also absorbs energy at 492 nm when the donor is excited at its maximum. We measured this factor from the excitation spectrum of Alexa Fluor 555 (discussed in **Section 3.4**, step 6) and found it to be 0.28.
3. In the ratio_A method, the enhanced fluorescence of Alexa Fluor 555 is used to determine FRET efficiency, *E*. However, spillover fluorescence from Alexa Fluor 488 interferes with the emission spectrum of Alexa Fluor 555. To remove the donor contribution from the acceptor fluorescence, the emission spectrum collected from a substrate labeled only with Alexa Fluor 488 (from **Section 3.4**, step 5) is fitted to the donor portion of the FRET spectrum. Subtraction of the fitted donor spectrum reveals the extracted emission spectrum of Alexa Fluor 555 (**Fig. 6.3**).

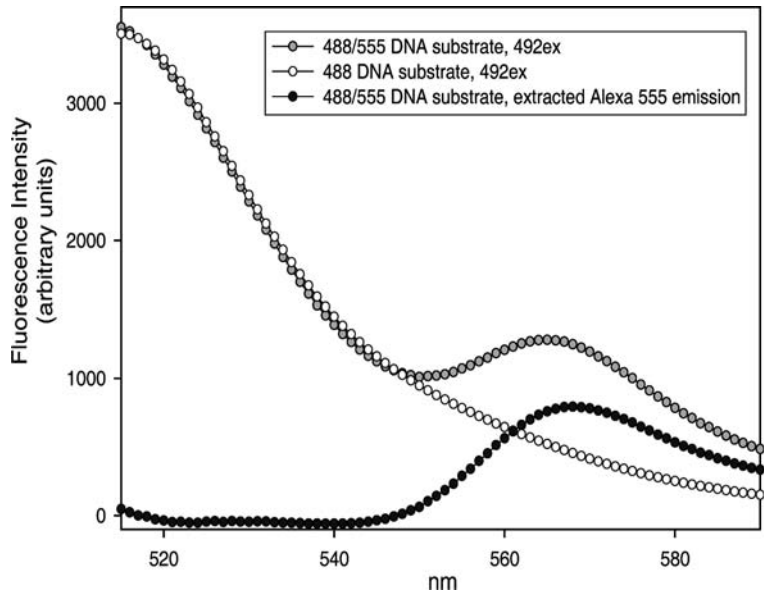

Fig. 6.3. **Example of extracting acceptor emission for calculating FRET**. The DNA substrate labeled with Alexa Fluor 488 and Alexa Fluor 555 was excited at 492 nm to obtain its emission spectrum (*gray circles*). A donor-only emission spectrum (*white circles*) was fitted to the donor portion of the doubly labeled substrate. The donor-only spectrum was subtracted from the FRET spectrum to obtain the extracted acceptor emission spectrum (*black circles*).

4. $Ratio_A$ is the extracted fluorescence intensity of the acceptor at 565 nm upon donor excitation at 492 nm (from step 3) divided by the fluorescence intensity of the acceptor at 565 nm upon direct excitation (no FRET) at 555 nm. Direct excitation of Alexa Fluor 555 and observation of its emission at 565 nm can be used in the calculation of $ratio_A$ because Alexa Fluor 488 does not absorb at 555 nm.
5. Solve equation [1] for *E*, the efficiency of energy transfer between Alexa Fluor 488 and Alexa Fluor 555. The changes in FRET efficiency can be measured and tracked for various conditions to monitor the conformational changes at the topo II DNA gate.

4. Notes

1. We prepare topo II containing an N-terminal hexahistidine tag and purify by Ni^{2+}-affinity and ion-exchange chromatography (11). Topo II can be stored at –20°C in a buffer containing 15 mM NaPi, pH 7.0, 0.1 mM EDTA, 0.1 M NaCl, 50% glycerol, 5 mM β-mercaptoethanol, 1 μg/ml leupeptin, and 1 μg/ml pepstatin.

2. Protect samples from light by covering samples with foil, storing fluorescent oligonucleotides in a dark environment, and manipulating samples in a dark room wherever possible.
3. Reserve some of the leftover gel in the flask and use a pasteur pipette to add additional liquid in case of a leak. Only dispose of the leftover gel once polymerization is complete.
4. To minimize exposure of the fluorescent oligonucleotides to light, create a box to cover the gel assembly, or place the assembly in a dark room.
5. Rigorously clean dirty cuvettes with a solution containing 10 g of potassium dichromate, 100 ml of distilled water, and 10 ml of sulfuric acid. To make this solution, dissolve potassium dichromate in water and slowly add the sulfuric acid. Fill cuvettes with the cleaning solution and soak overnight, rinsing with distilled water after cleaning.
6. Collect the fluorescence emission spectra at a wavelength at least 5 nm higher than the excitation wavelength to avoid interference from the incident light.
7. Avoid the formation of bubbles when mixing to eliminate artifacts in the fluorescence spectra. Mix gently to avoid precipitation of topo II, which will cause the solution to appear cloudy.
8. When topo II binds to the doubly labeled DNA substrate, the intensity of the donor decreases and the intensity of the acceptor increases, causing it to appear as if there were an increase in FRET if examining this spectrum without using the ratio_A method. However, when topo II binds to a donor-only labeled substrate, Alexa Fluor 488 is quenched, and when topo II binds to acceptor-only labeled substrate, the fluorescence intensity of Alexa Fluor 555 is enhanced. The ratio_A method accounts for this enhancement, because the acceptor emission due to FRET is normalized by the direct excitation of the acceptor.
9. We approximated a correction for donor quenching, which may occur under the conditions tested. For example, if the donor-only labeled substrate is quenched by 3% under a particular condition, we multiplied the extracted acceptor emission by 1.03 (increasing it by 3%). On the other hand, if acceptor quenching occurs, the FRET efficiency calculation is unaffected because of the ratio method used. The quantum yield of the acceptor does not enter into the energy transfer ratio calculation since this parameter cancels out when normalizing by the direct excitation of the acceptor.

10. Several methods can be used to determine FRET efficiency, but the ratio$_A$ method has multiple advantages, some of which include that virtually all measurements are collected on a single sample and that the fluorescence contribution of the donor can be completely and rigorously removed.

Acknowledgments

This work was supported by the National Institutes of Health Grant GM29006 (to T.-s. H.), and T. R. L. C. was supported in part by a grant from the Department of Defense Breast Cancer Research Program.

References

1. Champoux, J. J. (2001) DNA TOPOISOMERASES: structure, function, and mechanism. *Annu Rev Biochem* **70**, 369–413.
2. Corbett, K. D. and Berger, J. M. (2004) Structure, molecular mechanisms, and evolutionary relationships in DNA topoisomerases. *Annu Rev Biophys Biomol Struct* **33**, 95–118.
3. Wang, J. C. (2002) Cellular roles of DNA topoisomerases: a molecular perspective. *Nat Rev Mol Cell Biol* **3**, 430–440.
4. Roca, J. and Wang, J. C. (1992) The capture of a DNA double helix by an ATP-dependent protein clamp: a key step in DNA transport by type II DNA topoisomerases. *Cell* **71**, 833–840.
5. Baird, C. L., Harkins, T. T., Morris, S. K. and Lindsley, J. E. (1999) Topoisomerase II drives DNA transport by hydrolyzing one ATP. *Proc Natl Acad Sci USA* **96**, 13685–13690.
6. Liu, L. F. (1989) DNA topoisomerase poisons as antitumor drugs. *Annu Rev Biochem* **58**, 351–375.
7. Wilsterman, A. M. and Osheroff, N. (2003) Stabilization of eukaryotic topoisomerase II-DNA cleavage complexes. *Curr Top Med Chem* **3**, 321–338.
8. Sander, M. and Hsieh, T.-s. (1983) Double strand DNA cleavage by type II DNA topoisomerase from *Drosophila melanogaster*. *J Biol Chem* **258**, 8421–8428.
9. Smiley, R. D., Collins, T. R., Hammes, G. G. and Hsieh, T. S. (2007) Single-molecule measurements of the opening and closing of the DNA gate by eukaryotic topoisomerase II. *Proc Natl Acad Sci USA* **104**, 4840–4845.
10. Clegg, R. M. (1992) Fluorescence resonance energy transfer and nucleic acids. *Methods Enzymol* **211**, 353–388.
11. Hu, T., Sage, H. and Hsieh, T.-s. (2002) ATPase domain of eukaryotic DNA topoisomerase II. Inhibition of ATPase activity by the anti-cancer drug bisdioxopiperazine and ATP/ADP-induced dimerization. *J Biol Chem* **277**, 5944–5951.

Chapter 7

Single-Molecule Magnetic Tweezers Studies of Type IB Topoisomerases

Jan Lipfert, Daniel A. Koster, Igor D. Vilfan, Susanne Hage, and Nynke H. Dekker

Abstract

The past few years have seen the application of single-molecule force spectroscopy techniques to the study of topoisomerases. Magnetic tweezers are particularly suited to the study of topoisomerases due to their unique ability to exert precise and straightforward control of the supercoiled state of DNA. Here, we illustrate in a stepwise fashion how the dynamic properties of type IB topoisomerases can be monitored using this technique.

Key words: Single-molecule techniques, magnetic tweezers, topoisomerases, TopIB, spectroscopy.

1. Introduction

1.1. Topoisomerase Activity

Topoisomerases are enzymes that control the topological state of DNA, in particular supercoiling, by temporarily breaking one or two strands of the DNA double helix (1–3). They are generally classified as type I and type II topoisomerases, depending on the number of strands cut in their catalytic mechanism. Type II topoisomerases induce temporary double-strand breaks and have a strand passage mechanism that requires ATP hydrolysis. In contrast, type I topoisomerases act on a single strand of DNA and remove one or more supercoils by temporarily creating a single-strand break and rotating the DNA around the remaining intact strand. Topoisomerase IB (TopIB), a eukaryotic enzyme, releases the torsion built up in a supercoiled DNA in a manner that is very different from type II topoisomerases and does not require ATP for the reaction. The enzyme releases the torsion from the DNA by

D.J. Clarke (ed.), *DNA Topoisomerases*, Methods in Molecular Biology 582,
DOI 10.1007/978-1-60761-340-4_7,

surrounding the double-stranded DNA (dsDNA) like a clamp and temporarily cleaving one of the two strands. The accumulated torsional forces in the DNA are then spun out by swiveling about the intact strand. After a number of turns, the topoisomerase IB again firmly grabs the spinning DNA and neatly ligates the broken strands back together again (**Fig. 7.1**).

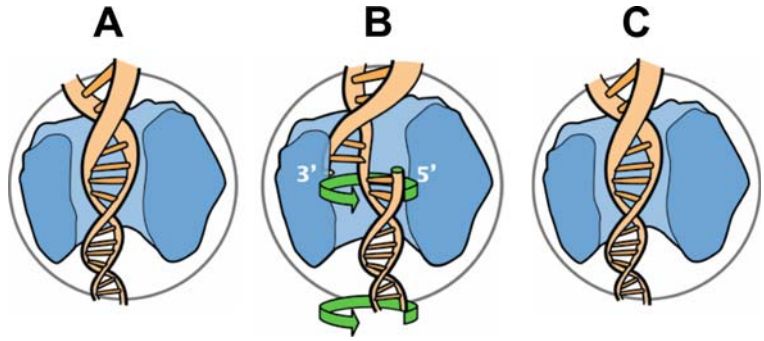

Fig. 7.1. **Schematic of the supercoil removal mechanism of topoisomerase IB**. The enzyme binds (non-covalently) to supercoiled double-stranded DNA (**A**). Topoisomerase IB then binds covalently to one strand of the DNA via its active tyrosine, creating a nick in the DNA strand. Rotation around the remaining DNA strand that acts as a swivel releases supercoils (**B**). Finally, the topoisomerase–DNA bond is broken and the DNA nick is resealed (**C**).

1.2. Magnetic Tweezers and DNA Manipulation

Magnetic tweezers (MT) are a single-molecule technique that permits the application of both stretching forces and torques to single DNA molecules (4). They are particularly well suited to the study of topoisomerases, as they enable straightforward and precise control of the supercoiling of DNA molecules (5–8). In the magnetic tweezers, a DNA molecule is tethered in a flow cell between a glass surface and a paramagnetic bead by means of non-covalent bonds which can resist forces on the order of ~100 pN (**Fig. 7.2**). Above the flow cell, a pair of permanent magnets or an electromagnet is suspended on a motorized stage (**Fig. 7.2**), exposing the flow cell to a magnetic field B (9). The magnetic field exerts an upward stretching force F on the bead given by

$$\vec{F} = \frac{1}{2}\vec{\nabla}\left(\vec{\mathbf{m}} \cdot \vec{\mathbf{B}}\right) \qquad [1]$$

where $\vec{\mathbf{m}}$ is the induced magnetization of the bead in the external magnetic field $\vec{\mathbf{B}}$. The magnitude of the stretching force can be controlled by controlling the distance of the magnets from the flow cell. Additionally, the magnets can be rotated, which in turn controls the rotation of the DNA-tethered beads. Rotating the bead attached to a torsionally constrained DNA molecule changes its linking number Lk. Starting from a torsionally relaxed molecule, the change in linking number is initially absorbed by elastic

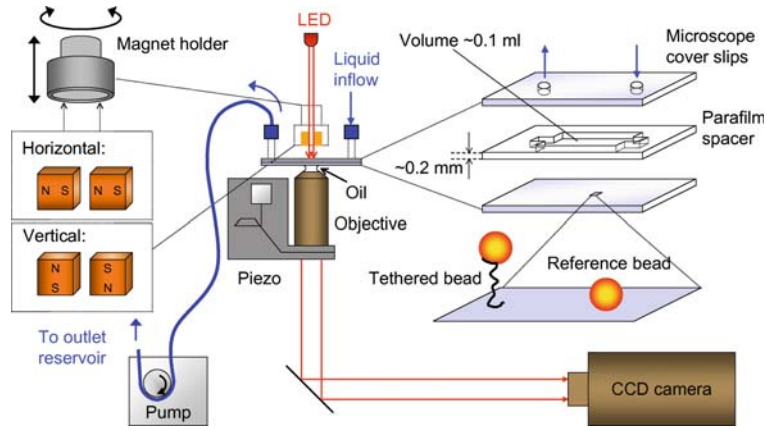

Fig. 7.2. **Schematic of the magnetic tweezers setup**. The basic components are shown schematically: the inverted microscope, the CCD camera, the flow cell system with fluid inlet and outlet connected to a pump, and the LED illumination. Shown in more detail are the flow cell with a tethered and a reference bead and pairs of magnets in horizontal and vertical geometry. Both horizontal and vertical magnet pairs provide field gradients appropriate for magnetic tweezers, however, with different characteristics. Lipfert et al. have carried out an extensive study of the different magnet geometries for magnetic tweezers (Jan Lipfert, Xiaomin Hao, and Nynke H. Dekker (2009) Quantitative modeling and optimization of magnetic tweezers. *Biophys J* 96, 5040–5049).

twist deformations and increases *Tw* of the molecule, while the Writhe *Wr* remains unchanged. In this regime, the torque Γ increases linearly with the number of turns *N*:

$$\Gamma = \frac{C}{L_c}(2\pi N) \qquad [2]$$

where *C* is the torsional modulus, $C \approx 90\ k_B T$ for DNA (10–12), and L_c is the length of the DNA. If one continues to rotate the magnets, the molecule undergoes a buckling transition where the additional mechanical energy is no longer stored as an elastic twisting deformation but rather in a loop, which leads to an observable decrease in the end-to-end extension of the DNA molecule (**Fig. 7.3**). Further rotations past the buckling transition do not increase *Tw*, and the torque remains constant. Instead *Wr* increases as plectonemic supercoils are formed, further decreasing the end-to-end distance of the molecule in a linear fashion (see the linear slopes shown as solid lines in **Fig. 7.3**).

Strick et al. have proposed a simple and approximate model for this plectonemic regime (13, 14), in which the postbuckling torque is equal to

$$\Gamma_B = \sqrt{2L_p k_B T F} \qquad [3]$$

where *F* is the force applied to the DNA molecule and $L_p \approx 50$ nm is the persistence length of DNA. The decrease in the length of the tethered molecule per turn in this approximate model is given by

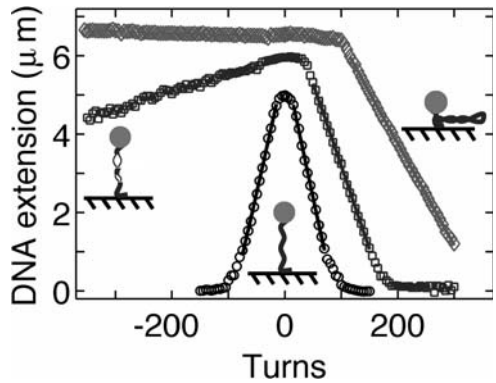

Fig. 7.3. **DNA extension as a function of linking number measured using the magnetic tweezers**. The data shown are for stretching forces of 0.25 (*black circles*), 1 (*dark gray squares*), and 5 pN (*light gray diamonds*). Initially, at zero turns, the DNA is torsionally relaxed. Introduction of positive turns eventually results in (positive) supercoiling of the DNA for all three measured forces. Negative turns result in (negative) supercoiling at low forces (*black symbols* and *line*), but at higher forces, the DNA melts locally under negative torque (*gray symbols*).

$$\Delta z = \pi \sqrt{\frac{2 L_p k_B T}{F}} \qquad [4]$$

It is the linear response of the DNA end-to-end extension to the number of induced supercoils that has to date proven so very useful to the study of topoisomerases, including TopIB. Since the supercoils are removed from the DNA as soon as the topoisomerase cuts through one of the two DNA strands, an increase in the length of the DNA is observed. Relating changes in length to changes in the degree of supercoiling, Koster et al. were able to determine the exact number of turns removed by the topoisomerase between "cutting" and "sealing" (**Fig. 7.4**) (6). In addition, by varying the applied force (and hence the torque in the plectonemic regime), the authors could monitor the torque dependence of the average number of turns removed. Finally, by monitoring the rate at which supercoils were removed by TopIB, the existence of friction of the rotating DNA in a cavity of the enzyme could be demonstrated. This methodology was recently also extended to study the influence of TopIB inhibitors on the dynamics of the enzyme (8).

1.3. The Magnetic Tweezers Microscope

1. Typically, the microscope is assembled in an inverted configuration for straightforward sample handling.
2. The focal length of the tube lens must be taken into account when computing the magnification of the experimental configuration. A calibrated grid (stage micrometer/G390010000, Linos, Germany) is useful for verifying that the magnification achieves the expected value.

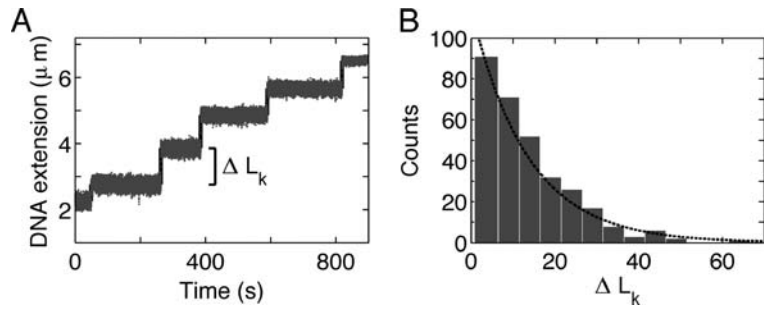

Fig. 7.4. **Single-molecule topoisomerase IB supercoil removal observed in the magnetic tweezers**. (**A**) Time trace of the DNA extension at a stretching force of 1 pN in the presence of wild-type human topoisomerase IB. The DNA is initially (time = 0) prepared in a positively supercoiled state by rotating the magnets +120 turns. Each time a topoisomerase molecule removes supercoils, a step in the extension is observed. Using the relationship between supercoils and the DNA extension (from the slope of the rotation curves, *see* **Fig. 7.3**), the steps in extension can be converted to a change in linking number ΔL_k. (**B**) A histogram of supercoil removal step sizes for human topoisomerase IB at a stretching force of 1 pN. The histogram is accumulated by recording many traces like the one shown in *panel A*. The data shown here comprise a total of $N = 309$ events and are well described by an exponential distribution (*dashed line*) of the form $P(\Delta L_k) = \exp(-\Delta L_k/\langle \Delta L_k \rangle)$ with $\langle \Delta L_k \rangle = 13.6 \pm 1.5$.

3. To reduce drift, it is recommended that the microscope be built as compactly as possible.

Magnetic tweezers setups are now also commercially available (www.picotwist.com). Our setup is similar to the one used by Croquette and coworkers (4) and described in further detail elsewhere (6) (I. D. Vilfan, J. Lipfert, D. A. Koster, S.G. Lemay and N. H. Dekker (2009) Magnetic tweezers for single-molecule experiments. P. Hinterdorfer and A. van Oijen (eds.), *Handbook of Single-Molecule Biophysics*, Springer).

1.4. The Magnetic Tweezers Software

1. In the magnetic tweezers, the force F applied to the DNA molecule is given by the following expression:

$$F = \frac{k_B T l}{\langle \delta x^2 \rangle} \qquad [5]$$

where k_B is Boltzmann's constant and T is the absolute temperature. Thus, to determine F, one needs to measure the extension of the molecule l and the variance of the bead excursions $\langle \delta x^2 \rangle$. These parameters are determined from the acquired data by image analysis of the diffraction pattern recorded by the CCD.

2. To monitor l, we use a method first designed by Gosse and Croquette, in which the objective's focal plane (OFP) is accurately shifted in the vertical direction while imaging the

diffraction rings of the bead attached to the nucleic acid (15). In this manner, a calibration profile is generated correlating the diffraction pattern of the bead to the distance between the bead and the OFP (I. D. Vilfan, J. Lipfert, D. A. Koster, and N. H. Dekker, Springer Handbook of Single-Molecule Biophysics, 2009).When this calibration profile is interpolated, the vertical displacements of the bead can be measured with an accuracy of up to ~10 nm (15). If one then measures a similar calibration profile for a reference bead fixed to the surface in the proximity of the tethered bead, the distance between the surface and OFP can be determined. Finally, the difference between the two measured distances yields l.

3. An additional advantage of tracking both a reference bead and the DNA-tethered bead is that this differential measurement minimizes the effect of drift between the objective and the sample holder (i.e., flow cell).
4. Processing of the bead's in-plane fluctuations allows one to compute $\langle \delta x^2 \rangle$. Changes in the x position of the bead are computed via cross-correlation analysis of the intensity profiles displayed by a bead at subsequent time intervals (16, 17). As in the case of tracking the vertical position, in-plane tracking can be carried out at subpixel resolution to an accuracy of a few nanometers (15).
5. In practice it can be advantageous, in particular for large forces ($\geq$10 pN), to determine the pulling force not directly from equation [5] but from Fourier analysis of the beads' fluctuations (I. D. Vilfan, J. Lipfert, D. A. Koster, and N. H. Dekker, Springer Handbook of Single-Molecule Biophysics, 2009).

2. Materials

Our measurements employ a home-built microscope equipped with a pair of permanent magnets whose position and rotation can be computer controlled. This MT setup is described in - **Section 2.1** (*see* **Note 1**).

2.1. Magnetic Tweezers Microscope

1. Microscope objective: An Olympus ACH 100X 1.25 numerical aperture objective (Olympus, Japan) is recommended for measurements of a single pair of beads, 60X for multibead tracking (18).

2. Nanometer-accurate objective positioner: A PI PIFOC P-721.CDQ piezo-driven microscope objective nanofocusing/scanning device (Physik Instrumente, Germany).
3. High-speed CCD camera: A Pulnix TM-6710CL CCD camera (to track the bead positions at 60 or 120 Hz).
4. Frame grabber: A NI PCIe-1429 frame grabber (National Instruments, USA) to read out the CCD camera images.
5. Permanent magnets with high magnetization: Cubic 5 × 5 × 5 mm neodymium–iron–boron (NdFeB) magnets (W-05-N50-G, Supermagnete, Germany).
6. Motorized stage (to control the magnets' position): A PI M-126.PD motorized stage (Physik Instrumente, Germany).
7. Motor to control the magnets' rotation: A PI C-150 (Physik Instrumente, Germany).
8. Syringe pump (Cole-Parmer, IL, USA) for buffer exchange in the flow cell.
9. Computer and software: A Dell Precision T5400 work station (Dell, USA) and software custom written in Labview 8.2 (National Instruments, USA) are used to control all of the components and for data acquisition.

2.2. Magnetic Tweezers Software

The software to control the magnets, read out the CCD camera, and track the DNA-tethered bead and reference bead positions in x, y, and z in real time is written in Labiew 8.2 (National Instruments, USA).

2.3. Flow Cells for Magnetic Tweezers

1. Coverslips: Glass coverslips 24 × 60 mm, 130 μm thickness (Merzel Gläser, Germany).
2. Polystyrene solution: 100,000 MW polystyrene powder (Sigma-Aldrich, USA) dissolved in toluene (1% polystyrene by weight).
3. Anti-digoxigenin antibodies: Fab fragments of anti-digoxigenin antibodies (Roche Diagnostics, The Netherlands) dissolved at 100 μg/ml in PBS.

2.4. Buffer Solutions

1. PBS: Dissolve phosphate-buffered saline tablets (Sigma-Aldrich, USA) in deionized MilliQ water to obtain a 1X solution. Filter through a 0.22-μm pore size Millex GV syringe driven filter unit (Millipore Corporation, USA) to remove impurities and to filter sterilize the solution. The solution can be stored at 4°C and should be replaced after 6–8 weeks.

2. Topoisomerase reaction buffer: 10 mM Tris-HCl, pH 8.0, 50mM KCl, 1 or 10 mM $MgCl_2$, 1mM DTT (dithiotheitol), 200 μg/ml BSA (bovine serum albumin), and 0.1% Tween-20 (molecular biology grade). Make up the solution in deionized MilliQ water and filter through a 0.22-μm pore size Millex GV syringe driven filter unit (Millipore Corporation, USA) to remove impurities and to filter sterilize the solution. The solution can be stored at 4°C and should be replaced after 6–8 weeks.
3. BSA or poly-L-glutamic acid solution: 10 mg/ml BSA or poly-L-glutamic acid (15,000–30,000 molecular weight, Sigma-Aldrich, USA).

2.5. DNA Constructs for Magnetic Tweezers

1. Supercos1 plasmid DNA (Stratagene, The Netherlands). The plasmid contains two nicking sites *Bbv*CI.
2. pbluescrIISK plasmid DNA (Stratagene, The Netherlands).
3. λ-phage DNA (Promega, The Netherlands).
4. LB (per l): 10 g bacto-tryptone, 5 g bacto-yeast extract, 10 g NaCl. Adjust the pH to 7.0 and autoclave to sterilize.
5. Midi kit: Qiafilter plasmid midi kit (Qiagen, Germany).
6. Restriction enzymes and buffers (New England Biolabs, MA, USA): *Mlu*I, *Xho*I, *Not*I.
7. Gel extraction kit: Nucleospin extract II kit (Macherey-Nagel, Germany).
8. PCR primers (for sequences *see* **Section 3.2**).
9. bio-dUTP: Bio-16-dUTP (biotin-16-2′-deoxyuridine-5′-triphosphate) (Roche, The Netherlands).
10. dig-dUTP: Dig-11-dUTP (digoxigenin-11-2′-deoxyuridine-5′-triphosphate) (Roche, The Netherlands).
11. T4 DNA ligase and buffer (New England Biolabs, MA, USA).
12. Go taq polymerase kit (Promega, WI, USA).
13. Phase lock tubes (Eppendorf, Germany).
14. Phenol:chloroform:isoamylalcohol: (49.5:49.5:1) (J.T. Baker, NJ, USA).
15. TE: 10 mM Tris–HCl, pH 8, 1 mM EDTA.

2.6. Superparamagnetic Beads

We employ streptavidin-coated Dynal MyOne beads (Invitrogen, USA) for most measurements. MyOne beads have a nominal diameter of 1.05 μm and exhibit good homogeneity in size and magnetic content, such that the variation in stretching forces from bead to bead is less than 5–10%. For measurements with higher stretching forces (see below), we also use streptavidin-

coated ≈ 1 μm diameter MagSense beads (MagSense, IN, USA), which have a higher content of magnetic material, or streptavidin-coated Dynal M280 beads (Invitrogen, USA), which have a diameter of 2.8 μm.

2.7. Topoisomerase Stocks

Topoisomerases can be purchased commercially or purified following overexpression in-house (6, 8). We routinely use human TopIB purchased from Topogen (TopoGEN, FL, USA). It is also available from Inspiralis (Inspiralis, UK).

3. Methods

3.1. Assembly of Flow Cells for Magnetic Tweezers

Flow cells are made from microscope cover slides on the top and bottom with a parafilm spacer in the middle. The bottom slides are coated with a layer of polystyrene to enhance the absorption of anti-digoxigenin antibodies that are used to specifically bind functionalized DNA molecules to the surface (*see* **Note 2**).

1. Drill holes in the microscope cover slips that are going to be the top slides for the flow cells. The holes are required for the fluid inlets and outlets to the cell (*see* **Note 3**).
2. Clean the top slides by sonication for 10 min in ethanol or isopropyl alcohol. Blow dry with compressed air or nitrogen stream.
3. Rinse the bottom slides with deionized MilliQ water. Blow dry with compressed air or nitrogen stream.
4. Coat the bottom slides with polystyrene: Fill the bottom of a small glass beaker with polystyrene solution. Rinse a thick 70 × 24 microscope cover slide with MilliQ water, blow dry with compressed air or nitrogen, and place in the beaker. Coat the bottom slides by dipping them into the beaker with tweezers and using the surface tension between the glass slides to evenly cover one surface with the polystyrene solution. Place the slides with the coated surface facing up into a glass Petri dish.
5. Heat the coated bottom slides in an oven at 100°C for 60 min.
6. Cut out spacers from a double layer of parafilm that form the reaction chamber of the flow cell, with channels that will connect to the holes of the top slide. This is easily done using a scalpel and a metal mould (*see* **Note 4**).

7. Assemble the flow cells: Place the parafilm spacers on the polystyrene-coated side of the bottom slides and close the top with the cleaned top slides. Using tweezers, place the assembled cell on a heater plate set to 80–100°C for ≈5 min (*see* **Note 5**). Allow the cells to cool off for a few minutes at room temperature.
8. Fill the flow cells with anti-digoxigenin solution using a standard pipette.
9. Cover the inlet and outlet holes with small pieces of parafilm.
10. Store the readymade flow cells in plastic Petri dishes, with a small piece of paper towel or Kimwipe soaked with MilliQ water to keep the cells from drying out. Seal the Petri dishes with parafilm.
11. Incubate for at least 12 h at 4°C (*see* **Note 6**).
12. Prior to mounting the cell, clean the microscope objective and apply a drop of objective oil, if an oil immersion objective is used.
13. Mount the flow cell on the magnetic tweezers microscope and connect the syringe pump to the outlet channel. Check the flow cell for leaks.
14. Passivate the flow cell surface by adsorbing inert proteins: Load into the flow cell BSA or poly-L-glutamic acid solution and incubate for 15–30 min to passivate the part of the surface not occupied by the nucleic acid attachment points (6, 19–22) (*see* **Note 7**).

3.2. Preparation of the Magnetic Tweezers DNA Constructs

The DNA construct described here is ≈21 kb in length, which corresponds to a contour length of ≈7 μm. Longer or shorter molecules can be used, depending on the requirements of particular measurements. To reduce the noise on traces and observe single steps in great detail, shorter constructs will improve the signal-to-noise ratio on the time traces (23). In contrast, for the determination of the step size distribution (see below), it is advantageous to use fairly long constructs so that a larger number of supercoils can be initially introduced. A long construct with a large number of initial supercoils reduces the bias of the distributions stemming from the finite number of supercoils (24). The ≈21 kb construct described here presents a compromise between the two requirements. The protocol can be modified to generate longer or shorter DNA constructs by using the same labeled ends and by changing the DNA construct that is used for the middle portion of the tether (Supercos1-lambda1,2 in this protocol) by a longer or shorter DNA construct.

3.2.1. Construction of the Supercos1-Lambda1,2 Vector

1. Digest the Supercos1 plasmid with *Mlu*I to delete the *Mlu*I fragment and then self-ligate the backbone of the plasmid. (This will remove one *Bbv*CI nicking site.) Transform the ligation product into *Escherichia coli* and recover the plasmid DNA, designated Supercos1-*Mlu*I.
2. Amplify a 9.5-kb lambda fragment by PCR using the forward primer 5′ AAGGAAAAAA GCGGCCGCTACATCTCGAG ATGGTGCATCCCTCAAAACGAG and the reverse primer 5′ GGAAAGGGCCCGTAAAGTGATAATGATTATCATC, and λ-phage DNA as the template DNA.
3. Digest the Supercos1-*Mlu*I plasmid with *Not*I and ligate the PCR product from step 2 into the cut plasmid. After recovering the ligation product in *E. coli* and isolating the plasmid DNA from *E. coli* clones, select clones having the orientation where the *Not*I site is 10 kb away from the *Bbv*CI site, designated Supercos1-lambda1-1.
4. Amplify a 5-kb lambda fragment by PCR using the forward primer 5′ TTGGCGCGC TTGATACATCAACTGCACCT-GATATTG and the reverse primer 5′ CCAGATCT ACGA CCTGCATAACCAGTAAG, and λ-phage DNA as the template DNA.
5. Digest the Supercos1-lambda1-1 plasmid from step 3 with *Bss*HII and *Bgl*II and ligate the PCR product from step 4 into the cut plasmid. Recover the ligation product into *E. coli*. This plasmid is designated Supercos1-lambda1,2.

3.2.2. Construction of the DNA Construct for Labeling

1. Inoculate the *E. coli* harboring the Supercos1-lambda1,2 plasmid into 100 ml of LB medium and grow overnight at 37°C.
2. Pellet the culture and isolate the plasmid DNA using the low copy protocol from the midiprep kit.
3. Digest approximately 18 μg of the Supercos1-lambda 1,2 plasmid with *Xho*I and *Not*I in NEB buffer 3, supplemented with BSA, according to the manufacturer's instructions. (The expected fragment lengths are 20,666 and 12 bp, which can be verified by gel electrophoresis.)
4. Purify the 20.6-kb fragment from the digest in step 3 using the gel extraction kit.

3.2.3. Preparation and Ligation of the Biotin and Digoxigenin Handles

1. Set up two PCR reactions to produce the biotin and digoxigenin fragments using the pbluescrIISK+ as the template DNA: In 50 μl volumes, make the PCR reaction solutions containing 0.2 μM forward primer 5′ GACCGAGATAGGGTTGAGTG, 0.2 μM reverse primer 5′ CAGGGTCGGAACAGGAGAGC, 0.2 mM dNTP, 100 ng of the pbluescrIISK+ plasmid DNA, 1X

PCR buffer, and 1 µl of Taq polymerase. To one of the reactions, add bio-dUTP (40 µM final concentration) and to the other reaction add dig-dUTP (40 µM final concentration).

2. Purify the PCR fragments using the gel extraction kit.
3. Determine the concentration of the DNA recovered from step 2 spectrophotometrically.
4. Digest approximately 8 µg of the biotin PCR fragment with *Xho*I according to the manufacturer's instructions. The expected digestion products are 534 and 665 bp.
5. Digest approximately 8 µg of the digoxigenin PCR fragment with *Not*I according to the manufacturer's instructions. The expected digestion products are 624 and 614 bp.
6. Purify the digested fragments from steps 4 and 5 with the gel extraction kit. These are designated the "handle constructs."
7. Determine the concentration of the handle constructs.
8. Ligate the handle constructs to the ends of the 20.6 kb Supercos1-lambda1,2 digested fragment from **Section 3.2.2**, step 5: Prepare the ligation mixture according to the manufacturer's instructions and using 7 µg of the 20.6 kb fragment with approximately a 20-fold molar excess of each of the handle constructs. Ligate overnight at 16°C.
9. Purify the ligation product by phenol:chloroform:isoamylalcohol extraction in phase-lock tubes and finally precipitate the DNA with ice-cold absolute ethanol.
10. Pellet the DNA from step 9 and resuspend the pellet in ~50 µl of TE to give a stock solution that is ~0.1 ng/µl. This is designated the "magnetic tweezers construct DNA" stock.

3.3. Preparation of Magnetic Beads and DNA for Magnetic Tweezers Measurements

3.3.1. Assembly of Tethered DNA Constructs in the Flow Cell

1. Sonicate the MyOne beads for 5 min.
2. Take an aliquot of 2 µl of the MyOne beads and dilute it with 10 µl of PBS. Wash twice with 10 µl of PBS using a magnetic pipette aid and resuspend in 10 µl of PBS.
3. Dilute 1 µl of the magnetic tweezers construct DNA stock from **Section 3.2**, step 10, into 50 µl of TE (*see* **Note 8**).
4. Add ca. 1–2 µl of the diluted DNA construct to the washed beads (*see* **Notes 9** and **10**).
5. Incubate the bead–DNA mixture for 15–30 min at room temperature.
6. Dilute the DNA–bead mixture into 100–300 µl PBS and load ca. 100 µl into the flow cell (*see* **Note 11**).

7. Incubate the beads in the flow cell for 30–60 min (*see* **Note 12**).
8. Flush the flow cell with ca. 1 ml of PBS. Most of beads will be flushed out and a small fraction of beads will remain either stuck to the surface through unspecific interactions or tethered to the surface through the DNA. Ideally, the density of beads is such that there are one to a few stuck and tethered beads per field of view.
9. Move the magnets down to within 1–2 mm of the flow cell surface to apply a stretching force to the tethered beads (*see* **Note 13**).

3.3.2. Calibration of the Tethered DNA in the Magnetic Tweezers

1. Search for coilable molecules in the flow cell. By introducing 30–60 turns of the magnets at a force of ≈ 0.25 pN (*see* **Section 1.4** on how to determine the stretching forces), one can test whether a tethered molecule is coilable. By comparing the behavior under positive and negative turns at forces of ≈ 1 pN, it can be checked whether the molecules are attached by a single or multiple tether. Additionally, appropriate fixed beads stuck to the bottom surface need to be identified, which can serve as a reference bead. Instead of using unspecifically attached magnetic beads as reference markers, it can be beneficial to use non-magnetic (e.g., polystyrene) beads as reference beads.
2. Record look-up tables for the z-position tracking and verify that the tethered and reference beads can be tracked by the tracking software (*see* **Section 1**).
3. Flush in the topoisomerase reaction buffer, without the enzyme added.
4. Run a rotation curve (measurement of the DNA extension as a function of the number of turns) at a stretching force of ≈ 0.25 pN to determine the number of turns at which the extension is maximal and at which the DNA molecule is torsionally relaxed. Define this point as "zero turns." For this step, it is useful to fit the rotation curve locally with a parabola or Gaussian to determine the center position (*see* **Note 14**).
5. Record a force–extension curve: At a series of ~ 10 magnet positions, determine the average extension of the molecule from the z-trace. In addition, at each magnet position determine the stretching force from the fluctuations in the x or y position, as described in **Section 1.4**. Fit the resulting force-extension data by the worm-like chain equation using the polynomial approximation by Bouchiat et al. (25). The fitted values of the persistence length should be ≈ 50 nm (in practice, values in the range 45–55 nm are acceptable), and

the fitted contour length should be close (typically within 10%) to the value expected for the DNA construct that is used in the measurements, using the relationship $L_{DNA} = 0.34$ Å*bp.

6. Record a number of rotation curves of the DNA molecule at different forces, where the forces included should correspond to forces at which data of topoisomerase activity are desired (*see* **Fig. 7.3** for examples of rotation curves). For each of these curves, determine the slope of the rotation curves in μm/turn by fitting a straight line to the slope of the rotation curve in the plectonemic supercoiling region (**Fig. 7.3**, solid lines) (*see* **Note 14**).

3.4. Monitoring DNA–Topoisomerase IB Interactions

1. Flush in TopIB at a concentration of 0.5–20 nM in topoisomerase reaction buffer.
2. Adjust the magnets to exert the desired pulling force and rotate the DNA molecule into the plectonemic regime.
3. Track the bead's position to obtain a time trace with stepwise increases in the DNA extension (**Fig. 7.4A**; these length changes are below referred to as "steps"). Troubleshooting strategies in case too many or two few events are observed are outlined in **Notes 15–18**.

3.5. Analysis of Topoisomerase IB Time Traces

The time traces of topoisomerase activity (**Fig. 7.4A**) should be saved in an appropriate format, e.g., as ASCII text files. We further analyze the time traces offline to quantitatively dissect different aspects of TopIB activity. An analysis that has revealed important fundamental mechanistic aspects of topoisomerase enzymatic activity is to determine step size histograms, i.e. the distribution of the number of supercoils relaxed in individual steps (6, 7).

1. To analyze the step sizes, first identify all of the steps due to topoisomerase activity in the time traces of DNA extension (**Fig. 7.4A**). The steps can be identified using a sliding average window after low-pass filtering (6). Alternatively, use the algorithm developed by Kerssemakers et al. that detects steps in time traces without any a priori assumptions about the step size (26) (solid lines in **Fig. 7.4A**) (*see* **Note 19**).
2. Convert the changes in DNA extension determined from the steps in the time traces to changes in linking number per step, ΔL_k. The slope of the rotation curve, recorded at the appropriate force, in the linear plectonemic regime (**Fig. 7.3**, solid lines) gives the necessary conversion factor (in μm/turn).
3. The step size histograms for TopIB are well described by exponential distributions of the form

$$P\Delta(L_k) = exp\frac{-\Delta L_k}{\langle \Delta L_k \rangle} \quad [6]$$

where $\langle \Delta L_k \rangle$ is the mean number of supercoils removed per step. To obtain an unbiased estimate of the step size distribution and of $\langle \Delta L_k \rangle$, correct for the finite number of initial supercoils using the method of Koster et al. (24) (*see* **Note 20**).

4. By repeating the same analysis (steps 1–3) for time traces recorded at different stretching forces, establish the relationship between $\langle \Delta L_k \rangle$ and the stretching force. This provides further insights into the mechanism of topoisomerase activity (6, 7).

Time traces of topoisomerase activity can be analyzed in a number of other ways, to quantitatively determine additional parameters and to reveal various further aspects of their mechanism. If time traces with sufficient temporal resolution were recorded, individual steps can be analyzed to determine the velocity of supercoil removal (6). This kind of analysis has provided particular valuable insights into the effects of TopIB inhibitors of the camptothecin class of chemotherapeutics on TopIB function (8, 27). In addition, time traces can be analyzed to determine the time between DNA cleavage and religation. This analysis, too, has been particularly useful to study the action of camptothecin-type TopIB inhibitors. The details of these analyses depend on the particular scientific question under study and are detailed in the literature.

4. Notes

1. Commercial MT systems that supply complete systems have recently become available (www.picotwist.com).
2. We typically prepare batches of five to ten flow cells at once. The cells can be stored at 4°C for several weeks without noticeable degradation. Each cell can last for several days of magnetic tweezers measurements.
3. We use a 190-070 Microetcher II sandblaster (Great Lake Orthodontics, NY, USA) to drill the holes.
4. A single layer of parafilm could be used if a particularly thin flow cell with a reduced volume is desired.
5. Pay attention that (1) the flow cell is well sealed, (2) the parafilm does not close off the holes that connect to the inlet and outlet, and (3) the glass slides are well aligned. To

ensure a good seal, it is recommended to stroke out bubbles in the parafilm using a large cotton swab. Poorly aligned glass slides can cause breaking and leaking of the cell upon mounting in the microscope.

6. The flow cells can be stored at 4°C for several weeks without noticeable degradation.
7. Alternatively, a monolayer composed of PEG and biotinylated PEG has been successfully used to reduce unspecific interactions between the inner surface and the components of the system (21). In addition, our laboratory has used nitrocellulose-based passivation of the flow cell surface (22), which is characterized by the ease of its preparation as well as high density of nucleic acid tethers.
8. The DNA suspended in TE buffer can be stored at 4°C for several weeks without significant degradation.
9. The amount of DNA added in this step can be adjusted: If the yield of tethered beads in the flow cell is very low, the amount of DNA added in this step should be increased. If many beads are tethered through multiple DNA molecules, the amount of DNA should be reduced.
10. When handling DNA constructs avoid unnecessary pipetting, as this can result in breaking or nicking of the DNA, in particular for long DNA constructs. Instead, mix solutions by shaking or gentle vortexing.
11. The dilution factor and amount loaded into the flow cell in this step can be adjusted, depending on the amount of beads present in the flow cell after the final incubation.
12. The surface of the flow cell should be covered with beads at this stage.
13. At pulling forces of $\geq$1 pN, tethered beads can easily be distinguished from beads stuck to the surface of the bottom slide by their different heights in the focus.
14. A Matlab (The Mathworks, USA) routine for this purpose is available from the authors upon request.
15. If there are no or too few stepping events during the tracking of the bead, we recommended to periodically (every 20–40 min) check for sticking of the bead and DNA to the surface. This can be accomplished by quickly changing the stretching force to a higher value ($\approx$5–10 pN). The bead should assume its new equilibrium position (at larger distances from the flow cell surface) almost instantaneously. If this is not the case, the flow cell surface should be treated with (additional) poly-L-glutamic acid (*see* **Section 3.1**) or a new flow cell should be used. If the rate of stepping events is very low ($<$1 step per $\sim$5 min) and if sticking has been excluded as a possible cause,

fresh topoisomerase reaction buffer containing TopIB solution should be flushed into the cell. If the event rate remains very low, a higher concentration of TopIB can be employed.

16. If there are too many stepping events: If the stepping events are observed in very short succession or if the molecule becomes uncoilable after introduction of TopIB, the data are uninterpretable as several TopIB molecules likely act on the DNA at the same time. Such "bursts" of activity are sometimes observed after introducing fresh TopIB-containing buffer. If the behavior persists after waiting for ~5 min, TopIB can be removed from the flow cell by flushing with a high-salt buffer (e.g., 1 M NaCl) and the TopIB concentration in the topoisomerase reaction buffer should be reduced.
17. The stepping behavior can be monitored in the plectonemic regime, i.e., for the range of extensions where the relationship between turns and DNA extension is approximately linear (**Fig. 7.3**). Once TopIB activity has removed all plectonemic supercoils, the DNA molecule needs to be recoiled by rotating the magnets. Recoiling of the magnets can be done manually, by following the online trace, or automatically by programming a threshold for rotation into the tracking routine.
18. Even though topoisomerase activity can sometimes be observed even after overnight incubation in a flow cell, the stepping activity typically decreases over time and it is necessary to flush in fresh TopIB buffer every ~60 min.
19. A Matlab implementation of the algorithm of Kerssemakers et al. is available from the authors upon request.
20. In general, for the accurate determination of step size histograms, it is advantageous to use fairly long DNA constructs, such that a large number of initial supercoils ($\geq$100) can be introduced.

Acknowledgments

We thank the many members of our laboratory who have contributed to the research effort on topoisomerases over the last few years, in particular Jacob W. J. Kerssemakers and Jaap Beekman for technical support. We are grateful to the laboratories of Stewart Shuman (Sloan Kettering Institute, New York, USA) and Mary-Ann Bjornsti (St. Jude Children's Research Hospital, Memphis, USA) for fruitful collaborations on topoisomerase research. Funding is acknowledged from the Dutch Foundation for Research on Matter (FOM), the Nederlandse Organisatie voor Wetenschappelijk Onderzoek (NWO)

via its Vidi program (JL, IDV, and NHD), Nanoned (NHD and IDV), the Human Frontiers Science Program (DAK), the European Science Foundation via a EURYI grant (NHD), and Delft University of Technology (NHD).

References

1. Wang, J. C. (1996) DNA topoisomerases. *Annu Rev Biochem* **65**, 635–692.
2. Champoux, J. J. (2001) DNA topoisomerases: structure, function, and mechanism. *Annu Rev Biochem* **70**, 369–413.
3. Wang, J. C. (2002) Cellular roles of DNA topoisomerases: a molecular perspective. *Nat Rev Mol Cell Biol* **3**, 430–440.
4. Strick, T. R., Allemand, J. F., Bensimon, D., Bensimon, A. and Croquette, V. (1996) The elasticity of a single supercoiled DNA molecule. *Science* **271**, 1835–1837.
5. Strick, T. R., Croquette, V. and Bensimon, D. (2000) Single-molecule analysis of DNA uncoiling by a type II topoisomerase. *Nature* **404**, 901–904.
6. Koster, D. A., Croquette, V., Dekker, C., Shuman, S. and Dekker, N. H. (2005) Friction and torque govern the relaxation of DNA supercoils by eukaryotic topoisomerase IB. *Nature* **434**, 671–674.
7. Taneja, B., Schnurr, B., Slesarev, A., Marko, J. F. and Mondragon, A. (2007) Topoisomerase V relaxes supercoiled DNA by a constrained swiveling mechanism. *Proc Natl Acad Sci USA* **104**, 14670–14675.
8. Koster, D. A., Palle, K., Bot, E. S., Bjornsti, M. A. and Dekker, N. H. (2007) Antitumour drugs impede DNA uncoiling by topoisomerase I. *Nature* **448**, 213–217.
9. Neuman, K. C., Lionnet, T. and Allemand, J. F. (2007) Single-molecule micromanipulation techniques. *Ann Rev Mater Res* **37**, 33–67.
10. Forth, S., Deufel, C., Sheinin, M. Y., Daniels, B., Sethna, J. P. and Wang, M. D. (2008) Abrupt buckling transition observed during the plectoneme formation of individual DNA molecules. *Phys Rev Lett* **100**, 4.
11. Strick, T., Dessinges, M.-N., Charvin, G., Dekker, N. H., Allemand, J.-F., Bensimon, D. and Croquette, V. (2003) Stretching of macromolecules and proteins. *Rep Prog Phys* **66**, 1–45.
12. Bryant, Z., Stone, M. D., Gore, J., Smith, S. B., Cozzarelli, N. R. and Bustamante, C. (2003) Structural transitions and elasticity from torque measurements on DNA. *Nature* **424**, 338–341.
13. Strick, T., Allemand, J., Croquette, V. and Bensimon, D. (2000) Twisting and stretching single DNA molecules. *Prog Biophys Mol Biol* **74**, 115–140.
14. Strick, T. R., Dessinges, M. N., Charvin, G., Dekker, N. H., Allemand, J. F., Bensimon, D. and Croquette, V. (2003) Stretching of macromolecules and proteins. *Rep Prog Phys* **66**, 1–45.
15. Gosse, C. and Croquette, V. (2002) Magnetic tweezers: micromanipulation and force measurement at the molecular level. *Biophys J* **82**, 3314–3329.
16. Cheezum, M. K., Walker, W. F. and Guilford, W. H. (2001) Quantitative comparison of algorithms for tracking single fluorescent particles. *Biophys J* **81**, 2378–2388.
17. Gelles, J., Schnapp, B. J. and Sheetz, M. P. (1988) Tracking kinesin-driven movements with nanometre-scale precision. *Nature* **331**, 450–453.
18. Ribeck, N. and Saleh, O. A. (2008) Multiplexed single-molecule measurements with magnetic tweezers. *Rev Sci Instrum* **79**, 094301.
19. Abels, J. A., Moreno-Herrero, F., van der Heijden, T., Dekker, C. and Dekker, N. H. (2005) Single-molecule measurements of the persistence length of double-stranded RNA. *Biophys J* **88**, 2737–2744.
20. Fulconis, R., Mine, J., Bancaud, A., Dutreix, M. and Viovy, J. L. (2006) Mechanism of RecA-mediated homologous recombination revisited by single molecule nanomanipulation. *Embo J* **25**, 4293–4304.
21. Kruithof, M., Chien, F., de Jager, M. and van Noort, J. (2008) Subpiconewton dynamic force spectroscopy using magnetic tweezers. *Biophys J* **94**, 2343–2348.
22. Skinner, G. M., Baumann, C. G., Quinn, D. M., Molloy, J. E. and Hoggett, J. G. (2004) Promoter binding, initiation, and elongation by bacteriophage T7 RNA polymerase. A single-molecule view of the transcription cycle. *J Biol Chem* **279**, 3239–3244.

23. Revyakin, A., Ebright, R. H. and Strick, T. R. (2005) Single-molecule DNA nanomanipulation: improved resolution through use of shorter DNA fragments. *Nat Methods* **2**, 127–138.
24. Koster, D. A., Wiggins, C. H. and Dekker, N. H. (2006) Multiple events on single molecules: unbiased estimation in single-molecule biophysics. *Proc Natl Acad Sci USA* **103**, 1750–1755.
25. Bouchiat, C., Wang, M. D., Allemand, J., Strick, T., Block, S. M. and Croquette, V. (1999) Estimating the persistence length of a worm-like chain molecule from force-extension measurements. *Biophys J* **76**, 409–413.
26. Kerssemakers, J. W., Munteanu, E. L., Laan, L., Noetzel, T. L., Janson, M. E. and Dogterom, M. (2006) Assembly dynamics of microtubules at molecular resolution. *Nature* **442**, 709–712.
27. Koster, D. A., Czerwinski, F., Halby, L., Crut, A., Vekhoff, P., Palle, K., Arimondo, P. B. and Dekker, N. H. (2008) Single-molecule observations of topotecan-mediated TopIB activity at a unique DNA sequence. *Nucleic Acids Res* **36**, 2301–2310.

Chapter 8

Dissolution of Double Holliday Junctions by the Concerted Action of BLM and Topoisomerase IIIα

Csanád Z. Bachrati and Ian D. Hickson

Abstract

In eukaryotic cells, topoisomerase III forms an evolutionarily conserved complex with a RecQ family helicase and two OB-fold containing proteins, replication protein A (RPA) and RMI1. One role for this complex is to catalyze the completion of homologous recombination reactions in which the recombining DNA molecules are covalently interlinked by a double Holliday junction structure. This process, which requires the single-stranded DNA decatenation activity of topoisomerase III, is termed Holliday junction "dissolution" to distinguish it from Holliday junction "resolution" catalyzed by endonucleases (resolvases) that simply cleave the four-way junction. Holliday junction dissolution gives rise exclusively to non-cross-over recombinant products, which would have the effect of suppressing sister chromatid exchanges and loss of heterozygosity between homologous chromosomes. In this chapter, we provide a detailed experimental protocol for the preparation of an oligonucleotide-based, double Holliday junction substrate and for the biochemical analysis of dissolution in vitro.

Key words: Double Holliday junction dissolution, Bloom's syndrome helicase, topoisomerase IIIα.

1. Introduction

Topoisomerase III is a type IA topoisomerase that cleaves single strands of DNA and forms a transient covalent linkage to the 5′ end of the cut DNA (1). In nearly all species, topoisomerase III cooperates with a 3′–5′ DNA helicase of the RecQ family; for example, RecQ in *Escherichia coli*, Sgs1 in *Saccharomyces cerevisiae*, Rqh1 in *Schizosaccharomyces pombe*, and BLM in human cells (2). BLM is the protein defective in Bloom's syndrome, a disorder associated with growth retardation, skin abnormalities, fertility defects, and cancer predisposition (3). Mutants lacking RecQ

D.J. Clarke (ed.), *DNA Topoisomerases*, Methods in Molecular Biology 582,
DOI 10.1007/978-1-60761-340-4_8,

helicases or topoisomerase III exhibit dysregulated homologous recombination and DNA replication defects (2, 4). Recently, it has become clear that these proteins also associate with the major ssDNA binding factor in each species (e.g. SSB in *E. coli* and RPA in eukaryotes) (2, 5) and in eukaryotes, with a more poorly conserved, OB-fold-containing factor called RMI1 (or BLAP75 in humans) (6–8). That these factors co-operate in vivo is clear from the wealth of genetic data that exist linking their function. For example, *top3* or *rmi1* mutants in *S. cerevisiae* grow very poorly, but this phenotype is suppressed by deletion of *SGS1* (9). Mutants lacking topoisomerase III or RMi1 in yeast accumulate X-shaped DNA structures that require homologous recombination factors for their generation (10). These and other data, including the existence of excessive numbers of sister chromatid exchanges in cells lacking Sgs1 (11), BLM (12), or topoisomerase III (13), led us to propose previously that the RecQ helicase/topoisomerase III combination acts to disentangle homologous recombination intermediates containing Holliday junctions. Consistent with this, human BLM can promote branch migration of Holliday junctions (14) and topoisomerase III binds with high affinity to such structures (our unpublished observation). Moreover, we showed that the combination of BLM and human topoisomerase IIIα (the isoform that binds BLM; topoisomerase IIIβ does not apparently bind) could disentangle unlinked DNA molecules containing two adjacent Holliday junctions through a combination of BLM-mediated, convergent, Holliday junction branch migration and topoisomerase IIIα-mediated decatenation of the resulting hemicatenane (15, 16). The mechanism of this reaction, which we termed Holliday junction dissolution (15), is such that junctions are eliminated without the potentially deleterious generation of so-called cross-over products, where the DNA flanking the original sites of the junctions is exchanged. Crossing-over in cells can be responsible for genomic instability in that it leads to sister chromatid exchanges and loss of heterozygosity in diploid organisms by recombining maternal and paternal homologous chromosomes. Subsequently, we and others showed that RMI1 strongly stimulates the dissolution reaction (17, 18). The mechanism of this stimulation appears to be via an ability to promote the loading of topoisomerase IIIα onto the substrate (17).

Here, we provide a step-by-step guide to the generation of double Holliday junction-containing DNA molecules and to the assaying of BLM/topoisomerase IIIα/RMI1 for Holliday junction dissolution activity. The procedures outlined below utilise an oligonucleotide-based double Holliday junction substrate described by Wu and Hickson (15) (**Fig. 8.1**). It is also possible to generate plasmid-sized DNA molecules containing a double Holliday junction using the elegant and elaborate procedure of Plank and Hsieh (19). Generation of this plasmid-based molecule,

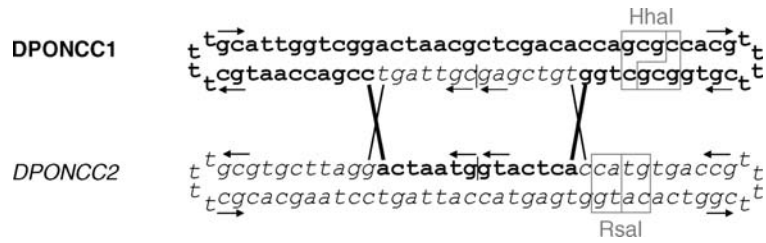

Fig. 8.1 **Schematic representation of the double Holliday junction substrate.** The oligonucleotides DPONCC1 and DPONCC2 are depicted in *bold* and *italics*, respectively. 5′–3′ orientation of the oligonucleotides is indicated by *small arrows*. Small *vertical black lines* denote the 5′/3′ boundaries of the two oligonucleotides, which are sealed during the ligation step of substrate preparation (**Section 3.1.3**). The RsaI and HhaI restriction endonuclease recognition sites and their respective cleavage positions are shown in *grey*.

however, requires the use of reagents that are not commercially available. Therefore, we focus here on the oligonucleotide-based substrate.

2. Materials

2.1. Substrate Preparation

1. 1 M Tris–HCl, pH 7.5.
2. 1 M $MgCl_2$.
3. 1 M DTT.
4. 100 mM ATP.
5. Oligonucleotides for the DHJ substrate: DPONCC1 and DPONCC2, phosphorylated and non-phosphorylated (*see* **Note 1**). DPONCC1: 5′-GTAATCACCG ACCAATGCTT TTGCATTGGT CGGACTAACG CTCGACACCA GCGC CACGTT TTCGTGGCGC TGGACTCATG-3′, DPO NCC2: 5′-CGTTAGTGGA TTCGTGCGTT TTCGCAC-GAA TCCTGATTAC CATGAGTGGT ACACTGGCTT TTGCCAGTGT ACCTGTCGAG-3′ (20) (**Fig. 8.1**).
6. T4 polynucleotide kinase (T4 PNK). Supplied with the manufacturer's 10X reaction buffer.
7. 1 mg/ml bovine serum albumin (BSA); molecular biology grade. Usually supplied with restriction endonucleases, but can be purchased separately.
8. γ^{32}P-ATP, 0.37 MBq/µl, 111 TBq/mmol (10 µCi/µl, 3000 Ci/mmol).
9. Sephadex G50-based microcentrifuge spin column (such as the mini Quick Spin DNA Columns of Roche Diagnostics, Indianapolis, IN, USA).

10. Mineral oil. Standard molecular grade oil typically used to overlay PCR reactions.
11. High concentration T4 DNA ligase (2000 units/μl, available from New England Biolabs) (*see* **Note 5**).
12. Dialysis cassette, such as the D-Tube Dialyzer midi from Novagen. A D-tube electroelution support tray is available separately also from Novagen.

2.2. Dissolution Reaction

1. 10X reaction buffer: 660 mM K-acetate (*see* **Note 12**), 330 mM Tris–acetate, pH 7.8 (adjust pH with KOH), 1 mM DTT. Stored in 100 μl aliquots at –20°C.
2. Further buffer components added fresh before each reaction (final concentration): 10 mM Mg-acetate, 100 mM Mg-acetate, 100 mM ATP, 10 mg/ml BSA.
3. HhaI and RsaI restriction enzymes.
4. Stop solution: 5% SDS, 50 mM EDTA, pH 8.0.
5. 100 mg/ml proteinase K.
6. BLM protein (*see* **Note 16**).
7. Topo3α protein (*see* **Note 16**).

2.3. Electrophoresis and Detection

1. 10X Tris–borate–EDTA gel electrophoresis running buffer (10X TBE): 890 mM Tris–borate and 20 mM EDTA, pH 8.3.
2. 40% acrylamide:bis-acrylamide (19:1).
3. 10% ammonium persulfate (APS): Prepared in Milli Q water, and stored in 400 μl aliquots at –20°C.
4. 10X non-denaturing loading dye: 50% glycerol, 100 mM Tris–HCl, pH 7.5, 50 mM EDTA, 0.05% bromophenol-blue, 0.05% xylene-cyanol, 0.05% Orange G.
5. 2X denaturing loading dye: Mix 950 μl formamide with 50 μl 6X non-denaturing loading dye.
6. X-ray film: Double sided is recommended, such as the Bio-Max MS film from Kodak.

3. Methods

3.1. Preparation of Substrates

3.1.1. Labelling the Oligonucleotides

1. Label 10 pmol of non-phosphorylated DPONCC1 or DPONCC2 (*see* **Notes 1** and **2**):
   (i) In a screw-cap microcentrifuge tube, add 10 pmol of DPONCC1 and adjust the volume to 5 μl with ddH_2O.

(ii) Boil for 5 min and then chill on ice for 5 min (*see* **Note 3**).

(iii) Centrifuge briefly to collect the liquid at the bottom of the tube.

(iv) While keeping on ice, add in order: 1.5 µl of 10X PNK buffer, 1.5 µl of 1 mg/ml BSA, 5 µl of γ^{32}P-ATP, and 1.5 µl of T4 PNK (15 units).

(v) Mix the contents and incubate at 37°C for 60 min.

2. Separate the labelled oligonucleotides from the non-incorporated γ^{32}P-ATP using a microcentrifuge spin column according to the manufacturer's instructions, keeping the elution volume low. Measure the elution volume. Save 1 µl of the labelled oligonucleotide.

3.1.2. Annealing the Oligonucleotides

1. Add 30 pmol of the phosphorylated complementary oligonucleotide to the labelled oligonucleotide from **Section 3.1.1**; that is, if you labelled DPONCC1, add p-DPONCC2 and vice versa (*see* **Note 1**).
2. Add 5 µl of 1 M Tris–HCl, pH 7.5 (to 50 mM final), and 1 µl, 1 M $MgCl_2$ (to 10 mM final).
3. Adjust the volume to 100 µl and overlay with mineral oil.
4. Set up the annealing reaction (ideally late in the working day) as follows:

(i) Bring to boil about 1800 ml of water in a 2 l glass beaker.

(ii) Transfer the beaker into a polystyrene box that can easily accommodate it (*see* **Note 4**).

(iii) Place the tube with the annealing mixture from step 3 into a polystyrene tube rack and float it on the surface of the hot water.

(iv) Close the polystyrene box with its lid. The box will provide efficient insulation to allow the hot water to cool very slowly to room temperature overnight.

3.1.3. Ligation of the Oligonucleotides

1. Remove the annealing reaction from the polystyrene box.
2. Add 1 µl of 100 mM ATP (to 1 mM final) and 0.5 µl of 1 M DTT (to 5 mM final) (*see* **Note 5**). Mix carefully (*see* **Note 6**).
3. Adjust the water temperature in the annealing chamber to 16°C.
4. Add 3.5 µl of high concentration T4 ligase to the annealing mixture, and mix carefully (*see* **Note 6**).
5. Close the lid of the polystyrene box and allow the ligation to proceed for approximately 24 h.

3.1.4. Casting the Denaturing Gel

The following instructions assume the use of a Bio-Rad Protean II xi/XL large vertical gel electrophoresis apparatus, but any other similar system can be used.

1. Clean the glass plates with detergent and, after thorough rinsing, wipe with ethanol.
2. Assemble the plates with the clamps into a sandwich using 1 mm spacers paying careful attention to the correct alignment of the spacers and glass plates at the bottom to prevent leakage.
3. Prepare 50 ml of gel solution for an 8% denaturing gel: Dissolve 25 g of urea in a mixture of 15.8 ml of Milli Q H_2O, 10 ml of 40% acrylamide:bis-acrylamide (19:1), and 5 ml of 10X TBE (*see* **Note 7**). Warm the mixture slightly to aid the dissolving of the urea.
4. When the urea has dissolved, de-gas the mixture under vacuum for about 10 min (*see* **Note 8**). Meanwhile, make sure that everything is at hand to cast the gel (glass plate assembly, comb, glass pipettes, and pipette aid).
5. Add 400 µl of APS and mix with gentle swirling. Add 20 µl of TEMED and mix quickly again with gentle swirling (*see* **Note 8**). In a 25 ml glass pipette, draw up about 30–35 ml of gel solution (or as much as it can safely take). Gently pipette the solution in between the glass plates on one side, close to the spacer. The liquid will sink to the bottom, and if the plates are clean enough, no bubbles will form. Fill the glass plate assembly close to the top edge. Immediately insert the comb (*see* **Note 9**).
6. Allow the gel to polymerise for at least 20 min.
7. Assemble the gel tank and the gel, and fill the reservoirs with 1X TBE. Remove the comb, and flush the wells gently with a Pasteur pipette. Pre-run the gel for about 30 min.

3.1.5. Gel Purification of the Substrate

1. Remove as much of the mineral oil from the ligated substrate mix as possible (*see* **Note 10**).
2. Add an equal amount (100 µl) of 2X denaturing loading dye.
3. Boil for 3 min, and then cool rapidly in iced water.
4. Flush the wells of the gel again, and then load the sample distributing it between four wells.
5. Run the electrophoresis at 35 mA until the xylene cyanol dye has migrated about 10 cm from the wells.
6. Remove the gel assembly from the tank, and lay it on layers of paper towel (*see* **Note 11**). Remove the clamps and the spacers. Carefully prise open the plates with a flexible spatula or a disused spacer to avoid chipping the plates. The gel should remain stuck to one of the plates.

7. Wrap the gel on the glass plate with Saran wrap. Expose the gel to X-ray film in a dark room for around 3–4 min. Put markers on the X-ray film by marking the corners of the glass plate with a marker pen to aid alignment of the film and the gel in the subsequent steps. Develop the film.
8. Cut out the area of the film that corresponds to the intact substrate with a scalpel. The band representing the intact substrate should be the topmost, about 3 cm from the wells.
9. Align the film with the gel, and using the film as a template, cut out the area of the gel that contains the substrate with a clean scalpel.
10. Lift the cut gel slice and transfer it into a D-Tube dialysis cassette. Fill with 1X TBE. Insert the D-Tube into its support tray with its windows facing sideways. Electroelute in a horizontal gel tank in 1X TBE, at 120 V for 2 h at 4°C. At the end of the electroelution, reverse the polarity of the current for 30 s to dissociate the DNA molecules from the dialysis membrane.
11. Transfer the D-Tube into a floating rack and dialyse against 1000 ml of 10 mM $MgCl_2$, 10 mM Tris–HCl, pH 7.5, at 4°C for at least 2 h, changing the dialysis buffer every 20 min.
12. Transfer the dialysed substrate into screw-capped microcentrifuge tubes in 100 µl aliquots and store at –20°C.
13. Dilute the labelled oligonucleotide you saved in step 2 of **Section 3.1.1** 100-fold in Milli Q H_2O. Measure the radioactivity of 1 µl of purified substrate and 1 µl of labelled oligonucleotide. Assuming 95% recovery from the Sephadex G50 spin column, calculate the approximate chemical concentration of the purified substrate from the above data.

3.2. Double Holliday Junction Dissolution

3.2.1. Enzyme Reaction

1. Assemble substrate mix: For one sample, add 1 fmol of substrate (*x* µl, where *x* is the volume of substrate solution that contains 1 fmol), 0.5 µl of 10X reaction buffer, 0.5 µl of 100 mM ATP, 2-x µl of 10 mM Mg-acetate (*see* **Note 13**); supplement with Milli Q H_2O to 5 µl. Make a master substrate mix by simply mixing multiples of the above volumes for the number of samples.
2. Make up the enzyme mix: For one sample, add 0.5 µl of 10X reaction buffer, 0.2 µl of 100 mM Mg-acetate, 0.1 µl of 10 mg/ml BSA, 1 µl of BLM protein at the required concentration, 1 µl of TOPO3α protein at the required concentration, and 2.2 µl Milli Q H_2O. A master enzyme mix can again be made as required by multiplying the volumes above for the number of samples (*see* **Note 14**).

3. Mix the substrate master mix thoroughly and then warm to 37°C.
4. Mix the enzyme master mix thoroughly, then aliquot 5 μl into reaction tubes. Transfer the tubes to 37°C.
5. As controls, include substrate digested with either HhaI or RsaI (*see* **Note 2**). These enzymes work in the dissolution reaction buffer. Instead of adding BLM and TOPO3α to the enzyme mix, add 0.5 μl of restriction enzyme and adjust the volume of H_2O to 3.8 μl.
6. Start the reaction by the addition of 5 μl of substrate mix. Incubate for 60 min.
7. Stop the reaction by the addition of 2 μl of stop solution.
8. Add 1 μl of 100 mg/ml proteinase K and incubate for a further 20 min.

3.2.2. Electrophoresis and Detection

1. Cast an 8% denaturing gel as before, but use a thinner (0.5 mm) spacer. This will require a slightly lower amount of gel mix: 15 g urea, 6 ml 40% acrylamide:bis-acrylamide 19:1, 3 ml 10X TBE, 9.5 ml Milli Q H_2O, 300 μl APS, and 20 μl TEMED. Otherwise follow the protocol as described in **Section 3.1.4**.
2. Mix the samples with an equal amount of 2X denaturing loading dye (13 μl). Boil for 3 min, snap chill in iced water, and centrifuge briefly.
3. Flush the wells of the gel and load samples.
4. Run the gel at 35 mA until the xylene-cyanol dye is about 10 cm from the wells.
5. Remove gel assembly from the tank and carefully disassemble it on a few sheets of paper towel (*see* **Note 11**).
6. Soak the gel on the glass plate in 500 ml of 10% acetic acid, 10% methanol rocking gently for 20 min at room temperature. Repeat this step with 500 ml of Milli Q H_2O (*see* **Note 15**).
7. Transfer the gel to a sheet of Whatman 3MM paper and dry on a gel dryer under vacuum.
8. Expose to a phosphorimager screen for detection and quantification.

4. Notes

1. Choose the non-phosphorylated oligonucleotide to label and anneal with its phosphorylated counterpart. This assures more efficient substrate building for two reasons: (1) the

forward kinase reaction (that is labelling non-phosphorylated oligonucleotides) is more efficient, and (2) this way only labelled molecules will circularize during the subsequent ligation step.

2. Either oligonucleotide can be labelled, but labelling both is not practical. We usually label DPONCC1 (depicted in bold in **Fig. 8.1**), in which case RsaI digestion, which cuts on DPONCC2 (the strand in italics in **Fig. 8.1**), liberates the labelled, covalently closed circular DPONCC1 molecule. Digesting with HhaI, which cuts DPONCC1, results in a labelled, linear 64-mer oligonucleotide (**Fig. 8.2**).

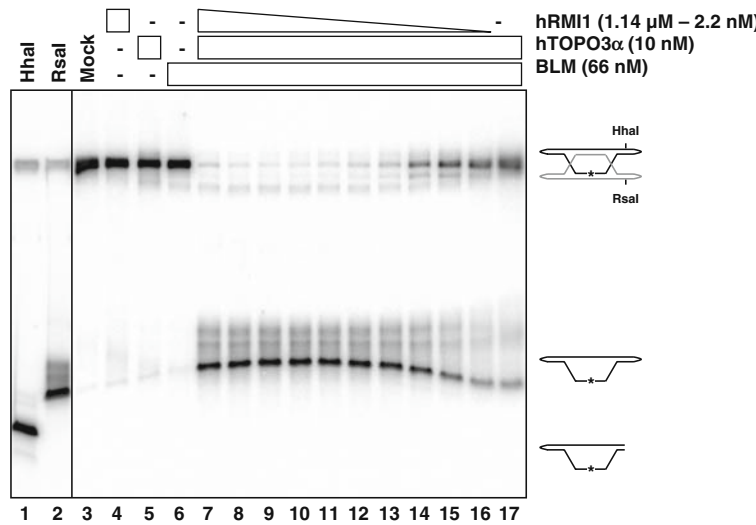

Fig. 8.2. **A typical example of a dissolution reaction showing the concentration-dependent effect of human RMI1.** The dissolution of double Holliday junction requires the concerted action of BLM and topoisomerase IIIα (compare lane 17 with lanes 5 and 6). Human RMI1 stimulates the reaction in a concentration-dependent manner, by modulating the binding of hTOPO3α to the substrate (17). In this experiment, 4 µl aliquots of enzyme mix (containing buffer, BSA, Mg-acetate, hTOPO3α, and BLM, as described in point 2 of **Section 3.2.1**) were added to 1 µl dilutions of hRMI1. Control reactions (lanes 1–6) were assembled separately. The gel also shows the position of the labelled linear DPONCC1 oligonucleotide after digestion with HhaI (lane 1). Digestion of the DPONCC2 oligonucleotide with RsaI releases the labelled circular DPONCC1 molecule, which co-migrates with the product of dissolution (lane 2).

3. These oligonucleotides assume strong secondary structure, which may interfere with T4 PNK. This denaturation step is, therefore, important to achieve efficient labelling.
4. Care must be taken while handling very hot water in large volumes.
5. The manufacturer's supplied ligase buffer is not used in this reaction. The annealing buffer used in the previous step must, therefore, be supplemented with ATP and DTT.

6. The annealing reaction is still overlaid with mineral oil. Pay particular attention to add the reaction components to the aqueous phase, and mix carefully by pipetting. As the mixture is highly radioactive, usage of barrier tips is highly recommended to avoid contamination of the micropipettes at this step.
7. The acrylamide:bis-acrylamide solution is a neurotoxin. Wear appropriate protection when handling it, and also treat the waste as toxic.
8. De-gassing the mixture is necessary to remove oxygen from the solution, which would interfere with polymerization. Also, gentle mixing of APS and TEMED into the mixture prevents the re-entry of oxygen into the solution.
9. After the APS and TEMED are added to the solution, polymerization will start immediately. The subsequent steps, therefore, need to be carried out swiftly. Bubbles can be removed by tapping the plate with a pen, or gently tapping the casting apparatus on the bench.
10. The oil will be contaminated with radioactivity; handle it accordingly.
11. The buffer in both the upper and lower reservoirs of the gel tank is likely to be contaminated with radioactivity. Discard the buffer accordingly. The paper towels are to trap radioactive liquid dripping from the gel assembly.
12. The optimal final concentration of monovalent cations should be around 70 mM for reactions in vitro. At more physiological concentrations (around 140 mM [K^+]), the reaction is largely inhibited and becomes completely dependent on the presence of additional proteins, such as RMI1 (18).
13. The substrate has been dialysed against 10 mM $MgCl_2$. The amount of Mg^{2+} which is subsequently necessary to put into the reaction along with the substrate must be adjusted accordingly.
14. Assembling the reaction in two steps this way allows the concentration of components to be varied (titration) or the effect of other proteins to be studied (**Fig. 8.2**). For example, serial dilutions of BLM can be made in 1 μl volume in the reaction tubes. Four microlitre aliquots of the enzyme master mix, which lacks the BLM component, should be added in this case, and then proceed as normal. Alternatively, the kinetics of the reaction can be followed in a time course experiment: Mix the enzyme and substrate master mixes together, remove 10 μl aliquots at desired time points, and add to reaction tubes already containing 2 μl stop solution. Treat with proteinase K and proceed as normal.

15. This step does not only fix the DNA molecules in the gel but also removes the urea. If the urea is not removed, the gel is liable to cracking during subsequent drying.
16. Purification of BLM (21) and Topo3 (22) recombinant proteins has been extensively described elsewhere.

References

1. Wang, J. C. (2002) Cellular roles of DNA topoisomerases: a molecular perspective. *Nat Rev Mol Cell Biol* **3**, 430–40.
2. Bachrati, C. Z. and Hickson, I. D. (2003) RecQ helicases: suppressors of tumorigenesis and premature aging. *Biochem J* **374**, 577–606.
3. German, J. (1993) Bloom syndrome: a mendelian prototype of somatic mutational disease. *Medicine (Baltimore)* **72**, 393–406.
4. Bachrati, C. Z. and Hickson, I. D. (2008) RecQ helicases: guardian angels of the DNA replication fork. *Chromosoma* **117**, 219–33.
5. Sharma, S., Doherty, K. M., and Brosh, R. M., Jr. (2006) Mechanisms of RecQ helicases in pathways of DNA metabolism and maintenance of genomic stability. *Biochem J* **398**, 319–37.
6. Yin, J., Sobeck, A., Xu, C., Meetei, A. R., Hoatlin, M., Li, L., and Wang, W. (2005) BLAP75, an essential component of Bloom's syndrome protein complexes that maintain genome integrity. *EMBO J* **24**, 1465–76.
7. Mullen, J. R., Nallaseth, F. S., Lan, Y. Q., Slagle, C. E., and Brill, S. J. (2005) Yeast Rmi1/Nce4 controls genome stability as a subunit of the Sgs1-Top3 complex. *Mol Cell Biol* **25**, 4476–87.
8. Chang, M., Bellaoui, M., Zhang, C., Desai, R., Morozov, P., Delgado-Cruzata, L., Rothstein, R., Freyer, G. A., Boone, C., and Brown, G. W. (2005) RMI1/NCE4, a suppressor of genome instability, encodes a member of the RecQ helicase/Topo III complex. *EMBO J* **24**, 2024–33.
9. Mankouri, H. W. and Hickson, I. D. (2007) The RecQ helicase-topoisomerase III-Rmi1 complex: a DNA structure-specific 'dissolvasome'? *Trends Biochem Sci* **32**, 538–46.
10. Mankouri, H. W. and Hickson, I. D. (2006) Top3 processes recombination intermediates and modulates checkpoint activity after DNA damage. *Mol Biol Cell* **17**, 4473–83.
11. Onoda, F., Seki, M., Miyajima, A., and Enomoto, T. (2000) Elevation of sister chromatid exchange in *Saccharomyces cerevisiae* sgs1 disruptants and the relevance of the disruptants as a system to evaluate mutations in Bloom's syndrome gene. *Mutat Res* **459**, 203–9.
12. Chaganti, R. S. K., Schonberg, S., and German, J. (1974) A many-fold increase in sister chromatid exchanges in Bloom's syndrome lymphocytes. *Proc Natl Acad Sci USA* **71**, 4508–12.
13. Ui, A., Seki, M., Ogiwara, H., Onodera, R., Fukushige, S., Onoda, F., and Enomoto, T. (2005) The ability of Sgs1 to interact with DNA topoisomerase III is essential for damage-induced recombination. *DNA Repair (Amst)* **4**, 191–201.
14. Karow, J. K., Constantinou, A., Li, J. L., West, S. C., and Hickson, I. D. (2000) The Bloom's syndrome gene product promotes branch migration of holliday junctions. *Proc Natl Acad Sci USA* **97**, 6504–8.
15. Wu, L. and Hickson, I. D. (2003) The Bloom's syndrome helicase suppresses crossing over during homologous recombination. *Nature* **426**, 870–4.
16. Plank, J. L., Wu, J., and Hsieh, T. S. (2006) Topoisomerase IIIα and Bloom's helicase can resolve a mobile double Holliday junction substrate through convergent branch migration. *Proc Natl Acad Sci USA* **103**, 11118–23.
17. Wu, L., Bachrati, C. Z., Ou, J., Xu, C., Yin, J., Chang, M., Wang, W., Li, L., Brown, G. W., and Hickson, I. D. (2006) BLAP75/RMI1 promotes the BLM-dependent dissolution of homologous recombination intermediates. *Proc Natl Acad Sci USA* **103**, 4068–73.
18. Raynard, S., Bussen, W., and Sung, P. (2006) A double Holliday junction dissolvasome comprising BLM, topoisomerase IIIalpha, and BLAP75. *J Biol Chem* **281**, 13861–4.
19. Plank, J. L. and Hsieh, T. S. (2006) A novel, topologically constrained DNA molecule containing a double Holliday junction: design, synthesis, and initial biochemical characterization. *J Biol Chem* **281**, 17510–6.

20. Fu, T. J., Tse-Dinh, Y. C., and Seeman, N. C. (1994) Holliday junction crossover topology. *J Mol Biol* **236**, 91–105.
21. Karow, J. K., Chakraverty, R. K., and Hickson, I. D. (1997) The Bloom's syndrome gene product is a 3′-5′ DNA helicase. *J Biol Chem* **272**, 30611–4.
22. Goulaouic, H., Roulon, T., Flamand, O., Grondard, L., Lavelle, F. and Riou, J. F. (1999) Purification and characterization of human DNA topoisomerase IIIalpha. *Nucleic Acids Res* **27**, 2443–50.

Chapter 9

ChIP-on-Chip Analysis of DNA Topoisomerases

Rodrigo Bermejo, Yuki-Mori Katou, Katsuhiko Shirahige, and Marco Foiani

Abstract

Here we describe an adapted ChIP-on-chip protocol for the analysis of DNA topoisomerase chromosomal binding in *Saccharomyces cerevisiae* cells. The ChIP-on-chip technique is based on the immunoprecipitation of crosslinked chromatin (ChIP, chromatin immunoprecipitation), followed by DNA amplification and hybridization to high-density oligonucleotide arrays (Chip). Comparison of the signal intensities of immunoprecipitated and control fractions provides a measurement of the protein–DNA association along entire genomes. ChIP-on-chip analysis of DNA topoisomerase binding to chromosomal DNA opens a window to the understanding of the in vivo contribution of these enzymes to the different DNA transactions taking place concomitantly within the context of the highly organized eukaryotic genome. Chromosomal binding profiles obtained from synchronized cells allow scoring the temporal and spatial restriction of these enzymes at different cell cycle stages. By using this approach, novel aspects of DNA topoisomerase function in chromosome metabolism might be unmasked.

Key words: Top1, Top2, chromatin immunoprecipitation, high-density oligonucleotide arrays, *Saccharomyces cerevisiae*.

1. Introduction

In the last decades, in vitro studies on topologically constrained circular DNA molecules have contributed to the characterization of the ability of DNA topoisomerases to relax torsional stress and to promote catenation/decatenation reactions. Structural studies revealed the fundamental mechanistic aspects through which these enzymes interact with DNA molecules and catalyze the breakage/religation steps that change their linkage status. Nevertheless, the way these topological transactions take place in vivo, within the context of the eukaryotic nucleus is largely unknown.

D.J. Clarke (ed.), *DNA Topoisomerases*, Methods in Molecular Biology 582,
DOI 10.1007/978-1-60761-340-4_9,

Eukaryotic chromosomal DNA exhibits a complex architectural organization. DNA is spatially organized and associated with fixed nuclear structures, such as the nuclear matrix and the chromosome scaffold. The generation and distribution of topological changes, and DNA topoisomerase function, in vivo is presumably subject to the constraints imposed by higher-order chromatin structure and chromosomal architecture. Hence, cells must coordinate the resolution of the topological distortions generated by the different DNA metabolic transactions that occur concomitantly within eukaryotic genomes (e.g., the advancement of replication and transcription machineries). The ChIP-on-chip methodology enables the genomewide analysis of DNA topoisomerase-mediated topological transactions within eukaryotic chromosomes.

The ChIP-on-chip technique exploits the DNA obtained by chromatin immunoprecipitation (ChIP) and PCR amplification as a probe for hybridization to DNA chips. The usage of high-resolution tilling arrays (oligonucleotide DNA chips; i.e., Affymetrix *Saccharomyces cerevisiae* chromosome VI tilling chip array) allows the detection of protein binding to chromosomal DNA at a resolution of 300 bp. Protein–DNA complexes are first crosslinked by formaldehyde treatment (**Fig. 9.1A**). Chromatin is then sheared by sonication to obtain suitable protein-bound DNA fragments, and immunoprecipitation is carried out with specific antibodies. For the ChIP-on-chip analysis in yeast cells, epitope-tagged proteins expressed under their endogenous promoters can be used for immunoprecipitation with highly specific commercial antibodies. Epitopes suitable for ChIP analysis are listed in **Table 9.1**. In this way, two fractions are separated: an IP fraction, enriched in the protein of interest, and a SUP fraction, containing non-immunoprecipitated DNA that is used as a hybridization control. After reversal of the formaldehyde crosslink (**Fig. 9.1B**), samples are treated with proteinase K and RNase. DNA fractions are then evenly amplified by tagged-random primer PCR, DNAse digested, and labeled with biotin. Enriched and non-enriched DNA pools are probed to independent chips and, after staining, washing, and scanning, signal intensities of each locus from IP and SUP-hybridized arrays are compared using an expression analysis protocol and the logarithmic ratio of the loci enrichment between IP and SUP fractions is calculated (**Fig. 9.2**). The statistical significance of the observed differences is based on three criteria (1, 2): (i) the reliability of the signal intensity at each locus, evaluated by the detection of p-value, (ii) the reliability of the IP/SUP detection ratio, judged by the change in p-value, and (iii) when the binding of a protein to a discrete chromosomal site results in the immunoprecipitation of DNA fragments containing that site and neighboring regions, only such clusters containing three or more loci fulfilling the previous two criteria are considered. Integration of the logarithmic expression of the IP/SUP signal ratio and the

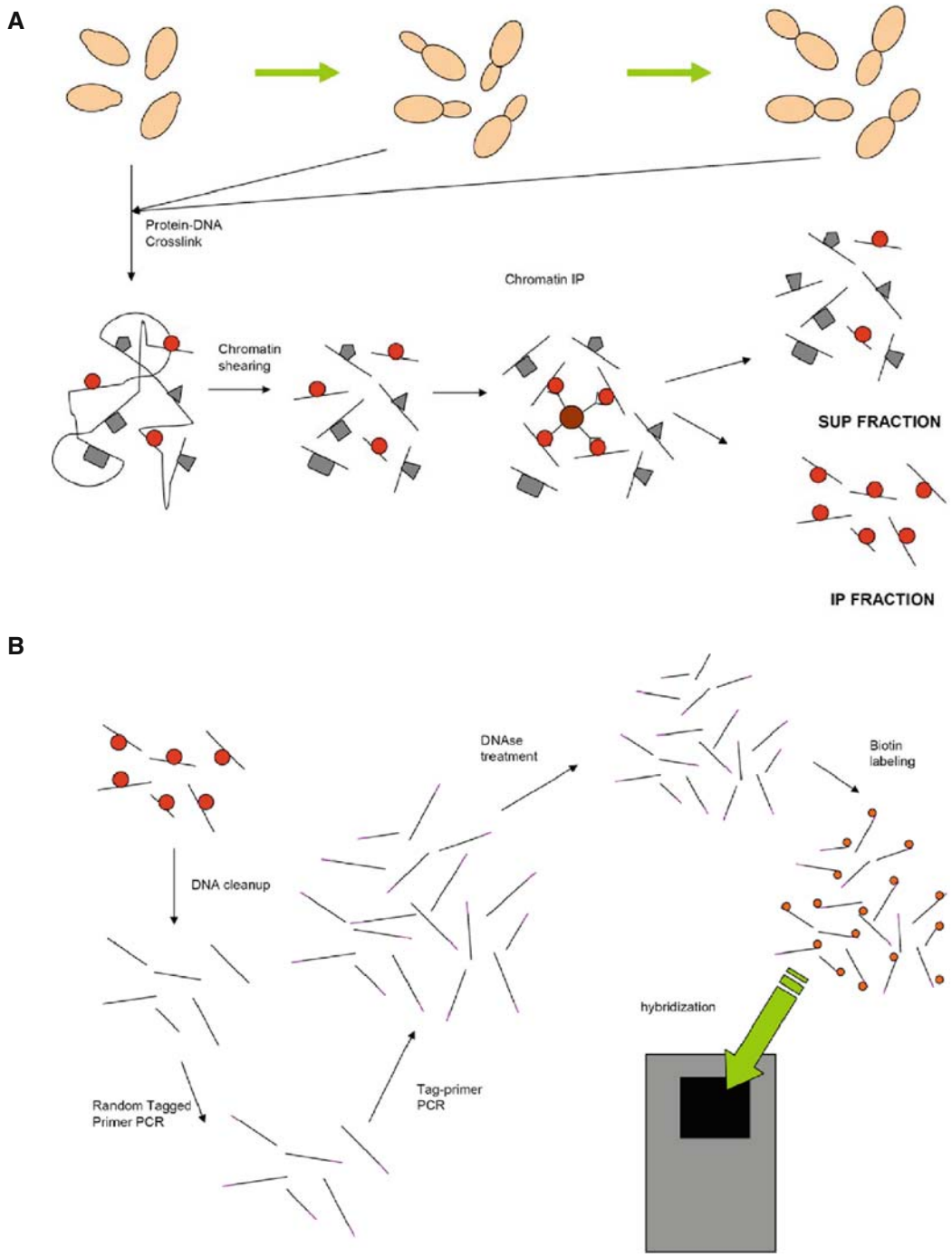

Fig. 9.1. **ChIP-on-chip procedure (I)**. Schematic representation of the Chip-on-chip technique: chromatin crosslink and immunoprecipitation (**A**); purification, amplification, and labeling of the immunoprecipitated and control DNA fractions (**B**) (see text for the details).

Table 9.1
Epitopes available for ChIP-on-chip analysis on budding yeast

TAG	Epitope	Working antibody for ChIP	Antibody_Host
HA	YPYDVPDYA	16B12(BAbCO HA11)	Mouse IgG1
FLAG	DYKDDDDK	M2(SIGMA F3165)	Mouse IgG1
PK	GKPIPNPLLGLD	SV5-Pk1(Serotec MCA1360)	Mouse IgG2a
Myc	EQKLISEEDL	PL14(MBL M047-3)	Mouse IgG1

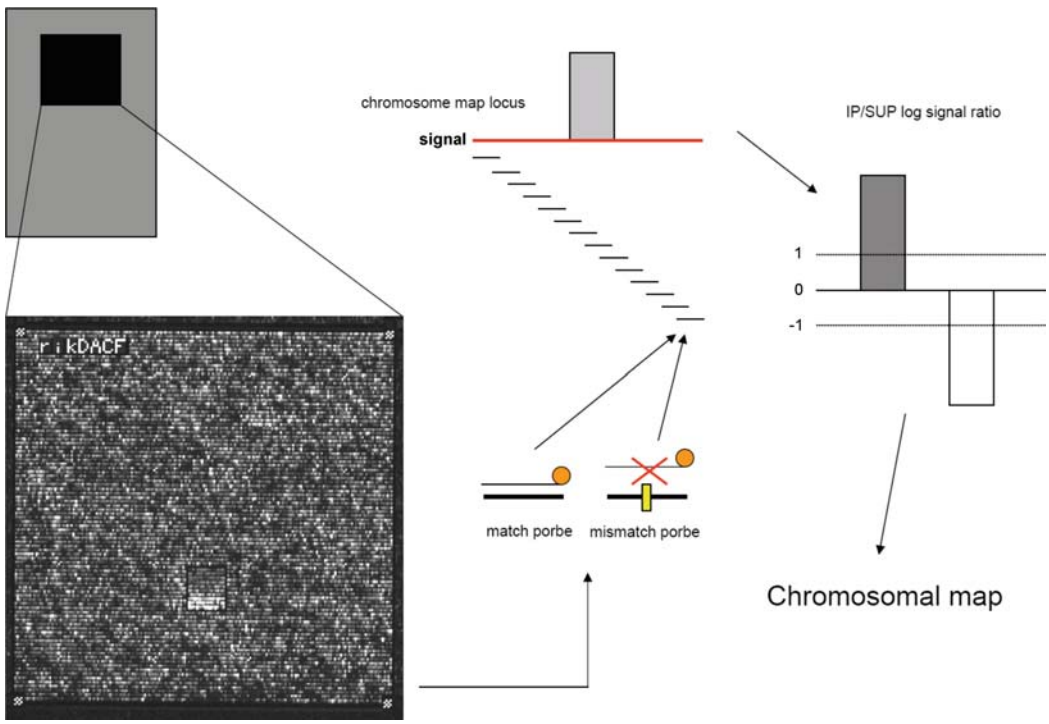

Fig. 9.2. **ChIP-on-chip procedure (II)**. Schematic representation of the statistical algorithm used to calculate the immunoprecipitated versus control signal logarithmic ratio for each chromosomal locus (see text for details).

annotated sequence of *S. cerevisiae* genome (http://www.yeastgenome.org/) allows the construction of maps displaying the binding pattern of the protein of interest along entire chromosomes.

A typical chromosomal binding profile observed for yeast topoisomerase I (Top1) and yeast topoisomerase II (Top2) in S-phase arrested cells is shown in **Fig. 9.3**. Consistent with its role in resolving torsional stress ahead of replication forks and physical association with replisome components, Top1 clusters are detected at regions containing or neighboring active replication

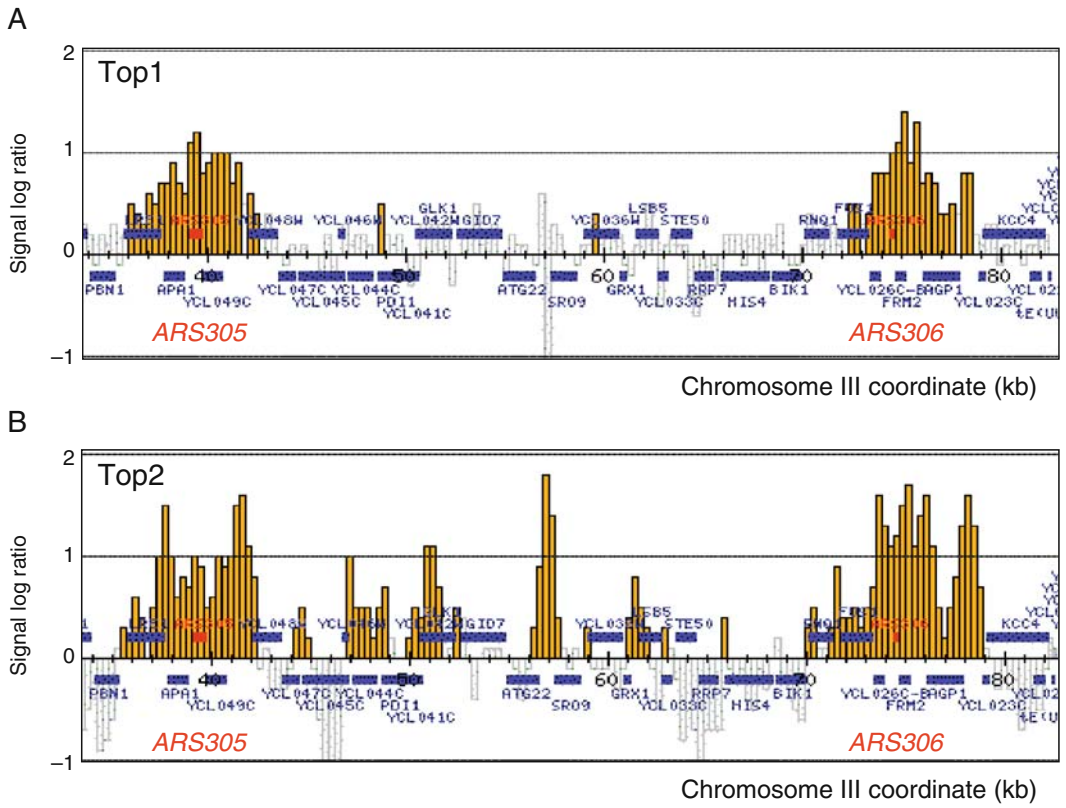

Fig. 9.3. **Chromosomal maps showing Top1 and Top2 distribution in S-phase**. Distribution of Top1 (**A**) and Top2 (**B**) on chromosomal DNA in S-phase arrested cells. The histogram bars in the *Y*-axis show the average signal ratio of loci significantly enriched in the immunoprecipitated fraction along a ~50 kb fragment of chromosome III containing *ARS305* and *ARS306* replication origins in $\log_2$ scale. The *horizontal bars* represent open reading frames (ORFs).

origins (**Fig. 9.3A**). Mutations in the ARS consensus sequence (ACS), that preclude origin firing, abolish the detection of Top1 clusters (4).

The Top2 protein is also enriched at regions containing or neighboring early replication origins on chromosomes (**Fig. 9.3B**). Top2 binding is also abolished when inactivating mutations are introduced in the ACS (4), indicating that Top2 acts to sustain DNA replication, most likely contributing to torsional stress removal and/or sister chromatid decatenation at replication forks. Top2 also clusters at specific intergenic regions in a fashion independent of origin activation (4). The Top2 intergenic clusters likely reflect the participation of this enzyme in transcription-dependent topological rearrangements at gene promoters during S-phase.

ChIP-on-chip represents a highly valuable technique for the in vivo analysis of topoisomerase interaction with chromosomal DNA in the nuclear context. In the future, the use of this genomic approach may contribute to the elucidation of the role played by these enzymes in the complex DNA transactions essential for

gene expression, genome duplication, and maintenance of genome integrity. Furthermore, considering that topoisomerases represent the molecular target of several drugs, this approach can also be used to characterize the action of topoisomerase inhibitors.

2. Materials

2.1. Preparation of Magnetic Beads

1. Magnetic beads: Protein A Dynabeads (Dynal, Lake Success).
2. 1.7 ml prelubricated Costar tubes (Corning, NY).
3. Magnetic grid (Dynal MPC–S, Dynal, Lake Success, NY).
4. PBS: 137 mM NaCl, 10 mM phosphate buffer, pH 7.4, 2.7 mM KCl.
5. PBS/BSA: 1X phosphate-buffered saline containing 5 mg/ml bovine serum albumin.
6. Anti-Flag antibody: M2 anti-flag antibody (Sigma).

2.2. Preparation of Chromatin Extracts and Immunoprecipitation

1. *TOP2-FLAG* yeast: *S. cerevisiae* strain expressing *FLAG*-tagged *TOP2* from the endogenous yeast *TOP2* promoter (available upon request).
2. Anti-Flag antibody: Mouse monoclonal antibody that is highly specific for the Flag epitope (*see* **Table 9.1**).
3. Formaldehyde solution: 37% formaldehyde.
4. TBS: 20 mM Tris–HCl, pH 7.5, 150 mM NaCl.
5. Lysis buffer: 50 mM Hepes–KOH, pH 7.5, 140 mM NaCl, 1 mM EDTA, 1% Triton-X100, 0.1% Na-deoxycholate.
6. PMSF stock solution: 100 mM phenylmethanesulfonyl fluoride.
7. Antiproteolytic cocktail: Complete protease inhibitor tablets (Roche, Indianapolis, IN).
8. 2-ml O-ring screw-cap tubes.
9. Acid-washed glass beads: 425–600 μm (Sigma).
10. Cell disruptor: Multibeads shocker® (Yasui-kikai, Osaka, Japan) or similar device.
11. Branson Sonifier 2508 (Danbury, CT).
12. 1.7 ml prelubricated Costar tubes.
13. 1.5 ml microcentrifuge tubes.
14. 2X Laemmli buffer: 4% SDS, 20% glycerol, 10% 2-mercaptoethanol, 0.004% bromophenol blue, 0.125 M Tris–HCl, pH 6.8.

2.3. Washing the Beads and Crosslink Reversal

1. 1.5 ml microcentrifuge tubes.
2. 2X Laemmli buffer: 4% SDS, 20% glycerol, 10% 2-mercaptoethanol, 0.004% bromophenol blue, 0.125 M Tris–HCl, pH 6.8.
3. Magnetic grid (Dynal MPC–S, Dynal, Lake Success, NY).
4. Wash buffer: 10 mM Tris–HCl, pH 8.0, 250 mM LiCl, 0.5% NP-40, 0.5% Na-deoxycholate, 1 mM EDTA.
5. Elution buffer: 50 mM Tris–HCl, pH 8, 10 mM EDTA, 1% SDS.
6. TE: 10 mM Tris–HCl, pH 8, 1 mM EDTA.
7. TE/1% SDS: TE with 1% SDS.

2.4. DNA Purification

1. Proteinase K buffer: 895 µl of TE, 30 µl of 10 mg/ml glycogen (Roche), and 75 µl of 50 mg/ml Proteinase K (Roche).
2. 5 M NaCl stock solution.
3. Phenol/chloroform/isoamylalcohol (Sigma).
4. 100% ice-cold ethanol.
5. 70% ice-cold ethanol.
6. RNase A (Sigma): DNAse-free RNase A powder. Store at –20°C.
7. Qiagen PCR purification kit (Qiagen, Valencia, CA).
8. 3 M sodium acetate.
9. 80% ice-cold ethanol.
10. Autoclaved MilliQ water (ddH_2O).

2.5. DNA Amplification

1. Sequenase Ver2.0 T7 DNA polymerase (USB).
2. Primer A: 5′-GTT TCC CAG TCA CGA TCN NNN NNN NN-3′.
3. Primer B: 5′-GTT TCC CAG TCA CGA TC-3′.
4. 0.1 M DTT stock solution.
5. 3 mM dNTPs stock solution.
6. Microcon centrifugal filter unit (YM30) cartridges (Millipore Corporation, Bedford, MA, USA).
7. KOD-Dash: DNA polymerase with proof-reading and high processivity (TOYOBO, Osaka, Japan).
8. WGA2 GenomePlex Complete Genome Amplification (WGA) Kit (Sigma).

2.6. DNAse Digestion

1. DNAseI: Amplification Grade (Gibco BRL, Grand Island, NY).
2. 10X One-Phor-All-Buffer plus (Pharmacia, Piscataway, NJ).
3. 25 mM $CoCl_2$.

2.7. DNA Labeling

1. Terminal transferase (Roche, Indianapolis, IN).
2. Biotin-11-ddATP (NEN).

2.8. Hybridization

1. rikDACF, chromosome VI tiling array (Affymetrix, CA).
2. GeneChip hybrid oven 320 (Affymetrix, CA).
3. 20X eukaryotic hybridization control (Genechip).
4. Herring sperm DNA: 10 mg/ml dissolved in ddH_2O. Store at –20°C.
5. 20X SSPE: 3 M NaCl, 200 mM sodium phosphate, 20 mM EDTA, pH 7.4.
6. 0.1% Triton-X100.
7. Control OligoB2 (Affymetrix, CA).

2.9. Washing, Staining, and Scanning of the Chips

1. Acetylated BSA (Invitrogen).
2. SAPE: Streptavidin, R-phycoerythrin conjugate, premium grade (Invitrogen).
3. GeneChip fluidics station 450 (Affymetrix, CA).
4. Affymetrix GeneChip Scanner 3000 7G (Affymetrix CA).

3. Methods

Here, we describe a version of the ChIP-on-chip protocol (1) adapted for analysis of the binding pattern of endogenously expressed Flag-epitope-tagged DNA topoisomerases on *S. cerevisiae* chromosome VI (3, 4).

3.1. Preparation of the Magnetic Beads

1. Transfer 60 µl of the magnetic beads to a 1.7-ml prelubricated tube and centrifuge at 2300*g* for 1 min at 4°C.
2. Place the tube in a magnetic grid and aspirate the supernatant with a vacuum pump.
3. Wash beads twice as follows: Resuspend the magnetic beads in 0.5 ml of ice-cold PBS/BSA by removing the tube from the magnetic grid and gently shaking (*see* **Note 1**). Place the tube back in the magnetic grid, and wait until the beads attach to the magnet leaving a clear solution and aspirate the supernatant with a vacuum pump.
4. Resuspend the beads in 60 µl of PBS/BSA and add 20 µg of anti-Flag antibody. Incubate with rotation overnight (*see* **Note 2**).
5. Immediately before use, remove the antibody-containing solution, wash twice with ice-cold PBS/BSA, and resuspend in 60 µl of PBS/BSA. (Magnetic beads, 15 µl, are added to each 0.4 ml lysis buffer aliquot.)

3.2. Preparation of Chromatin Extracts and Immunoprecipitation

1. Collect 100 ml of *TOP2-FLAG* yeast culture at a concentration of 1×10^7 cells/ml and transfer into two 50-ml centrifuge tubes.
2. Add formaldehyde to a 1% final concentration (1.350 ml of a 37% solution to each tube) and incubate at room temperature for 30 min, gently shaking (*see* **Note 3**).
3. Wash the cells three times as follows: Pellet the fixed cells by centrifugation at 1850*g* for 3 min at 4°C and resuspend in 20 ml of ice-cold 1X TBS by vortexing. After the last washing step, discard the supernatant and carefully remove the remaining liquid with a vacuum pump.
4. Resuspend each cell pellet in 0.8 ml of lysis buffer (supplemented with a final concentration of 1 mM PMSF and 1X antiproteolytic cocktail, immediately before use). Transfer 0.4 ml lysis buffer aliquots into 2-ml O-ring screw-cap tubes and add glass beads up to 1 mm below the buffer's meniscus. (You now have four, 2-ml O-ring screw-cap tubes.)
5. Break the cells with a Multibeads Shocker® using the following pattern: 60 min of total time (1 min shaking/1 min pause) at 2500 rpm and 4°C (*see* **Note 4**).
6. Recover the cell lysates as follows: Wipe each of the four O-ring tubes with a tissue paper, puncture the bottom with a hypodermic syringe needle, and put each O-ring tube into a 15 ml centrifuge tube. Centrifuge at 2850*g* for 1 min at 4°C, resuspend the flow-through extracts in the 15 ml tubes, and then transfer to four 1.5 ml microcentrifuge tubes. Repeat the centrifugation step once more and collect the remaining extract.
7. Centrifuge the extracts at 13,400*g* for 1 min at 4°C. Add a 5 µl aliquot of the soluble fraction (SOL) to 5 µl of 2X Laemmli buffer for Western blot analysis of IP efficiency (*see* **Fig. 9.4A**, **Note 5**). Discard the supernatant containing the soluble protein fraction and resuspend the pellets in 0.4 ml of lysis buffer supplemented with PMSF and antiproteolytic cocktail, as described in step 4.
8. Shear the chromatin by applying five sonication cycles of 15 s at 1.5 output (*see* **Note 6**) After each sonication cycle, pellet the chromatin by centrifuging at 2300*g* for 1 min at 4°C (*see* **Note 7**).
9. Centrifuge at $\geq$16,000*g* for 5 min at 4°C and transfer the supernatants to 1.7-ml prelubricated tubes. This is the whole cell extract (WCE).
10. Take a 5 µl aliquot of the WCE and add 5 µl of 2X Laemmli buffer for Western blot analysis (*see* **Fig. 9.4A**).
11. Add the previously washed antibody-bound magnetic beads (15 µl per tube) to the remaining WCE in the 1.7-ml prelubricated tubes. Incubate on a rotating wheel at 4°C overnight (*see* **Note 8**).

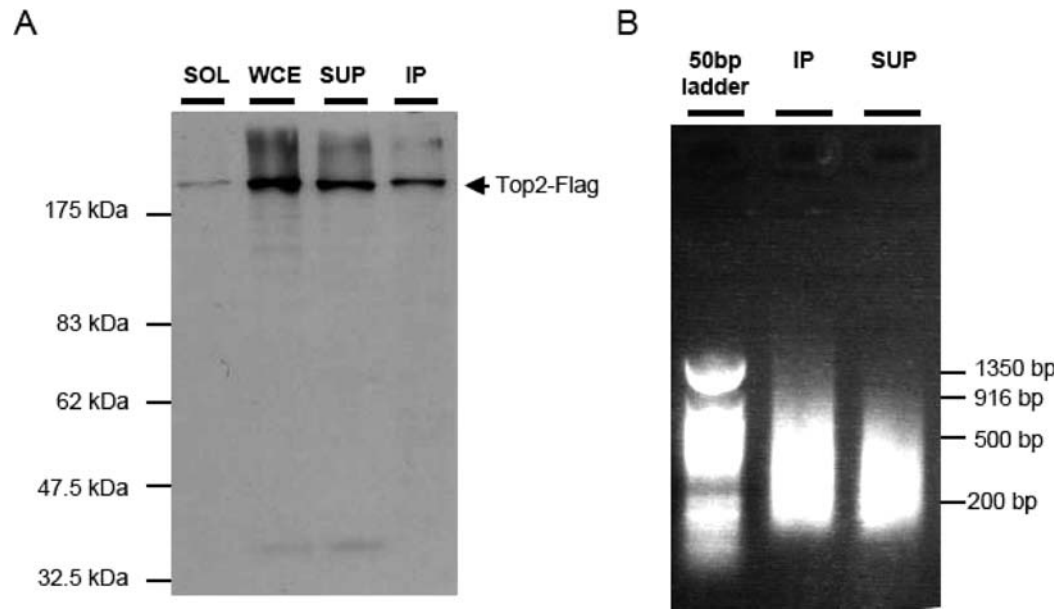

Fig. 9.4. **Immunoprecipitation and amplification controls**. (**A**) Evaluation of the efficiency of chromatin crosslink and immunoprecipitation: Western blot analysis of Top2 abundance in the soluble (SOL), chromatin (WCE), supernatant (SUP), and immunoprecipitated (IP) fractions from a typical ChIP-on-chip experiment. (**B**) Qualitative analysis of DNA amplification: Ethidium bromide-stained agarose gel electrophoresis of an aliquot of the DNA amplified from immunoprecipitated (IP) and control (SUP) fractions. Fragments show a smeared distribution with sizes ranging from 100 to 1000 bp.

3.3. Washing the Beads and Crosslink Reversal

1. Place the four 1.7-ml prelubricated tubes containing the beads and WCE in a magnetic grid. Wait until the beads attach to the magnet leaving a clear supernatant. Transfer 5 µl of the supernatant (the SUP fraction; used in step 7) to a 1.5 ml microcentrifuge tube to be used as the hybridization control and another 5 µl to a tube containing 5 µl of 2X Laemmli buffer for Western blot analysis of IP efficiency (*see* **Fig. 9.4A**).
2. Wash the beads as follows using the magnetic grid as described in **Section 3.1**:
   - 2X with 1 ml of ice-cold lysis buffer (without antiproteolytics).
   - 2X with 1 ml of ice-cold lysis buffer supplemented with 360 mM NaCl.
   - 2X with 1 ml of ice-cold wash buffer.
   - 1X with 1 ml of ice-cold TE.
3. Remove the TE (*see* **Note 9**) and centrifuge the beads at 800*g* for 3 min at 4°C. Place the tubes back in the magnetic grid and remove the remaining liquid with a vacuum pump.
4. Add 40 µl of elution buffer to each tube, resuspend the beads by pipetting up and down, and incubate at 65°C for 10 min (*see* **Note 10**).

5. Centrifuge the tubes for 1 min at $\geq$16,000*g* at RT.
6. Place the tubes back in the magnetic grid (this is the IP fraction) and transfer 5 µl to a tube containing 5 µl of 2X Laemmli buffer. [For Western blot analysis of the IP efficiency, boil the samples at 95°C for 30 min prior to separation on an SDS-PAGE gel, then following blotting, probe the membrane with α-flag antibody at a dilution of 1:30,000 (*see* **Fig. 9.4A**, **Note 11**).]
7. Transfer the remaining IP fractions (about 35–40 µl per tube) to four new 1.5-ml microcentrifuge tubes containing 4 volumes (140–160 µl) of TE/1% SDS.
8. Add 95 µl of TE/1% SDS to the SUP fraction (collected in step 1).
9. Incubate overnight at 65°C to reverse the crosslink (*see* **Note 12**).

3.4. DNA Purification

1. Consolidate the SUP and IP fractions by pulse-spinning and, if necessary, add TE to each of the IP samples to reach a volume of 200 µl.
2. Add 100 µl of proteinase K buffer to the IP samples and 44.75 µl of proteinase K buffer to the SUP sample.
3. Mix, without vortexing, and incubate at 37°C for 2 h.
4. Add 12 µl or 6 µl of a 5 M NaCl stock to the IP or SUP samples, respectively.
5. Extract twice by adding an equal volume of phenol/chloroform/isoamylalcohol and centrifuging at 13,400*g* for 5 min at RT.
6. Add 2 volumes of cold 100% ethanol, vortex, and incubate at –20°C for at least 20 min (*see* **Note 13**).
7. Centrifuge at $\geq$13,400*g* for 10 min at 4°C.
8. Discard the supernatants and wash with 1 ml of cold 80% ethanol.
9. Let the pellets dry (*see* **Note 14**), resuspend each pellet in 30 µl of TE containing 10 µg of RNase A. Incubate for 1 h at 37°C. (The RNase A powder should be added to the TE immediately before use and boiled for 10 min.)
10. Pool the 30 µl IP samples together to obtain two 60 µl samples and purify the IP and SUP DNA samples using a PCR purification kit following the manufacturer's instructions. Elute the DNA from each sample with 50 µl of EB buffer.
11. Pool the two 50 µl IP samples together.

12. Precipitate the IP DNA sample by adding 5 µl of 3 M sodium acetate, 2 µl of glycogen (10 mg/ml), and 2.5 volumes of cold 100% ethanol. Precipitate the SUP DNA sample by adding 2.5 µl of 3 M sodium acetate, 1 µl of glycogen (10 mg/ml), and 2.5 volumes of cold 100% ethanol.
13. Incubate at –20°C for at least 20 min.
14. Centrifuge at ≥13,400*g* for 10 min at 4°C.
15. Discard the supernatants and wash with 0.5 ml of cold 70% ethanol.
16. Resuspend the pellets in 7 µl of TE or 10 µl of ddH_2O (for amplification using method I or method II, respectively).

3.5. DNA Amplification

Amplification of the IP and SUP DNA is required to obtain a sufficient amount (≥5 µg) of DNA to be labeled and used as hybridization probes. We describe here two methods for random PCR amplification that give comparable outcomes.

3.5.1. Method I

1. Prepare Round A setup as follows:

DNA	7 µl
5X sequenase buffer	2 µl
Primer A (40 mM)	1 µl

2. Prepare reaction mix (for each reaction):

5X sequenase buffer	1 µl
dNTPs (3 mM each)	1.5 µl
DTT (0.1 M)	0.75 µl
BSA (0.5 mg/ml)	1.5 µl
Sequenase	0.3 µl

3. Incubate Round A setup in a thermocycler as follows: 94°C for 2 min, 10°C for 5 min, hold. During the hold time add 5.05 µl of reaction mix to each sample.
4. Ramp to 37°C over 8 min. Hold at 37°C for 8 min, at 94°C for 2 min, and then at 10°C for 5 min. During this time, add 1.2 µl of diluted sequenase (diluted 1:4 in 5X sequenase dilution buffer).
5. Ramp to 37°C over 8 min.
6. Concentrate the DNA using a Microcon centrifugal filter unit (YM30) according to the manufacturer's instructions, and adjust the sample volume to 40 µl with ddH_2O.
7. Prepare Round B reaction as follows:

DNA template	40 µl
KOD-Dash	2 µl
10X KOD-Dash PCR buffer	10 µl

dNTPs (2 mM each)	10 µl
Primer B (100 µM)	1 µl
ddH_2O	37 µl

8. Perform the following amplification cycle (*see* **Note 15**): 94°C for 5 min (94°C for 20 s, 40°C for 30 s, 50°C for 30 s, 74°C for 3 min) × 32 cycles, 74°C for 7 min.

3.5.2. Method II

1. Use the WGA2 GenomePlex Complete Genome Amplification (WGA) Kit. Follow the manufacturer's instructions from the *Library Preparation* step onward.
2. Check the amplified DNA by running an aliquot (2.5 µl for Method I, 1.9 µl for Method II) of the reaction on a 1.2% agarose gel. A smear ranging from 100 to 1000 bp should be observed (*see* **Fig. 9.4B**).
3. Concentrate the DNA using a Microcon centrifugal filter unit (YM30) according to the manufacturer's instructions.
4. Measure the DNA concentration by spectrometry at A260.

3.6. DNAse Digestion (see Note 16)

1. Prepare DNAse reaction (for 13 samples):

DNAse I (1 U/µl)	2 µl
10X One-Phor-All-Buffer plus	2 µl
25 mM $CoCl_2$	1.2 µl
ddH_2O	14.8 µl

2. Prepare the following reaction mix:

DNAse I setup	1.5 µl
10X One-Phor-All-Buffer plus	4.85 µl
25 mM $CoCl_2$	2.9 µl
DNA (5–10 µg) + ddH_2O (IP/SUP) samples	40.75 µl

3. Incubate at 37°C for 30 sec and then transfer to 95°C for 15 min.

3.7. DNA Labeling

1. Transfer the DNA into new 1.5-ml microcentrifuge tubes.
2. Add 5 µl of TdT reaction buffer, 1 µl terminal transferase (25 U/µl), and 1 µl biotin-N11-ddATP (1 nM/µl).
3. Mix and incubate at 37°C for 1 h.

3.8. Hybridization

Hybridization, chip-staining, washing and scanning, as well as discrimination analysis, are performed as described by the manufacturer's instructions (Affymetrix), as follows:

1. Prehybridize the chips with 200 µl of prehybridization solution. Incubate in an Affymetrix oven at 42°C for 10–20 min.

2. Prepare a mix with the DNA samples in 1.5 ml tubes:

DNA (5–10 μg)	55 μl
3 nM control OligoB2	3.3 μl
Herring sperm DNA (10 mg/ml)	2 μl
20X eukaryotic hybridization control	10 μl
20X SSPE	60 μl
0.1% Triton-X100	10 μl
ddH2O	64.7 μl

3. Boil the mix for 10 min and transfer immediately to ice.
4. Spin the samples at 14,000*g* for 2–3 min in a microcentrifuge.
5. Remove the prehybridization solution and spot the boiled DNA probes onto the microarray chips. Hybridize with 150 μl of probe for 16 h at 42°C in a hybridization oven at 60 rpm.

3.9. Washing, Staining, and Scanning of Chips

1. Remove the hybridization solution.
2. Add 200 μl of washing buffer (wash A) to the chips.
3. Prepare 600 μl of staining buffer as follows:

2X stain buffer	300 μl
ddH_2O	270 μl
Acetylated BSA (50 mg/ml)	24 μl
SAPE (1 mg/ml)	6 μl

4. Insert the chips in a Fluidics Station and run the washing and staining protocol (Midi_euk1 ver2) provided by Affymetrix.
5. Scan the chips.
6. Compare the signal intensities of each locus on the DNA chips hybridized with IP and SUP fractions using GCOS expression analysis.
7. Discrimination analysis can be carried out using the statistical algorithms developed by Affymetrix (extensive information can be downloaded from the manufacturer's web site: http://www.affymetrix.com). Comparison analysis of the IP/SUP fractions is employed to generate DNA topoisomerase binding profiles (1, 4).

4. Notes

1. During the washes, excessive shaking is not desirable as it might revert the magnetic bead–antibody crosslinking.

2. Incubation time can be shortened, but bead–antibody crosslinking times under 2 h are not recommended.
3. Crosslink efficiency can be extended by gently shaking the extracts overnight at 4°C, though immunoprecipitation efficiency might decrease.
4. Breakage time can be extended if broken cells are not over 90% of the total. Cell breakage can be assessed by analyzing a small aliquot of the lysate by phase contrast microscopy. Broken cells appear phase-dark while intact cells appear bright.
5. Western blot detection of this fraction indicates the proportion of protein that is not associated with chromatin after the formaldehyde crosslink.
6. During the sonication step, it is important to avoid sample overheating that can result in crosslink reversal.
7. The size of the sheared chromatin can be assessed by running the extract on a 1.2% TAE agarose gel. A smear of DNA fragments ranging from approximately 100–1000 base pairs should be observed. If not, additional sonication cycles can be performed.
8. The duration of the chromatin immunoprecipitation can be reduced down to 5 h, but overnight incubation is recommended to obtain a better efficiency.
9. After the last wash, TE should be removed with a micropipette to avoid bead aspiration.
10. Flick the tubes three times to resuspend the beads during the incubation time.
11. A good IP efficiency is essential to obtain a significant enrichment ratio. A distinct band should be observed for the IP fraction by Western blotting.
12. Crosslink reversal can be performed in an oven to avoid condensation of the sample.
13. The duration of the precipitation steps at –20°C can be extended without a decrease in the DNA yield.
14. A heated vacuum-centrifuge can be used at this step to completely remove ethanol from the sample.
15. The number of cycles of Round B PCR can be raised to increase the DNA yield. It is not advisable to perform more than 40 cycles as background DNA can be amplified.
16. Short DNAse incubation is performed to reduce the size of the amplified DNA and increase its suitability for the hybridization on the array.

Acknowledgments

Work in M.F. lab is supported by grants from the Associazione Italiana per la Ricerca sul Cancro, Association for International Cancer Research, and, partially, from European Union, Telethon-Italy, and the Italian Ministry of Education. K.S. is supported by a grant of the Genome Network Project and Grant-in-Aid for Scientific Research (S) from the MEXT. Y.K. is supported by Global COE program from MEXT. We thank all the members of our laboratories for helpful discussions and criticisms.

References

1. Katou, Y., Kaneshiro, K., Aburatani, H. and Shirahige, K. (2006) Genomic approach for the understanding of dynamic aspect of chromosome behaviour. *Methods Enzymol* **409**, 389–410.
2. Katou, Y., Kanoh, Y., Bando, M., Noguchi, H., Tanaka, H., Ashikari, T., Sugimoto, K. and Shirahige, K. (2003) S-phase checkpoint proteins Tof1 and Mrc1 form a stable replication-pausing complex. *Nature* **424**, 1078–83.
3. De Antoni, A. and Gallwitz, D. (2000) A novel multi-purpose cassette for repeated integrative epitope tagging of genes in *Saccharomyces cerevisiae*. *Gene* **246**, 179–85.
4. Bermejo, R., Doksani, Y., Capra, T., Katou, Y. M., Tanaka, H., Shirahige, K. and Foiani, M. (2007) Top1- and Top2-mediated topological transitions at replication forks ensure fork progression and stability and prevent DNA damage checkpoint activation. *Genes Dev* **21**, 1921–36.

Chapter 10

Analyzing Top2 Distribution on Yeast Chromosomes by Chromatin Immunoprecipitation

Melissa Baldwin, Tariq Warsi, and Jeff Bachant

Abstract

In vertebrate cells, DNA topoisomerase II (Topo II), named Top2 in yeast, localizes along chromosome axes early in mitosis and concentrates within centromeric chromatin during metaphase. The factors controlling these changes in enzyme distribution are largely unknown. Insight into Topo II dynamics could potentially be derived through genetic approaches in yeast. In practice, however, the small size and limited compaction of yeast chromosomes has precluded a detailed analysis of Top2 localization along mitotic chromosomes. As an alternative approach, we describe a method for examining Top2 distribution using chromatin immunoprecipitation (ChIP). By adding a detergent solubilization step, this method allows efficient recovery of DNA sequences associated with Top2 in the insoluble chromosome scaffold fraction.

Key words: DNA topoisomerase II (Top2), chromatin immunoprecipitation (ChIP).

1. Introduction

Following cell lysis, the majority of Topo II partitions with an insoluble, nuclease-resistant, protein fraction. Historically, this insolubility was found to correspond with Topo II being a prominent component of a linear protein structure, or scaffold, that remained following extraction of vertebrate mitotic chromosomes (1, 2). The scaffold came to be viewed as an important architectural element of chromosome structure, serving as a platform to mediate higher-order DNA packing [for a discussion, *see* (3)].

More recent experiments have shown that vertebrate Topo II is actually quite dynamic, exchanging rapidly between chromosomally bound and unbound pools (4, 5). This would seem to rule

D.J. Clarke (ed.), *DNA Topoisomerases*, Methods in Molecular Biology 582,
DOI 10.1007/978-1-60761-340-4_10,

out Topo II assembling into a static structural scaffold in vivo. However, it is possible that Topo II engages in more transient interactions that contribute to chromosome organization, or that there is a small but functionally relevant population that associates with chromatin in a more stable fashion. Along these lines, fixed and live cell studies have revealed that, superimposed on fast Topo II turnover, there are also processes that cause the enzyme to localize (or, alternatively, to be preferentially retained) at specific chromosomal regions, most prominently at the centromere/primary constriction of metaphase cells [reviewed in (6)]. It is likely that a more complete understanding of these chromosome dynamics will provide insight into Topo II function in mitotic chromosome structure and segregation.

Because of the difficulties in visualizing individual mitotic chromosomes in yeast, we have a comparatively limited knowledge of Top2 chromosome distribution in this organism. Fortunately, ChIP affords a direct (and high resolution) approach to examine this issue. Using this method, it has been recently shown that Top2 associates with replicating chromosomal regions during S phase as well as certain intergenic loci (7). It has also been reported that a Top2-SUMO fusion protein appears to cross-link more robustly to centromeric regions than the wild-type protein (8). In our efforts to implement Top2 ChIP, we were concerned that the insolubility of Top2 might preclude sampling of a subset of Top2-associated sequences. To avoid this caveat, we developed a modified ChIP procedure in which Top2 and cross-linked DNA sequences are solubilized prior to immunoprecipitation. In our hands, this protocol works robustly for the recovery and amplification of Top2-associated chromatin and has proven applicable to other chromosomal proteins.

2. Materials

2.1. Analysis of Top2 Association with Chromatin

Our best results with Top2 ChIP have been obtained using an 18X-myc tagged form of the protein. *TOP2-Myc$_{18X}$* can be expressed either as a gene replacement of the endogenous *TOP2* locus or from an episomal plasmid. These strains and reagents are described below. We have also successfully performed Top2 ChIP using 3X-HA tagged Top2, and reagents for expressing TOP2-HA$_{3X}$ are described in **Chapter 16**.

1. pTW009 (p*CEN ARS URA3 TOP2-Myc-kanMX4*): Yeast episomal plasmid for expressing *TOP2-Myc$_{18X}$*. Base vector: pRS416 (9).
2. pTW007: A *TOP2-Myc$_{18X}$-kanMX* gene replacement cassette can be liberated from this plasmid via DraIII restriction.

3. JBY1403 (*MATa his3-11, leu2-3 trp1-1, ura3-1 ade2-1 can1-100 TOP2-18Xmyc-kanMX4*): In this strain, *TOP2* has been replaced with *TOP2-myc-kanMX*.
4. CRY1 (*MATa ade2-1 trp1-1 leu2-3,112 his3-11,15 ura3-1 can1-100*): This strain is congenic with JBY1403 and can be used as a no-tag control for non-specific recovery of DNA sequences.

2.2. Cell Culture and Lysis

1. YPD: 2% glucose, 1% yeast extract, 2% bacto-peptone. Autoclave and store at room temperature.
2. Nocodazole (Sigma): For a 1000X stock solution, dissolve 15 mg/ml in DMSO, store in aliquots at –20°C.
3. α-factor (Bio Synthesis, Inc): For a 1000X stock solution, dissolve 5 mg/ml in water, store in aliquots at –80°C.
4. Formaldehyde: 37% (w/v).
5. 2.5 M glycine: Dissolve in water, store at room temperature.
6. Protease inhibitors (100X stock solutions):
   (a) Cocktail: leupeptin (1 mg/ml), aprotinin (2 mg/ml), benzamidine (1.6 mg/ml); prepare in sterile water, store in aliquots at –20°C.
   (b) Phenylmethylsulfonyl fluoride (PMSF): 10 mg/ml in 95% ethanol, store in aliquots at –20°C.
   (c) Pepstatin A: 0.1 mg/ml in 95% ethanol, store in aliquots at –20°C.
   (d) *N*-ethylmalemide (NEM): 10 mM in ethanol, make fresh.
7. Lysis buffer: 25 mM HEPES, pH 7.5, 150 mM NaCl, 5 mM EDTA, 10% glycerol. Dissolve in water and store at 4°C.
8. 20% (w/v) sodium dodecyl sulfate (SDS). Dissolve in water and store at room temperature.
9. 10% (v/v) Triton X-100: Dilute in water and store at room temperature.

2.3. Chromatin Immunoprecipitation

1. Primary antibodies:
   (a) α-Myc antibody: 9E10 monoclonal antibody (Covance), 3–5 mg/ml ascites.
   (b) α-HA antibody: 12CA5 monoclonal antibody (Roche Applied Science), 5 mg/ml ascites.
2. Proteins G plus/protein A-agarose beads (Calbiochem).
3. Lambda BstEII digest (NEB), 0.5 mg/ml or other source of DNA to compete non-specific binding (*see* **Note 7**).
4. High-salt wash: 20 mM Tris–HCl, pH 8.0, 2 mM EDTA, 500 mM NaCl, 1% Triton X-100; dissolve in water and store at room temperature.

5. Buffer III: 0.25 M LiCl, 1% NP40, 1% Na deoxycholate, 1 mM EDTA, 10 mM Tris–HCl, pH 8.0; dissolve in water and store at room temperature.
6. Low-salt wash: 20 mM Tris–HCl, pH 8.0, 2 mM EDTA; dissolve in water and store at room temperature.
7. TE/1% SDS: 20 mM Tris–HCl, pH 8.0, 2 mM EDTA, 1% SDS. Dissolve in water and store at room temperature.
8. 20 mg/ml Proteinase K (Promega): Dissolve in water and store at –20°C.
9. QIAQuick PCR Purification Kit (Qiagen).

2.4. Semi-quantitative PCR Analysis of Recovered Chromatin

1. Primers: **Table 10.1** describes primers that will amplify fragments at ~2000 bp intervals along a 34-kb *CEN4*-proximal chromosomal region.
2. ChromaTaq DNA polymerase reaction mixture with dNTPs (Denville Scientific).
3. Agarose: Gel electrophoresis grade.
4. Ethidium bromide: 1000X stock solution; 50 mg/ml in water.

Table 10.1
PCR primers for ChIP analysis of sequences flanking CEN4

Name[a]	Sequence[b]	Length[c]	Midpoint[d]
JB.168–17000 UP	GATAAAGGGTCGCGAATAACC		
JB.169–17000 DOWN	GTTTGGAACAGTTCCTCTACC	245	432,760
JB.170–15000 UP	GGAATCCACAAAAGGGAATCG		
JB.171–15000 DOWN	ATGGAAGCTGCAAATGCAAGC	399	434,723
JB.172–13000 UP	AGTTCGAGGATAAGGACATCG		
JB.173–13000 DOWN	AACTACCGGCATAGAAAGTGG	360	436,828
JB.174–11000 UP	AGAGTTACCGTTAACACACCC		
JB.175–11000 DOWN	CTGAATTTCTCTCTCACCACC	315	438,796
JB.176–9000 UP	TAGCGTGTGATGGATTATGGG		
JB.177–9000 DOWN	GTCGACCACTGGAGATAATGG	468	440,829
JB.64–7000 UP	GTTGCATCATCATTTCTGCTCC		
JB.65–7000 DOWN	GTCAATCATCAATCTCCTAGGC	512	442,416
JB.178–5000 UP	ACTTGCCACCAATAAGGGTCC		

(continued)

Table 10.1 (continued)

Name[a]	Sequence[b]	Length[c]	Midpoint[d]
JB.179–5000 DOWN	GGAGAAAAGTGGCCTGTTTGG	229	444,834
JB.180–3000 UP	ATTAGGAATCGTCTGCCCACG		
JB.181–3000 DOWN	TCCTCTGGCTGCTAATGTACC	206	446,725
JB.182–1000 UP	TGATGAATGCTTGTACACTCCC		
JB.183–1000 DOWN	CATAGAAACTTTACCGCTGTATGC	468	448,701
JB.66 *CEN4* UP	GTGTGGAAGTCCTAATATCGG		
JB.67 *CEN4* DOWN	TTTAAGCTATGAAAGCCTCG	693	449,560
JB.184–1000 UP	TTTTCTGTGCTTGCTCCTTCG		
JB.185–1000 DOWN	GTTAGAGAATCTGGACACGAC	324	450,898
JB.186–3000 UP	GTAATCTCCTTATATCTATGCAGTTGG		
JB.187–3000 DOWN	AAAGAAACGACAGGAGCATCG	324	452,694
JB.188–5000 UP	GACTTCAATCTGCTAAGACCC		
JB.189–5000 DOWN	CCGATGAATTGACTGTTCTGG	338	454,784
JB.68–7000 UP	GCCTGTACTCGAATTTAGACG		
JB.69–7000 DOWN	TCTGATTGCTATCCTCAACGC	333	457,145
JB.190–9000 UP	TAAACCTCTGGATGCAATCGC		
JB.191–9000 DOWN	ACCCCTCAGTGAAGTTTATGG	270	458,810
JB.192–11000 UP	TGCTGCTTGTTCTTTGTGTGG		
JB.193–11000 DOWN	AACGCCACTAACAACGATAGC	299	460,733
JB.194–13000 UP	ATGACCCGATTCTTGCTAGCC		
JB.195–13000 DOWN	TTGACGACTTGAGGCTGATGG	272	462,896
JB.196–15000 UP	ACTGTACATGAAGCCTCTACG		
JB.197–15000 DOWN	TAGGAACAAGGTGGATAGTGC	366	464,662
JB.198–17000 UP	CGGTGAAGTAGCATATGATGG		
JB.199–17000 DOWN	GGCTTTTGCGTATTCTAAGGC	396	466,768

[a] JB designations are reference numbers for our primer stocks; other numbers indicate the approximate distance of the PCR product amplified by each primer set from *CEN4*.
[b] All sequences are 5′ to 3′.
[c] The size (bp) of the PCR product amplified by each pair of primers.
[d] The chromosome IV bp coordinate of the midpoint of each PCR product.

3. Methods

Our initial attempts to perform Top2 ChIP using standard lysis buffers met with limited success. The percent recovery of DNA sequences was low or absent, and there was considerable sample-to-sample variability. These difficulties corresponded with the majority of Top2 fractionating with the insoluble pellet (**Fig. 10.1A**), leading us to suspect that we were recovering only a small fraction of Top2-associated chromatin. We found Top2 could be efficiently solubilized by extracting the cross-linked lysates with 2.5% SDS, leading to the development of the protocol described below. In this method, ChIP is performed essentially as described (10, 11), but with the addition of a detergent extraction step. This is followed by dilution of the sample to allow immunoprecipitation of the solubilized protein and associated chromatin. We also describe a set of primers for analyzing Top2 association with DNA sequences in a 34-kb region surrounding *CEN4* (**Table 10.1**). A representative data set obtained using this method is shown in **Fig. 10.1**.

3.1. Cell Culture and Protein Preparation

1. Grow cultures of *Saccharomyces cerevisiae* expressing epitope-tagged *TOP2* and untagged controls in YPD at 30°C overnight with shaking, aiming for a late log phase culture with an OD_{600} of 1–2. If *TOP2-myc* is being expressed from pTW009, it is necessary to maintain selection for the plasmid in synthetic complete medium.
2. Dilute the overnight cultures to an OD_{600} of 0.6 in YPD or minimal media for 3–4 h and culture at 30°C. A 50-ml culture should be sufficient for this procedure. As appropriate for the experiment, the cultures can also be supplemented with nocodazole (to block cells in mitosis) or other drugs (*see* **Note 1**).
3. At the end of the 3–4 h period, verify any drug arrest by observing cells under a microscope. For nocodazole-treated cultures, ~90% of the cells should be arrested as large budded cells. Once this level of arrest is achieved, measure the OD_{600} and remove a sufficient volume of the culture to achieve the equivalent of 50 ml of cells at an OD_{600} of 0.7. Readjust the volume to 50 ml and add 1.35 ml of formaldehyde. Fix cells for 2 h (*see* **Note 2**).
4. Quench the formaldehyde by adding 2.7 ml of 2.5 M glycine and mixing by swirling.
5. Pellet the cells at 3000*g* for 3 min.
6. Rinse the cells into a 2.0 ml screw-capped tube with 1 ml of distilled water, pellet the cells at 2000*g*, and aspirate the water from the pellet.

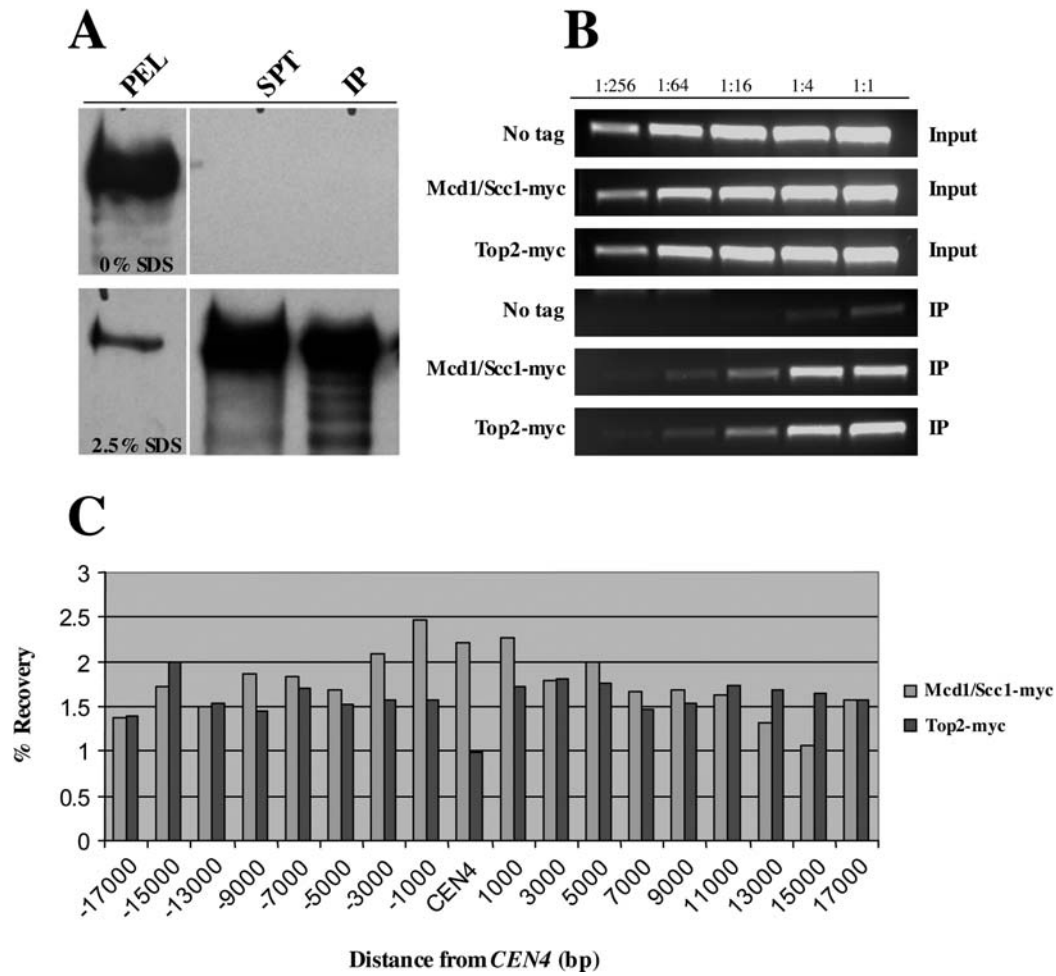

Fig. 10.1. **Recovery of Top2-associated chromatin by ChIP**. (**A**) Top2 release from the chromosome scaffold. Protein lysates (500 μl) from Top2-myc cells (JBY1403) were prepared with or without 2.5% SDS and partitioned into soluble and insoluble (PEL) fractions. Soluble fraction of 100 μl was removed (SPT), and Top2 was recovered from the remaining lysate by α-myc immunoprecipitation (IP). Equivalent volumes of PEL, SPT, and IP samples were analyzed by α-myc immunoblotting. (**B**) PCR analysis of Top2 ChIP samples. Using the method described in this chapter, ChIP samples were obtained from nocodazole-arrested cells. A four-fold dilution series was then prepared, 0.5 μl of each dilution was amplified by PCR (–17,000 primer set; **Table 10.1**), and the products were examined by gel electrophoresis. This type of data can be quantified using the NIH Image J application to determine sample dilutions and the number of reaction cycles necessary to produce a linear relationship between input DNA and PCR amplification. No tag control strain (CRY1), Mcd1/Scc1-myc (JBY705), and Top2-myc (JBY1403). (**C**) Top2 association with *CEN* proximal chromatin. The primer array described in **Table 10.1** was used to examine the recovery of DNA sequences association with both Top2-myc (JBY1403) and the cohesin subunit Mdc1/Scc1-myc (JBY705) over a 34-kb region surrounding *CEN4*.

7. Disrupt the cells with eight 30 s bursts in a BioSpec bead beater, placing the tubes on ice for 1 min in between each burst. Break the cells in 500 μl of lysis buffer supplemented with protease inhibitors, using 300 μl of glass beads (*see* **Note 3**).

8. Recover the cell lysate by puncturing the bottom of the lysis tube with an 18-gauge needle and transferring the contents into a fresh screwcap tube (the capture tube) by centrifugation for 5 min at 3000*g* at 4°C, as follows: Seat a new 2.0 ml screw-capped tube at the bottom of a 15 ml conical tube, set the punctured lysis tube on top of the capture tube, and then place the entire assemblage into the centrifuge rotor.
9. Shear the chromosomal DNA by sonication. We use a hand-held Fisher Sonic Dismembrator on setting 3 for five 12 s bursts on ice. Let the tubes sit on ice for 30 s in between each burst. The goal is to generate DNA fragments ranging from 300 to 1000 bp, with the bulk of fragments migrating at ~700 bp.
10. As precisely as possible, adjust the volume of the lysate to 500 µl with fresh lysis buffer. Add 72 µl of 20% SDS to bring the final concentration of SDS in the lysate to approximately 2.5%. Rotate on a nutator at room temperature for 5 min (*see* **Note 4**).
11. Pellet the insoluble cell debris by spinning in a microfuge at the high-speed setting (~14,000*g*) for 5 min. Remove the solubilized lysate to a 15 ml Falcon tube.
12. Remove 100 µl of the solubilized lysate to a screw-capped tube and keep on ice to use as an input sample. Dilute the remaining ~472 µl into 4.5 ml of lysis buffer supplemented with 150 µl of 10% Triton X-100 and protease inhibitors (*see* **Note 5**).

3.2. Chromatin Immunoprecipitation

1. Add 5–20 µl of the appropriate antibody to the Falcon tube and allow the sample to rotate on a nutator at 4°C for 2 h to overnight (*see* **Note 6**).
2. Add 300 µl of Protein A beads and 20 µl of the lambda BstEII digest and rotate for an additional hour (*see* **Note 7**).
3. Recover the Protein A beads and immunoprecipitated material by spinning at a low-speed setting in a microfuge (~500*g*) for 3 min.
4. Wash the beads as follows, recovering beads by spinning at low speed for 3 min after each wash:
   (a) Two 2-min washes using 1 ml of lysis buffer supplemented with protease inhibitors.
   (b) One 2-min wash using 1 ml of high-salt wash supplemented with protease inhibitors.
   (c) One 2-min wash using 1 ml of buffer III supplemented with protease inhibitors.
   (d) Two 2-min washes with 1 ml of low-salt wash supplemented with protease inhibitors.

5. Recover the immunoprecipitated material by eluting in 150 µl of TE/1% SDS for 15 min at 65°C. Spin at a high-speed setting in a microfuge (~14,000*g*) for 1 min, then remove the eluted supernatant from the beads and transfer to a fresh screw-capped tube. Repeat the elution, and combine the two supernatants.
6. Reverse the crosslinks by incubation at 65°C overnight. Be sure to include the input control tubes during this incubation step!
7. Treat with 5 µl of 20 mg/ml Proteinase K for 2 h at 37°C.
8. Recover the DNA using a Qiagen QIAquick PCR purification spin column:
   (a) Add five volumes of Buffer PB to the IP and input samples.
   (b) Pass the samples through the column (this will require multiple spins to get all of the immunoprecipitated samples through the column).
   (c) Wash once with 750 µl of Buffer PE.
   (d) Elute in 50 µl of elution buffer. This is your final sample (*see* **Note 8**).

3.3. Semi-quantitative PCR Analysis of Immunoprecipitated Chromatin

1. Set up an appropriate dilution of the input and IP samples. This will need to be determined experimentally, but fortunately is usually the same between experiments (*see* **Note 9** and **Fig. 10.1B**).
2. Set up 35 µl PCR reactions as follows, using Denville Scientific ChromaTaq:
   (a) 10X ChromaTaq reaction buffer (5 µl).
   (b) 50 mM of $MgCl_2$ solution (1.05 µl).
   (c) 10 mM of dNTP mix (0.7 µl).
   (d) 10 pmol/µl of each primer (3.5 µl, 10 mM primer stocks; *see* **Table 10.1**).
   (e) 1 unit of ChromaTaq Polymerase (1 µl) (*see* **Note 10**).
   (f) 0.5 µl of purified DNA at appropriate dilution.
   (g) 19.75 µl of dH_2O.
3. Run the PCR reactions using the following conditions:
   (a) 92°C for 2 min.
   (b) 92°C for 30 s.
   (c) 44°C for 30 s.
   (d) 65°C for 90 s.
   (e) Cycle steps B-D 25–30 times (*see* **Note 11**).
   (f) 68°C for 5 min.
   (g) Hold at 4°C.

4. Run the PCR products on a 2% agarose gel with EtBr (5 mg/ml) for 40 min at 120 V constant voltage.
5. Record the data with an appropriate gel documentation system, and then quantify band intensities using a densitometry application such as NIH Image J. We calculate percentage recovery for any given sample as [(IP peak area) × (1.2) × (dilution factor)]/[(input peak area) × (5.8) × (dilution factor)] × 100. The 1.2 and 5.8 values are correction factors for the distribution of the lysate between input and IP samples. The actual experimental percentage recovery for each primer set is then corrected for background using percentage recovery (sample)–percentage recovery (no tag control).

4. Notes

1. Nocodazole is used at a final concentration of 15 μg/ml. In our experience, a more efficient arrest in nocodazole is achieved in YPD as opposed to synthetic complete media. We have also performed Top2 ChIP using samples prepared from cells that had been arrested in G1 with α-factor (5 μg/ml at start of arrest and supplement at 1.5 h for *BAR1* strains).
2. We have achieved the best solubilization and most robust recovery of Top2-associated chromatin using the equivalent of 50 ml of cells at an OD_{600} of 0.7. If too many cells are used, lysis will not be efficient, Top2 may be solubilized inefficiently, or levels of non-specific amplification may be high. A 2 h fixation has worked well for us, but potentially could be reduced.
3. We include NEM because we are interested in the role of Top2 sumoylation on chromosomal distribution; NEM blocks hydrolysis of Top2 SUMO conjugates. A small aliquot should be prepared for each experiment immediately proceeding cell disruption. If sumoylation is not a consideration, NEM can be eliminated from the lysis buffer.
4. Due to fluid retention with the glass beads, at this point you may not have a full 500 μl. It is important to adjust the volume to 500 μl with lysis buffer to ensure the concentration of SDS is fairly accurate. As described in **Note 5**, if the concentration of SDS is too high, it will come out of solution when the temperature of the solution is lowered.
5. If the Triton-X100 was not added before moving samples to 4°C, or if the concentration of SDS is too high, the SDS will come out of solution at 4°C and appear cloudy. In our

experience, once this happens the IP will not work even if the SDS precipitate is warmed back into solution. If SDS precipitation is a problem, the IP can be done at room temperature, incubating in primary antibody for 2 h. For ChIP with other proteins (the cohesin subunits Mcd1/Scc1 and Pds5), we have reduced the final concentration of SDS to 2% and performed the entire IP procedure at room temperature. This has worked well and greatly minimized the SDS solubility problems.

6. The IPs have worked within the suggested range of antibody. Unfortunately, at least for us more (i.e., 20 μl) does appear to be better, giving the best yield and reproducibility from sample to sample.
7. The purpose of adding the exogenous DNA is to compete non-specific binding during recovery of the immune complexes. We have used the lambda BstEII digest with the idea that the relatively low-sequence complexity would minimize spurious PCR amplification. A different source of competitor DNA (such as sheared salmon sperm DNA) could probably also be used.
8. You can run some of the input DNA samples on a 0.8% agarose gel to verify the fragment size range.
9. For Top2-myc ChIP, we frequently find input dilutions of 1:10 or 1:20 and using the IP sample straight puts us in the linear amplification range. The method described here is for traditional PCR amplification; we have also used samples obtained by this method successfully for real-time PCR.
10. The Denville ChromaTaq has proven a useful reagent for us, providing more robust and reproducible amplification of ChIP samples compared to conventional Taq polymerase.
11. The amplification conditions and number of cycles are what we have routinely used for analysis of Top2 samples. This is of course another set of parameters that can be adjusted and optimized as required.

Acknowledgments

The authors would like to thank members of the Bachant laboratory for useful discussions and input in developing this protocol. This work was supported by an NIH grant (R01 GM-66190) to J.B.

References

1. Earnshaw, W. C., Halligan, B., Cooke, C. A., Heck, M. M. and Liu, L. F. (1985) Topoisomerase II is a structural component of mitotic chromosome scaffolds. *J Cell Biol* **100**, 1706–15.
2. Gasser, S. M., Laroche, T., Falquet, J., Boy de la Tour, E. and Laemmli, U. K. (1986) Metaphase chromosome structure. Involvement of topoisomerase II. *J Mol Biol* **188**, 613–29.
3. Belmont, A. S. (2002) Mitotic chromosome scaffold structure: new approaches to an old controversy. *Proc Natl Acad Sci USA* **99**, 15855–7.
4. Christensen, M. O., Larsen, M. K., Barthelmes, H. U., Hock, R., Andersen, C. L., Kjeldsen, E., Knudsen, B. R., Westergaard, O., Boege, F. and Mielke, C. (2002) Dynamics of human DNA topoisomerases IIalpha and IIbeta in living cells. *J Cell Biol* **157**, 31–44.
5. Tavormina, P. A., Come, M. G., Hudson, J. R., Mo, Y. Y., Beck, W. T. and Gorbsky, G. J. (2002) Rapid exchange of mammalian topoisomerase II alpha at kinetochores and chromosome arms in mitosis. *J Cell Biol* **158**, 23–9.
6. Porter, A. C. and Farr, C. J. (2004) Topoisomerase II: untangling its contribution at the centromere. *Chromosome Res* **12**, 569–83.
7. Bermejo, R., Doksani, Y., Capra, T., Katou, Y. M., Tanaka, H., Shirahige, K. and Foiani, M. (2007) Top1- and Top2-mediated topological transitions at replication forks ensure fork progression and stability and prevent DNA damage checkpoint activation. *Genes Dev* **21**, 1921–36.
8. Takahashi, Y., Yong-Gonzalez, V., Kikuchi, Y. and Strunnikov, A. (2006) *SIZ1/SIZ2* control of chromosome transmission fidelity is mediated by the sumoylation of topoisomerase II. *Genetics* **172**, 783–94.
9. Sikorski, R. S. and Hieter, P. (1989) A system of shuttle vectors and yeast host strains designed for efficient manipulation of DNA in *Saccharomyces cerevisiae*. *Genetics* **122**, 19–27.
10. Strahl-Bolsinger, S., Hecht, A., Luo, K. and Grunstein, M. (1997) *SIR2* and SIR4 interactions differ in core and extended telomeric heterochromatin in yeast. *Genes Dev* **11**, 83–93.
11. Meluh, P. B. and Koshland, D. (1997) Budding yeast centromere composition and assembly as revealed by in vivo cross-linking. *Genes Dev* **11**, 3401–12.

Chapter 11

Binding of DNA Topoisomerases I and II to Replication Origins

Arturo Falaschi

Abstract

The interaction of DNA topology modifying enzymes with eukaryotic DNA replication origins can be detected with nucleotide precision exploiting the action of enzyme poisons specific for type I or type II DNA topoisomerases. Using the topoisomerase I poison camptothecin and the topoisomerase II poison VP16, the precise sites of interaction of these enzymes around the lamin B2 origin have been identified at different points in the cell cycle. The procedure can be applied to any origin for which the sequence has been identified within approximately 1 kb.

Key words: DNA replication, camptothecin, VP16, LM-PCR, TD-PCR.

1. Introduction

Modulation of DNA topology is essential for the process of activation and deactivation of DNA replication origins in all studied organisms and viruses; hence DNA topoisomerases can be expected to interact with the origins at specific points in the cell cycle and carry out the necessary variations and adaptations of the local topological status of the origin DNA. A type II DNA topoisomerase, gyrase, is required for the processes of activation of ori C of *Escherichia coli* (1). Other topoisomerases are required for the function of several viral DNA origins: SV40 (2), BPV (3), and EBV (4). In vitro DNA synthesis in a *Saccharomyces cerevisiae* system requires the introduction of negative supercoiling through the action of DNA topoisomerase I (5). Negatively supercoiled DNA is essential for the binding of the *Drosophila* ORC to replication origins (6). The essential role of human DNA topoisomerase I for the initiation of synthesis at the origin located near the lamin B2

D.J. Clarke (ed.), *DNA Topoisomerases*, Methods in Molecular Biology 582,
DOI 10.1007/978-1-60761-340-4_11,

gene has been recently demonstrated (7); in the same article, procedures were established for identifying the precise sites of interaction of the two types of topoisomerases, that can be applied, in principle, to any eukaryotic replication origin for which the sequence is known with a precision of approximately 1 kb.

The procedures rely on the use of specific poisons that freeze the covalent enzyme-DNA phosphate intermediates formed by both enzymes and preclude the reformation of the phosphodiester linkage which is normally achieved by the topoisomerases. The poisons, both corresponding to molecules widely used in cancer chemotherapy for their inhibitory effect on DNA replication, are camptothecin for topoisomerase 1 (8) and the etoposide VP16 for topoisomerase II (9). The frozen intermediates carry a break at the precise nucleotide where the topoisomerase bound in the first place. This position, if specific enough, can be detected by exploiting appropriate PCR-based amplification procedures using the protein-bound DNA fragment as a template. The amplification procedures used are ligation-mediated PCR (LM-PCR) for the 3′-phosphate-enzyme intermediate produced by topoisomerase I and terminal deoxynucleotidyl transferase-mediated PCR (TD-PCR) for the 5′-phosphate-enzyme intermediate produced by topoisomerase II (10–12). For each amplification, a set of three primers, appropriate for the sequence under study, is used (see legend to **Fig. 11.2** for an example). The LM-PCR procedure is depicted in **Fig. 11.1**, and an example of the application to the lamin B2 origin and of the choice of primers is shown in **Fig. 11.2**. The TD-PCR procedure is depicted in **Fig. 11.3**, and an example of the application to the lamin B2 origin is shown in **Fig. 11.4**. The study of the lamin B2 origin revealed a surprising precision of the bound nucleotides, at specific moments of the origin functional cycle (7). Here, we describe in detail the procedures utilized to this purpose.

2. Materials

2.1. Cell Culture

1. HeLa cells or other human or mammalian cell lines.
2. Complete culture medium: D-MEM/F-12 (1:1) supplemented with GlutaMAX^{TM} I (Invitrogen), 10% final volume of fetal calf serum (Invitrogen), and 50 μg/ml gentamicin.

2.2. Topoisomerase I Mapping

1. Camptothecin: 100 mM stock solution of camptothecin (Sigma) dissolved in DMSO. Store at –20°C.
2. Lysis buffer: 250 mM Tris–HCl, pH 8.0, 25 mM EDTA, 5 mM NaCl, 0.5% SDS, 800 μg/ml proteinase K (Sigma).

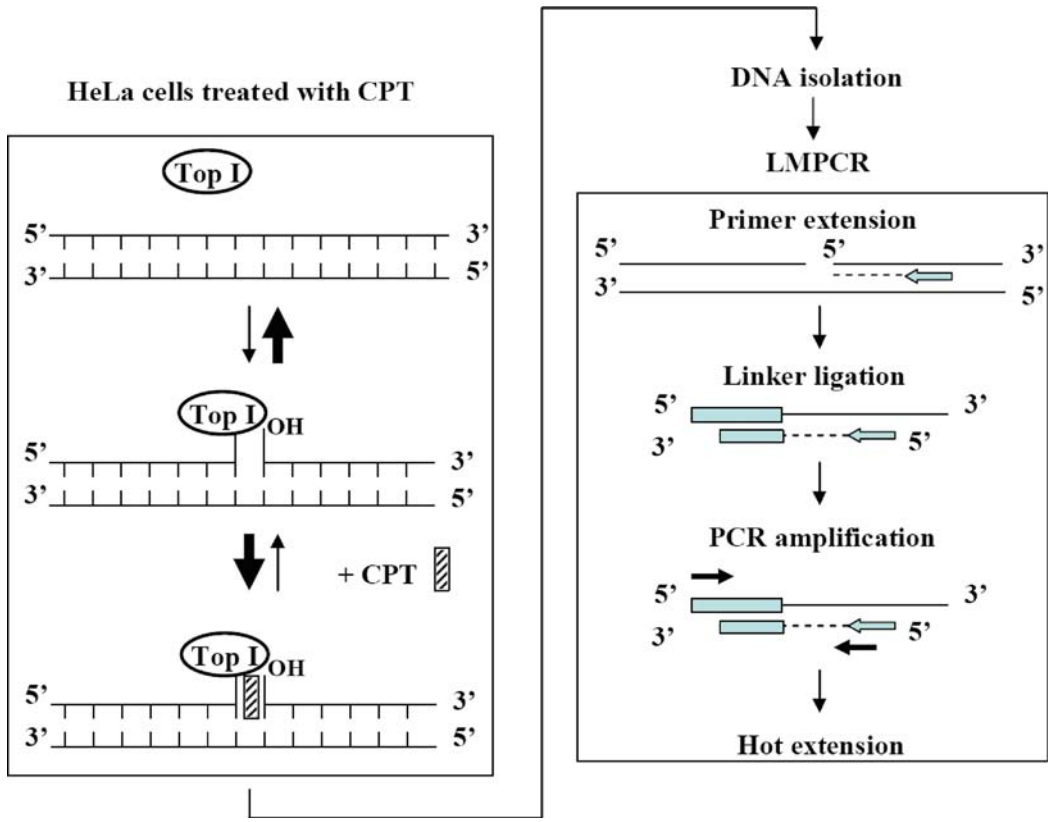

Fig. 11.1. **Mapping of the topoisomerase I-DNA cleavage complexes**. HeLa cells are treated with 1 μM CPT for 1 min to stabilize the topoisomerase I-DNA covalent complexes (*left panel*). The cells are then lysed, and the total genomic DNA is isolated and used for ligation-mediated PCR (LM-PCR) analysis (*right panel*). To perform LM-PCR analysis, the 5′-end of the DNA must be phosphorylated, therefore the genomic DNA is subjected first to an in vitro phosphorylation reaction. As a first step in LM-PCR, a sequence-specific primer (primer 1) is annealed to the region of interest and extended to obtain a double-stranded DNA blunt end, which, in turn, is ligated to an asymmetric linker. The next step is a PCR amplification of the substrate using a second sequence specific primer (primer 2) and a primer complementary to the linker sequence. As a final step, a third sequence specific primer (primer 3), radioactively labeled, is used for hot extension and the product is then visualized, following sequencing gel electrophoresis, by autoradiography.

3. PNK reaction buffer: 1 U/μl of polynucleotide kinase (New England Biolabs), 1 mM ATP, 1X PNK buffer (New England Biolabs).
4. PNK-gamma reaction buffer: 1 U/μl of polynucleotide kinase (New England Biolabs), 1 mM γ-^{32}P-ATP (3000 Ci/mmol at 10 mCi/ml), 1X PNK buffer (New England Biolabs).
5. Vent polymerase: Vent exo-DNA polymerase (New England Biolabs; 2000 U/ml).
6. Vent polymerase buffer: 1X Vent exo-DNA polymerase buffer (New England Biolabs).

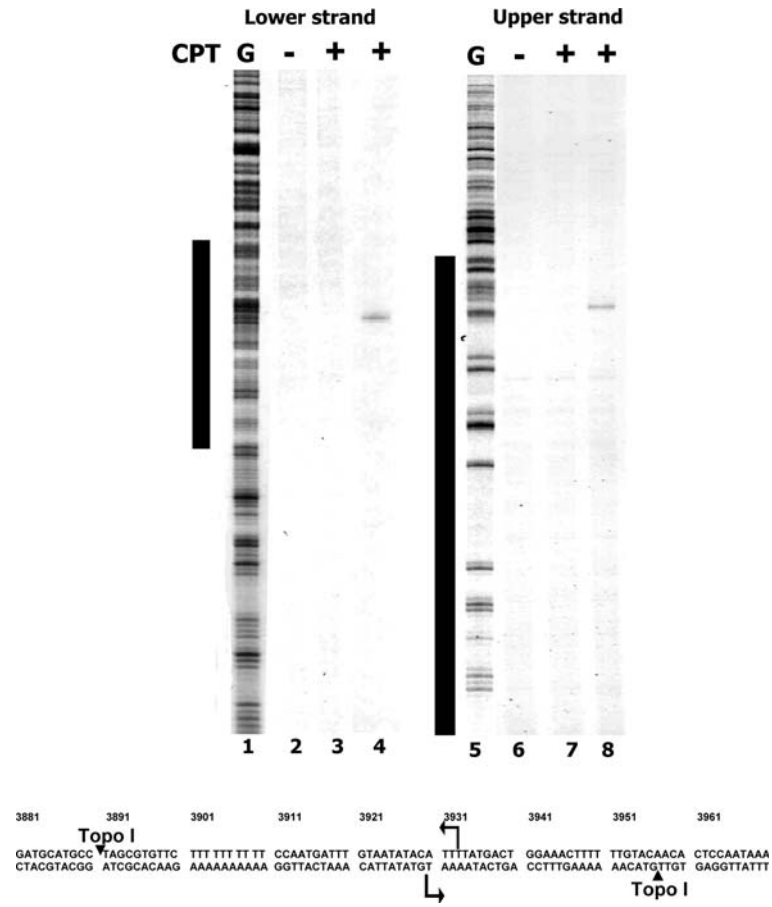

Fig. 11.2. **Positions of topoisomerase I residues in the lamin B2 origin sequence**. In asynchronous HeLa cells, topoisomerase I cleaves the region of the lamin B2 origin, which is covered by the replicative complexes. On both the *upper* and *lower strands*, respectively, one LM-PCR stop corresponding to one CPT-stabilized topo I cleavage complex can be detected. These stops correspond to the DNA 5′-end arisen from the topo I action at the origin. The *black bars* indicate the origin area covered by a protein footprint in asynchronous HeLa cells. Lanes 4, 8 – cells treated with 1 μM CPT for 1 min. Lanes 3, 7 – cells treated with DMSO only. G – In vitro DMS-treated genomic DNA. The *lower panel* shows the position of the topoisomerase I cleavage sites at the lamin B2 origin in asynchronous HeLa cells. The set of three primers used for the lower strand corresponds to nt 3795–3821, 3813–3837, and 3826–3851 of the lamin B2 origin (GeneBank accession number M94363), and those for the upper strand to nt 4049–4074, 4026–4052, 4016–4042.

7. dNTP mix: A mixture of the four dNTPs, each at a concentration of 5 mM.
8. Oligonucleotides: Long-linker oligonucleotide (5′-GCGG TGACCCGGGAGATCTGAATTC) and short-linker oligonucleotide (5′-GAATTCAGATC), each dissolved in distilled water at 400 pmol/μl.

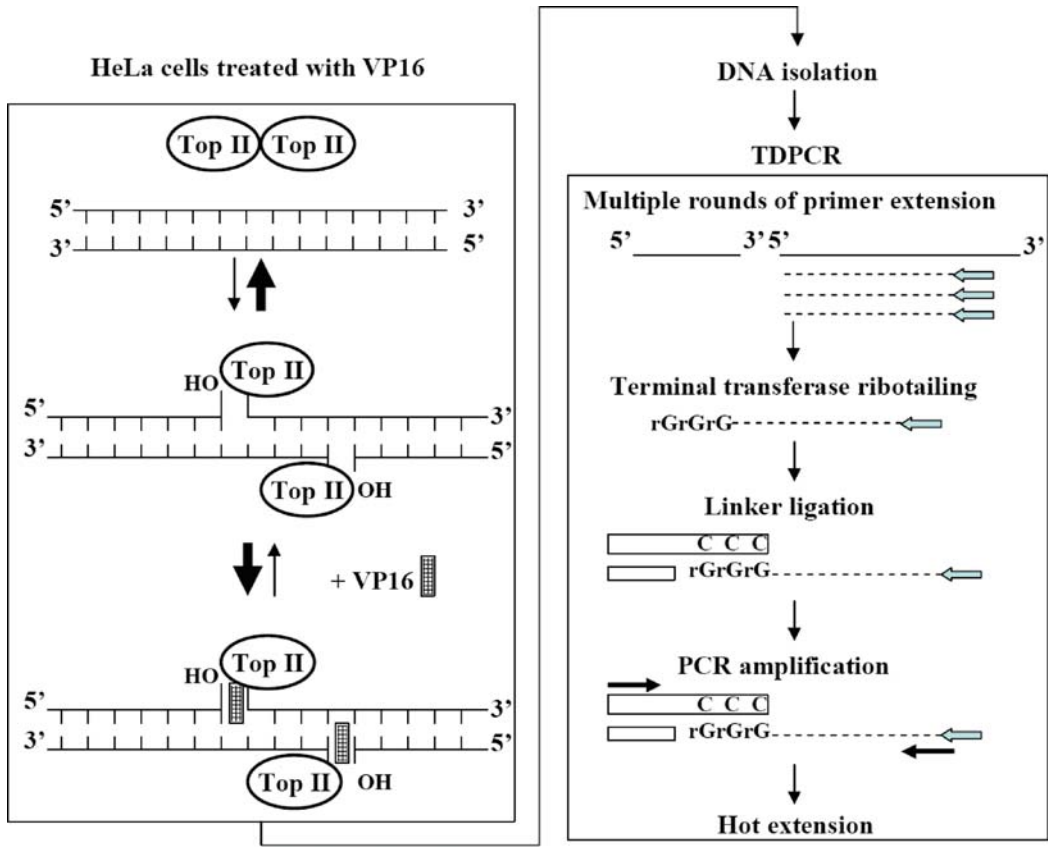

Fig. 11.3. **Mapping of the topoisomerase II-DNA cleavage complexes**. HeLa cells are treated with 10 nM VP16 for 1 min to stabilize the topo II-DNA covalent complexes (*left panel*). The cells are then lysed, and the total genomic DNA is isolated and used for terminal transferase dependent PCR (TD-PCR) analysis (*right panel*). As a first step, a sequence-specific primer (primer 1) is annealed to the region of interest and multiple rounds of polymerase extension are performed. The extension products, thus obtained, are subjected to 3′-end ribotailing using terminal transferase (TdT) and rGTP. This ribonucleotide is not the preferred substrate for TdT, and under determined conditions, the enzyme is able to add only three nucleotides (on average). The three rGs are complementary to an overhang of three C residues contained in the asymmetric linker, which aides the linker ligation reaction. The next step involves PCR amplification of the substrate using a second sequence specific primer (primer 2) and a primer complementary to the linker sequence (long asymmetric linker primer). As a final step, a third sequence specific primer (primer 3), radioactively labeled, is used for hot extension and the product is then visualized, following sequencing gel electrophoresis, by autoradiography.

9. Ligation mixture (Topo I mapping): 3 μl of Vent polymerase buffer, 3 μl of T4 DNA ligase buffer (New England Biolabs), 5 μl of annealed asymmetric linker [*see* **Section 3.2**, step 20; (13)], 19 μl of 40% PEG 8000.
10. T4 DNA ligase: 400 U/μl of T4 DNA ligase (New England Biolabs).
11. Loading buffer: 95% formamide, 100 mM EDTA, 0.5% bromophenol blue, 2.5% xylene cyanol.

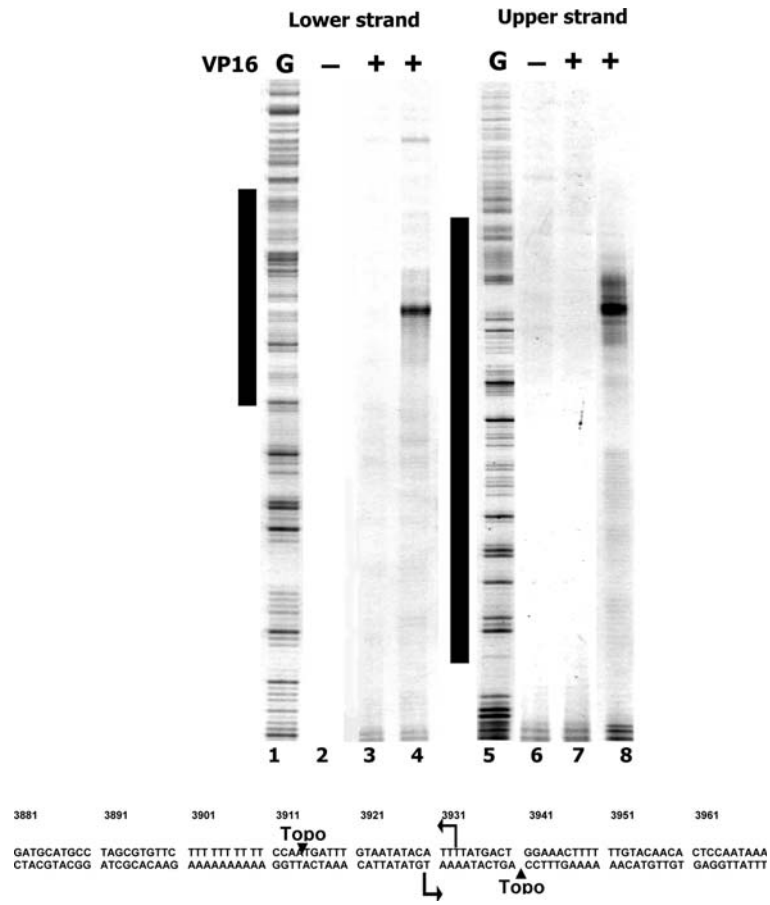

Fig. 11.4. **Positions of topoisomerase II residues in the lamin B2 origin sequence**. In asynchronous HeLa cells, topoisomerase II cleaves the region of the lamin B2 origin, which is covered by the replicative complexes. On both the *upper* and *lower strands*, respectively, one TD-PCR stop corresponding to one VP16-stabilized topoisomerase II cleavage complex can be detected. These stops correspond to the DNA 5′-end arisen from the topoisomerase II action at the origin. The *black bars* indicate the origin area covered by a protein footprint in asynchronous HeLa cells. Lanes 4, 8 – cells treated with 10 nM VP16 for 1 min. Lanes 3, 7 – cells treated with 10 nM VP16 for 1 min, and the drug washed from the cells and then incubated in drug-free complete culture medium for 5 min. Lanes 2, 6 – cells treated with DMSO only. G – In vitro DMS-treated genomic DNA. The *lower panel* shows the position of the topoisomerase II cleavage sites at the lamin B2 origin in asynchronous HeLa cells. The primer sets used are the same as in **Fig. 11.2**.

12. PBS (per l): 8 g NaCl, 0.2 g KCl, 1.15 g Na_2HPO_4, 0.2 g KH_2PO_4, pH 7.4.
13. TE: 1 mM EDTA, 10 mM Tris–HCl, pH 7.5.

2.3. Topoisomerase II Mapping

1. VP16: 10 mM stock solution of VP16 (Sigma) dissolved in DMSO. Store at –20°C.

2. Lysis buffer: 250 mM Tris–HCl, pH 8.0, 25 mM EDTA, 5 mM NaCl, 0.5% SDS, 800 μg/ml proteinase K (Sigma).
3. PNK reaction buffer: 1 U/μl of polynucleotide kinase (New England Biolabs), 1 mM ATP, 1X PNK buffer (New England Biolabs).
4. PNK-gamma reaction buffer: 1 U/μl of polynucleotide kinase (New England Biolabs), 1 mM γ-^{32}P-ATP (3000 Ci/mmol at 10 mCi/ml), 1X PNK buffer (New England Biolabs).
5. Vent polymerase: Vent exo-DNA polymerase (New England Biolabs; 2000 U/ml).
6. Vent polymerase buffer (New England Biolabs): 1X Vent exo-DNA polymerase buffer.
7. dNTP mix: A mixture of the four dNTPs, each at a concentration of 5 mM.
8. Ligation solution (Topo II mapping): 100 mM Tris–HCl, pH 7.5, 20 mM $MgCl_2$, 20 mM DTT, 2 mM ATP.
9. Loading buffer: 95% formamide, 100 mM EDTA, 0.5% bromophenol blue, 2.5% xylene cyanol.
10. T4 DNA ligase (for topoisomerase II mapping): 3 U/μl T4 DNA ligase (Promega).
11. Asymmetric linker primers: Long top-strand oligonucleotide, 5′-GCGGTGACCCGGGAGATCTGAATTCCC; short bottom-strand oligonucleotide, 3′-CGCCACTGGGCCCTCT AGACTTAA.
12. TdT mix: 1 U/μl of terminal deoxynucleotidyl transferase (TdT; Gibco BRL), 2X buffer supplied by the manufacturer, 4 mM rGTP.
13. Vent exo-mix: 0.07 U/μl Vent polymerase, 1.43X ThermoPol buffer, 2.9 mM $MgSO_4$, 0.4 mM each dNTP, 0.15 pmol/μl of primer 2 (see legend to **Fig. 11.3**), 0.15 pmol/μl of the long asymmetric linker primer (5′-GCGGTGACCCGGGAGATC TGAATTCCC).
14. PBS (per l): 8 g NaCl, 0.2 g KCl, 1.15 g Na_2HPO_4, 0.2 g KH_2PO_4, pH 7.4.
15. TE: 1 mM EDTA, 10 mM Tris–HCl, pH 7.5.

3. Methods

3.1. Cell Cultures

Culture the cells as monolayers in complete culture medium at 37°C, 5% CO_2. Maintain the cells in log phase growth, and subculture them at the necessary intervals to avoid the cells reaching confluence.

3.2. Topoisomerase I Mapping

1. Add to $\sim 10^7$ HeLa cells that are growing in log phase in complete culture medium a final concentration of 1 μM camptothecin.
2. Incubate the cells at 37°C, 5% CO_2 for 1 min.
3. Wash the cells twice with PBS containing 1 μM camptothecin (*see* **Notes 1** and **2**).
4. Lyse the cells by adding 1.5 ml of lysis buffer.
5. Incubate the cell lysates overnight at 37°C.
6. Isolate the DNA from the cell lysates by phenol/chloroform/isoamyl alcohol extraction.
7. Precipitate the DNA using 2.5 volumes of cold absolute ethanol.
8. Pellet the DNA by centrifugation and resuspend in 20 μl of TE.
9. Denature the DNA (using the whole 20 μl sample from step 8) by incubating for 5 min at 95°C.
10. Add to the DNA 0.1 pmol of primer 1 (*see* **Fig. 11.1**) and 10 μl of 1X Vent polymerase buffer. Allow the primer to anneal to the DNA by incubating for 30 min at 60°C.
11. Make up the second-strand DNA synthesis reaction as follows: Add to the DNA+primer mixture (from step 10) 2 μl of dNTP mix and 1 U of Vent polymerase. Make the mixture up to a final volume of 20 μl with distilled H_2O.
12. Allow the extension reaction to proceed by incubating the second-strand DNA synthesis reaction at the annealing temperature of the primer for 5 min, followed by a 10-s incubation at 65°C, a 10-s incubation at 70°C, and a 10-min incubation at 76°C.
13. Isolate the DNA by phenol/chloroform/isoamyl alcohol extraction.
14. Precipitate the DNA using 2.5 volumes of cold absolute ethanol.
15. Pellet the DNA by centrifugation and resuspend in 20 μl of TE.
16. To phosphorylate the 5′-OH ends generated by the extension reaction, set up the following: Add the 20 μl of DNA (from step 15) to PNK reaction buffer to give a final volume of 50 μl.
17. Incubate at 37°C for 30 min.
18. Extract the DNA once with phenol/chloroform/isoamyl alcohol.
19. Precipitate the DNA using 2.5 volumes of cold absolute ethanol in the presence of 0.3 M sodium acetate, pH 7.2, and 2 μg of glycogen.

20. Prepare the annealed asymmetric linker as follows:
    (a) Make a solution of the long-linker oligonucleotide and the short-linker oligonucleotide each at 200 pmol/μl.
    (b) Heat the solution at 95°C for 5 min then allow it to cool gradually.
21. Pellet the DNA and resuspend in 20 μl of ligation mixture and add 1 μl of T4 DNA ligase.
21. Incubate the ligation reaction overnight at 16°C.
22. Add to the ligation reaction 150 μl of TE and extract the DNA with phenol:chloroform.
23. Precipitate the DNA with 2.5 volumes of cold absolute ethanol in the presence of 2 μl of glycogen (20 mg/ml) and 0.3 M ammonium acetate.
24. Pellet the DNA and wash in 70% ethanol. Dry the pellet and resuspend in 20 μl of distilled H_2O.
25. Set up the PCR amplification reaction as follows: In a total reaction volume of 50 μl, add the 20 μl of the ligated product from step 24, 10 pmol of primer 2 (*see* **Fig. 11.1**), 10 pmol of the long-linker primer (*see* **Fig. 11.1**), 1 U of Vent polymerase and final concentrations of 1X Vent buffer, 4 mM $MgSO_4$, 0.2 mM of each of the four dNTPs.
26. Perform an 18-cycle PCR reaction using the following conditions: Pre-PCR denaturation, 3 min at 95°C; denaturation, 1 min at 95°C; annealing, 2 min at the temperature indicated for each primer 2; extension, 3 min at 76°C plus 3 s added to each subsequent cycle.
27. Prepare the γ-^{32}P-labeled oligonucleotide (primer 3) as follows (take the appropriate precautions needed for the use of radioactivity):
    (a) Add 20 μl of primer 3 (*see* **Fig. 11.1**) (0.5 pmol/μl) to 30 μl of PNK-gamma reaction buffer. (The primer must not be phosphorylated at the 5′ end.)
    (b) Incubate at 30°C for 30 min.
    (c) Extract the DNA once with phenol/chloroform/isoamyl alcohol.
    (d) Precipitate the DNA using 2.5 volumes of cold absolute ethanol in the presence of 0.3 M sodium acetate, pH 7.2, and 2 μg of glycogen.
28. Take 20 μl of the PCR reaction from step 26 and subject this to a radioactive extension by making up the reaction mixture as follows: In a final volume of 30 μl, combine 0.8 pmol of γ^{32}P-labeled primer 3 (from step 27 above), 0.5 U of Vent polymerase and final concentrations of 1X Vent buffer, 2.6 mM $MgSO_4$, 0.2 mM of each dNTP.

29. Perform a 5-cycle PCR reaction using the following conditions: Pre-PCR denaturation, 3 min at 95°C; denaturation, 1 min at 95°C; annealing, 2 min at the temperature indicated for each primer 3; extension, 7 min at 95°C.
30. Block the extension reaction by adding EDTA (final concentration, 40 mM).
31. Purify the DNA by phenol:chloroform extraction.
32. Precipitate the DNA with 2.5 volumes of cold absolute ethanol in the presence of 0.3 M sodium acetate.
33. Pellet the DNA and wash with 70% ethanol. Dry the pellet and resuspend in 7 µl of loading buffer.
34. Denature the samples by incubating for 3 min at 95°C. Subject the samples to electrophoresis on an 8% sequencing acrylamide gel.

3.3. Topoisomerase II Mapping

1. Add to $\sim 10^7$ HeLa cells that are growing in log phase in complete culture medium a final concentration of 10 nM VP16.
2. Incubate the cells at 37°C, 5% CO_2 for 1 min.
3. Wash the cells twice with PBS containing 10 nM VP16 (*see* **Notes 1** and **2**).
4. Lyse the cells by adding 1.5 ml of lysis buffer and incubating at room temperature for 5 min.
5. Incubate the cell lysates overnight at 37°C.
6. Isolate the DNA from the cell lysates by phenol/chloroform/isoamyl alcohol extraction.
7. Precipitate the DNA using 2.5 volumes of cold absolute ethanol in the presence of 0.3 M sodium acetate, pH 7.2, and 2 µg of glycogen.
8. Pellet the DNA by centrifugation and resuspend it in 10 µl of 0.1X TE.
9. Denature the DNA (the whole sample from step 8) by incubating for 5 min at 95°C.
10. Add to the DNA 0.1 pmol of primer 1 (*see* **Fig. 11.3**) and 10 µl of 1X Vent polymerase buffer. Allow the primer to anneal to the DNA by incubating for 30 min at 60°C.
11. Make up the second-strand DNA synthesis reaction as follows: Add to the DNA+primer mixture (from step 10) 2 µl of dNTP mix and 1 U of Vent polymerase. Make the mixture up to a final volume of 20 µl with distilled H_2O.
12. Allow the extension reaction to proceed by incubating the second-strand DNA synthesis reaction at the annealing temperature of the primer in each set for 5 min, followed by a 10-s incubation at 65°C, a 10-s incubation at 70°C, and a 10-min incubation at 76°C.

13. Isolate the DNA by phenol/chloroform/isoamyl alcohol extraction.
14. Precipitate the DNA using 2.5 volumes of cold absolute ethanol.
15. Pellet the DNA by centrifugation and resuspend in 10 µl of 0.1X TE.
16. Add to the DNA 10.5 µl of TdT mix and incubate at 37°C for 15 min.
17. Precipitate the DNA by adding sequentially: 80 µl of 2.5 M ammonium acetate, 4 µl of 250 mM EDTA, and 300 µl of ethanol.
18. After pelleting the DNA, dissolve it in 15 µl of 1/10 TE.
19. Prepare the TD-PCR asymmetric linker (*see* **Fig. 11.3**) as follows:
    (a) Phosphorylate the 5′-terminus of the bottom-strand oligonucleotide (*see* **Section 2.3**, reagent #11) according to the procedure in **Section 3.2**, steps 16–19.
    (b) Combine equal volumes each at 200 µM of the phosphorylated bottom-strand oligonucleotide and the top-strand oligonucleotide (*see* **Section 2.3**, reagent #11).
    (c) Heat the mixture at 95°C for 5 min and allow it to cool gradually.
20. Combine 10.5 µl of ligation solution, 3 µl of 20 µM TD-PCR asymmetric linker (from step 19), and 2 µl of T4 DNA ligase.
21. Incubate the mixture at 17°C overnight.
22. Make up the TD-PCR reaction as follows: Add to the 30 µl mixture from step 21, 70 µl of Vent exo-mix.
23. Perform PCR using 18 cycles as follows: 1 min at 95°C (5 min at 95°C for the first cycle), 2 min at 70°C, 3 min at 76°C (plus 3 s added per cycle), and 5 min at 76°C.
24. Prepare the γ-^{32}P-labeled oligonucleotide (primer 3) as follows (take the appropriate precautions needed for the use of radioactivity):
    (a) Add 20 µl of primer 3 (*see* **Fig. 11.3**) (0.5 pmol/µl) to 30 µl of PNK-gamma reaction buffer. (The primer must not be phosphorylated at the 5′-end.)
    (b) Incubate at 30°C for 30 min.
    (c) Extract the DNA once with phenol/chloroform/isoamyl alcohol.
    (d) Precipitate the DNA using 2.5 volumes of cold absolute ethanol in the presence of 0.3 M sodium acetate, pH 7.2, and 2 µg of glycogen.

25. Take 40 µl of the PCR reaction from step 23 and subject this to a radioactive extension by making up the reaction mixture as follows: In a final volume of 60 µl, combine 1 pmol of γ^{32}P-labeled primer 3, 1 U of Vent polymerase and final concentrations of 1X ThermoPol buffer, 2.6 mM $MgSO_4$, 0.2 mM of each dNTP.
26. Perform a 5-cycle PCR reaction using the following conditions: 1 min at 95°C (5 min at 95°C for the first cycle), 2 min at 72°C, 7 min at 76°C.
27. Purify the DNA by phenol:chloroform extraction.
28. Precipitate the DNA with 2.5 volumes of cold absolute ethanol in the presence of 0.3 M sodium acetate.
29. Pellet the DNA and wash with 70% ethanol. Dry the pellet and resuspend in 7 µl of loading buffer.
30. Denature the samples by incubating for 3 min at 95°C. Subject the samples to electrophoresis on an 8% sequencing acrylamide gel.

4. Notes

1. The inclusion of the drug in the PBS avoids reversal of the cleavable complexes.
2. Two different controls can be employed. First, the cells can be treated with DMSO only (i.e. a no drug control). Second, for both enzymes, it is advisable to check for the reversal of the drug-induced cleavage. This can be achieved by washing the drug from the treated cells (i.e. wash with drug-free PBS) and then incubate the cells in complete culture medium for 10–30 min before the DNA extraction and LM-PCR or TD-PCR procedure.

References

1. Kornberg, A. (1984) Enzyme studies on the replication of the *Escherichia coli* chromosome. *Adv Exp Med Biol* **179**, 3–16.
2. Halmer, L., Vestner, B. and Gruss, C. (1998) Involvement of topoisomerases in the initiation of simian virus 40 minichromosome replication. *J Biol Chem* **273**, 34792–34798.
3. Hu, Y., Clower, R. V. and Melendy, T. (2006) Cellular topoisomerase I modulates origin binding by bovine papilloma virus type 1 E1. *J Virol* **80**, 4363–4371.
4. Kawanishi, M. (1993) Topoisomerase I and II activities are required for Epstein-Barr virus replication. *J Gen Virol* **74**, 2263–2268.
5. Mitkova, A.V., Biswas-Fiss, E. E. and Biswas, S.B. (2005) Modulation of DNA synthesis in *Saccharomyces cerevisiae* nuclear extract by DNA polymerases and the origin recognition complex. *J Biol Chem* **280**, 6285–6292.
6. Remus, D., Beall, E.L. and Botchan, M.R. (2004) DNA topology, not DNA sequence,

is a critical determinant for Drosophila. ORC-DNA binding. *EMBO J* **23**, 897–907.

7. Abdurashidova, G., Radulescu, S., Sandoval, O., Zahariev S., Danailov, M. B., Demidovich, A., Santamaria, L., Biamonti, G., Riva, S. and Falaschi, A. (2007) Functional interactions of DNA topoisomerases with a human replication origin. *EMBO J* **26**, 998–1009.
8. Pommier, Y., Pourquier, P., Fan, Y. and Strumberg, D. (1998) Mechanism of action of eukaryotic DNA topoisomerase I and drugs targeted to the enzyme. *Biochim Biophys Acta* **1400**, 83–105.
9. Burden, D.A. and Osheroff, N. (1998). Mechanism of action of eukaryotic topoisomerase II and drugs targeted to the enzyme. *Biochim Biophys Acta* **1400**, 139–154.
10. Strumberg, D., Pilon, A.A., Smith, M., Hickey, R., Malkas, L. and Pommier, Y. (2000) Conversion of topoisomerase I cleavage complexes on the leading strand of ribosomal DNA into 5′-phosphorylated DNA double-strand breaks by replication runoff. *Mol Cell Biol* **20**, 3977–3987.
11. 11.Mueller, P.A., Wold, B. and Garrity, P.A. (2001) Ligation-mediated PCR for genomic sequencing and footprinting. In *Current protocols in molecular biology* (New York: John Wiley & Sons, Inc.), pp. 15.3.1–15.3.26.
12. Komura, J. and Riggs, A.D. (1998) Terminal transferase-dependent PCR: a versatile and sensitive method for in vivo footprinting and detection of DNA adducts. *Nucleic Acids Res* **26**, 1807–1811.
13. Quivy, J. P. and Becker P.B. (1993) An improved protocol for genomic sequencing and footprinting by ligation-mediated PCR. *Nucleic Acids Res* **21**, 2779–2781.

Chapter 12

Cytometric Assessment of DNA Damage Induced by DNA Topoisomerase Inhibitors

Zbigniew Darzynkiewicz, Dorota H. Halicka, and Toshiki Tanaka

Abstract

Exposure of cells to inhibitors of DNA topoisomerase I (topo I) or topoisomerase II (topo II) leads to DNA damage that often involves formation of DNA double-strand breaks (DSBs). DNA damage, particularly induction of DSBs, manifests by phosphorylation of histone H2AX on *Ser*-139 which is mediated by one of the protein kinases of the phosphoinositide kinase family, namely ATM, ATR, and/or DNA-PK. The presence of *Ser*-139 phosphorylated H2AX (γH2AX) is thus a reporter of DNA damage. This protocol describes quantitative assessment of γH2AX detected immunocytochemically in individual cells combined with quantification of cellular DNA content by cytometry. The bivariate analysis of γH2AX expression versus DNA content allows one to correlate DNA damage with the cell cycle phase or DNA ploidy. The protocol can also be used to assess activation (*Ser*-1981 phosphorylation) of ATM; this event also revealing DNA damage induced by topo I or topo II inhibitors. Examples where DNA damage was induced by topotecan (topo I) and etoposide (topo II) inhibitors are provided.

Key words: Histone H2AX phosphorylation, ataxia telangiectasia mutated, ATM, DNA double-strand breaks, flow cytometry, apoptosis, cell cycle, topotecan, etoposide.

1. Introduction

DNA topoisomerase I (topo I) and topoisomerase II (topo II) inhibitors are among the most widely used anticancer drugs. These drugs stabilize otherwise transient covalent complexes (*cleavable complexes*), consisting of DNA bound to topo I or topo II, in the process of untangling the DNA helix (1, 2). During DNA replication, the replication forks collide with these complexes converting them to DNA double-strand breaks (DSBs). DSBs can also be formed during transcription when the RNA polymerase

D.J. Clarke (ed.), *DNA Topoisomerases*, Methods in Molecular Biology 582,
DOI 10.1007/978-1-60761-340-4_12,

molecules, progressing along the transcribed DNA strand, collide with the cleavable complexes (3). Binding of topo inhibitors to DNA in live cells also causes condensation of the DNA-inhibitor complexes (4). In addition to the mechanism involving formation of cleavable complexes, certain topo II inhibitors induce DNA damage, including formation of DSBs, by generating reactive oxygen intermediates (5, 6). Induction of DSBs may trigger apoptosis, and cells replicating their DNA were shown to be particularly susceptible to apoptosis when treated with topo I inhibitors of the camptothecin family or with the topo II inhibitors mitoxantrone or etoposide (6–8).

DNA damage, particularly involving formation of DSBs, triggers phosphorylation of histone H2AX (9), a variant of nucleosome core histone H2A (10). The phosphorylation, mediated by one of the members of the phosphoinositide kinase family, ATM, ATR, or DNA-PK, occurs on *Ser*-139 within the C terminus of H2AX. Nucleosomes containing this modified H2AX are located within a megabase domain of DNA flanking the DSBs (11). Phosphorylated H2AX, defined as γH2AX, can be detected immunocytochemically using γH2AX phospho-specific antibodies (Abs). Shortly after induction of DSBs, the appearance of γH2AX on chromatin manifests in the form of discrete immunofluorescent (IF) nuclear foci, each focus representing a single DSB (12). The intensity of γH2AX IF within an individual cell correlates with extent of DNA damage (frequency of DSBs) in its nucleus. Flow- or laser scanning-cytometry allows the rapid quantification of γH2AX IF in large cell populations, and multiparameter analysis of the cytometric data makes it possible to correlate DNA damage with other attributes of the cell, e.g., cell cycle phase or induction of apoptosis (13–16). Assessment of H2AX phosphorylation combined with the assessment of activation of ATM provides more specific and definitive evidence of DNA damage, particularly formation of DSBs, than analysis of H2AX phosphorylation alone, and the immunocytochemical probe to reveal ATM activation is available (5, 6, 8). This cytometric approach utilizing either γH2AX alone or both γH2AX and ATM-S1981P probes to measure DNA damage is rapid, more sensitive, and less cumbersome compared with the alternative, commonly used method, the comet assay (17).

The method presented in this chapter is designed to assess the intensity of γH2AX and/or ATM-S1981P immunofluorescence (IF) for evaluation of the extent of DNA damage. The detection of γH2AX or ATM-S1981P is combined with differential staining of DNA to measure cellular DNA contents and thus to define the cell cycle phase of the cells in which DNA damage is measured (*see* **Note 1**). The procedure is based on indirect IF detection of γH2AX using the primary Ab unlabeled and the secondary Ab conjugated with FITC or Alexa Fluor 488 (*see* **Note 2**). DNA is

counterstained with propidium iodide (PI) whose emission spectrum (red) is separated from the green color emission of FITC or Alexa Fluor 488. The cells are briefly fixed in methanol-free formaldehyde and then transferred into 70% ethanol in which they can be kept briefly ($\geq$2 h) or stored at –20°C for weeks or longer. Ethanol treatment makes the plasma membrane permeable to the γH2AX Ab; further permeabilization is achieved by including the detergent Triton X-100 in a solution used to incubate cells with the Ab. After incubation with the primary γH2AX Ab, the cells are incubated with FITC or Alexa Fluor 488-labeled secondary Ab and their DNA is counterstained PI in the presence of RNase A to remove RNA, which otherwise, similar to DNA, would be stained with PI. The intensity of cellular green (FITC or Alexa Fluor 488) and red (PI) fluorescence is measured by flow cytometry.

It should be noted that H2AX undergoes constitutive phosphorylation in healthy cells, not treated with radiation or genotoxic agents. This constitutive presence of γH2AX, which is more pronounced in S and G_2M than in G_1 cells, is considered to be in large part a reflection of oxidative DNA damage caused by metabolically generated oxidants (18, 19). Furthermore, extensive DNA fragmentation that takes place during apoptosis (20) leads to the formation of a large quantity of DSBs which triggers high level of H2AX phosphorylation (21). Strategies are presented in this chapter to differentiate between the DNA damage induced by topo inhibitors versus the constitutive damage occurring in untreated cells (*see* **Note 3**), or versus apoptosis-associated (AA) DSBs (*see* **Note 4**).

2. Materials

2.1. Reagents

1. Cells to be analyzed: 10^6–5×10^6 cells, untreated (control) and treated in culture with topo I or topo II inhibitors, are suspended in 1 ml of tissue culture medium. It is adequate to expose cells to 0.1–2 μM of camptothecin, topotecan, mitoxantrone, or etoposide for 1 h in culture to obtain extensive DNA damage that can be easily detected and measured according to this protocol.
2. 70% ethanol.
3. Abs: There are several commercially available phospho-specific Abs monoclonal as well as polyclonal, unconjugated and FITC- or Alexa Fluor 488-conjugated, applicable to cytometry, that can be used to detect gH2AX or ATM-S1981P (e.g., from BioLegend, San Diego, CA; Cell Signaling/Santa Cruz Biotechnology, Danvers, MA; Molecular Probes/Invitrogen,

Eugene, OR; Millipore/Upstate, Lake Placid, NY). The same companies also offer FITC- or Alexa 488-tagged secondary Abs to be used in conjunction with the unconjugated primary Abs.

4. 12 × 75 mm polypropylene tubes.
5. Methanol-free formaldehyde fixative: Prepare 1% (v/v) solution of methanol-free formaldehyde (Polysciences, Warrington, PA) in phosphate-buffered saline (PBS). This solution may be stored at 4°C for up to 2 weeks.
6. BSA–T–PBS: Dissolve bovine serum albumin (BSA; Sigma) in PBS to obtain 1% (w/v) BSA solution. Add Triton X-100 (Sigma Chemical Co., St. Louis, MO) to obtain 0.2% (v/v) of its concentration. This solution may be stored at 4°C for up to 2 weeks.
7. PI stock solution: Dissolve propidium iodide (PI; Molecular Probes/Invitrogen) in distilled water to obtain a 1 mg/ml solution. This solution can be stored at 4°C in the dark (e.g., in the tube wrapped in aluminum foil) for several months.
8. PI staining solution: Dissolve DNase-free RNase A (e.g., from Sigma) in PBS to obtain 0.1% (w/v; 100 mg/ml) solution. Add an appropriate aliquot of PI stock solution (e.g., 5 µl per 1 ml) to obtain its 5 µg/ml final concentration. Store the PI staining solution in the dark. This solution may be stored at 4°C for up to 2 weeks.

2.2. Instrumentation

Flow cytometers of different types, offered by several manufacturers, can be used to measure cell fluorescence following staining according to the protocol given below. The most common flow cytometers are from Coulter Corporation (Miami, FL), Becton Dickinson Immunocytometry Systems (San Jose, CA), Cytomation/DAKO (Fort Collins, CO), and PARTEC (Zurich, Switzerland).

3. Methods

1. Centrifuge cells collected from tissue culture (suspended in culture medium) at 300*g* for 4 min at room temperature. Suspend cell pellet (1–2 × 10^6 cells) in 0.5 ml of PBS.
2. With a Pasteur pipette, transfer this cell suspension into a polypropylene tube (*see* **Note 5**) containing 4.5 ml of ice-cold 1% methanol-free formaldehyde solution in PBS. Keep on ice for 15 min.
3. Centrifuge at 300*g* for 4 min at room temperature and suspend the cell pellet in 4.5 ml of PBS. Centrifuge again as above and suspend the cell pellet in 0.5 ml of PBS. With a

Pasteur pipette, transfer the suspension to a tube containing 4.5 ml of ice-cold 70% ethanol. The cells should be stored in the 70% ethanol at –20°C for at least 2 h, but may be stored under these conditions for up to 2 weeks.

4. Centrifuge at 200*g* for 4 min at room temperature, remove the ethanol, and suspend the cell pellet in 2 ml of BSA–T–PBS solution.
5. Centrifuge at 300*g* for 4 min at room temperature and suspend the cells again in 2 ml of BSA–T–PBS. Keep at room temperature for 5 min.
6. Centrifuge at 300*g* for 4 min at room temperature and suspend the cells in 100 µl of BSA–T–PBS containing 1 µg of the primary γH2AX Ab (*see* **Notes 2** and **6**).
7. Cap the tubes to prevent drying and incubate them overnight at 4°C (*see* **Note 7**).
8. Add 2 ml of BSA–T–PBS and centrifuge at 300*g* for 4 min at room temperature.
9. Centrifuge at 300*g* for 4 min at room temperature and suspend the cells in 2 ml of BSA–T–PBS.
10. Centrifuge at 300*g* for 4 min at room temperature and suspend the cell pellet in 100 µl of BSA–T–PBS containing the appropriate (anti-mouse or anti-rabbit, depending on the source of the primary Ab) FITC- or Alexa Fluor 488-tagged secondary Ab (*see* **Note 6**).
11. Incubate for 1 h at room temperature, occasionally gently shaking. Add 5 ml of BSA–T–PBS, and after 2 min, centrifuge at 300*g* for 4 min at room temperature.
12. Suspend the cells in 1 ml of the PI staining solution. Incubate at room temperature for 30 min in the dark.
13. Set up and adjust the flow cytometer for excitation within the blue wavelength range (488-nm laser line or BG-12 excitation filter).
14. Measure the intensity of green (530 ± 20 nm) and red (>600 nm) fluorescence of the cells by flow cytometry. Record the data.

4. Notes

1. On the bivariate distributions (scatterplots), subpopulations of cells in G_1, versus S versus G_2/M, are distinguished based on differences in their DNA content (intensity of PI fluorescence; *see* **Fig. 12.1**). To assess the mean extent of DNA

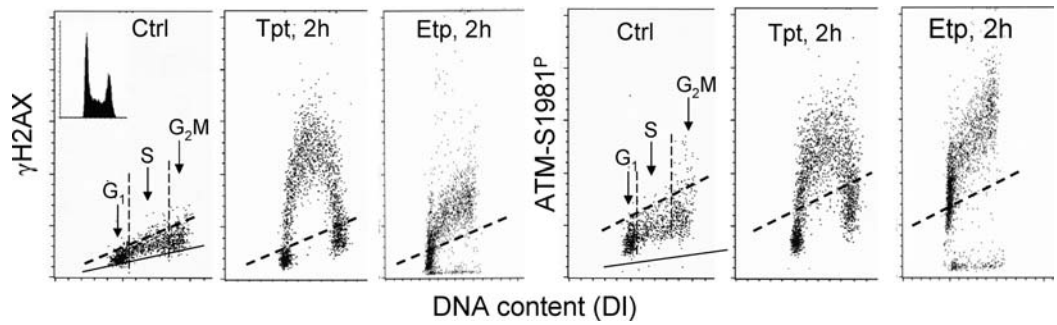

Fig. 12.1. **Bivariate flow cytometry**. Detection of histone H2AX phosphorylation on *Ser*139 and ATM activation (phosphorylation on *Ser*-1981) induced by topotecan (Tpt) or etoposide (Etp) in relation to the cell position in the cell cycle. Bivariate (cellular DNA content versus γH2AX IF or DNA content versus ATM-S1981P IF) distributions (scatterplots) of human lymphoblastoid TK6 cells are shown under the following conditions: untreated (Ctrl) or treated in cultures with 0.15 μM Tpt or 10 μM of Etp for 2 h. The cells were processed as described in the protocol; their fluorescence was measured by flow cytometry (FACScan; Becton Dickinson Immunochemistry, San Jose, CA). Note increased γH2AX and ATM-S1981P IF of S-phase cells from the Tpt-treated culture and the cell cycle phase-indiscriminative (overall) increase of γH2AX and ATM-S1981P IF of cells from the Etp-treated culture. Based on differences in DNA content, the subpopulations of cells in G_1, versus S versus G_2M phases of the cycle, may be distinguished and gated as shown in the Ctrl samples (*vertical dashed lines*). The mean γH2AX IF or ATP-S1981P IF may be then calculated for each cell cycle-phase subpopulation. To estimate the extent of the *treatment-induced* H2AX phosphorylation or ATM activation, the γH2AX or ATM-S10981P IF mean values of the untreated cells have to be subtracted from the respective G_1, S, and G_2M means of the treated samples to obtain the drug-induced increase (Δ) of the mean values. The *dashed line* represents the upper γH2AX or ATM-S1981P IF threshold for 95% of the cells from the untreated (Ctrl) cultures. The *solid skewed lines* represent the upper 95% threshold of the fluorescence intensity for the nonspecific isotype control. The cellular DNA content histogram of the cells subjected to Tpt or Etp treatment is shown in the *left panel inset*.

damage for cells at a particular phase of the cycle, the mean values of γH2AX or ATM-S1981P IF are calculated separately for G_1, S, and G_2/M cells distinguished based on differences in DNA content, by the computer-interactive "gating" analysis. The gating analysis should be carried out to obtain mean values of γH2AX or ATM-S1981P IF for G_1 (DNA index, DI = 0.9–1.1), S (DI = 1.2–1.8), and G_2M (DI = 1.9–2.1) cell subpopulations.

2. If primary Ab conjugated with fluorochrome (e.g., with FITC or Alexa Fluor 488) is being used, replace the unlabelled Ab in step 5 with the conjugated one and move to step 10, omitting steps 6–9.
3. A low level of γH2AX or ATM-S1981P IF seen in the cells that have not been treated with inducers of DSBs represents the "background," constitutive H2AX phosphorylation, and ATM activation, most of which reflects oxidative DNA damage induced by metabolically generated reactive oxygen species (ROS) (18, 19). The level of constitutive γH2AX phosphorylation and ATM activation is generally higher in S- and G_2M- than in G_1-phase cells and varies between different cell lines. To quantify the γH2AX or ATM-S1981P IF

induced by external factors that damage DNA (e.g., topo I or topo II inhibitors), the constitutive component of γH2AX IF or ATM-S1981P has to be subtracted. Toward this end, the means of γH2AX or ATM-S1981P IF of G_1, S, and G_2/M-phase of the untreated cells are subtracted from the respective means of the G_1, S, and G_2/M subpopulations of the drug-treated cells, respectively (*see* **Fig. 12.1**). After the subtraction, the extent of *increase* in intensity of γH2AX (ΔγH2AX IF) or ATM-S1981P (ΔATM-S1981P IF) over the untreated sample represents the *treatment-induced phosphorylation* of this protein. The irrelevant isotype control can be used to estimate the nonspecific Ab binding component, although its use may be unnecessary when one is interested only in the assessment of the drug-induced increase (Δ) in IF.

4. DNA undergoes extensive fragmentation during apoptosis (20), which leads to the appearance of a multitude of DSBs in apoptotic cells, triggering H2AX phosphorylation and ATM activation (6, 8, 21). It is often desirable, therefore, to distinguish between primary DSBs induced by DNA damaging agents (e.g., topo inhibitors) versus DSBs generated during apoptosis. The following attributes of γH2AF IF allow one to distinguish the cells with the radiation-, drug- or carcinogen-induced H2AX phosphorylation from the cells that have phosphorylation of this histone triggered by apoptosis-associated (AA) DNA fragmentation: (a) The γH2AX IF induced by external DNA damaging agents is seen rather early during the treatment (10 min to 2 h) whereas AA γH2AX IF is seen later (>3 h) (6, 8, 21); (b) The intensity of AA γH2AX IF is generally much higher than that of DNA damage-induced γH2AX IF, unless the cells are at a late stage of apoptosis (21); (c) The induction of AA γH2AX IF is prevented by cell treatment with the caspase inhibitor z-VAD-FMK, which precludes activation of endonucleases responsible for DNA fragmentation. In its presence, thus, the AA γH2AX IF is suppressed (16); and (d) the AA H2AX phosphorylation occurs concurrently with activation of caspase-3 in the same cells. Multiparameter analysis (active caspase-3 versus γH2AX IF), thus, provides a direct approach to distinguish cells in which DSBs were caused by inducers of DNA damage (active caspase-3 is undetectable) from the cells that have H2AX phosphorylation and ATM activation additionally triggered in response to apoptotic DNA fragmentation (active caspase-3 is present). These strategies are discussed in more detail elsewhere (16).
5. If the sample initially contains a small number of cells, they may be lost during repeated centrifugations. To minimize cell loss, polypropylene or siliconized glass tubes are

recommended. Since transferring cells from one tube to another causes electrostatic attachment of a large fraction of cells to the surface of each new tube, all steps of the procedure (including fixation) preferentially should be done in the same tube. Addition of 1% BSA to rinsing solutions also decreases cell loss. When the sample contains very few cells, carrier cells (e.g., chick erythrocytes) may be included; they may be recognized during analysis based on differences in DNA content (intensity of PI fluorescence).

6. Quality of the primary and of the secondary antibody is of utmost importance. The ability to detect γH2AX or ATM-S1981P is often lost during improper transport or storage conditions of the Ab. We have occasionally observed that Abs provided by vendors are defective. Also of importance is the use of the Abs at optimal concentration. It is recommended that with the first use of every new batch, the primary and secondary Abs should be tested at serial dilutions (e.g., within the range between 0.2 and 2.0 μg/100 μl) to determine their optimal titer for detection of γH2AX or ATM-S1981P. The optimal titer is recognized as giving maximal signal-to-noise ratio, i.e., the maximal ratio of the mean IF intensity of the drug-treated cells to the untreated cells. The titer recommended by the vendor is not always the optimal one.
7. Alternatively, incubate for 1 h at 22–24°C. The overnight incubation at 4°C, however, appears to yield somewhat higher intensity of γH2AX IF or ATM-S1981P IF compared with 1-h incubation.

Acknowledgment

Supported by NCI grant RO1 28704.

References

1. Hsiang, Y.H., Lihou, M.G., and Liu, L.F. (1989) Arrest of replication forks by drug stabilized topoisomerase I-DNA cleavable complexes as a mechanism of cell killing by camptothecin. *Cancer Res* **49**, 5077–5082.
2. D'Arpa, P., Beardmore, C., and Liu, L.F. (1990) Involvement of nucleic acid synthesis in cell killing mechanisms of topoisomerase poisons. *Cancer Res* **50**, 6916–6924.
3. Wu, J., and Liu, L.F. (1997) Processing of topoisomerase I cleavable complexes into DNA by transcription. *Nucleic Acids Res* **25**, 4181–4186.
4. Kapuscinski, J., and Darzynkiewicz, Z. (1986) Relationship between the pharmacological activity of antitumor drugs Ametantrone and Mitoxantrone (Novantrone) and their ability to condense nucleic acids. *Proc Natl Acad Sci USA* **83**, 6302–6306.
5. Huang, X., Kurose, A., Tanaka, T., Traganos, F., Dai, W., and Darzynkiewicz, Z. (2006) Activation of ATM and histone H2AX phosphorylation induced by

mitoxantrone but not by topotecan is prevented by the antioxidant *N*-acetyl-L-cysteine. *Cancer Biol Ther* **5**, 959–964.

6. Tanaka, T., Halicka, H.D., Traganos, F., Seiter, K., and Darzynkiewicz, Z. (2007) Induction of ATM activation, histone H2AX phosphorylation and apoptosis by etoposide: relation to the cell cycle phase. *Cell Cycle* **6**, 371–376.
7. Del Bino, G., Bruno, S., Yi, P.N., and Darzynkiewicz, Z. (1992) Apoptotic cell death triggered by camptothecin or teniposide: the cell cycle specificity and effects of ionizing radiation. *Cell Prolif* **25**, 537–548.
8. Kurose, A., Tanaka, T., Huang X., Halicka, H.D., Traganos F., Dai, W., and Darzynkiewicz, Z. (2005) Assessment of ATM phosphorylation on *Ser*-1981 induced by DNA topoisomerase I and II inhibitors in relation to *Ser*-139-histone H2AX phosphorylation, cell cycle phase and apoptosis. *Cytometry A* **68A**, 1–9.
9. Rogakou, E.P., Pilch, D.R., Orr, A.H., Ivanova, V.S., and Bonner, W.M. (1998) DNA double-stranded breaks induce histone H2AX phosphorylation on serine 139. *J Biol Chem* **273**, 5858–5868.
10. West, M.H., and Bonner, W.M. (1980) Histone 2A, a heteromorphous family of eight protein species. *Biochemistry* **19**, 3238–3245.
11. Rogakou, E.P., Boon, C., Redon, C., and Bonner, W.M. (1999) Megabase chromatin domains involved in DNA double-strand breaks in vivo. *J Cell Biol* **146**, 905–916.
12. Sedelnikova, O.A., Rogakou, E.P., Panuytin, I.G., and Bonner, W. (2002) Quantitative detection of 125IUdr-induced DNA double-strand breaks with γ-H2AX antibody. *Radiat Res* **158**, 486–492
13. MacPhail, S.H., Banath, J.P., Yu, T.Y., Chu, E.H., Lambur, H., and Olive, P.L. (2003) Expression of phosphorylated histone H2AX in cultured cell lines following exposure to X-rays. *Int J Radiat Biol* **79**, 351–358.
14. Huang, X, Okafuji, M., Traganos, F., Luther, E., Holden, E., and Darzynkiewicz, Z. (2004) Assessment of histone H2AX phosphorylation induced by DNA topoisomerase I and II inhibitors topotecan and mitoxantrone and by DNA cross-linking agent cisplatin. *Cytometry* **58A**, 99–110.
15. Huang, X., Halicka, H.D., Traganos, F., Tanaka, T., Kurose, A., and Darzynkiewicz, Z. (2005) Cytometric assessment of DNA damage in relation to cell cycle phase and apoptosis. *Cell Prolif* **38**, 223–243.
16. Tanaka, T., Huang, X., Halicka, H.D., Zhao, H., Traganos, F., Albino, A.P., Dai, W., and Darzynkiewicz, Z. (2007) Cytometry of ATM activation and histone H2AX phosphorylation to estimate extent of DNA damage induced by exogenous agents. *Cytometry A* **71A**, 648–661.
17. Speit, G., and Hartmann, A. (1999). The comet assay (single cell gel test). *Methods Mol Biol* **113**, 203–212.
18. Zhao, H., Tanaka, T., Halicka, H.D., Traganos, F., Zarebski, M., Dobrucki, J., and Darzynkiewicz, Z. (2007) Cytometric assessment of DNA damage by exogenous and endogenous oxidants reports the aging-related processes. *Cytometry A* **71A**, 905–914.
19. Tanaka, T., Halicka, H.D., Huang, X., Traganos, F., and Darzynkiewicz, Z. (2006) Constitutive histone H2AX phosphorylation and ATM activation, the reporters of DNA damage by endogenous oxidants. *Cell Cycle* **5**, 1940–1945.
20. Kajstura, M., Halicka, H.D., Pryjma, J., and Darzynkiewicz, Z. (2007) Discontinuous fragmentation of nuclear DNA during apoptosis revealed by discrete "sub-G1" peaks on DNA content histograms. *Cytometry A* **71A**, 125–131.
21. Tanaka, T., Kurose, A., Huang, X., Dai, W., and Darzynkiewicz, Z. (2006) ATM kinase activation and histone H2AX phosphorylation as indicators of DNA damage by DNA topoisomerase I inhibitor topotecan and during apoptosis. *Cell Prolif* **39**, 49–60.

Chapter 13

Analysis of the Topoisomerase II-Dependent Decatenation G2 Checkpoint and Checkpoint Kinases in Human Cells

William K. Kaufmann

Abstract

Inhibition of Topo II function using poisons and catalytic inhibitors triggers checkpoints that act to delay progression of G2 cells into mitosis. Topo II poisons induce Topo II-associated DNA double-strand breaks that activate ATM and the DNA damage G2 checkpoint. Topo II catalytic inhibitors do not induce DNA double-strand breaks but block decatenation of intertwined daughter chromatids. Complete decatenation before anaphase of mitosis is required for chromatid segregation. G2 cells appear to sense the degree of chromatid arm catenations and actively delay the onset of mitosis by sustaining the inhibition of mitosis-promoting factor (MPF) and polo-like kinase 1 (Plk-1) kinase activities that normally propel G2 cells into mitosis. This chapter details the methods for assay of decatenation G2 checkpoint function and checkpoint kinase activities.

Key words: Topoisomerase II, checkpoint, decatenation, mitosis-promoting factor, Plk-1.

1. Introduction

Type II topoisomerases (Topo II) perform the functions of unknotting DNA and separating intertwined daughter chromatids following DNA replication (1, 2). Intertwined daughter DNA duplexes are considered to be catenated, and the Topo II-catalyzed reaction of separating the intertwined duplexes is termed decatenation. Cells must decatenate daughter chromatids before the anaphase period of mitosis or risk being unable to segregate daughter chromatids and suffering non-disjunction errors upon completion of mitosis at the point of cytokinesis (3). The embryo lethality of knockout of Topo IIα may reflect the essential nature of chromatid decatenation in the mammalian cell biology (4).

D.J. Clarke (ed.), *DNA Topoisomerases*, Methods in Molecular Biology 582,
DOI 10.1007/978-1-60761-340-4_13,

Eukaryotic cells appear to recognize the condition of incomplete decatenation of daughter chromatids prior to anaphase and generate a checkpoint signal to slow or arrest progression toward the anaphase, pending sufficient or complete decatenation (2, 5–7). In budding yeast cells, mutant alleles of *top2* have been described that cause an arrest in G2/M and require the spindle damage checkpoint genes *MAD1* and *MAD2* to prevent anaphase onset (8). In mammalian cells, two checkpoints may operate prior to anaphase: one acting in G2 to delay the onset of mitosis until a sufficient level of chromatid arm decatenation has been achieved (7) and another acting at the metaphase to delay the onset of anaphase until the remaining set of centromeric catenations is removed (9, 10).

Mitosis-promoting factor (MPF) is a cyclin-dependent kinase composed of the cyclin B1 and Cdk1 subunits (11, 12). MPF is capable of initiating the steps of mitosis including nuclear membrane vesiculation, chromatid condensation, and formation of the mitotic spindle. Checkpoints that operate in G2 cells to delay the onset of mitosis appear to function by inhibiting the accumulation and activation of MPF inside the interphase nucleus (13). The decatenation G2 checkpoint causes G2 cells to delay entry to mitosis when Topo II catalytic activity is inhibited (2, 5, 7). The G2 delay that is elicited by treating cells with Topo II catalytic inhibitors is an active response that requires signaling by the ATM and Rad3-related (ATR) checkpoint kinase (5). The breast tumor suppressor gene BRCA1 appears to mediate signaling by ATR (5). Polo-like kinase I (Plk-1) is required for several biological events that are associated with mitosis, and it can be inhibited by signaling from ATM and ATR (14, 15). The decatenation G2 checkpoint is associated with the inhibition of Plk-1 and MPF activation in G2 cells (6). This chapter describes the methods for assay of decatenation G2 checkpoint function and MPF and Plk-1 kinase activities as indices of decatenation G2 checkpoint function.

2. Materials

2.1. Human Cell Culture

1. Human dermal fibroblasts (or other cells of interest growing as monolayers or in suspension; *see* **Note 1**).
2. Culture medium: Dulbecco's Minimal Essential Medium, supplemented with final concentrations of 10% fetal bovine serum and 2 mM L-glutamine.
3. Trypsin solution: 0.5% trypsin–EDTA.
4. Hank's balanced salt solution.
5. Aphidicolin: 2 mg/ml stock solution dissolved in DMSO. Store at –20°C.

2.2. Checkpoint Biology

1. ICRF-193 (MP Biomedicals): 4 mM stock of 4-[2-(3,5-dioxo-1-piperazinyl)-1-methylpropyl]piperazine-2,6-dione (ICFR-193) dissolved in dimethylsulfoxide. Freeze aliquots at –80°C.
2. Colcemid: 100 μg/ml stock solution dissolved in culture medium.
3. Cytometry fix solution: 95% ethanol with 5% glacial acetic acid.
4. Cytometry buffer: 4% fetal bovine serum, 10 mM HEPES, pH 7.4, 150 mM NaCl, 0.1% sodium azide, 0.5% Tween 20 (Tween 20 must be added fresh daily).
5. Primary antibody solution: 80% cytometry buffer, 20% 1 mg/ml DNase-free RNase A, supplemented with 2 μg/ml anti-phospho-histone H3 mouse monoclonal antibody (Millipore).
6. Secondary antibody solution: 1:20 dilution of fluorescein isothiocyanate (FITC)-labeled anti-mouse antibody (Santa Cruz Biotechnology, Inc.) in cytometry buffer (the FITC-labeled anti-mouse antibody should be sedimented for 5 min at ~14,000*g* in a microcentrifuge before dilution in cytometry buffer).
7. Cytometry staining solution: cytometry buffer supplemented with 50 μg/ml of propidium iodide and 5 μg/ml of DNase-free RNase A.

2.3. Checkpoint Kinase Biochemistry

1. MPF kinase assay lysis buffer: 10 mM sodium phosphate, pH 7.2, 150 mM NaCl, 1% Nonidet P-40, 1 mM ethylenediamine tetraacetic acid, 5 mM ethyleneglycol bis(β-aminoethylether)-*N*,*N*,*N*′,*N*′-tetraacetic acid, 5 mM β-glycerolphos phate, 2 mM dithiothreitol, 5 mM sodium fluoride, 2.5 mM phenylmethylsulfonyl fluoride, 120 Komberg IU (KIU)/ml aprotinin, 10 μg/ml leupeptin, and 1 mM sodium vanadate.
2. MPF kinase reaction buffer: 20 mM HEPES, pH 7.3, 80 mM β-glycerolphosphate, 20 mM ethyleneglycol bis(β-aminoethylether)-*N*,*N*,*N*′,*N*′-tetraacetic acid, 50 mM $MgCl_2$, 5 mM $MnCl_2$, 1 mM dithiothreitol, 2.5 mM phenylmethylsulfonyl fluoride, 60 KIU/ml aprotinin, 10 μg/ml leupeptin, and 10 mM cyclic AMP-dependent protein kinase inhibitory peptide.
3. Kinase assay reaction mixture: 20 μCi [γ-^{32}P]ATP (~3000 Ci/mmol; Amersham), 1 mM unlabeled ATP, and 32 μg histone H1 protein (Boehringer Mannheim).
4. Electrophoresis sample buffer: 4% sodium dodecylsulfate, 150 mM Tris–HCl, pH 6.8, 20% glycerol, 0.02% bromophenol blue, and 2 mM sodium vanadate.

5. Plk-1 kinase assay lysis buffer: 50 mM Tris–HCl, pH 7.4, 1% Nonidet P-40, 250 mM NaCl, 10 mM NaF, and 5 mM ethylene diamine tetraacetic acid.
6. Plk-1 kinase reaction buffer: 20 mM HEPES, pH 7.4, 150 mM NaCl, 10 $MgCl_2$, 1 mM ethyleneglycol bis(β-aminoethylether)-N,N,N',N'-tetraacetic acid, 0.5 mM dithiothreitol, 5 mM NaF, and 10 mM orthovanadate.
7. Cyclic AMP-dependent protein kinase inhibitory peptide.
8. Mouse monoclonal cyclin $B1^{Hs}$ antibody (Upstate Biotechnology, Inc.).
9. Rabbit polyclonal Plk-1 antibody (Millipore).
10. Non-specific mouse IgG (Millipore).
11. Non-specific rabbit IgG (Millipore).
12. Protein G-agarose beads (GIBCO-BRL).
13. $[\gamma]^{32}$P-labeled ATP (~3000 Ci/mmol).
14. Dephosphorylated α-casein.
15. HyperFilm MP (Amersham).

3. Methods

3.1. Assay of Decatenation G2 Checkpoint

The decatenation G2 checkpoint causes G2 cells to delay progression to mitosis in response to inhibition of Topo II decatenatory activity. Inhibition of Topo II decatenatory activity without introduction of Topo II-associated DNA double-strand breaks is typically accomplished using the Topo II catalytic inhibitor ICRF-193. Three different methods for the assay of decatenation G2 checkpoint function are described below. Using these assays, we have found that several lines of diploid human fibroblasts express 55–98% inhibition of G2/M progression after treatment with 4 μM ICRF-193. Cells with a defective decatenation checkpoint display less inhibition of mitosis, and some cultures with severe attenuation of the checkpoint actually display more mitotic cells after treatment with ICRF-193, apparently because ICRF-193 can delay the metaphase/anaphase transition and therefore cause cells to transiently accumulate in mitosis. This effect on mitosis can be seen even in diploid human fibroblasts after treatment with high concentrations of ICRF-193 (>20 μM; *see* **Note 2**). However, after treatment with the lower concentrations of ICRF-193 that we use to quantify decatenation G2 checkpoint function (2–4 μM), diploid human fibroblasts exit from mitosis substantially within 2 h after the 15-min treatment with the drug (*see* **Note 2**).

Mitotic cells are quantified by flow cytometry using a primary mouse monoclonal antibody to phospho-histone H3 and a fluorescein isothiocyanate-labeled secondary rabbit antibody to the mouse primary antibody. As mammalian cells express phospho-ser10 histone H3 in mitosis at vastly higher levels than in interphase compartments, the mitotic cells can be easily and accurately quantified. With effective G2 delay and exit of mitotic cells to interphase, the mitotic compartment in an asynchronous cell population may decline by as much as 95% within 2 h after treatment with 2–4 μM ICRF-193 (16, 17).

3.1.1. Assaying G2/M Progression in Unsynchronized Cells

1. The day before the experiment, seed one million diploid human fibroblast cells per sample in 10-cm tissue culture dishes in the culture medium.
2. The next day, add to the samples a final concentration of 2–4 μM ICRF-193 or an equivalent volume of DMSO to a control sample.
3. Return the cells to the tissue culture incubator for 15 min, and then remove the drug by briefly washing the cells in prewarmed culture medium and then adding drug-free culture medium. (A significant reduction in the mitotic index can be noted 2 h later; *see* **Note 3**.)
4. Quantify the percent of cells in mitosis using the flow cytometry method described in **Section 3.2**.

3.1.2. Assaying G2/M Progression in Synchronized Cells Treated with Colcemid

A second method for assay of the decatenation G2 checkpoint uses synchronized cells and employs collection of the cells in mitosis with colcemid (6). Compared with the above protocol, in this case a larger percentage of the cell population will be in G2-phase when treated with the topo II inhibitor (*see* **Note 4**).

1. Arrest cultures of diploid human fibroblasts in G0 by allowing them to grow to confluence or by removal of the serum from the culture medium.
2. The day before the experiment, add back the serum to the culture medium or replate the cells at subconfluent density, about one million cells per 10-cm culture dish. (The cells will transit parasynchronously from G0 into G1 and then to S-phase.)
3. Two hours later, when cells are in G1, add to the culture medium the DNA polymerase inhibitor aphidicolin at 2 μg/ml final concentration. (Within 24 h after replating diploid human fibroblasts and addition of aphidicolin, as many at 80% of cells can be collected at the beginning of the S-phase (18).)

4. On the day of the experiment, about 24 h later, replace the culture medium with pre-warmed aphidicolin-free culture medium and return the cells to the tissue culture incubator. (The cells will progress through S-phase as a uniform cohort completing DNA synthesis within 6–7 h.)
5. Eight hours later, add to the samples a final concentration of 2–4 μM ICRF-193 or an equivalent volume of DMSO to a control sample.
6. Return the cells to the tissue culture incubator for 15 min, and then remove the drug by briefly washing the cells in pre-warmed culture medium and adding pre-warmed culture medium supplemented with 100 ng/ml of colcemid.
7. After 2–4 h, prepare the samples for flow cytometry and quantify the percent of cells in mitosis using the method described in **Section 3.2**.

About 8 h after release from the aphidicolin block, 50–70% of cells are in G2 and poised to enter mitosis within the next 4 h. The addition of the colcemid to the culture medium prevents the cells that enter mitosis from progressing to metaphase and beyond. In our experiments, addition of colcemid to the medium for 4 h beginning 8 h after release from aphidicolin typically collects 20–30% of the cells in mitosis (19). Treatment of G2 cells for 15 min with 2 μM ICRF-193 before addition of colcemid blocks their progression to mitosis by 85% (6).

3.1.3. Assaying G2/M Progression in Unsynchronized Cells Treated with Colcemid

A third method for the assay of decatenation G2 checkpoint function uses asynchronous cells and monitors the increment of mitotic cells during a 2–6 h incubation with colcemid (16) (*see* **Note 4**).

1. The day before the experiment, seed one million diploid human fibroblast cells per sample (six samples for this example) in 10-cm tissue culture dishes in culture medium.
2. On the day of the experiment, add 100 ng/ml of colcemid to the dishes, and then add to three of the dishes, a final concentration of 4 μM ICRF-193. Add to the other three dishes, an equivalent amount (0.1% final) of DMSO as a control.
3. After 2, 4, and 6 h, prepare pairs of samples (treated with ICRF and DMSO) for flow cytometry and quantify the percent of cells in mitosis using the method described in **Section 3.2**.

A typical outcome of this experiment is as follows. The control cells that are treated with the DMSO solvent collect in mitosis during the 6-h incubation. The ICRF-193-treated cells are delayed in G2, and the mitotic index does not increase during incubation with colcemid. The slope of the line of increasing mitotic cells during the 0–6 h incubation with colcemid is a

measure of the rate of G2/M progression. In diploid human fibroblasts, the slope of the line during incubation with colcemid and ICRF-193 is quite shallow. In multiple analyses with three different fibroblast cell lines, 4 μM ICRF-193 reduced the rate of G2/M progression by an average value of 98% relative to the control.

3.2. Quantification of Mitotic Cells by Flow Cytometry

1. Harvest the cells by releasing them from the dishes with trypsin solution, and then inactivate the trypsin by adding five volumes of culture medium. Generally, we process two million cells per sample.
2. Sediment the cells by centrifugation at 800*g* for 5 min at room temperature.
3. Resuspend the cell pellet in Hank's balanced salt solution at 4°C.
4. Sediment the cells by centrifugation at 800*g* for 5 min.
5. Resuspend the cell pellet in cytometry fix solution at 4°C. Allow the cells to fix for 1 h at 4°C; the cells may be held at 4°C overnight.
6. Sediment the cells at 800*g* for 5 min, remove the supernatant, and resuspend in 3 ml of cytometry buffer.
7. Sediment the cells by centrifugation at 800*g* for 5 min.
8. Resuspend the cell pellet in 0.2 ml of primary antibody solution. Incubate overnight at 4°C.
9. Add 3 ml of cytometry buffer and mix briefly.
10. Sediment the cells by centrifugation at 800*g* for 5 min.
11. Resuspend the cell pellet in 0.2 ml of secondary antibody solution. Incubate the suspension for 1 h at room temperate in the dark.
12. Add 3 ml of cytometry buffer and mix.
13. Sediment the cells by centrifugation at 800*g* for 5 min.
14. Resuspend the cell pellet in 1 ml of cytometry staining solution. Samples may be stored for 1–2 days at 4°C in the dark before analysis with a FACScan flow cytometer.
15. Perform flow cytometry using two channels to detect propidium iodide and FITC fluorescence signals (*see* **Note 5**).

3.3. Assay of MPF Kinase

MPF is a cyclin-dependent kinase that phosphorylates various substrates to induce mitosis. MPF kinase activity is assayed by quantifying the transfer of the ^{32}P-labeled gamma phosphate of ATP ([γ-^{32}P]ATP) to histone H1 in a reaction that depends upon the cyclin B1-associated Cdk1 protein kinase. There are three steps in the assay: extraction and isolation of cyclin B1/Cdk1

complexes, incubation of cyclin B1/Cdk1 complexes with histone H1 and [γ-^{32}P]ATP in an appropriate reaction cocktail, and quantification of transfer of [γ-^{32}P] to histone H1.

3.3.1. Extraction and Isolation of Cyclin B1/Cdk1 Complexes

Following treatment with ICRF-193 to induce G2 delay, cyclin B1/Cdk1 complexes are isolated from human cells by immunoprecipitation using a monoclonal antibody to cyclin B1.

1. Harvest cells that grow in suspension by sedimentation from the medium by centrifugation at 800*g* for 5 min. If the cells are growing as a monolayer, detach with trypsin, then mix with culture medium to inactivate the trypsin, and collect by sedimentation, as described in **Section 3.2**, steps 1 and 2.
2. Resuspend the cell pellet in ice-cold phosphate-buffered saline (PBS). (An additional wash using a small volume of PBS can be used to transfer the cells to a 1.5-ml plastic tube.)
3. Sediment the cells by centrifugation at 800*g* for 5 min and remove the supernatant. (The packed dry pellet of cells can be frozen in an ethanol-dry ice bath and stored at –80°C before further processing.)
4. Solubilize the cell pellets on ice in MPF kinase assay lysis buffer.
5. Clarify the lysates by sedimentation at 100,000*g* for 1 h at 4°C.
6. Determine the protein concentration within the lysate using a commercial kit (e.g., Pierce) and bovine serum albumin to generate a standard curve.
7. Incubate lysate containing 200 µg of total protein overnight at 4°C with 2.5 µl of mouse monoclonal cyclin B1^{Hs} antibody.
8. Add 25 µl of protein G-agarose beads and incubate at 4°C for 1 h.
9. Wash the beads three times by sedimentation (800*g* for 5 min at 4°C) and resuspension in ice-cold kinase assay lysis buffer. [To control for non-specific kinase activity in immunoprecipitates, an equivalent sample of cell lysate can be incubated with non-specific mouse IgG (as described in step 7) followed by protein G-agarose beads (as described in steps 8 and 9).]

3.3.2. Assay of MPF Kinase Activity

1. Resuspend the washed beads (that should contain the immunoprecipitated cyclin B1/Cdk1 complexes) in 20 µl of ice-cold MPF kinase reaction buffer.
2. Add 12 µl of kinase assay reaction mixture. After mixing, incubate the samples at 30°C for 15 min.
3. Stop the kinase reaction by the addition of an equal volume of electrophoresis sample buffer.

4. Heat at 100°C for 5 min.
5. Separate the proteins by SDS-PAGE in a 10% polyacrylamide gel.
6. Stain the SDS-PAGE gel with Coomassie blue to verify equal loading of histone protein.
7. Dry the gel with a gel-drier and subject to autoradiography with HyperFilm MP. This provides a radiographic image of MPF kinase activity.
8. To quantify the kinase activity, excise the regions of the gel that contain the histone H1, soak in 30% hydrogen peroxide overnight at 37°C, and quantify the radioactivity by scintillation spectrometry. (Alternatively, radioactivity associated with the histone H1 protein bands can be quantified using a Molecular Dynamics PhosphorImager and ImageQuant software.)

Radioactivity that is associated with histone H1 is determined for samples that were incubated with anti-cyclin B1 immunoprecipitates containing MPF and for control samples with non-specific IgG immunoprecipitates. Net cyclin B1-associated histone H1 kinase activity is determined by subtraction of the non-specific radioactivity. MPF kinase activity in ICRF-193-treated cells is then compared with that recovered from DMSO-treated control cells to determine the inhibition of MPF that is associated with activation of the decatenation G2 checkpoint. For proper control of experimental and biological variability in the assay, experiments should be repeated a minimum of three times.

3.3.3. Assay of Plk-1 Kinase Activity

1. Harvest the cells and make cell pellets as described in **Section 3.3.1**, steps 1–3.
2. Lyse the pelleted cells in Plk-1 kinase activity lysis buffer by incubating on ice for 20 min.
3. Clarify the cell lysates by sedimentation at 100,000*g* for 20 min at 4°C.
4. Pre-clear the lysates (which should contain 300–500 μg of total protein) with washed protein G-agarose beads for 30 min at 4°C. (The protein G-agarose beads should be washed with 10X PBS and then with Plk-1 kinase activity lysis buffer.)
5. Sediment the beads by centrifugation at 800*g* for 5 min.
6. Transfer the supernatant to a new tube and add 1 μg of rabbit polyclonal anti-Plk-1 antibody. (To control for non-specific kinase activity in immunoprecipitates, a non-specific rabbit IgG can be used in place of the anti-Plk-1 antibody.)
7. Incubate for 2 h at 4°C.

8. Add 20 μl of washed protein G-agarose beads and incubate at 4°C for 30 min.
9. Wash the beads four times with Plk-1 kinase activity lysis buffer, sedimenting the beads by centrifugation at 800*g* for 5 min.
10. Wash the beads once with Plk-1 kinase reaction buffer, sedimenting the beads by centrifugation at 800*g* for 5 min.
11. Resuspend the beads in 20 μl of Plk-1 kinase reaction buffer supplemented with 5 mg of dephosphorylated α-casein and 1 μCi of [γ-^{32}P]ATP (~3000 Ci/mmol).
12. Incubate at 34°C for 50 min.
13. Stop the reaction by adding an equal volume of electrophoresis sample buffer.
14. Subject the samples to electrophoresis through 12% SDS-PAGE gels.
15. Radioactivity that is associated with casein can be imaged by autoradiography and quantified by scintillation spectrometry or using a PhosphorImager. Plk-1-specific kinase activity is determined by subtracting radioactivity associated with the non-specific IgG control. Plk-1 kinase activity in ICRF-193-treated cell lysates is expressed as a percent of the activity in DMSO-treated control cell lysates.

4. Notes

1. It is also important to note that cancer cell lines are highly idiosyncratic and can display highly variable responses to ICRF-193 ranging from stable growth arrest to death by apoptosis. While it is important to understand the consequences of reduced or defective decatenation G2 checkpoint function in cancer cells, understanding of the mechanisms of decatenation G2 checkpoint function is more fruitfully addressed in genetically stable cell lines, such as telomerase-expressing diploid human fibroblasts.
2. When assaying for the decatenation G2 checkpoint, it is important to consider the effect of concentration of Topo II catalytic inhibitor. ICRF-193 at concentrations of >25 μM is capable of producing a block in the metaphase/anaphase transition. This block will prevent mitotic completion, and the mitotic index may not decrease significantly in the first 2 h after the treatment with ICRF-193. It should not be concluded that high concentrations of ICRF-193 block the decatenation G2 checkpoint that inhibits progression of G2 cells

into mitosis. Lower concentrations of ICRF-193 in the range of 1–4 μM do not produce a significant inhibition of the metaphase/anaphase transition, and following treatment with these lower concentrations of ICRF-193, the mitotic index may decrease by up to 90% within 2 h.

3. This reduction in the mitotic index is thought to reflect two effects, one being the active, checkpoint-dependent, delay of progression of G2 cells into mitosis, and the second being the recovery and exit from mitosis of cells that were in mitosis during the drug treatment.
4. We find that while the assay of decatenation G2 checkpoint that is based on inhibition of mitosis 2 h after treatment with ICRF-193 has the advantage of simplicity and low cost, it is prone to error in certain genetic contexts that may sensitize cells to the effect of ICRF-193 on the metaphase/anaphase transition. For this reason, we assay the rate of G2 to mitosis progression with synchronized cells or during incubation of asynchronous cells with colcemid to confirm the suspected effects on decatenation G2 checkpoint function.
5. We use Summit version 4.3 software to analyze flow cytometry profiles. We first gate on whole cells, then on singlets to exclude doublets. Finally, in the singlet population of cells, we monitor propidium iodide fluorescence as a measure of DNA content and FITC as a measure of histone H3 phosphorylation. Cells with 4 C DNA content and high expression of phospho-histone H3 are considered to be in mitosis. We analyze 30,000 cells per sample. For proper control of experimental and biological variability in the assay, experiments should be repeated a minimum of three times.

Acknowledgment

Supported in part by PHS grants CA81343, CA16086, and ES10126.

References

1. Holm, C. (1994) Coming undone: how to untangle a chromosome. *Cell* **77**, 955–7.
2. Downes, C. S., Clarke, D. J., Mullinger, A. M., Gimenez-Abian, J. F., Creighton, A. M. and Johnson, R. T. (1994) A topoisomerase II-dependent G2 cycle checkpoint in mammalian cells. *Nature* **372**, 467–70.
3. Clarke, D. J., Johnson, R. T. and Downes, C. S. (1993) Topoisomerase II inhibition prevents anaphase chromatid segregation in mammalian cells independently of the generation of DNA strand breaks. *J Cell Sci* **105**, 563–9.
4. Wang, J. C. (2002) Cellular roles of DNA topoisomerases: a molecular perspective. *Nat Rev Mol Cell Biol* **3**, 430–40.

5. Deming, P. B., Cistulli, C. A., Zhao, H., Graves, P. R., Piwnica-Worms, H., Paules, R. S., Downes, C. S. and Kaufmann, W. K. (2001) The human decatenation checkpoint. *Proc Natl Acad Sci USA* **98**, 12044–9.
6. Deming, P. B., Flores, K. G., Downes, C. S., Paules, R. S. and Kaufmann, W. K. (2002) ATR enforces the topoisomerase II-dependent G2 checkpoint through inhibition of Plk1 kinase. *J Biol Chem* **277**, 36832–8.
7. Clarke, D. J., Vas, A. C., Andrews, C. A., Diaz-Martinez, L. A. and Gimenez-Abian, J. F. (2006) Topoisomerase II checkpoints: universal mechanisms that regulate mitosis. *Cell Cycle* **5**, 1925–8.
8. Andrews, C. A., Vas, A. C., Meier, B., Gimenez-Abian, J. F., Diaz-Martinez, L. A., Green, J., Erickson, S. L., Vanderwaal, K. E., Hsu, W. S. and Clarke, D. J. (2006) A mitotic topoisomerase II checkpoint in budding yeast is required for genome stability but acts independently of Pds1/securing. *Genes Dev* **20**, 1162–74.
9. Skoufias, D. A., Lacroix, F. B., Andreassen, P. R., Wilson, L. and Margolis, R. L. (2004) Inhibition of DNA decatenation, but not DNA damage, arrests cells at metaphase. *Mol Cell* **15**, 977–90.
10. Diaz-Martinez, L. A., Gimenez-Abian, J. F., Azuma, Y., Guacci, V., Gimenez-Martin, G., Lanier, L. M. and Clarke, D. J. (2006) PIASy is required for faithful chromosome segregation in human cells. *PLoS ONE* **1**, e53.
11. Morgan, D. O. (1997) Cyclin-dependent kinases: engines, clocks, and microprocessors. *Annu Rev Cell Dev Biol* **13**, 261–91.
12. Morgan, D. O. (1995) Principles of CDK regulation. *Nature* **374**, 131–4.
13. Takizawa, C. G. and Morgan, D. O. (2000) Control of mitosis by changes in the subcellular location of cyclin-B1-Cdk1 and Cdc25C. *Curr Opin Cell Biol* **12**, 658–65.
14. Smits, V. A., Klompmaker, R., Arnaud, L., Rijksen, G., Nigg, E. A. and Medema, R. H. (2000) Polo-like kinase-1 is a target of the DNA damage checkpoint. *Nat Cell Biol* **2**, 672–6.
15. van Vugt, M. A., Smits, V. A., Klompmaker, R. and Medema, R. H. (2001) Inhibition of Polo-like kinase-1 by DNA damage occurs in an ATM- or ATR-dependent fashion. *J Biol Chem* **276**, 41656–60.
16. Kaufmann, W. K., Campbell, C. B., Simpson, D. A., Deming, P. B., Filatov, L., Galloway, D. A., Zhao, X. J., Creighton, A. M. and Downes, C. S. (2002) Degradation of ATM-independent decatenation checkpoint function in human cells is secondary to inactivation of p53 and correlated with chromosomal destabilization. *Cell Cycle* **1**, 210–9.
17. Doherty, S. C., McKeown, S. R., McKelvey-Martin, V., Downes, C. S., Atala, A., Yoo, J. J., Simpson, D. A. and Kaufmann, W. K. (2003) Cell cycle checkpoint function in bladder cancer. *J Natl Cancer Inst* **95**, 1859–68.
18. Kaufmann, W. K. and Wilson, S. J. (1990) DNA repair endonuclease activity during synchronous growth of diploid human fibroblasts. *Mutat Res* **236**, 107–17.
19. Zhou, T., Chou, J., Mullen, T. E., Elkon, R., Zhou, Y., Simpson, D. A., Bushel, P. R., Paules, R. S., Lobenhofer, E. K., Hurban, P. and Kaufmann, W. K. (2007) Identification of primary transcriptional regulation of cell cycle-regulated genes upon DNA damage. *Cell Cycle* **6**, 972–81.

Chapter 14

Assaying Topoisomerase II Checkpoints in Yeast

Katherine Furniss, Amit C.J. Vas, Andrew Lane, and Duncan J. Clarke

Abstract

Topoisomerase II activity is crucial to maintain genome stability through the removal of catenanes in the DNA formed during DNA replication and scaffolding the mitotic chromosome. Perturbed Topo II activity causes defects in chromosome segregation due to persistent catenations and aberrant DNA condensation during mitosis. Recently, novel *top2* alleles in the yeast *Saccharomyces cerevisiae* revealed a checkpoint control that responds to perturbed Topo II activity. Described in this chapter are protocols for assaying the phenotypes seen in *top2* mutants on a cell biological basis in live cells: activation of the Topo II checkpoint using spindle morphology, chromosome condensation using fluorescently labeled chromosomal loci, and cell cycle progression by flow cytometry. Further characterization of this novel checkpoint is warranted so that we can further our understanding of the cell cycle, genomic stability, and the possibility of identifying novel drug targets.

Key words: Topoisomerase II checkpoint, anaphase, spindle elongation, chromosome condensation, budding yeast.

1. Introduction

To perform mitosis successfully, DNA topoisomerase II (Topo II) must resolve catenations between the sister chromatid DNA molecules (1, 2). This is essential for the separation of the sister chromatids in anaphase (3, 4). Topo II also contributes to the process of chromosome condensation, which facilitates accurate chromosome segregation in anaphase (4–9). When Topo II activity is perturbed, cell cycle checkpoints are triggered, which delay mitotic progression (10–17). The budding yeast, *Saccharomyces cerevisiae*, has a single Topo II protein, Top2 (18). Top2 functions in both chromosome condensation and segregation, and a preanaphase (G2/M) cell cycle checkpoint is activated in strains possessing

D.J. Clarke (ed.), *DNA Topoisomerases*, Methods in Molecular Biology 582,
DOI 10.1007/978-1-60761-340-4_14,

mutant *top2* alleles (11). In the following sections, we will explain how to perform cell cycle synchronization of cultures of *S. cerevisiae* cells so that the checkpoint induced in response to perturbed Top2 can be analyzed. This analysis employs FACScan determination of DNA content and characterization of cell cycle stage using spindle morphology as a criterion. We also describe a method that allows measurement of chromosome condensation defects in *top2* mutants (9). Use of these assays will allow further characterization of the Topo II checkpoint and will allow the process of chromosome condensation to be studied in a genetically tractable eukaryote.

1.1. Cell Cycle Synchronization of Yeast Cells

All of the yeast strains used in these assays are mating type **a** (*MAT***a**) and are *bar1Δ*. This genotype is important for the cell cycle synchronization in G1-phase. Yeast that are mating type **a** respond to a peptide mating pheromone called α-factor, which in the wild is secreted by mating type $\boldsymbol{\alpha}$ cells. The pheromone induces the *MAT***a** cells to prepare for mating by arresting in G1-phase of the cell cycle. Upon arrest, the cells form a mating projection called a shmoo that is employed in the conjugation process. We can exploit this behavior to achieve cell cycle synchrony in G1 and the shmoo is a useful marker for efficient G1 arrest. *MAT***a** cells that have the *BAR1* locus deleted (i.e., *bar1Δ* strains) are unable to degrade α-factor and therefore can be arrested in G1 in the presence of low concentrations of the mating pheromone. This is an advantage because the peptide mating pheromone is expensive.

1.2. Analysis of Spindle Morphologies in Yeast Cells

The "spindle assay" described below allows the monitoring of cell cycle progression by scoring spindle morphologies visualized by expression of a GFP-Tub1 fusion protein (GFP fused to the alpha tubulin protein) (19). There are two advantages to using this approach. First, it avoids the need to immunostain the microtubules to visualize the mitotic spindle. Second, the cells can be visualized live (i.e., there is no need to fix the cells before performing the microscopy). Analysis of spindle morphologies gives an accurate view of cell cycle progression (*see* **Figs. 14.1**–**14.9**). When a yeast cell is in G1, the GFP-Tub1 reveals a single, bright dot with small projections; these are the spindle pole body and the astral microtubules (**Fig. 14.1**). As the cell enters S-phase (which corresponds with the emergence of a bud), it duplicates its spindle pole body; however, because the spindle pole bodies do not immediately separate, a single bright dot, or two very closely aligned dots, are seen. Again, the duplicated spindle pole bodies are associated with astral microtubule projections (**Fig. 14.2**). Approximately coincident with the completion of DNA replication, and defined as the beginning of G2/M-phase, the spindle pole bodies separate and the mitotic spindle assembles (**Fig. 14.3**).

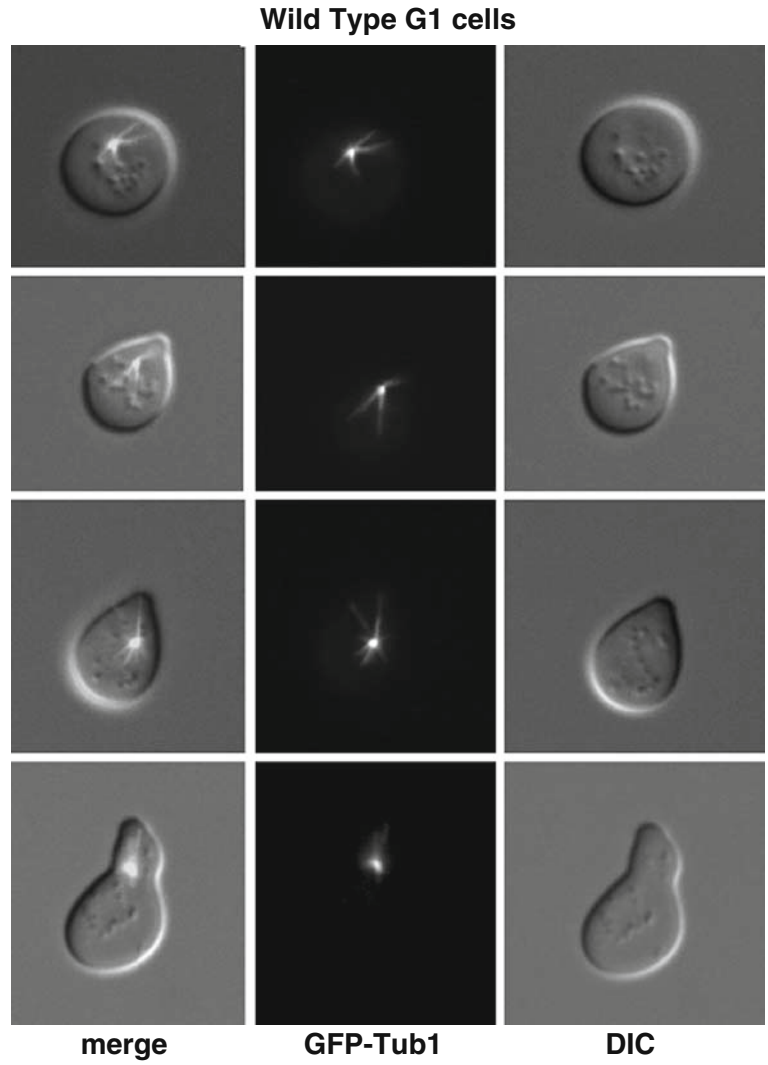

Fig. 14.1. **Microtubule morphologies in wild-type G1 cells**. Wild-type G1 cells visualized using the DIC setting on the microscope as well as the green fluorescence channel to observe the GFP-Tub1 fusion protein. G1 cells appear round and unbudded. However, when *bar1Δ* cells are exposed to α factor, projections called shmoos form (these are the mating projections that cells of opposite mating type form to initiate conjugation). The mating projections can be confused with buds. Notice that buds have a pinched (constricted) neck while the projections do not (compare the images in **Figs. 14.1 and 14.2**). The GFP-Tub1 fusion protein in G1-phase cells localizes to a single, bright spot, which is the spindle pole body as well as to the astral microtubules that can be seen to project from the spindle pole body. When scoring the percent of G1 cells in a population, combine the percent of cells that are round and unbudded with the percent of cells that are unbudded with a shmoo.

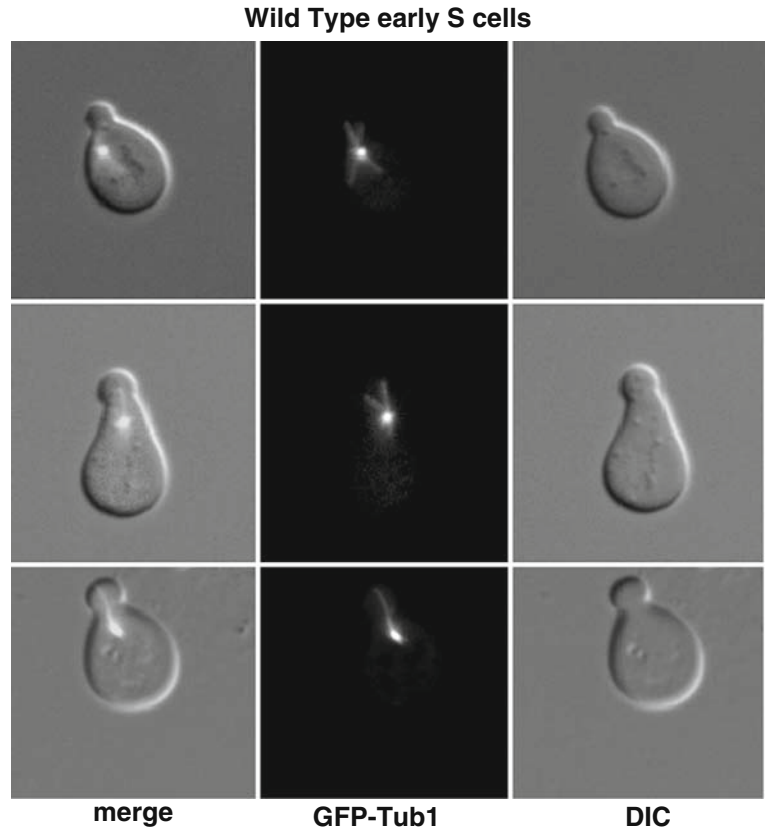

Fig. 14.2. **Microtubule morphologies in wild-type early S-phase cells**. Wild-type early S-phase cells visualized using the DIC setting on the microscope as well as the green fluorescence channel to observe the GFP-Tub1 fusion protein. The onset of DNA replication (when S-phase begins) coincides with the initiation of bud formation. S-phase cells have relatively small buds, up to a maximum of about 2/3 of the mother cell volume. The bud can form at the tip of the shmoo (as seen in the second image) or in a new location on the cell surface. In the S-phase, cells duplicate their spindle pole body and this is initiated along with budding and DNA replication. However, the spindle pole bodies do not separate until late S-phase and a single fluorescent spot is visualized. Astral microtubules emanate from the spindle pole bodies.

At this stage, the spindle is first viewed as a short (1–2 μm) thick bar of microtubules with a bright dot at each end (the spindle pole bodies). The spindle pole bodies have astral microtubule projections pointing toward the edges of the mother cell (commonly in the vicinity of the bud neck) and the edges of the daughter bud. The spindle continues to elongate and can reach about 3–4 μm but remains thick and bright. At this stage, a lower density of microtubules in the middle region of the spindle can often be observed. This is because kinetochore microtubules (those that connect the spindle pole bodies to each kinetochore) do not reach all the way to the middle of the spindle (20, 21). There are 16 kinetochore

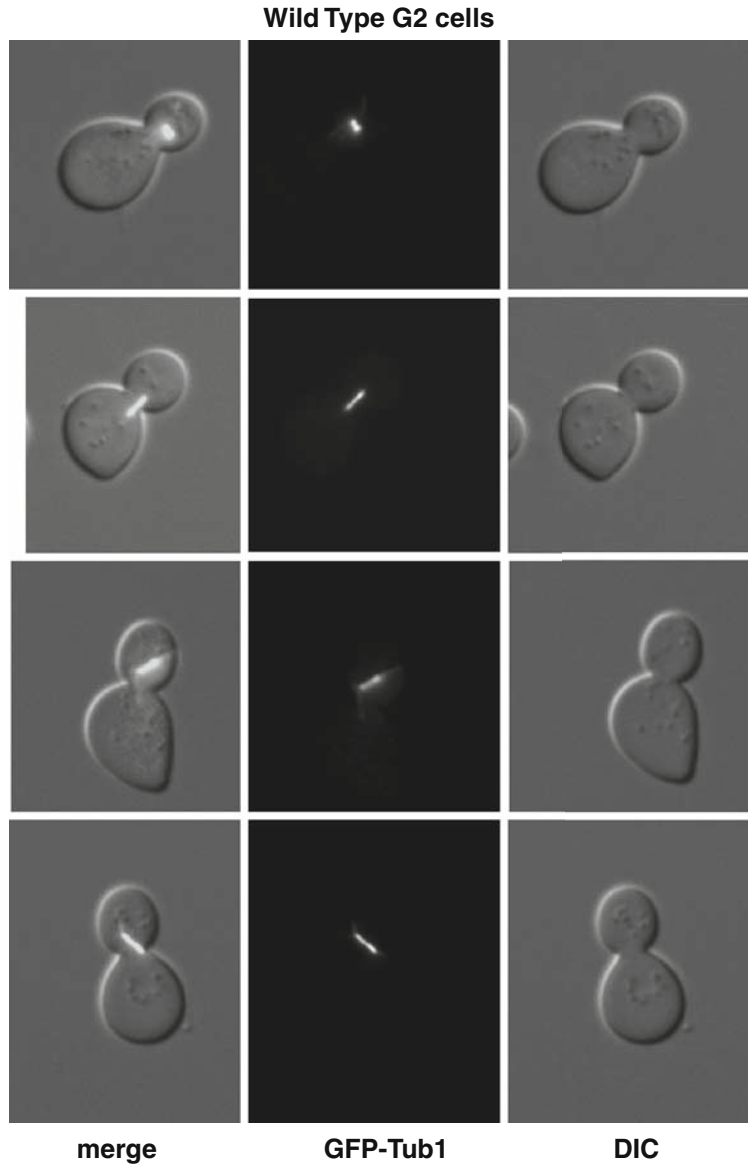

Fig. 14.3. **Microtubule morphologies in wild-type G2/M cells**. Wild-type G2/M cells visualized using the DIC setting on the microscope as well as the green fluorescence channel to observe the GFP-Tub1 fusion protein. In G2/M-phase, the buds have grown to about 2/3 of the mother cell volume. The spindle pole bodies have separated and a thick, bright metaphase spindle can be seen. Upon assembly, the metaphase spindle is initially 1–2 μm in length but typically increases in length up to about 3–4 μm during G2/M-phase. The cell at the top of this figure is an early G2/M-phase cell, its spindle pole bodies having begun to separate – the GFP-Tub1 image shows that there are two fluorescent dots. Astral microtubules can sometimes be seen to emanate from both spindle pole bodies. The spindle pole body that will ultimately remain in the mother cell has astral microtubules, which contact the mother cell cortex, usually close to the neck of the bud. The spindle pole body that will ultimately segregate to the daughter cell has astral microtubules, which contact the bud cortex.

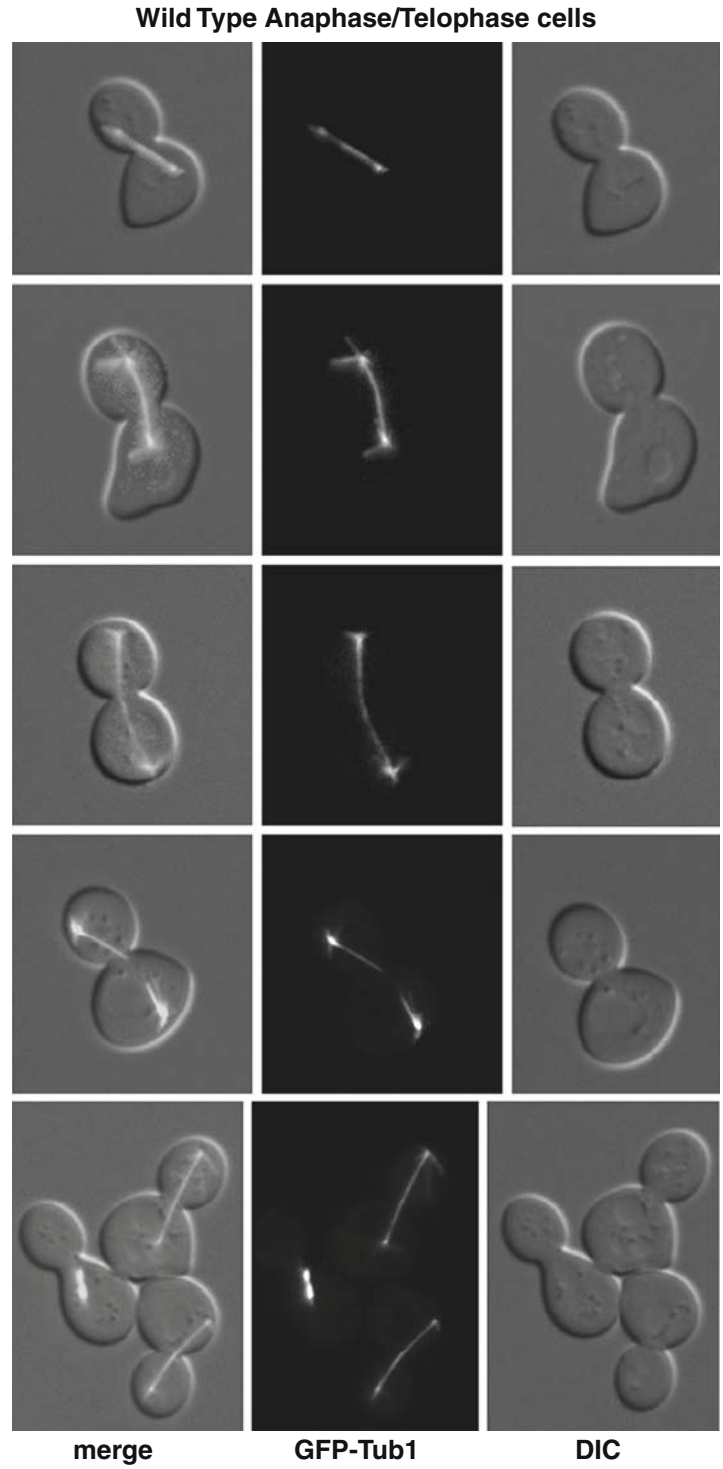

Fig 14.4. **Microtubule morphologies in wild-type anaphase/telophase cells**. Wild-type anaphase/telophase cells visualized using the DIC setting on the microscope as well as the green fluorescence channel to observe the GFP-Tub1 fusion protein. Cells in

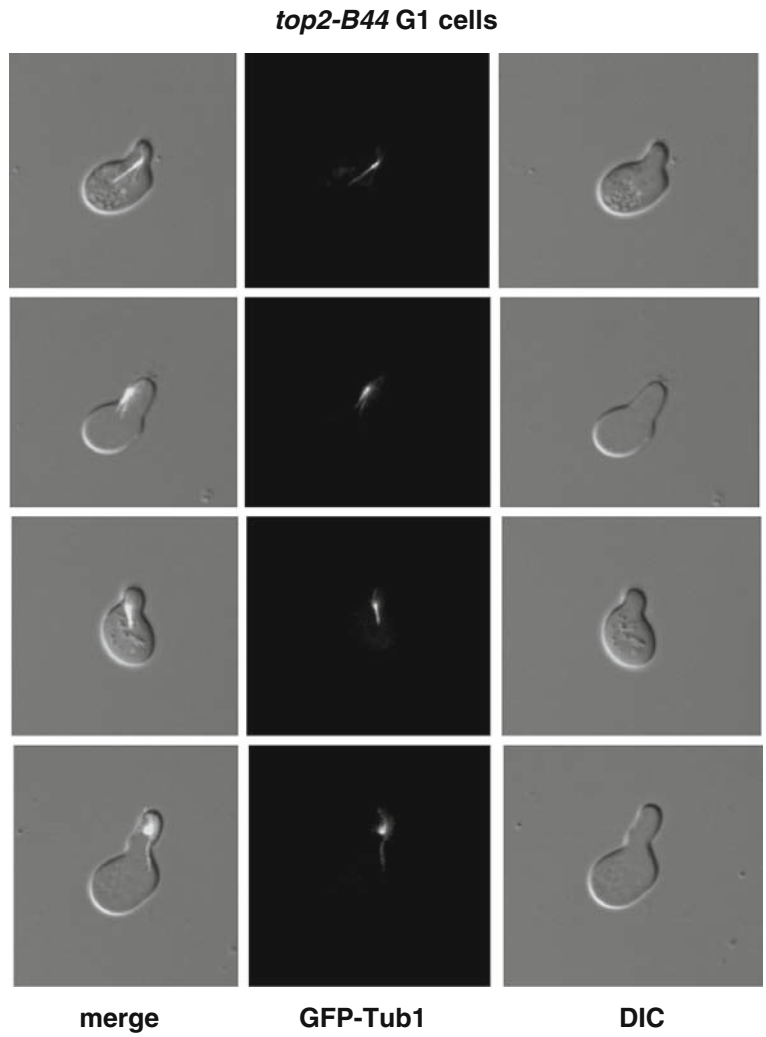

Fig. 14.5. **Microtubule morphologies in *top2-B44* G1 cells**. *top2-B44* G1 cells visualized using the DIC setting on the microscope as well as the green fluorescence channel to observe the GFP-Tub1 fusion protein. Mutant cells can look similar to wild-type cells, but some different morphologies that are seen are depicted here. As shown in **Fig. 14.1**, there is a single spindle pole body with astral microtubule projections.

Fig. 14.4. (continued) anaphase and telophase also have buds that are approximately 2/3 the size of the mother cell. The spindle elongates as the spindle pole bodies migrate away from each other. The elongated spindle is composed of fewer microtubules and so it appears fainter than G2/M spindles. In the fourth image (from the *top*; telophase), the spindle has broken in preparation for cytokinesis. Astral microtubules can be seen to emanate from the SPBs to contact the cell cortexes. The image at the *bottom* has one G2/M cell (on the *left*) and two anaphase/telophase cells. This image contrasts the size and brightness of G2/M versus anaphase/telophase spindles.

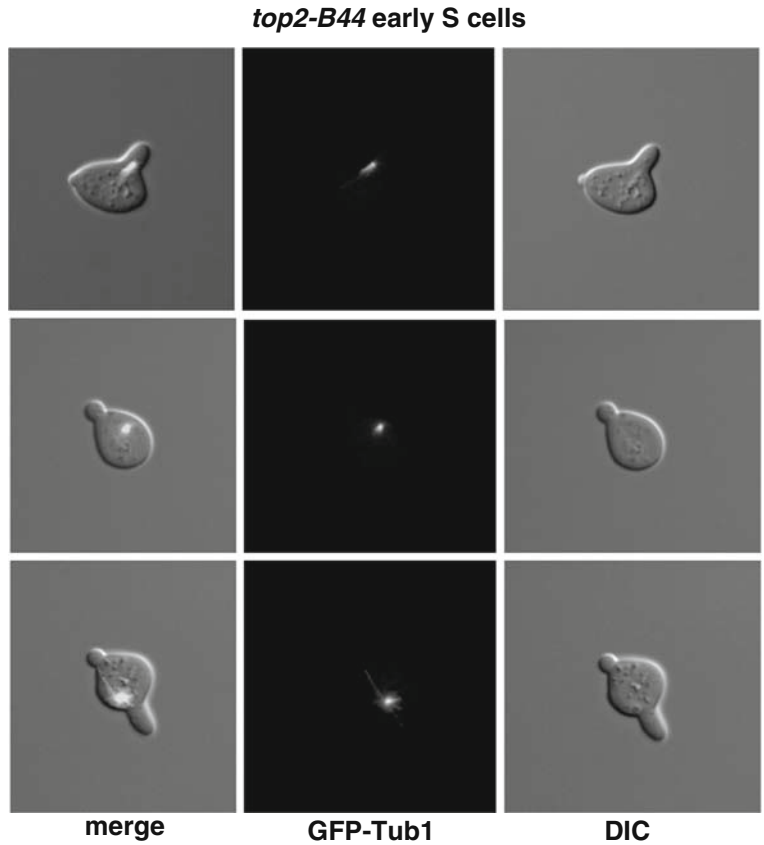

Fig. 14.6. **Microtubule morphologies in *top2-B44* early S-phase cells**. *top2-B44* early S-phase cells visualized using the DIC setting on the microscope as well as the green fluorescence channel to observe the GFP-Tub1 fusion protein. Much like the wild-type cells shown in **Fig. 14.2**, these cells have formed a small bud, identified by the constriction at the bud neck. Two of the cells have both a bud and a shmoo, the buds are at the top left of the cells. The spindle pole body has duplicated but has not yet separated so a single dot with astral microtubules is present.

microtubules in each half of the spindle. A smaller number of overlap microtubules emanate from both spindle pole bodies and are crosslinked in the middle region of the spindle. Once anaphase begins, the G2/M bar spindle morphology is dramatically changed. The anaphase spindle is much longer (typically 7–10 μm when fully elongated) and is markedly thinner so that it is no longer as bright as the G2/M spindle (**Fig. 14.4**). This is because the

Fig. 14.7. (continued) delay, the bud, and to some extent the mother cell, continue growth. As a result, the bud can reach the size of the mother cell. Mutant cells can have a variety of shapes. In the second image, the bud has formed at the end of an elongated shmoo so that there is a long neck between the shmoo and bud. In the *bottom* two figures, the shmoo has enlarged greatly and the bud has formed at the opposite end. As seen in **Fig. 14.3**, the spindle pole bodies have separated and the spindle is thick and bright with astral microtubules projecting from the spindle pole bodies. Because the overall cell size can be larger than wild-type G2/M cells, the metaphase spindle can also become slightly longer than is typical.

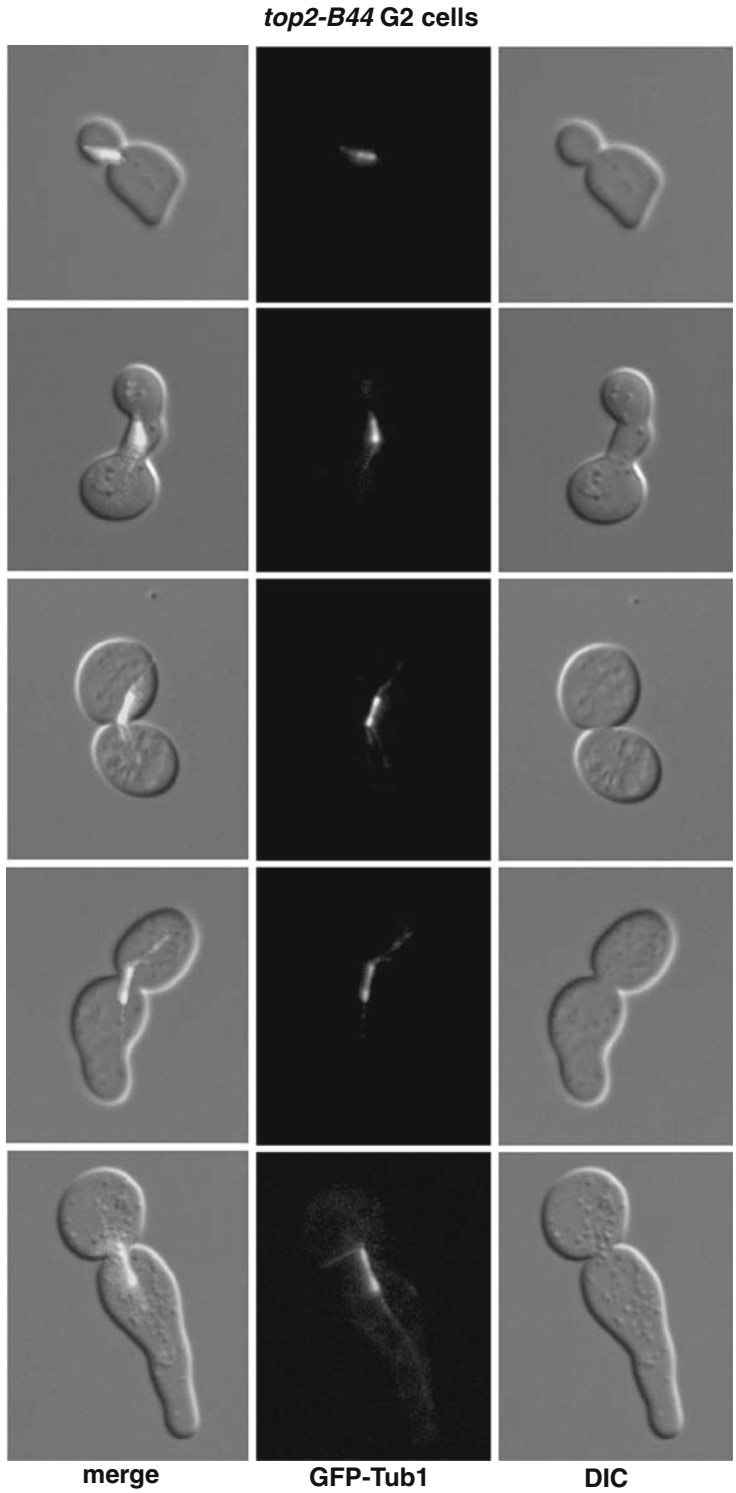

Fig. 14.7. **Microtubule morphologies in *top2-B44* G2/M cells**. *top2-B44* G2/M-phase cells visualized using the DIC setting on the microscope as well as the green fluorescence channel to observe the GFP-Tub1 fusion protein. Because the Topo II checkpoint is activated in these cells they spend about three times the normal time in G2/M-phase. During this

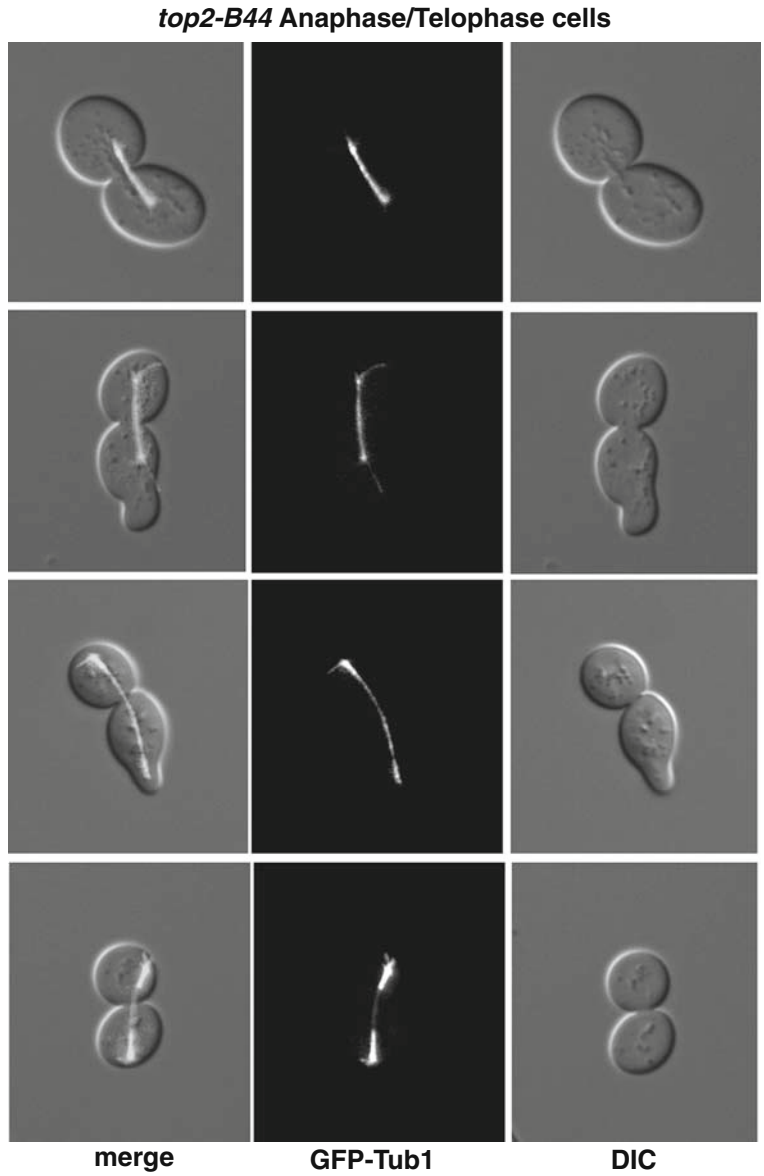

Fig. 14.8. **Microtubule morphologies in *top2-B44* anaphase/telophase cells**. *top2-B44* anaphase/telophase cells visualized using the DIC setting on the microscope as well as the green fluorescence channel to observe the GFP-Tub1 fusion protein. In mutant cells with G2/M delays, the daughter cell can continue to grow and therefore become approximately equal in size to the mother cell. As in **Fig. 14.4**, the spindle has elongated and thinned so that it is less bright. The *bottom image* is of a cell in which the spindle is about to break just prior to cytokinesis.

kinetochore microtubules shorten during chromosome segregation toward the spindle pole bodies, and it is the smaller number of overlap microtubules that are seen in the anaphase spindle. Finally, in telophase, the elongated spindle begins to break down. At this stage, the spindle pole bodies are seen close to the extremities of the mother and daughter cells, with short astral microtubules

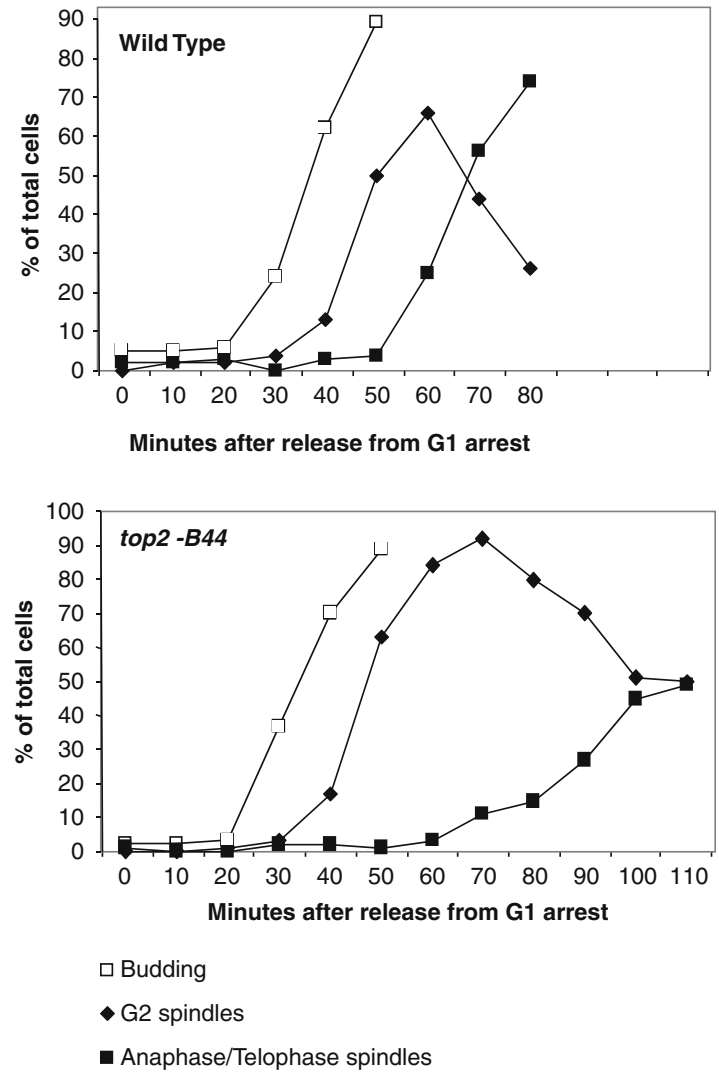

Fig. 14.9. **A typical time course experiment in which spindle morphologies were monitored**. Wild-type and *top2-B44* cells were counted according to the previously defined categories of spindle morphologies (**Figs. 14.1**–**14.8**). In a typical time course of wild-type cells budding begins to increase around 30 min and peaks around 80–90% between 50 and 60 min after release from G1. The formation of G2 spindles increases at an approximately equal rate but with about a 10-min delay. Anaphase spindle formation should also increase in an approximately equal rate, about 14–18 min after G2 spindle formation. In a typical time course of *top2-B44* cells, budding and G2 spindle formation occur with kinetics similar to wild-type cells. However, in this mutant, due to Topo II checkpoint activation, there is a delay between G2 spindle formation and anaphase spindle elongation of about 300%, such that anaphase spindles are seen 46 min after G2 spindles. Additionally, because of the delay the yeast cells do not undergo anaphase as synchronously as wild-type cells.

connecting them to the cells' edges. The cell then completed the cell cycle and following cytokinesis, the mother and daughter cells return to G1 and possess a single spindle pole body with astral microtubule projections. Because the yeast topoisomerase II checkpoint extends the G2/M-phase of the cell cycle, checkpoint duration can be assayed by measuring the interval between spindle assembly (i.e., at the beginning of G2/M-phase) and spindle elongation (i.e., at the onset of anaphase). In wild-type cells that have normal levels of topoisomerase II activity (i.e., when the checkpoint has not been triggered) and also in mutant cells that lack the checkpoint response, the G2/M period is typically around 15 min (11) (*see* **Fig. 14.9**). In *top2* mutants that activate the checkpoint response, the G2/M period can be extended by at least an additional 30 min (11).

1.3. Analysis of Chromosome Arm Condensation in Yeast Cells

Chromosome condensation is a necessary prerequisite for segregation of the genome in mitosis. As such, this process is regulated through the cell cycle. Through the end of S-phase, the genome is in a decondensed state. However, approximately at the onset of G2/M-phase of the cell cycle, the chromosome becomes compacted and condensed, a topoisomerase II-dependent process (9). This cell cycle stage in yeast is thought to correspond with prophase of mitosis in higher eukaryotes, where the condensation of the chromosomes is a cytologically dramatic event. In yeast, because chromosomes are very small, molecular tools needed to be developed to allow the analysis of the condensation process (9, 22). These methods allow the monitoring of chromosome condensation in live cells and can provide insight into aspects of Topoisomerase II function under experimental conditions.

A GFP-LacR fusion protein in combination with *LacO* sequences integrated into the yeast genome was utilized to produce a suitable strain (a "condensation strain") that can be used to monitor linear condensation of a chromosome arm during G2/M-phase (9). This system exploits features of the Lac operon in which the GFP-LacR fusion protein binds with sequence specificity to *LacO* DNA sequences. In the condensation strain, long stretches of tandemly repeated *LacO* sequences were inserted at two loci: one at the *trp1* locus (512 copies of *LacO*) and one at the *lys4* locus (256 copies of *LacO*). As GFP-LacR localizes to these repeats, it renders the *trp1* and *lys4* loci visible by fluorescent microscopy. When the chromosome is decondensed, the loci are separated by the intervening chromatin and appear as two discrete GFP foci under the microscope; the centers of the dots are separated on average by 1.6 μm (9). As the chromosome condenses, however, the foci coalesce and appear as two tightly associated GFP foci, or in some cases one single GFP focus, with an average distance of 0.6 μm between their centers (9). Examples are given in **Fig. 14.10**, and **Fig. 14.11** shows a typical cell cycle analysis of condensation.

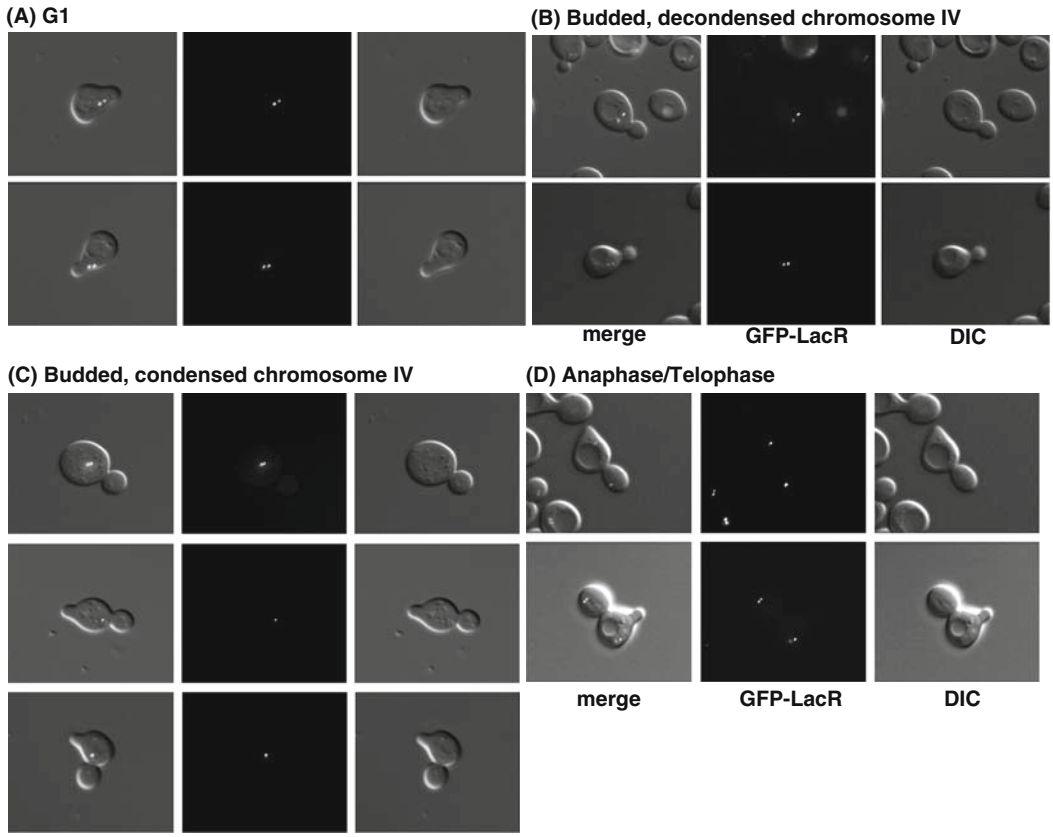

Fig. 14.10. **Visualization of the linear compaction of the chromosome IV right arm**. Yeast cells visualized using the DIC setting on the microscope as well as the green fluorescence channel to observe the GFP-LacR fusion protein in the "condensation strain" described in **Section 1.3**. (**A**) In G1 cells, the chromosome IV arm is decondensed, and thus two GFP foci are seen. If cells have not been arrested in α-factor, there is often only a single GFP focus visible in G1 cells. This is because round cells can lie in any orientation on the microscope slide and the two GFP foci can be vertically stacked, thus appearing as one dot or closely opposed dots. In α-factor arrested cells, the shmoo mating projection constrains the orientation in which the cells can lie on the slide and seems to cause the foci to more often appear next to each other rather than vertically stacked. The centers of the dots, which correspond to the *TRP1* and *LYS4* loci on the chromosome IV right arm, are separated by about 1.6 μm. This corresponds to a distance of $\sim$450 kb between *TRP1* and *LYS4*. (**B**) Budded cells with decondensed chromosomes: As the cells enter the S-phase, a small bud appears. During this phase, the chromosome remains decondensed, indicated by two visible GFP foci. For the purposes of this assay, the chromosome arm is considered to be decondensed, if the distance between the dots is greater than approximately two to three times the width of the GFP focus as seen under the fluorescent microscope. Care should be taken to focus up and down to search the entire cell for GFP foci as they may not appear in the same focal plane. (**C**) Budded cells with condensed chromosomes: As the cells enter G2/M, the bud continues to grow and the chromosomes condense. Cells are judged to have condensed chromosomes when the two GFP foci appear closely associated (less than about one GFP focus-width apart) or as a single focus. (**D**) Anaphase/telophase cells: When cells enter the anaphase/telophase, one pair of closely associated GFP foci (i.e., corresponding to one copy of the condensed chromosome IV) will move through the bud neck and appear in the daughter bud. The other pair of closely associated GFP foci segregates the extremity of the mother cell. The chromosomes often decondense rapidly once chromosome segregation has occurred.

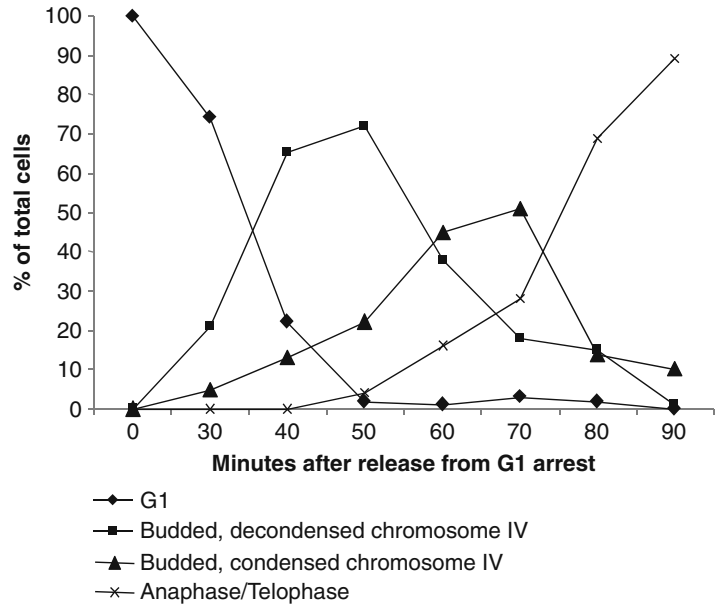

Fig. 14.11. **A typical time course experiment in which chromosome condensation was monitored.** To meaningfully relate chromosome condensation to cell cycle progression, the GFP-LacR condensation assay is coupled with analysis of budding, an indicator of entry into S-phase and therefore a useful cell cycle "landmark." This is useful, as cells will not synchronously release from G1, if too much α-factor is used or if they are left in α-factor for longer than approximately 2.5 h. In the graph shown, cells are considered to pass through the four states shown in **Fig. 14.10**. In a normal cell cycle following release from α-factor arrest, approximately 90% of cells are budded within 50–60 min (**Fig. 14.10B**). Chromosome condensation, indicated by the appearance of closely apposed GFP foci, or a single GFP focus (**Fig. 14.10C**), peaks at approximately 70 min. By 90 min, 90% of cells have completed anaphase (**Fig. 14.10D**). Because the period between chromosome condensation and the onset of anaphase is relatively short, the peak for the category in **Fig. 14.10C** is relatively low.

2. Materials

2.1. Yeast Strains and Plasmids

The following yeast strains and plasmids are available from the authors of the papers in which they were originally described. All of the yeast strains described below are derived from BF264-15 15DU: *MAT**a** ura3Δns ade1 his2 leu2-3,112 trp1-1a* (23).

1. pAFS91: A plasmid used to integrate *GFP-TUB1* (GFP-tagged α-tubulin) into the yeast genome at the *URA3* locus. The *GFP-TUB1* gene fusion is located in the KpnI to XhoI sites of plasmid pRS306. Integration at the *URA3* locus requires digestion of the plasmid with StuI followed by transformation into a *ura3* strain and selection for transformants on solid medium lacking uracil (19).
2. DCY1671: *MAT**a** bar1Δ ura3::HIS3:GFP-TUB1(URA3) ARG4*. This is a yeast strain, mating type **a**, that has the *bar1* locus deleted. The *ura3* gene is replaced with the

GFP-tagged α-tubulin fusion gene, which is under the control of the *HIS3* promoter. The integrated construct is linked to *URA3* so that this yeast strain is *URA3* (24).

3. DCY2769: *MAT**a** bar1Δ top2::top2-B44(KAN) ura3::HIS3:GFP-TUB1(URA3)*. This is a yeast strain, mating type **a**, that has the *bar1* locus deleted. The endogenous *TOP2* locus has been replaced with a recessive hypomorphic mutant allele of *TOP2* that causes activation of the Topo II checkpoint at temperatures that are semipermissive for growth. This strain is temperature sensitive at 37°C. This replacement is linked to resistance to kanamycin (11).
4. DCY2299: *MAT**a** bar1Δ top2-4 ura3::HIS3:GFP-TUB1(URA3)*. This is a yeast strain, mating type **a**, that has the *bar1* locus deleted. The endogenous *TOP2* locus has been replaced with an allele of *TOP2* that causes a chromosome condensation defect but does not cause activation of the Topo II checkpoint. This allele is temperature sensitive at 30°C (11).
5. AVY461: *MAT**a** bar1Δ trp1::LacO(TRP1, LEU2) LYS4::LacO(LEU2) his3::GFP-LacI(HIS3)* (9). This is the condensation strain described in **Section 1.3**.
6. AVY91: *MAT**a** bar1Δ top2-4 trp1::LacO(TRP1, LEU2) LYS4::LacO(LEU2) his3::GFP-LacI(HIS3)* (9). This is the condensation strain described in **Section 1.3** and carries a temperature-sensitive allele of *TOP2*.

2.2. Yeast Cell Growth and Synchronization

1. YPD: 2% glucose, 1% yeast extract, 2% bacto-peptone in distilled H_2O. Autoclave and store the solution at room temperature.
2. SD-Ura: 2% glucose, 0.67% yeast nitrogen base, 0.5% casamino acids in distilled H_2O. Autoclave and store the solution at room temperature.
3. α-Factor (mating pheromone peptide used for inducing G1 arrest in yeast): Dissolve 1 mg/ml of α-factor peptide in distilled H_2O. Store aliquots at –20°C (*see* **Note 1**).
4. 100X adenine solution: 0.3 g of adenine in 100 ml of distilled H_2O. Autoclave and store the solution at room temperature.

2.3. FACScan Analysis

1. Tris–HCl solution: 50 mM Tris–HCl, pH 8.0. Store at room temperature.
2. Sytox green (Molecular Probes): 1:1000 dilution of sytox green stock solution (5 mM in DMSO; store at –20°C) in 50 mM Tris–HCl, pH 8.0. Make up the solution immediately before use.

3. Pepsin solution: 5 mg/ml of pepsin dissolved in acidified water. Make up the solution immediately before use, add 45 µl of concentrated HCl to 10 ml of distilled H_2O, and then add 50 mg of pepsin.
4. RNase A solution: 1 mg/ml of RNase A in 50 mM Tris–HCl, pH 8.0. Make up the solution immediately before use, boil it for 10 min to ensure the complete inactivation of contaminating DNase, and then let it cool to room temperature.
5. 70% ethanol: Store at –20°C and transfer to ice before use.

3. Methods

3.1. Cell Culture and Synchronization

1. Grow cultures of *S. cerevisiae* overnight in 25 ml of SD-Ura containing 500 µl of 100X adenine solution (*see* **Note 2**) at 30°C in a conical flask in a shaking water bath (*see* **Note 3**). Aim for a late log phase culture that is near to reaching stationary phase, typically with an OD_{600} of 2–5 (*see* **Note 4**).
2. To synchronize the cells, dilute the cultures to an OD_{600} of 0.2 in 25 ml of YPD supplemented with α-factor solution (diluted in the range of 1:1000–1:5000 from the stock solution) (*see* **Note 5**). Grow the cells for 1.5–2.5 h at 30°C in a shaking water bath (*see* **Note 6**).
3. Verify the completion of the G1 arrest as follows: Take a 500-µl aliquot of the culture, pellet the cells by centrifugation briefly at 14,000*g* in a microcentrifuge, resuspend the cells in 10 µl of distilled H_2O, and place on a microscope slide with a coverslip on top. Score G1 arrest according to the criteria described in **Fig. 14.1**.
4. When the G1 arrest is complete (ideally greater than 90%), pellet the entire culture by centrifugation at 3000*g* for 5 min.
5. Wash the α factor from the cells by resuspending 2 times in 1 ml of distilled H_2O and sedimenting by centrifugation briefly at 14,000*g* in a microcentrifuge (*see* **Note 7**).
6. Release the cells from the synchrony by resuspending the pellet in 1 ml of YPD and inoculating this into 25 ml of prewarmed YPD in a conical flask in a shaking water bath (*see* **Note 7**).
7. Take samples at time points every 10 min beginning at the time of the release from the synchrony by removing 1 ml of the culture into a 1.5-ml tube. Sediment the cells by brief centrifugation at 14,000*g* in a microcentrifuge. Decant the supernatant.

8. Process the samples as described below for analysis by fluorescence microscopy to assay spindle morphologies (**Sections 3.2** and **3.2.1**); fluorescence-activated cell scanning to determine DNA content (**Section 3.3**); and fluorescence microscopy to assay chromosome condensation (**Sections 3.2** and **3.2.2**).

3.2. Processing the Samples for Analysis by Fluorescence Microscopy

1. Wash each sample with 1 ml of water and sediment the cells by brief centrifugation at 14,000*g* in a microcentrifuge. Decant the supernatant (*see* **Note 8**) and store the sample on ice, if unable to visualize immediately (*see* **Notes 9** and **10**).
2. To prepare the samples on microscope slides for analysis, completely resuspend the sample in the remaining supernatant by pipetting up and down. Put 3 µl of the resuspended sample on a microscope slide and place a coverslip over the sample on the slide (*see* **Note 11**).

3.2.1. Analysis of Spindle Morphologies

1. Score the cells into the following categories based on the analysis of spindle morphology and budding: G1, G2/M, anaphase/telophase. Images and descriptions of the morphological criteria are found in **Figs. 14.1**–**14.8**.
2. For each sample, count a total of 100–300 cells in triplicate. A graph of a typical time course is found in **Fig. 14.9**.

3.2.2. Analysis of Chromosome Condensation

1. Score the cells into the following categories based on the analysis of the fluorescent signals marking the *TRP1* and *LYS4* loci, as well as bud morphology: G1, S-phase and G2/M decondensed chromosome IV, S-phase and G2/M condensed chromosome IV, and anaphase/telophase. Images and descriptions of the morphological criteria are shown in **Fig. 14.10**.
2. For each sample, count a total of 100–300 cells in triplicate. A graph of a typical time course is shown in **Fig. 14.11**.

3.3. Fluorescence-Activated Cell Scanning (FACScan) Analysis of DNA Content

1. To process the samples for FACScan analysis, pellet the cells by centrifugation in a microcentrifuge at 14,000*g* for 30 s.
2. Discard the liquid supernatant and add 1 ml of distilled H_2O to the 1.5 ml tube to resuspend the pellet and wash the cells by vortexing the sample for 3–5 s.
3. Centrifuge the sample for 30 s at 14,000*g* to pellet the cells. Discard the supernatant.
4. Fix the cells by adding 1 ml of ice-cold 70% ethanol to the pellet and vortexing the sample until cell clumps are completely resuspended (*see* **Note 12**). Store the cells at 4°C for a minimum of 12 h to ensure complete fixation prior to processing the cells further.

5. The day prior to the FACScan analysis of the samples, wash the fixed cells in Tris–HCl solution: First, pellet the cells by centrifugation in a microcentrifuge at 3000*g* for 5 min. After discarding the ethanol, add 1 ml of Tris–HCl solution to the cell pellet and vortex briefly to resuspend.
6. Treat the cells with RNase A to degrade RNA in the cells (preferably this is done at the end of the working day): Centrifuge the washed cells at 3000*g* for 5 min and resuspend the pelleted cells in 200 µl of RNase A solution. Incubate the cells at 37°C for 12 h.
7. Wash the cells with Tris–HCl solution: Pellet the cells by centrifugation in a microcentrifuge at 3000*g* for 5 min. After discarding the supernatant, resuspend the cells in 1 ml of Tris–HCl solution by vortexing.
8. Add 200 µl of pepsin solution to the cells from the previous step. Incubate the samples at 37°C for 25–30 min (*see* **Note 13**).
9. Add 1 ml of Tris–HCl solution to the samples and centrifuge the samples in a microcentrifuge at 3000*g* for 5 min. Discard the supernatant and resuspend the pelletted cells in 500 µl of Tris–HCl solution.
10. Stain the cellular DNA with sytox green dye: First, label suitable FACScan analysis tubes and then aliquot 500 µl of the sytox green solution into the tubes. Add 100 µl of processed cells to the FACScan analysis tubes and store the samples in the dark at 4°C for 2 h (*see* **Note 14**).
11. Just prior to FACScan analysis of the samples, gently sonicate the cells for 2–5 s to disrupt any cell clumps in the sample (*see* **Note 15**).

4. Notes

1. The volume of the aliquots should correspond to the typical amount used in each experiment so that the peptide is not thawed and refrozen, which would reduce activity.
2. Addition of the adenine reduces the background fluorescence.
3. The optimum growth temperature is 30°C, but this should be adjusted if the strains being used are temperature sensitive.
4. In late log phase, the proportion of cells in G1 will be increased and this will aid in synchronizing the cells upon the addition of mating pheromone. If the cells are overgrown

and have become stationary, then the release from the synchrony will not be efficient and this will reduce the synchrony of cell cycle progression.

5. α-Factor differs in its effectiveness between batches and manufacturers. It is useful to empirically determine an appropriate working concentration for each batch because it is an expensive reagent. Each batch should be titrated to obtain 90% G1 arrest within 2 h of yeast growth at 30°C. If there is an insufficient α-factor concentration, the cells will not arrest during this time frame. If the concentration is too high, the cells will not release synchronously upon removal of the peptide. A minimum concentration of α factor present for a minimum amount of time will provide an optimally synchronous release. The concentration of α-factor and the time required for 90% arrest will vary according to each strain used. Typically, mutant strains require more time and higher concentrations of α-factor to achieve arrest. If more than 3.5 h is required to achieve the G1 arrest, then the cells rarely release synchronously.
6. α-Factor treatment should arrest 85–100% of cells in G1. Do not leave cells in the α-factor for longer than 3.5 h as the cells will not release synchronously.
7. Water for washing the cells and the medium the cells will be released into should be prewarmed to the release temperature so that the cells release as quickly and as synchronously as possible. If the synchrony is performed at a low temperature and then release at high temperature is desired (for example, when working with temperature-sensitive mutants), care must be taken to avoid heat shocking the cells, which would result in G1 arrest at the START transition point. Two methods can be used to avoid heat shocking: (i) after inoculating the cells into medium at the low temperature, allow the water bath to transition to the high temperature over a period of about 10 min and (ii) inoculate the cells into the medium at the low temperature, incubate with shaking for 10–15 min to allow the cells to pass the START transition, and then transfer the flask of cells to another water bath set at the high temperature.
8. When decanting, pour the supernatant off but leave a small amount of liquid, usually about 50–100 μl.
9. Washing the cells decreases the background fluorescence.
10. Storing the samples on ice will prevent the cells from continuing through the cell cycle. However, long-term storage on ice can lead to microtubule breakdown so it is preferable to visualize the spindle morphologies as quickly as possible. Alternatively, the cells can be fixed, which will provide more

time to perform the analysis. However, fixation reduces the fluorescence intensity of the GFP and can make the spindle morphologies more difficult to characterize. If fixation is required, add a final concentration of 3.7% formaldehyde solution directly to the cells in the medium, incubate at room temperature for 10 min, and then wash the cells with 1 ml of phosphate-buffered saline.

11. The goal is to immobilize the cells between the glass surfaces. Performing the microscopy when the cells are moving across the slide surface is almost impossible. Several factors will lead to the cells moving (i) if too large a sample volume is applied; (ii) if the cells are too concentrated; and (iii) if the cells are not fully resuspended.
12. Store the 70% ethanol at –20°C and transfer to ice before use to achieve optimal fixation. Less variance within the sample (in the widths of the G1 and G2 peaks for DNA content) can be obtained by dripping the ethanol into the 1.5 ml tube while vortexing the sample to be fixed. The use of sytox green rather than other DNA dyes such as propidium iodide also significantly reduces sample variance (25).
13. Do not treat the cells with pepsin for more than 30 min as this can result in increased sample variance.
14. Cells stained with sytox green must be kept in the dark until analysis as the dye is sensitive to light.
15. Settings for the sonicator must be determined empirically to achieve an appropriate level of cell disruption. Too much disruption can cause cell breakage and too little disruption can leave clumps of cells. The amount of cell disruption required can also vary between yeast strains.

References

1. Porter, A. C. and Farr, C. J. (2004) Topoisomerase II: untangling its contribution at the centromere. *Chromosome Res* **12**, 569–83.
2. Warburton, P. E. and Earnshaw, W. C. (1997) Untangling the role of DNA topoisomerase II in mitotic chromosome structure and function. *Bioessays* **19**, 97–9.
3. Holm, C., Stearns, T. and Botstein, D. (1989) DNA topoisomerase II must act at mitosis to prevent nondisjunction and chromosome breakage. *Mol Cell Biol* **9**, 159–68.
4. Uemura, T., Ohkura, H., Adachi, Y., Morino, K., Shiozaki, K. and Yanagida, M. (1987) DNA topoisomerase II is required for condensation and separation of mitotic chromosomes in *S. pombe*. *Cell* **50**, 917–25.
5. Adachi, Y., Luke, M. and Laemmli, U. K. (1991) Chromosome assembly in vitro: topoisomerase II is required for condensation. *Cell* **64**, 137–48.
6. Wood, E. R. and Earnshaw, W. C. (1990) Mitotic chromatin condensation in vitro using somatic cell extracts and nuclei with variable levels of endogenous topoisomerase II. *J Cell Biol* **111**, 2839–50.
7. Roberge, M., Th'ng, J., Hamaguchi, J. and Bradbury, E. M. (1990) The topoisomerase II inhibitor VM-26 induces marked changes in histone H1 kinase activity, histones H1 and H3 phosphorylation, and chromosome condensation in G2 phase and mitotic BHK cells. *J Cell Biol* **111**, 1753–62.

8. Newport, J. and Spann, T. (1987) Disassembly of the nucleus in mitotic extracts: membrane vesicularization, lamin disassembly, and chromosome condensation are independent processes. *Cell* **48**, 219–30.
9. Vas, A. C., Andrews, C. A., Kirkland Matesky, K. and Clarke, D. J. (2007) In vivo analysis of chromosome condensation in *Saccharomyces cerevisiae*. *Mol Biol Cell* **18**, 557–68.
10. Clarke, D. J., Vas, A. C., Andrews, C. A., Diaz-Martinez, L. A. and Gimenez-Abian, J. F. (2006) Topoisomerase II checkpoints: universal mechanisms that regulate mitosis. *Cell Cycle* **5**, 1925–8.
11. Andrews, C. A., Vas, A. C., Meier, B., Gimenez-Abian, J. F., Diaz-Martinez, L. A., Green, J., Erickson, S. L., Vanderwaal, K. E., Hsu, W. S. and Clarke, D. J. (2006) A mitotic topoisomerase II checkpoint in budding yeast is required for genome stability but acts independently of Pds1/securing. *Genes Dev* **20**, 1162–74.
12. Skoufias, D. A., Lacroix, F. B., Andreassen, P. R., Wilson, L. and Margolis, R. L. (2004) Inhibition of DNA decatenation, but not DNA damage, arrests cells at metaphase. *Mol Cell* **15**, 977–90.
13. Mikhailov, A., Shinohara, M. and Rieder, C. L. (2004) Topoisomerase II and histone deacetylase inhibitors delay the G2/M transition by triggering the p38 MAPK checkpoint pathway. *J Cell Biol* **166**, 517–26.
14. Gimenez-Abian, J. F., Weingartner, M., Binarova, P., Clarke, D. J., Anthony, R. G., Calderini, O., Heberle-Bors, E., Moreno Diaz de la Espina, S., Bogre, L. and De la Torre, C. (2002) A topoisomerase II-dependent checkpoint in G2-phase plant cells can be bypassed by ectopic expression of mitotic cyclin B2. *Cell Cycle* **1**, 187–92.
15. Deming, P. B., Flores, K. G., Downes, C. S., Paules, R. S. and Kaufmann, W. K. (2002) ATR enforces the topoisomerase II-dependent G2 checkpoint through inhibition of Plk1 kinase. *J Biol Chem* **277**, 36832–8.
16. Deming, P. B., Cistulli, C. A., Zhao, H., Graves, P. R., Piwnica-Worms, H., Paules, R. S., Downes, C. S. and Kaufmann, W. K. (2001) The human decatenation checkpoint. *Proc Natl Acad Sci USA* **98**, 12044–9.
17. Downes, C. S., Clarke, D. J., Mullinger, A. M., Giménez-Abián, J. F., Creighton, A. M. and Johnson, R. T. (1994) A topoisomerase II-dependent G2 cycle checkpoint in mammalian cells. *Nature* **372**, 467–70.
18. Goto, T. and Wang, J. C. (1984) Yeast DNA topoisomerase II is encoded by a single-copy, essential gene. *Cell* **36**, 1073–80.
19. Straight, A. F., Marshall, W. F., Sedat, J. W. and Murray, A. W. (1997) Mitosis in living budding yeast: anaphase a but no metaphase plate. *Science* **277**, 574–8.
20. Winey, M., Mamay, C. L., O'Toole, E. T., Mastronarde, D. N., Giddings, T. H., Jr., McDonald, K. L. and McIntosh, J. R. (1995) Three-dimensional ultrastructural analysis of the *Saccharomyces cerevisiae* mitotic spindle. *J Cell Biol* **129**, 1601–15.
21. Pearson, C. G., Maddox, P. S., Salmon, E. D. and Bloom, K. (2001) Budding yeast chromosome structure and dynamics during mitosis. *J Cell Biol* **152**, 1255–66.
22. Straight, A. F., Belmont, A. S., Robinett, C. C. and Murray, A. W. (1996) GFP tagging of budding yeast chromosomes reveals that protein-protein interactions can mediate sister chromatid cohesion. *Curr Biol* **6**, 1599–608.
23. Richardson, H. E., Wittenberg, C., Cross, F. R. and Reed, S. I. (1989) An essential G1 function for cyclin-like proteins in yeast. *Cell* **59**, 1127–33.
24. Clarke, D. J., Segal, M., Mondesert, G. and Reed, S. I. (1999) The Pds1 anaphase inhibitor and Mec1 kinase define distinct checkpoints coupling S phase with mitosis in budding yeast. *Curr Biol* **9**, 365–8.
25. Haase, S. B. and Reed, S. I. (2002) Improved flow cytometric analysis of the budding yeast cell cycle. *Cell Cycle* **1**, 132–6.

Chapter 15

Cytological Analysis of Chromosome Structural Defects that Result from Topoisomerase II Dysfunction

Juan F. Giménez-Abián and Duncan J. Clarke

Abstract

For analyzing chromosome structural defects that result from topoisomerase II (topo II) dysfunction, we have adapted classical cell cycle experiments, classical cytological techniques, and the use of a potent topo II inhibitor (ICRF-193). In this chapter, we describe in detail the protocols used and we discuss the rationale for our choice and for the adaptations applied. We clarify in which cell cycle stages each of the different chromosomal aberrations induced by inhibiting topo II take place: lack of chromosome segregation, undercondensation, lack of sister chromatid resolution, and lack of chromosome individualization. We also put these observations into the context of the two topo II-dependent cell cycle checkpoints.

Key words: Topoisomerase II, chromatid resolution, condensation, chromosome individualization, ICRF-193, topo II checkpoint.

1. Introduction

Topoisomerase II (topo II) is required for several mitotic processes that prepare chromosomes for accurate segregation in anaphase. Topo II is the major eukaryotic enzyme that can decatenate/concatenate DNA; that is, it can transiently break a double strand of DNA, pass another double strand through the gap, and then reseal the gap. Given that inter-chromatid catenations arise as a consequence of DNA replication, the first expected consequence of the lack of topo II activity is a block to the segregation process. In fact, this was the first phenotype to be described, when yeast topo II (*top2*) mutants were analyzed. The, so-called, *cut* phenotype (*Chromosomes Untimely Torn*) corresponded to attempts at cytokinesis in the absence of genome segregation (1). However,

D.J. Clarke (ed.), *DNA Topoisomerases*, Methods in Molecular Biology 582,
DOI 10.1007/978-1-60761-340-4_15,

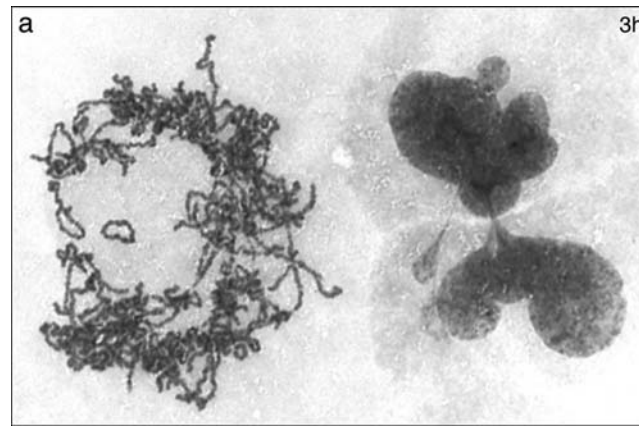

Fig. 15.1. **Long treatments with topo II inhibitors (ICRF-193, 2 μg/ml) generate a wide variety of phenotypes coexisting in the same preparation**. The cell on the *left* is a metaphase cell in polar view (i.e., as if the observer is at the spindle pole) and displays (1) lack of chromosome segregation (this cell would end up attempting cytokinesis in the absence of segregation as has occurred in the case of the cut phenotype displayed by the cell on the *right*); (2) chromosome undercondensation (chromosomes are long and thin); (3) lack of sister chromatid resolution (sister chromatids are indistinguishable and chromosomes appear as a single rod); and (4) deficient chromosome individualization: the chromosomes have intra-chromosomal tangles (these are described as Ω-figures, based on their shape, and can be seen in the left cell at the *top*) and are also tangled with each other. Identification of the cell cycle stage at which each phenotype is produced requires the use of cell cycle synchrony protocols and cytological techniques, which are described in detail in this chapter.

detailed analysis of topo II inhibition in mammalian cells, which carry considerably larger chromosomes, has revealed a wide variety of different phenotypes (**Fig. 15.1**) depending on the precise moment in which topo II activity is perturbed (2, 3). These phenotypes include (**Fig. 15.2**):

- Block of sister chromatid segregation (i.e., when the cell reaches metaphase, the chromosomes are unable to separate their sister chromatids and eventually proceed to cytokinesis in the absence of chromosome segregation) (**Fig. 15.3**).
- Deficient chromosome condensation (i.e., chromosomes that condensed in the presence of topo II inhibitors are longer than control chromosomes when topo II is inhibited prior to late metaphase) (**Figs. 15.4, 15.5, 15.6**, and **15.7**).
- Lack of chromosome resolution (i.e., chromosomes of cells that enter mitosis in the presence of topo II inhibitors do not display distinguishable sister chromatids in metaphase) (**Figs. 15.5, 15.6**, and **15.7**).
- Lack of chromosome individualization (i.e., chromosomes of cells that enter G_2 in the presence of topo II inhibitors reach metaphase with intra- and inter-chromosomal tangles) (**Figs. 15.6** and **15.7**).

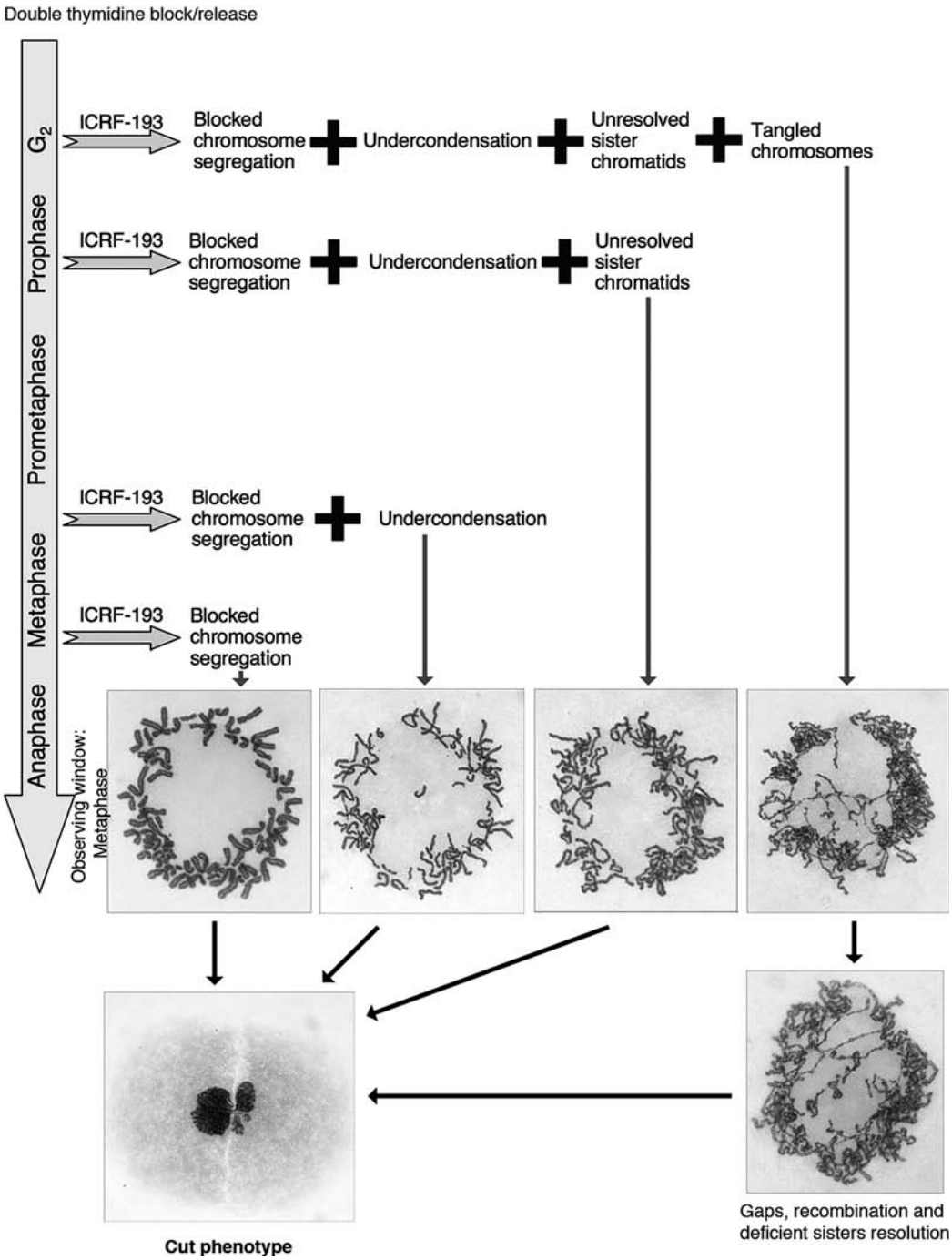

Fig. 15.2. **Rationale for the protocols described in this chapter**. Cells are presynchronized by a double thymidine block schedule then released into S-phase. We add the topo II inhibitor (ICRF-193) at different times as the cells progress through the cell cycle and we keep the drug present until the peak of the metaphase wave (10–10.5 h after the release from the second thymidine block). Then, we fix the material and compare the effects of different length treatments at a single observation window: metaphase in the case of the scheme shown and as illustrated in **Figs. 15.3, 15.4**, and **15.5** or prometaphase as illustrated in **Fig. 15.6**. Comparing phenotypes seen after the different length treatments allows one to determine at which cell cycle stage topo II activity is required for a specific function. All of the different categories eventually end up, after some delay, undergoing the cut phenotype.

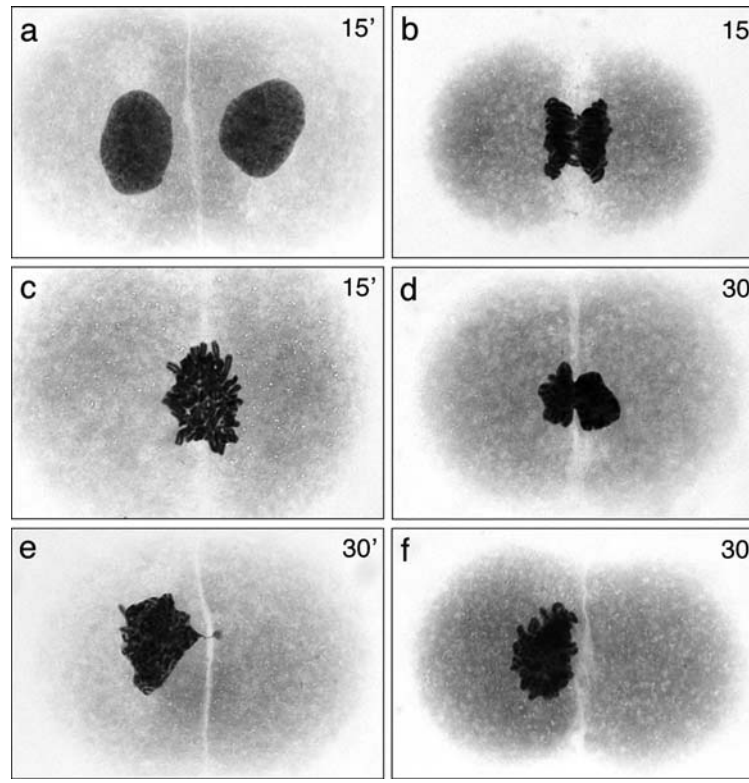

Fig. 15.3. **The *cut* (*C*hromosomes *U*ntimely *T*orn) phenotype**. As described in the protocols section, we use presynchronized HeLa cells and we add ICRF-193 at different times before the peak of the metaphase wave; the longer the treatment, the more complex the mixture of phenotypes observed; the shorter the treatment, the lesser the extent of different phenotypes. Ten minutes is the minimum treatment time required to obtain a detectable phenotype. The *Cut* (*C*hromosomes *U*ntimely *T*orn) phenotype is the first phenotype to be observed after short topo II inhibitor treatment. At first, this phenotype coexists with control-like telophase or early G1 cells (**a**). Although it is commonly remarked that failed segregation attempts result in the ingression of the cytokinesis ring into the chromatin mass (**b**), this phenotype is extremely infrequent. Most commonly, there is no observable chromosome segregation attempt and no separation of the centromeres (or the chromosome arms) is observed (**c**), but cytokinesis takes place to one side of the chromatin mass (**d, e**). These cells also display a delay in the process of chromosome decondensation as chromosomes can be clearly observed while cells are entering G1 (**c**, **f**, judging by the advanced stage of cytokinesis). During the deficient attempt at cell division, the trapped unsegregated chromosomes usually take up a position away from the center of the cell (**c**, **d**) and are progressively displaced toward one of the daughter cells (**e**, notice a small chromatin fragment on the right side cell) or are completely included within one of the daughters (**f**). We interpret these cut phenotypes as the result of cells being inhibited at late/very late metaphase stages (i.e., after the metaphase topo II checkpoint). Slightly longer treatments result in an increase in cells delayed in metaphase, which can remain in metaphase for up to 1–1.5 h (examples shown in **Fig. 15.4a, b**), that show no signs of undercondensation, indicating that the cell was already in metaphase when the inhibitor was added.

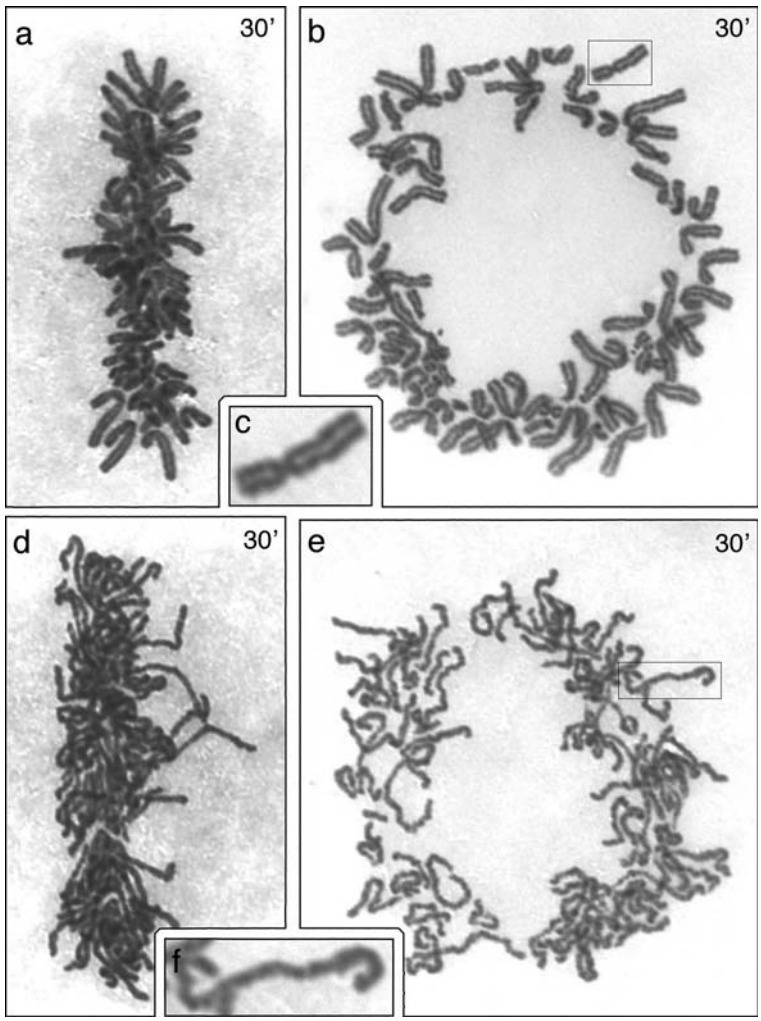

Fig. 15.4. **Transient arrest in metaphase**. Longer ICRF treatments (30 min to 1.5 h) result in the appearance of cells that are blocked/delayed in the metaphase (**a**, side view; **b**, polar view). These cells were already in the metaphase at the time the inhibitor was added (otherwise they would show chromosome undercondensation, not shown). The chromosomes in these cells show control-like sister chromatid resolution (sisters are distinguishable, insert **c**). They are easily differentiated from cells hit with the inhibitor in late prophase, in which case, the cells also reach metaphase during the length of the treatment (**d**, side view; **e**, polar view) but, in addition to the lack of chromosome segregation they show undercondensed chromosomes and a lack of sister chromatid resolution (chromosome in insert **f**) as sister chromatids are cytologically undifferentiated. Sister chromatid resolution takes place in late prophase in HeLa cells and in early prometaphase in *M. muntjac* cells. These latter cells also delay in metaphase and so they can appear in treatments as long as 3 h.

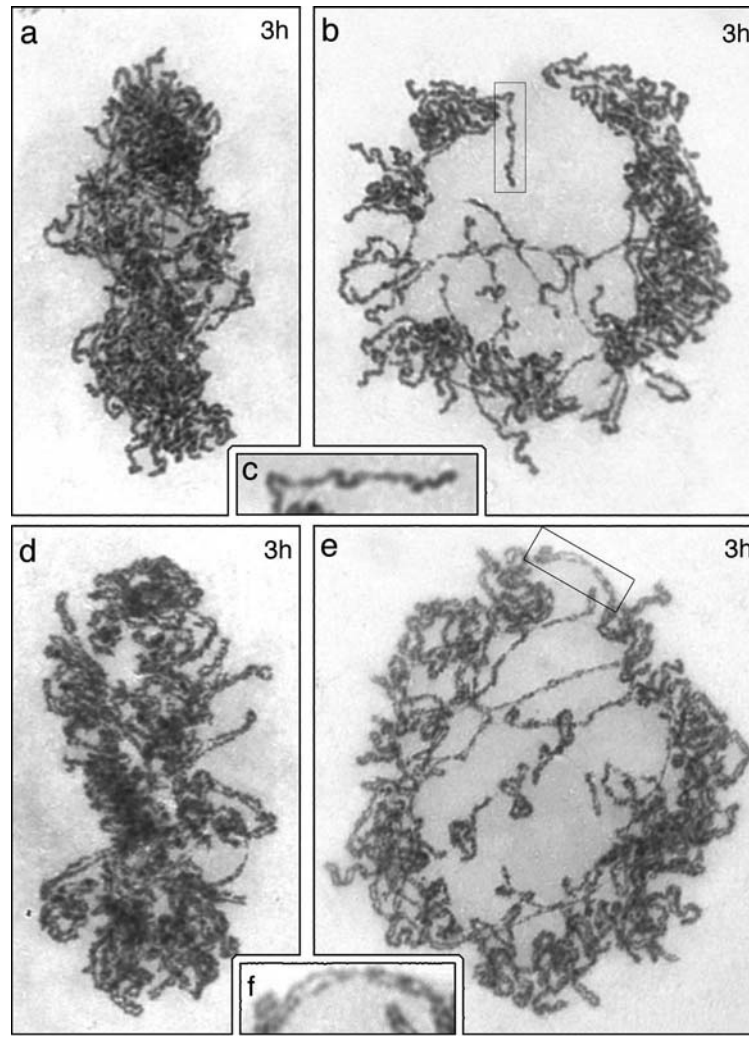

Fig. 15.5. **Inter- and intra-chromosomal tangles**. Treatments with topo II inhibitors (ICRF-193) initiated 1.5–3 h before the peak of the metaphase wave (i.e., when the cells were in late interphase) render new phenotypes mixed with the phenotypes described in **Figs. 15.1, 15.2, 15.3**, and **15.4**. As before, cells show a lack of chromosome segregation, chromosome undercondensation, and lack of sister chromatid resolution; but now a new phenotype appears: intra- and inter-chromosomal tangles. Part (**a**) represents a metaphase cell in side view while (**b**) shows a polar view of a metaphase cell. In both cases, the tangling between chromosomes is obvious. The selected chromosome in (**c**) displays three (different in size) Ω-figures visualized as chromosome bends that we interpret as intra-chromosomal tangles. These cells also delay in metaphase but the morphology of their chromosomes changes with time and despite being unable to segregate they end up resolving their sister chromatids, which now become visible (**d**, metaphase in side view; **e**, polar view metaphase). Sister chromatids become visible but they show a discontinuous appearance (**f**) and chromosome recombination events can sometimes be observed (**d**, **e**). This latter category of cell appears after 3 h of inhibitor treatment and becomes more frequent after longer (up to 4–5 h) treatments.

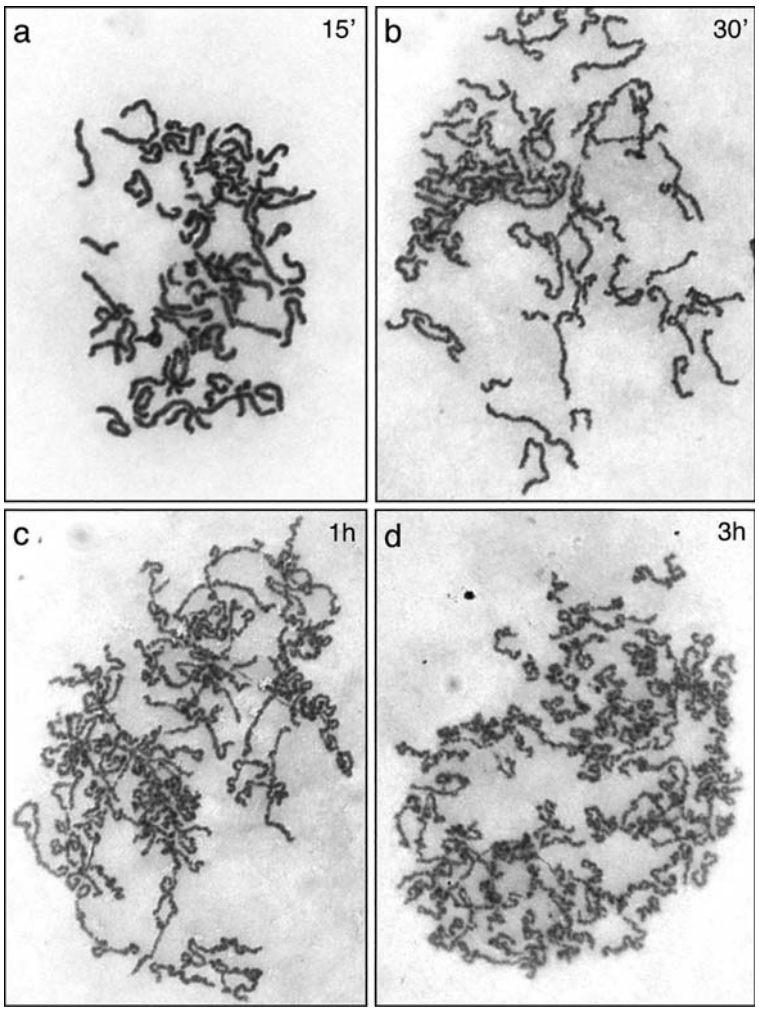

Fig. 15.6. **Prometaphase as the observation window**. In the previous figures (**Figs. 15.2, 15.4**, and **15.5**) we have shown typical results obtained when following the protocols described above, when a fixed observation window (metaphase) is used. The same kind of analysis can be performed using a different observation window. In this figure, we show prometaphases obtained after different length treatments with the same topo II inhibitor (ICRF-193). (**a**) Shows a prometaphase cell after a short time (15 min) with ICRF-193; the chromosomes display undercondensation and a lack of sister chromatid resolution indicating that the cell was hit with drug before sister chromatid resolution, which takes place in control cells in late prophase. (**b**) A very similar cell that displays more severe undercondensation, indicating that it was hit with drug earlier in prophase than the previous cell. (**c**) The presence of massive numbers of Ω-figures (chromosome bends and kinks) and inter-chromosomal tangles adds a new phenotype (in addition to undercondensation and a lack of sister chromatid resolution) suggesting that the cell was hit with drug in interphase. (**d**) A more severe display of each of these phenotypes, indicating that this cell was hit with drug earlier in interphase than the cell in (**c**).

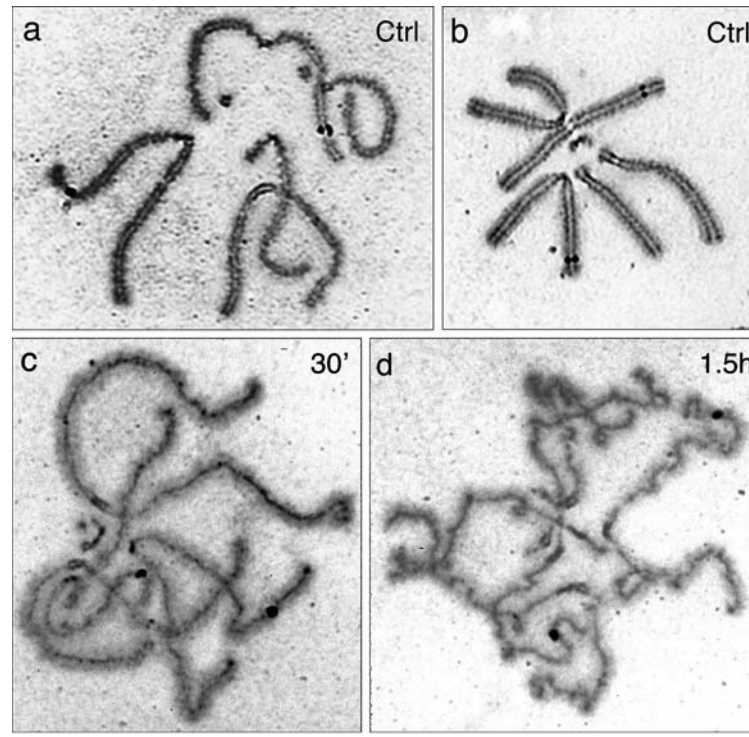

Fig. 15.7 . **Silver staining of chromosome cores**. Silver staining of chromosome cores is a simple procedure but which suffers from poor reproducibility. It allows the visualization of several chromosome and cellular features, such as the chromatin halo (*light staining intensity*), the chromosome core (*medium staining intensity*), the NOR (Nucleolar Organizing Regions) in *black*, and kinetochores (*dark staining intensity*). The cells shown here are of *M. muntjac*, a small deer with a very low chromosome number and very large chromosomes. The cell in (**a**) is a control prometaphase cell in the process of resolving its sister chromatids, thus, together with regions of the chromosomes showing two sister chromatid cores we can observe stretches of apparently single core regions (unresolved regions). (**b**) A metaphase cell; two cores are observed per chromosome (sisters are already resolved) and the long muntjac kinetochores (in *black*) are grouped in the center of the cell (the metaphase plate). Two chromosomes bear near distal *black dots*, which correspond to the NORs. (**c**) Shows a metaphase cell after a 30′ treatment with ICRF-193; kinetochores are grouped and are under spindle tension (they are seen as double unlike the chromosome arms), the chromosomes are largely undercondensed and lack sister chromatid resolution (both sister chromatid cores are apposed, running through the middle of each chromosome). (**d**) This cell has in addition to the phenotypes in (**c**), the presence of multiple inter-chromosomal and intra-chromosomal (numerous Ω-figures involving the chromosome cores are observed) tangles.

Taking a fixed window of observation (e.g., metaphase), the longer the elapsed time since addition of the topo II inhibitor to the cells, the greater the variety in the different phenotypes that accumulate within the same cell (**Fig. 15.2**). Thus, it is important to be able to study chromosome morphology and mitotic stages in great cytological detail to understand the consequences of topo II perturbation at different times during the cell cycle.

1.1. Protocols

There are two strategies that can be used to perform such cell cycle experiments:

(i) Using this approach the observation window remains constant while the cells progress (**Fig. 15.2**). The fixed window of observation, for chromosome cytology, is preferably metaphase (**Figs. 15.4, 15.5**, and **15.7**) or prometaphase (**Fig. 15.6**) because most chromosome characteristics related to topo II function are observed at these cell cycle stages: lack of segregation, lack of condensation, lack of sister resolution (the ability to distinguish both sister chromatids), and lack of individualization (the physical separation of the chromosomes from the intertwined interphase chromosomes). The topo II inhibitor is added at different times prior to fixation of the cells with Carnoy's solution. For example, if the observation window is metaphase and the cells are fixed 10 min after adding the inhibitor, defects will be revealed that are related to topo II inhibition in early metaphase and late prometaphase. If the inhibitor is added 3 h before fixation, a cell in metaphase at the time of fixation will display the cumulative effects of topo II inhibition through G2, prophase, prometaphase, and metaphase. The phenotypes that are observed after treatments differing in length can be compared and subtracted: the longer the treatments, the more complex the phenotypes that are observed.

(ii) Using this approach the observation window moves as cells progress through the cell cycle. The most straightforward way of performing this approach is by observing live cells by time-lapse microscopy. However, the optical resolution of chromatin/chromatids/chromosomes is far below what can be achieved in Carnoy's fixed cells, even when using topo II-GFP cell lines (4). Thus, we prefer the analysis of fixed material and combine this with cell cycle synchronization.

To achieve the pseudo-synchronous passage of mammalian cells into and through mitosis, the cells are presynchronized by a double-thymidine block/release protocol. For HeLa cells, for instance, a good working protocol is 15 h with 2 mM thymidine, 10 h release in normal medium, 15 h with thymidine, final release (*see* **Section 2.1**). Different cells, even different HeLa isolates, require adjustments to the timing of the protocol (*see* **Note 1**). Essentially, during the first thymidine block, the cells in G2, mitosis, and in G1 cycle through and accumulate at the beginning of S-phase, while cells that were in S-phase at the time of thymidine addition remain dispersed through the S-phase period. During the first 10-h release, all cells progress and leave S-phase. The second thymidine block then allows all of the cells to accumulate at the beginning of S-phase. The second release thus renders a synchronous cell cycle wave involving the whole cell population, though

synchrony is lost to some extent as the cells reach mitosis. The topo II inhibitor can be added at different times after the release of the second thymidine block. The first cells will reach mitosis after about 8–10 h following the thymidine removal. Cells are then collected and processed at a fixed time after adding the inhibitor. This protocol, however, presents two main problems: (i) During the synchronization protocol, because some cells will have spent more time arrested in S-phase than others, cell mass differs as well as chromosome damage that might arise as a consequence of S-phase arrest. For these reasons, the cells progress at different rates towards mitosis, and there is some cell cycle desynchronization. The further through the cell cycle from the release point, the wider the synchrony wave. (ii) The assays described here rely on studying chromosome structure cytologically. Most cell cycle stages are recalcitrant to the study of chromosome structure as the chromosomes need to be reasonably well condensed, as they are in prometaphase and metaphase. For example, studying chromosome structure in G2-phase following a 1-h treatment at the end of S-phase would be complicated due to the lack of condensation. This limitation can be overcome by combining the methods described here with the induction of premature chromosome condensation (PCC), which itself requires some expertise, and a good PCC-inducer (e.g., Calyculin A-treatment or cell-fusion experiments). Furthermore, not all cell lines are amenable to PCC protocols. Thus, we do not include these methods here, but refer the reader to published work (2).

In our hands, the best protocol for analyzing the cytological effects of topo II inhibition is a combination of two previously described methods: we use presynchronized cells and we add the topo II inhibitor at different times during the cell cycle wave keeping the inhibitor present until we fix the cells at the peak of the mitotic wave (**Fig. 15.2**). Sometimes caffeine can be added to avoid the G2-phase topo II checkpoint as this allows interphase cells with inhibited topo II to reach mitosis without delay. Caffeine addition renders higher frequencies of cells with aberrations generated in interphase (so it can be important in studies of cell cycle timing or when frequencies of aberrations are being determined), but its addition can be omitted given the leaky nature of the G2-phase topo II checkpoint, especially when only chromosome structural defects are of interest.

1.2. Mitotic Chromosome Preparations

To analyze the cytology of mitotic cells and chromosomes, we routinely perform chromosome preparations similar to previous descriptions but with modifications that are described in this chapter (2, 3, 5). Most chromosome preparation methods, typically used in cytogenetics, aim to spread the chromosomes well, so that chromosome aberrations can be scored. However, in this chapter, we describe modifications to this procedure that allow

analysis of chromosomes "in situ" on the mitotic spindle. The method allows visualization of individual chromosomes and chromatids and differentiation of telomeres, arms, and centromeres within each chromosome. Remarkably, under these conditions mitotic cells appear in one plane but possess the major features of well-preserved 3D mitotic morphologies. The idea is to be able to study chromosome behavior during mitosis and to be able to accurately distinguish the different mitotic stages. This allows, in particular, the transition from metaphase to anaphase to be studied with clarity. This method is applicable to the study of the effects of any treatment on the mitotic process, but we have found it particularly effective in analyzing chromosome structural defects and aberrant chromosome behavior after topoisomerase II perturbation.

1.3. Impregnation of Silver into Chromosomes

Of particular relevance to the study of the mitotic functions of topo II is the analysis of the chromosome core, or scaffold. This is thought to be a proteinaceous structure that forms the skeleton of the mitotic chromosome, to which loops of chromatin are attached and on which they become organized during chromosome condensation. Topo II is a component of the chromosome core (2, 6). Silver impregnation produces a range of color tints including the black of nucleoli, the dark brown of chromosomal cores, the golden color of interphase nuclei, and the chromatin halo that surrounds chromosome cores. Reproducible silver staining requires attention to detail and, unavoidably, some good luck!

2. Materials

2.1. Cell Culture and Synchrony

1. Mammalian cells growing as monolayers (*see* **Note 1**).
2. Tissue culture medium: DMEM (Dulbecco's Minimal Essential Medium) supplemented with final concentrations of 10% FCS (fetal calf serum), 2 mM L-glutamine, and antibiotics.
3. Trypsin solution: 0.1–0.5% trypsin–EDTA.
4. ICRF-193 (MP Biomedicals): 4 mg/ml stock of 4-[2-(3,5-Dioxo-1-piperazinyl)-1-methylpropyl]piperazine-2,6-dione dissolved in dimethylsulfoxide. Freeze aliquots at –20°C. Use at a final concentration of 2 μg/ml.
5. Thymidine: 50 mM stock of thymidine in tissue culture medium. Filter to sterilize (when prepared) and store at 4°C.
6. Caffeine: 50 mM caffeine stock solution in tissue culture medium (*see* **Note 2**). Filter to sterilize (when prepared) and store at 4°C.

2.2. Chromosome Preparations

1. Carnoy's fixative: 75% methanol, 25% glacial acetic acid. Make fresh every hour (*see* **Notes 3** and **4**).
2. Clean microscope slides (*see* **Note 5**).
3. Giemsa solution: 7% Giemsa (EMD) made in phosphate buffer, pH 6.8 (Harleco) (*see* **Note 6**). It can be reused two to three times.
4. Entellan mounting agent (Merck) (*see* **Note 7**).

2.3. Silver Impregnation

1. 2XSSC: 300 mM sodium chloride, 30 mM sodium citrate. Adjust to pH 7.0 with 1 N HCl.
2. Silver staining solution: Freshly prepare 0.05% formic acid (*see* **Note 8**) in water and then add 150 µl of this to 0.1 g of silver nitrate (obtained from Probus or Panreac; *see* **Notes 9** and **10**). The solution should be prepared immediately before use as the silver will precipitate rapidly. Shake the mixture for 30 s (tapping) to dissolve the silver nitrate.

3. Methods

3.1. Growing and Synchronizing the Cells

The double thymidine block/release protocol is an inexpensive and reliable method to efficiently synchronize cells at the G1/S boundary. The timing of the steps in this protocol should be adjusted for each cell line depending on the doubling time and on the relative duration of each cell cycle phase (*see* **Note 1**). We should say, however, that this protocol does not work for rodent cells or for *Muntiacus muntjac* cell lines. Here, we describe the protocol used for our stock of the HeLa cell line that has a doubling time of approximately 24 h.

1. Culture monolayers of HeLa cells in a tissue culture incubator under standard conditions of growth at 37°C with 5% CO_2 (*see* **Note 11**).
2. Three days before the experiment, seed the exponentially growing HeLa cells at 10–30% confluence in tissue culture dishes with tissue culture medium. Incubate the cells for at least 24 h (*see* **Note 12**).
3. Add pre-warmed (37°C) thymidine to a final concentration of 2 mM. Incubate the cells for 15 h. (During this time cells in mitosis, G2, and G1 at the time of the thymidine addition will progress through the cell cycle and accumulate at the G1/S boundary while cells in S-phase delay/block their progression and remain at different stages of the S-phase.)
4. Release the thymidine block by removing the tissue culture medium from the cells and replacing it with prewarmed tissue culture medium without thymidine (*see* **Note 13**).

5. Ten hours after the thymidine was removed, again add thymidine to a final concentration of 2 mM. Incubate the cells for 15 h. (During the thymidine release, both the group of cells blocked at the G1/S boundary and those dispersed through the S period progress beyond the S-phase. Thus, this second thymidine block gathers together all of the cells at the next G1/S boundary.)
6. Release the cells from the second thymidine block as described in step 3.
7. At the desired time following release from the second thymidine block (*see* **Section 1.1**), add the prewarmed topo II inhibitor (ICRF-193) to achieve a final concentration of 2 μg/ml (*see* **Notes 14** and **15**). (Optional: add prewarmed caffeine to achieve a final concentration of 2 mM; *see* **Note 16**.)

3.2. Preparation of Mitotic Chromosome Morphologies that Maintain the 3D-Organization of Chromosomes on the Mitotic Spindle

1. Carefully aspirate off the majority of the tissue culture medium from the dish (*see* **Note 17**).
2. Transfer the mitotic cells in about 2–3 ml of tissue culture medium into a 15 ml tube (shake-off or scrape the cells from the dish; *see* **Notes 17–19**).
3. Hypotonic treatment: Add tap water (rapidly) so that the ratio is 40% medium/60% water (i.e., hypotonic) to swell the cells. For 2 ml of medium plus cells add 3 ml of tap water (*see* **Note 20**).
4. Leave the cells for 5.5 min at room temperature (*see* **Note 21**).
5. Stop the hypotonic treatment by rapidly adding at least an equal volume of freshly prepared Carnoy's solution (i.e., fill the rest of the 15 ml tube with Carnoy's) (*see* **Notes 22** and **23**). This procedure results in rapid fixation ("freezing") of the cells.
6. Pellet the cells by centrifugation at 800–1000*g*, ~4–5 min.
7. Quickly aspirate off the liquid using a vacuum pump assembly taking care not to disturb the cell pellet (*see* **Notes 24** and **25**).
8. Resuspend the cells by tapping the side of the tube (*see* **Note 26**).
9. Gently fill the tube with Carnoy's solution (along the side of the tube), and mix the cells and fixative gently by inverting the capped tube twice.
10. Let the tube stand for ~5 min at room temperature.
11. Pellet the cells by centrifugation at 800–1000*g*, ~4–5 min, resuspend the cell pellet, and add fresh Carnoy's fixative, as described in steps 6–9. Repeat this process so that the fixative

is changed at least four times (the cells should go through at least 3X changes in pure fixative with no water or tissue culture medium) (*see* **Note 27**).

12. After the final wash, resuspend the cell pellet in 2–5 ml of Carnoy's solution so that the cells are at an appropriate dilution for making the chromosome spreads (half an ml of cells in 4 ml of fixative) and store at 4°C overnight (*see* **Note 28**).
13. For spreading the cells on microscope slides, first let the fixations warm to room temperature then drop (a small drop) from a 5 cm height onto pre-cleaned glass slides and allow the cells to dry at room temperature (*see* **Note 29**).
14. Stain the air-dried slides in a coplin jar in freshly made 5% Giemsa solution for 7 min (*see* **Notes 30** and **31**).
15. After staining, wash the slides briefly in tap water, let them air dry.
16. Mount the slides with Entellan (Merck).
17. Analyze on the microscope (*see* **Note 32**).

3.3. Impregnation of Silver into Fixed Mitotic Chromosomes

1. Collect the cells and perform the hypotonic swelling, fixation, and chromosome spreads as described in **Section 3.2**, steps 1–13 (*see* **Notes 33** and **34**).
2. Incubate the dried slides with 2 × SSC in a coplin jar placed in a water bath at 60°C for 23 min (*see* **Note 35**).
3. Rinse the slides with running tap water for 5 min in the coplin jar and then briefly rinse in distilled water.
4. Allow the slides to air dry.
5. Prepare the silver staining solution as described in **Section 2.3** (*see* **Note 36**).
6. Put three drops (about 20 µl each) of silver staining solution onto each slide and then immediately cover with a coverslip (50–60 mm) and place the slides immediately into a wet, hot chamber at 70–80°C.
7. After 3–4 min, remove the slides from the chamber and monitor for staining intensity under the microscope. (The slides become yellow-brownish; *see* **Note 37**.)
8. Once the staining is sufficiently intense, remove the coverslips under tap water and rinse the slides for 20 s to completely remove the silver staining solution (*see* **Note 38**).
9. Allow the slides to air dry.
10. Mount with Entellan.

4. Notes

1. The protocols described in this chapter, especially the synchrony protocols, are optimized for HeLa cells but are applicable to a variety of immortalized mammalian cell lines. Some further optimization may be needed in some cases, for example, the timing of the thymidine addition and release can be optimized for each cell line. In our experience, even different isolates of HeLa cells require some optimization of the protocol timing ranging from 14 h/8.5 h/14 h to 16 h/11 h/16 h. There are some notable exceptions that we have encountered. Primary cultures of human cells, rodent cell lines, and *M. muntjac* cell lines are difficult to synchronize using the double thymidine approach.
2. Dissolving the caffeine requires warming up the solution. Caffeine does not lose activity as a result of heating (think about hot coffee).
3. It is important that the fixative is made fresh, at least every hour. Both methanol and acetic acid (glacial) should be of high quality. If old bottles of methanol and acetic acid are used, the quality of fixation can be diminished substantially.
4. The acetic acid is noxious. Take care not to breathe it in. It also burns the skin and appropriate care must be taken. Never keep acetic acid anywhere near a fluorescence microscope; in the event of an accidental spill, the acid will strip the coating from expensive microscope filters.
5. Sometimes the cytoplasm stains strongly. In that case, the slides should be cleaned with methanol before being used.
6. The source of the Giemsa solution is important, and Giemsa solution that works well for chromosome banding is not necessarily ideal for the analysis described here. In this protocol, the chromosomes ought to be solid stained with the Giemsa solution and the extent of staining is important in terms of yielding maximal optical resolution.
7. Entellan DPX mounting medium (BDH Laboratory Supplies, Poole, England) can also be used. Be careful not to touch the microscope objectives with the mounting agent before it is completely dried.
8. There are different sources of formic acid at different concentrations. Keep this in mind while preparing the silver nitrate solution (we usually obtain formic acid at 18%).
9. We have used different silver nitrate sources and, surprisingly, high-quality sources such as from Merck give worse results (except when silver staining for electron microscopy).

10. Larger amounts of silver nitrate are not recommended as they tend to precipitate.
11. During the routine culturing of the cells, make sure that the cells do not reach confluence or become starved. Subculture the cells every 3 days at a dilution that allows the cells to grow exponentially at all times. It is also important that the cells do not spend too much time in the presence of the trypsin solution as this will increase the time needed for recovery of growth. Monitor the trypsinization of the cells under the inverted microscope and inactivate the trypsin by the addition of tissue culture medium as soon as the cells detach from the dish.
12. It is important to be sure that cells are plated at the proper density and growing exponentially. Leave the cells at least 24 h to settle down before starting a synchrony.
13. Most protocols suggest washing the dishes twice with PBS or medium. In our hands, the washing step should be skipped as it takes too much time and results in the cooling down of the cells, which causes a cell cycle delay (7). For obtaining a proper synchrony, great care must be taken to avoid the cooling down of the cells at any step. When doing experiments with large numbers of dishes, we take only four dishes out of the incubator each time.
14. For very long treatments, replacement of the medium plus ICRF-193 should be considered (i.e., every 12–24 h).
15. ICRF-193 is taken up rapidly by the cells and its inhibition of topo II is almost instant; the first effects can be observed after only 10 min.
16. The effects of caffeine and uptake by the cells are very fast and, when cells are blocked in G2, its addition can result in the massive entrance of the cells into mitosis within 30 min to 1 h.
17. By removing most of the medium from the dish before doing the mitotic shake-off or scraping the cells from the dish, the final volume of medium that the cells are transferred to the 15 ml tube can be kept to around 2–3 ml. This saves a centrifugation step diminishing the disturbance of cells before fixation. It is important to take care during this step, so as to not detach too many mitotic cells from the dish. These would be lost during the aspiration.
18. Cells can be harvested by mitotic shake off, cell scraping, or trypsin treatment, depending on the experimental requirements. For best chromosome morphology and good-quality pictures, mitotic shake off is preferred, though for statistical analysis scraping must be performed (to include the whole cell population). For the shake off, do it strongly and rapidly but once it is done do not disturb the cells.

19. We usually take the content of a shake off from three 150 mm, almost confluent, dishes into a 15 ml tube, or the content of one 150 mm dish when the cells are being scraped (higher concentrations of cells do not fix well, so use more tubes when necessary).
20. If the volume of cells plus medium plus water is too large (i.e., more than 8 ml), quickly pellet the cells by centrifugation at 800*g* to reduce the volume to 2 ml. Tap the tube to resuspend the cells.
21. We have monitored hypotonic treatments by video microscopy of H2B-GFP HeLa cell lines and no disturbance of the positioning of the chromosomes on the spindle is observed during the 5.5 min incubation. However, longer incubation times will not only disturb the position of chromosomes on the spindle but will also perturb mitotic progression.
22. Mix the cells and fixative gently by inverting the tube twice (NB. The fixative is added rapidly and strongly to the tube and then the mixing of the cells should be done gently).
23. The mixture has far too much water to be a good fixative, and so the water should be removed rapidly by the successive centrifugation steps.
24. Aspirating the acetic acid may cause damage to typically used vacuum pump assemblies. Acid-resistant pumps are available but they are expensive. An alternative is to pipette off the liquid, but care must be taken not to disturb the pellet, which is quite fluffy. Moreover, the initial steps of fixation need to be done rapidly to achieve optimum fixation.
25. Leave just 1–2 mm of liquid above the pellet so that it does not dry out when resuspending. Leaving more liquid will result in an excess of water in the fixative. This is a very important step because it is when the cells are going to receive the true fixation mixture after being "stopped and prefixed" in the previous step.
26. It should be efficient as cells not resuspended at this step will not resuspend in the later steps.
27. The quality of the fixation improves with each wash in fresh Carnoy's solution. At least three washes are required. Fixed material can be stored for many years at –20°C.
28. The fixed material can be dropped onto microscope slides immediately following the last wash (we commonly do it), though the quality of the preparations is typically improved by the overnight storage at 4°C. The fixed material can be stored for years, but changes of fixative (every year) improve preservation.

29. A 200p micropipette is commonly used for convenient drop size. We usually add three drops evenly distributed on the same slide. Slides with frosted edges and labeled in pencil will be resistant to the fixative. If wider spreading of the chromosomes is required, put the slides in methanol, let them half-dry and then when the interference edges appear, drop the cells onto the slide. Help the material to dry out by gently blowing wet air across the slide surface (wet your lips continuously).
30. Quite commonly, a silvery-greenish surface is observed at the top of the Giemsa solution during the staining procedure. That surface results in dirtiness in some regions of the slide. To get rid of it, remove as much as possible from the Giemsa solution surface with a tissue paper (while staining). In addition, place a slide with useless cells on one side of the coplin jar, next to the slides from the experiment. After staining, remove the Giemsa solution by tilting the coplin jar in the direction of the useless slide. This will ensure that the useless slide receives the tainted surface from the solution.
31. The color of the chromosomes will depend largely on the time of staining. Short times (5–6 min) give reddish chromatin while long times (8 min) give blue chromatin. Ideally, stop the staining when the chromosomes are just changing color from pink to violet. This will ensure the best contrast under the microscope.
32. Notes on microscopy. We find that an accurate representation of the stained chromatin (in terms of color, contrast, and resolution) can be achieved using a Zeiss Axioplan II microscope with an alpha Plan Fluar 100X/1.45 n.a. objective, captured by an AxioCam MRC5 camera using Axiovision software.
33. We have observed that the reproducibility of the technique is greatly reduced when a standard hypotonic treatment in 25% HBSS is used.
34. When cells that are blocked in mitosis are required, mitotic arrest induced by high-pressure nitrous oxide treatment is preferable to nocodazole- or colcemid-induced arrest. These latter treatments more rapidly produce hypercondensed chromosomes that are not easily impregnated with silver.
35. We have optimized the length of the SSC treatment specifically for Indian muntjac chromosomes. Other mammalian cell types may require treatments of 15–30 min and this must be determined empirically.
36. Silver staining should be performed on the same day as the $2 \times$ SSC pretreatment.

37. The staining largely stops as the slides cool (monitor the cells really fast in case the slides need to go back to the hot chamber), but there is still some increase in the background precipitation.
38. Rinse the slides over a surface lacking cells, otherwise loss of material is prone to occur.

Acknowledgments

The chromosome preparation technique was originally devised in Prof. Robert T Johnson's laboratory (Mammalian Cell DNA Repair Group, University of Cambridge, U.K.) and has been modified over the years by Drs. Giménez-Abián and Clarke. Silver impregnation was developed for mammalian mitotic chromosomes by Dr. Giménez-Abián, but is based on methods used to stain meiotic grasshopper chromosomes by Rufas et al. (8, 9). Development of the protocols described in this chapter was partly dependent on funding from grants BFU2008-03579/BMC and 2008201165 from the VICT (MCI, Spain) and NIH grant CA099033 to D.J.C.

References

1. Hirano, T., Funahashi, S. I., Uemura, T. and Yanagida, M. (1986) Isolation and characterization of *Schizosaccharomyces pombe* cutmutants that block nuclear division but not cytokinesis. *EMBO J* **5**, 2973–2979.
2. Giménez-Abián, J. F., Clarke, D. J., Mullinger, A. M., Downes, C. S. and Johnson, R. T. (1995) A postprophase topoisomerase II-dependent chromatid core separation step in the formation of metaphase chromosomes. *J Cell Biol* **131**, 7–17.
3. Giménez-Abián, J. F., Clarke, D. J., Devlin, J., Giménez-Abián, M. I., De la Torre, C., Johnson, R. T., Mullinger, A. M. and Downes, C. S. (2000) Premitotic chromosome individualization in mammalian cells depends on topoisomerase II activity. *Chromosoma* **109**, 235–244.
4. Tavormina, P. A., Côme, M. G., Hudson, J. R., Mo, Y. Y., Beck, W. T. and Gorbsky, G. J. (2002) Rapid exchange of mammalian topoisomerase II alpha at kinetochores and chromosome arms in mitosis. *J Cell Biol* **158**, 23–29.
5. Hauf, S., Cole, R. W., LaTerra, S., Zimmer, C., Schnapp, G., Walter, R., Heckel, A., van Meel, J., Rieder, C. L., Peters, J. M. (2003) The small molecule Hesperadin reveals a role for Aurora B in correcting kinetochore-microtubule attachment and in maintaining the spindle assembly checkpoint. *J Cell Biol* **161**, 281–294.
6. Earnshaw, W. C., Halligan, B., Cooke, C. A., Heck, M. M. and Liu, L. F. (1985) Topoisomerase II is a structural component of mitotic chromosome scaffolds. *J Cell Biol* **100**, 1706–1715.
7. Mikhailov, A., Shinohara, M., Rieder, C. L. (2005) The p38-mediated stress-activated checkpoint. A rapid response system for delaying progression through antephase and entry into mitosis. *Cell Cycle* **4**, 57–62.
8. Rufas, J. S., Suja, J. A. and Garcia de la Vega, C. (1987) Chromosome organization in meiosis revealed by light microscopy of silver stained cores. *Genome* **29**, 706–712.
9. Sentis, C., Rodriguez-Campos, I., Stockert, L. and Fernandez-Piqueras, J. (1984) Morphology of the axial structures in the neo-XY sex bivalent of Pycnogaster cucullata (Orthoptera) by silver impregnation. *Chromosoma* **90**, 317–321.

Chapter 16

Top2 SUMO Conjugation in Yeast Cell Lysates

Melissa Baldwin and Jeff Bachant

Abstract

DNA topoisomerase II (Topo II), named Top2 in budding and fission yeast, is a conserved target of the SUMO modification pathway, with SUMO-conjugated forms of Topo II accumulating specifically during mitosis in both yeast and vertebrate cells (Bachant et al., *Mol Cell* 9, 1169–82, 2002; Azuma et al., *J Cell Biol* 163, 477–87, 2003; Dawlaty et al., *Cell* 133, 103–15, 2008). As with many SUMO substrates, the functional significance of this modification is still incompletely understood and, perhaps surprisingly, better characterized in vertebrates than yeasts. It seems likely, however, that continued analysis of yeast Top2 SUMO modification will reveal commonalities with vertebrate cells, leading to a deeper understanding of how sumoylation regulates Topo II function. Toward this end, we describe a protocol for analyzing yeast Top2 SUMO conjugates in vivo.

Key words: Smt3/SUMO, sumoylation, DNA topoisomerase II (Top2), centromere.

1. Introduction

In vertebrates, Topo II accumulates at centromeres and axial chromosome regions during mitosis (4, 5). Although the underlying mechanisms are obscure, recent studies have revealed a role for SUMO modification in controlling Topo II chromosome localization [(3, 6–8); for an overview of SUMO modification, *see* (9)]. Perturbations that interfere with Topo II sumoylation have been reported to either delay/block sister chromatid disjunction and induce pre-anaphase checkpoint arrest (6, 8) or to lead to anaphase bridging, chromosome segregation errors, and the formation of aneuploid cells (3). From these results, it has been suggested that sumoylation may direct Topo II to sites of residual catenation to facilitate chromatid untangling as cells transition into anaphase (6).

D.J. Clarke (ed.), *DNA Topoisomerases*, Methods in Molecular Biology 582,
DOI 10.1007/978-1-60761-340-4_16,

Whether Top2 sumoylation functions in a similar capacity in yeast has not yet been resolved. Top2-SUMO fusion proteins can either exhibit robust cross-linking to centromeric DNA (10) or accumulate in the nucleolus (11), indicating that sumoylation has the potential to regulate Top2 trafficking on yeast chromosomes. Furthermore, *top2-SNM* mutants in which Top2 sumoylation is abolished show altered centromere compaction as kinetochores biorient on the mitotic spindle and are placed under tension (1). These observations are consistent with a functional role for Top2 sumoylation within centromeric chromatin. However, there is currently no evidence that Top2 is preferentially targeted to yeast centromeres during mitosis. In addition, *top2-SNM* mutants do not have an obvious defect in decatenating sister chromatids and segregate chromosomes as proficiently as wild-type cells (T. Warsi and J. Bachant, *unpub. obs.*). The significance of yeast Top2 SUMO modification is therefore currently unclear.

Along these lines, accumulating evidence suggests that Topo II sumoylation may be functioning in other capacities besides serving as a localization tag. In *Xenopus*, blocking SUMO conjugation appears to stabilize the interaction of Topo II with mitotic chromatin (2). In addition, Topo II sumoylation is stimulated in response to Topo II poisons and catalytic inhibitiors (7, 12), potentially acting in a pathway that stimulates turnover of trapped Topo II–DNA reaction intermediates by ubiquitin proteolysis (13). These findings are consistent with the idea that cycles of Topo II SUMO conjugation and removal may play a general role in controlling enzyme turnover on chromatin. Biochemical approaches to examine this or other hypotheses for the function of Top2 SUMO modification necessitate a protocol for reliably detecting Top2 SUMO conjugates. Herein, we describe a simple method that has worked well in our laboratory.

2. Materials

2.1. Analysis of Top2 SUMO Conjugates

Reagents for analyzing Top2 SUMO conjugates are described below and are available upon request. Detailed information concerning plasmid and yeast strain construction is also available but is not included here. To visualize Top2, we either use HA_{3X} epitope-tagged *TOP2* (14) or a Myc_{18X}-tagged *TOP2* constructed in our laboratory. The sensitivity of the Myc_{18X} tag is an advantage for some applications, but it is easier to resolve individual SUMO conjugates on SDS-PAGE gels using Top2-HA_{3X}.

1. pJBN214 (p*CEN ARS URA3 TOP2-HA-kanMX*): Yeast episomal plasmid for expressing *TOP2-HA$_{3X}$*. The base vector is pRS416 [p*CEN ARS URA3*; (15)].

2. pJBN227 (p*CEN ARS URA3 top2-SNM-HA-kanMX*): Yeast episomal plasmid for expressing *top2-SNM-HA$_{3X}$*. Base vector, pRS416.
3. JBY1083 (*MATa his3-11,15-LacI-GFP-HIS3 leu2-3,112 trp1-1-LacO-TRP1-LEU2 ura3-1 ade2-1 can1-100 TOP2-HA$_{3X}$-kanMX4*): This is a W303-derived yeast strain (CRY1 background) in which the endogenous *TOP2* gene has been replaced by a *TOP2-HA-kanMX* cassette. The strain also contains two sets of Lac operator arrays targeted to the *TRP1* locus, as well as a Lac repressor-GFP fusion protein for visualizing chromosome IV by GFP tagging (16).
4. JBY1087 (*MATa his3-11,15-LacI-GFP-HIS3 leu2-3,112 trp1-1-LacO-TRP1-LEU2 ura3-1 ade2-1 can1-100 top2-SNM-HA$_{3X}$-kanMX4*): This strain is congenic with JBY1083 but *TOP2* has been replaced with *top2-SNM-HA-kanMX*.
5. pTW009 (p*CEN ARS URA3 TOP2-Myc-kanMX*): Yeast episomal plasmid for expressing *TOP2-Myc$_{18X}$*. Base vector, pRS416.
6. pTW010 (p*CEN ARS URA3 top2-SNM-Myc-kanMX*): Yeast episomal plasmid for expressing *top2-SNM-Myc$_{18X}$*. Base vector, pRS416.
7. JBY1403 (*MATa his3-11,15 leu2-3,112 trp1-1 ura3-1 ade2-1 can1-100 TOP2-Myc$_{18X}$-kanMX4*): W303-derived (CRY1) stain in which *TOP2* has been replaced with a *TOP2-Myc-kanMX* cassette.
8. TWY126 (*MATa his3-11,15 leu2-3,112 trp1-1 ura3-1 ade2-1 can1-100 top2-SNM-Myc$_{18X}$-kanMX4*): Congenic with JBY1403 but *TOP2* is replaced with *top2-SNM-Myc-kanMX*.

2.2. Cell Culture and Lysis

1. YPD: 2% glucose, 1% yeast extract, 2% bacto-peptone. Autoclave and store at room temperature.
2. Nocodazole (Sigma): For a 1000X stock solution, dissolve 15 mg/ml in DMSO and store in aliquots at –20°C.
3. Protease inhibitors (100X stock solutions):
   (a) Cocktail: Leupeptin (1 mg/ml), aprotinin (2 mg/ml), benzamidine (1.6 mg/ml); prepare in sterile water and store in aliquots at –20°C.
   (b) Phenylmethylsulfonyl fluoride (PMSF): 10 mg/ml in 95% ethanol and store in aliquots at –20°C.
   (c) Pepstatin A: 0.1 mg/ml in 95% ethanol and store in aliquots at –20°C.
   (d) *N*-Ethylmalemide (NEM): 10 mM in ethanol, make fresh.
4. 20% (v/v) trichloroacetic acid (TCA): Dilute in water and store at 4°C.

5. Acid-washed glass beads: 425–600 μm (Sigma).
6. 1 M Tris base: Store at 4°C (*see* **Note 1**).
7. HEPES solution: 25 mM HEPES, pH 7.5, 100 mM KCl, 2 mM EDTA, and 10% glycerol. Store at 4°C.
8. 20% (w/v) sodium dodecyl sulfate (SDS): Dissolve in water and store at room temperature.
9. 6X protein loading buffer: 35% 1 M Tris, pH 6.8, 2% SDS, 0.6 M DTT, 60% glycerol, and 1.5 mg/ml bromophenol blue. Store in aliquots at –20°C.

2.3. SDS-Polyacrylamide Gel Electrophoresis (SDS-PAGE)

1. Polyacrylamide (Biorad): 30% acrylamide/bis solution 37.5:1.
2. 1.5 M Tris–HCl, pH 8.8: Store at room temperature.
3. 1 M Tris–HCl, pH 6.8: Store at room temperature.
4. 10% (w/v) ammonium persulfate (APS): Dissolve in water and store in aliquots at –20°C.
5. *N*,*N*,*N*,*N*'-Tetramethyl-ethylenediamine (TEMED): Store at 4°C.
6. 20% (w/v) sodium dodecyl sulfate (SDS): Dissolve in water and store at room temperature.
7. Laemmli running buffer (10X): 250 mM Tris, pH 8.3, 1.92 M glycine; add 5 ml of 20% SDS per liter when preparing 1X.
8. Prestained molecular weight markers (Biorad): Precision Plus All Blue Protein Standards.

2.4. Western Blot for SUMO Modified Top2

1. Transfer buffer (10X): 250 mM Tris–HCl, 1.92 M glycine, pH 8.3. Add methanol to 20% (v/v) when preparing 1X.
2. Nitrocellulose membrane: 0.45 μm (Fisher).
3. Whatman chromatography paper: 0.34 mm (Fisher).
4. Tris-buffered saline with Tween (TBST, 10X): 250 mM Tris–HCl pH 7.5, 1.37 M NaCl, add 0.5 ml Tween 20 per liter when preparing 1X.
5. Blocking buffer: 3% nonfat dry milk in TBST.
6. Incubation buffer: TBST supplemented with 0.03% (m/v) bovine serum albumin (BSA).
7. Primary antibodies:
   (a) α-HA antibody: HA.11 monoclonal antibody (Covance), 2–3 mg/ml ascites, use 1:1000.
   (b) α-Myc antibody: 9E10 monoclonal antibody (Covance), 3–5 mg/ml ascites, use 1:1000.

8. Secondary antibody: Peroxidase-conjugated AffiniPure goat anti-mouse IgG (Jackson ImmunoResearch): reconstitute to 0.8 mg/ml in sterile water, use 1:25,000.
9. Enhanced chemiluminescent (ECL) reagents: Western Lightning Chemiluminescence Reagent Plus (Perkin Elmer).

3. Methods

Top2 is SUMO modified at three acceptor lysines within the non-catalytic C-terminus of the enzyme (K1220, K1246, K1277), resulting in higher molecular weight species that can be separated by SDS-PAGE (1, 10). As with most other SUMO substrates, the investigator faces two challenges when analyzing Top2 SUMO conjugates. First, even during mitosis only ~10% of Top2 is found in a SUMO-modified form at any given time (**Fig. 16.1**).

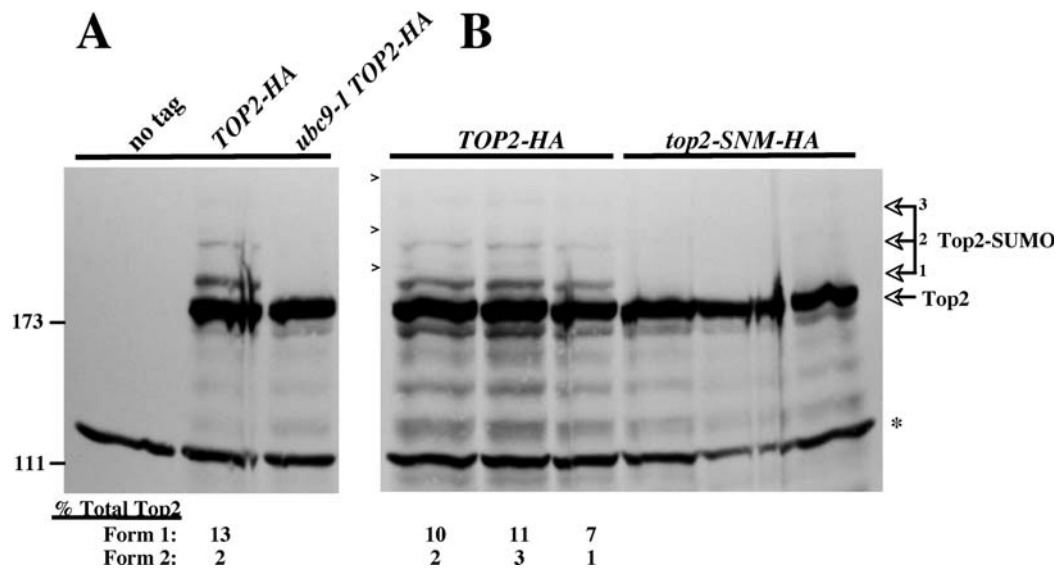

Fig. 16.1. **Top2 SUMO conjugates**. (**A**) Yeast strains were transformed with pRS416 (JBY1041; no tag) or pJBN214 (JBY1042; *TOP2-HA*; and JBY1043; *ubc9-1 TOP2-HA*). Transformants were cultured at 25°C, and then shifted to 35°C in media containing 15 μg/ml nocodazole for 4 h to inactivate Ubc9-1 (defective for E2 SUMO conjugating enzyme activity) and arrest cells in mitosis. (**B**) Three cultures of JBY1083 (*TOP2-HA*) and three cultures of JBY1087 (*top2-SNM-HA*) were treated with 15 μg/ml nocodazole at 30°C for 4 h. For **A** and **B**, protein extracts were analyzed by α-HA immunoblotting to detect Top2 SUMO conjugates. *Arrows*: Unmodified Top2-HA and three SUMO-conjugated Top2 species. These three forms are likely to represent a single SUMO moiety added in different combinations to each of the three SUMO acceptor lysines, but this has not been examined directly. Carets on the left side of **B** indicate the position of three additional species that are variably observed in different experimental preparations. The percentage of Top2 in the two indicated SUMO forms (quantified using Image J) is indicated below the gel panels. *Asterisk*: An α-HA cross-reacting band useful for evaluating protein load. Numbers left of **A**, molecular weight markers (kDa).

Second, upon cell lysis, these conjugates are quite labile. In the following method, the sensitivity challenge is addressed by using polyepitope-tagged forms of Top2. The stability challenge is addressed by performing cell lysis in trichloroacetic acid to minimize conjugate proteolysis, as well as through the use of *N*-ethylmaleimide, a sulfhydryl alkylating agent that inactivates cysteine-directed proteases by covalently modifying cysteine residues on proteins. NEM prevents cleavage of SUMO conjugates [for example, *see* (7)] and is included throughout the protein preparation procedure. The following protocol is an amalgamation of a TCA cell lysis method described previously (17) and a previously described method for analyzing yeast SUMO conjugates (18).

3.1. Cell Culture and Protein Preparation

1. Grow cultures of *Saccharomyces cerevisiae* with epitope-tagged *TOP2* and appropriate controls in YPD at 30°C overnight (~12–15 h) with shaking, aiming for a late log phase culture with an OD_{600} of approximately 1–2. If *TOP2* is being expressed from an episomal yeast plasmid (for example, pJBN214), it will be necessary to maintain selection for the plasmid in appropriate synthetic complete media (19).
2. Dilute the cultures to an OD_{600} of approximately 0.8, and culture with shaking in YPD supplemented with nocodazole (15 μg/ml) for 3–4 h at 30°C. A 10 ml culture should be sufficient for detecting Top2 SUMO conjugates (*see* **Note 2**).
3. Verify the mitotic arrest by microscopy. Typically, ~90% of the cells in the culture should be arrested as large budded cells. When arrested, pellet cells by centrifugation at 2000*g* for 3 min and pour off the media supernatant (*see* **Note 3**).
4. Rinse the cells into a 2.0 ml screw-capped tube with 1 ml of distilled water, pellet the cells at 2000*g*, and aspirate the water from the pellet. Keep the tubes on ice from this point forward.
5. Resuspend the pellet in 300 μl of 20% TCA supplemented with protease inhibitors (*see* **Section** 2.2, step 3a–d). Add an equal volume of acid-washed glass beads. Disrupt the cells for 4 min in a BioSpec bead beater. Immediately return the tubes to ice when finished (*see* **Note 4**).
6. Recover the TCA pellet by puncturing the bottom of the lysis tube with an 18-gauge needle and transferring the contents into a clean tube by centrifugation for 5 min at 3000*g* at 4°C, as follows: Seat a new 2.0 ml screw-capped tube (a capture tube) at the bottom of a 15 ml conical tube, set the punctured lysis tube on top of the capture tube, and then place the entire assemblage into the centrifuge rotor.

7. Aspirate off the liquid and resuspend the TCA pellet at the bottom of the capture tube in 200 µl of a 1:1 mixture of 1 M Tris base and HEPES solution supplemented with protease inhibitors as described above (*see* **Note 5**).
8. Remove an aliquot for protein quantification if desired (Bio-Rad Protein Assay Dye). To the remaining lysate, add 100 µl of 20% SDS and 60 µl of 6X protein-loading buffer. If the resulting solution turns yellow, add 1 M Tris base in 20 µl aliquots until the solution has been neutralized and turns blue.

3.2. SDS-Polyacrylamide Gel Electrophoresis (SDS-PAGE)

1. These instructions are for the use of a GIBCO V16-2 electrophoresis system. They can be adapted to other formats, including minigels. The glass plates for the gels should be cleaned with glassware detergent (PEX) and rinsed with distilled water, and then wiped with ethanol before use.
2. Prepare a 1.5-mm thick, 6% gel. For this, we prepare a separating gel mixture using 6 ml of the 30% acrylamide/bis solution, 7.5 ml of 1.5 M Tris, pH 8.8, 300 µl of 10% APS, 300 µl of 20% SDS, 30 µl TEMED, and enough distilled water to bring the volume to 30 ml. Pour the gel, leaving space for a stacking gel, and overlay with water. Allow the gel to polymerize for about 30 min (*see* **Note 6**).
3. Pour off the water and prepare the stacking gel by mixing 3.4 ml of the 30% acrylamide/bis solution, 2.5 ml of 1 M Tris–HCl, pH 6.8, 200 µl of 10% APS, 200 µl of 20% SDS, 20 µl TEMED, and enough distilled water to bring the volume to 20 ml. Fill to the top of the glass plates and insert the comb. Allow the gel to polymerize for about 30 min.
4. Prepare the running buffer by diluting 200 ml of the 10X running buffer with 1800 ml of water and adding 10 ml of 20% SDS; mix thoroughly.
5. Once the stacking gel has polymerized, carefully remove the comb and clamp the gel onto the apparatus. Add the running buffer to the upper and lower chambers of the gel unit and use a 60 cc syringe with a bent needle filled with running buffer to rinse the bubbles out from in between the glass plates at the bottom of the gel.
6. Before electrophoresis, heat the samples at 98°C for 5 min and clarify in a microfuge at a high-speed setting (~14,000*g*) for 3 min. Load 75–150 µg of each sample in a well. In one well, load 20 µl of the prestained molecular weight markers.
7. Attach the cover of the apparatus and connect to a power supply. The gel can be run either overnight at 50 V (approximately 18 h) or, if a faster run is desired, for 6–8 h at 50 mA.

For the best separation of the SUMO-conjugated Top2 forms, the gel should be run for 1–2 h after the dye front has run completely off the gel (*see* **Note 7**).

3.3. Transfer to Nitrocellulose and Western Blot for SUMO-Modified Top2

1. Once the gel has finished running, transfer the proteins to a nitrocellulose membrane. These directions are for the use of a Biorad TRANS-BLOT CELL transfer tank system. Prepare 3 l of transfer buffer by diluting 300 ml of 10X transfer buffer and 600 ml of methanol into 2100 ml of water.
2. Disassemble the gel apparatus and glass plates. Remove the stacking gel (optional) and place the separating gel in a tray partially filled with transfer buffer (*see* **Note 8**).
3. Assemble the following onto the transfer cassette. In between layers, gently roll a glass pipet over the surface to remove any air bubbles trapped between layers. Wear gloves to protect the nitrocellulose sheet.
   (a) One wet transfer sponge.
   (b) Two sheets of Whatman paper previously wetted in transfer buffer.
   (c) Carefully transfer the gel out of the tray, sliding either the wetted Whatman paper or the nitrocellulose sheet under the gel as a support. We typically flip the gel to preserve the lane orientation on the nitrocellulose sheet after transfer.
   (d) Two sheets of Whatman paper previously wetted in transfer buffer.
   (e) The second wet transfer sponge.
4. Close the transfer cassette and place it into the transfer tank such that the nitrocellulose membrane is between the gel and the anode. The cassette must be placed into the tank in this orientation or the proteins will run from the gel into the buffer rather than being transferred to the nitrocellulose. Fill the tank with transfer buffer.
5. Place the cooling coil and a magnetic stir-bar into the tank, turn on the water supply for the cooling coil, and place the lid onto the tank.
6. Connect the lid to the power supply. Transfer is accomplished at 50 V (should be ~1 A) for 4 h.
7. Once the transfer is complete, remove the cassette from the tank and disassemble. Remove and discard the sheets of Whatman paper and the gel. The molecular weight markers should be clearly visible on the membrane.
8. Incubate the nitrocellulose in blocking buffer for 1 h at room temperature on a rocking platform, or if desired the membrane can be placed in blocking buffer at 4°C overnight.

9. Rinse the membrane in TBST, and then incubate in 20 ml of incubation buffer with a 1:1000 dilution of the primary antibody in TBST/0.03% BSA for 1 h at room temperature on a rocking platform.
10. Wash the membrane three times for 10 min each with TBST.
11. Incubate in 20 ml of incubation buffer with a 1:25,000 dilution of the secondary antibody in TBST/0.03% BSA for 1 h at room temperature on a rocking platform.
12. Wash the membrane three times for 10 min each with TBST.
13. Once the final wash is removed from the blot, 5-ml portions of the ECL reagents are mixed together and added to the blot. Slowly rotate the blot by hand for 1 min to ensure even coverage.
14. Remove the blot from the ECL reagents, blot excess reagent from the bottom edge of the membrane onto a paper towel, and then place the membrane between two sheets of clear overhead projector plastic that have been cut to the size of the X-ray film cassette. Carefully smooth excess reagent and air bubbles out from between the sheets.
15. Place the sheets in an X-ray film cassette and move to a dark room. Expose sheets of film for a suitable period of time, typically 15 s to 1 min, and develop.

4. Notes

1. Unless stated otherwise, all solutions should be prepared in water. All cell lysate working solutions should be kept cold.
2. In our experience, a more efficient arrest in nocodazole is achieved when culturing in YPD as opposed to the selective synthetic complete media. It is also possible to visualize conjugates in mid to late log phase cultures of yeast that have not been synchronized.
3. Once pelleted, arrested cells can be stored at –80°C prior to lysate preparation. Successful visualization of Top2 SUMO conjugates has been achieved following freezing for up to 1 week. Longer freezing periods have not been tried.
4. Fresh NEM appears to be important in preventing Top2 desumoylation during resuspension of the TCA pellet. A small aliquot should be prepared for each experiment immediately proceeding cell disruption.

5. At this point you will have a protein slurry that will not go completely back into solution. Just make sure it is thoroughly mixed before removing a sample for protein quantification. With appropriate scaling up, these lysates can also be used for the purification of SUMO conjugates via affinity column chromatography procedures as described in (1, 18).
6. We visualize the conjugates as higher molecular weight forms using a standard acrylamide:bis-acrylamide ratio of 37.5:1.
7. Top2 and Top2 SUMO conjugates are visualized between ~175 and 275 kDa (175 kDa for unmodified Top2, with three conjugated variants appearing above it, **Fig. 16.1**). The best separation is achieved when the gel is allowed to run past the point where the dye front has run off the gel due to the large size of these proteins.
8. Removing the gel from the glass plate requires utmost care, as it sometimes sticks to the plate in spots and can tear when rolling off into the transfer buffer.

Acknowledgments

The authors would like to thank members of the Bachant laboratory for helping to develop this method into a reliable protocol. Tariq Warsi constructed reagents for visualizing Top2-myc. Dr. Andrew Murray initially provided reagents for generating Top2-HA_{3X} yeast strains. This work was supported by an NIH grant (R01 GM-66190) to J.B.

References

1. Bachant, J., Alcasabas, A., Blat, Y., Kleckner, N. and Elledge, S. J. (2002) The SUMO-1 isopeptidase Smt4 is linked to centromeric cohesion through SUMO-1 modification of DNA topoisomerase II. *Mol Cell* **9**, 1169–82.
2. Azuma, Y., Arnaoutov, A. and Dasso, M. (2003) SUMO-2/3 regulates topoisomerase II in mitosis. *J Cell Biol* **163**, 477–87.
3. Dawlaty, M. M., Malureanu, L., Jeganathan, K. B., Kao, E., Sustmann, C., Tahk, S., Shuai, K., Grosschedl, R. and van Deursen, J. M. (2008) Resolution of sister centromeres requires RanBP2-mediated SUMOylation of topoisomerase IIalpha. *Cell* **133**, 103–15.
4. Rattner, J. B., Hendzel, M. J., Furbee, C. S., Muller, M. T. and Bazett-Jones, D. P. (1996) Topoisomerase II alpha is associated with the mammalian centromere in a cell cycle- and species-specific manner and is required for proper centromere/kinetochore structure. *J Cell Biol* **134**, 1097–107.
5. Sumner, A. T. (1996) The distribution of topoisomerase II on mammalian chromosomes. *Chromosome Res* **4**, 5–14.
6. Diaz-Martinez, L. A., Gimenez-Abian, J. F., Azuma, Y., Guacci, V., Gimenez-Martin, G., Lanier, L. M. and Clarke, D. J. (2006) PIASgamma is required for faithful chromosome segregation in human cells. *PLoS ONE* **1**, e53.
7. Agostinho, M., Santos, V., Ferreira, F., Costa, R., Cardoso, J., Pinheiro, I., Rino, J., Jaffray, E., Hay, R. T. and Ferreira, J. (2008) Conjugation of human topoisomerase 2 alpha with small ubiquitin-like modifiers 2/3 in

response to topoisomerase inhibitors: cell cycle stage and chromosome domain specificity. *Cancer Res* **68**, 2409–18.

8. Azuma, Y., Arnaoutov, A., Anan, T. and Dasso, M. (2005) PIASy mediates SUMO-2 conjugation of Topoisomerase-II on mitotic chromosomes. *Embo J* **24**, 2172–82.
9. Johnson, E. S. (2004) Protein modification by SUMO. *Annu Rev Biochem* **73**, 355–82.
10. Takahashi, Y., Yong-Gonzalez, V., Kikuchi, Y. and Strunnikov, A. (2006) SIZ1/SIZ2 control of chromosome transmission fidelity is mediated by the sumoylation of topoisomerase II. *Genetics* **172**, 783–94.
11. Takahashi, Y. and Strunnikov, A. (2008) In vivo modeling of polysumoylation uncovers targeting of topoisomerase II to the nucleolus via optimal level of SUMO modification. *Chromosoma* **117**, 189–98.
12. Mao, Y., Desai, S. D. and Liu, L. F. (2000) SUMO-1 conjugation to human DNA topoisomerase II isozymes. *J Biol Chem* **275**, 26066–73.
13. Zhang, A., Lyu, Y. L., Lin, C. P., Zhou, N., Azarova, A. M., Wood, L. M. and Liu, L. F. (2006) A protease pathway for the repair of topoisomerase II-DNA covalent complexes. *J Biol Chem* **281**, 35997–6003.
14. Bhalla, N., Biggins, S. and Murray, A. W. (2002) Mutation of *YCS4*, a budding yeast condensin subunit, affects mitotic and nonmitotic chromosome behaviour. *Mol Biol Cell* **13**, 632–45.
15. Sikorski, R. S. and Hieter, P. (1989) A system of shuttle vectors and yeast host strains designed for efficient manipulation of DNA in *Saccharomyces cerevisiae*. *Genetics* **122**, 19–27.
16. Robinett, C. C., Straight, A., Li, G., Willhelm, C., Sudlow, G., Murray, A. and Belmont, A. S. (1996) In vivo localization of DNA sequences and visualization of large-scale chromatin organization using lac operator/repressor recognition. *J Cell Biol* **135**, 1685–700.
17. Foiani, M., Marini, F., Gamba, D., Lucchini, G. and Plevani, P. (1994) The B subunit of the DNA polymerase alpha-primase complex in *Saccharomyces cerevisiae* executes an essential function at the initial stage of DNA replication. *Mol Cell Biol* **14**, 923–33.
18. Johnson, E. S. and Blobel, G. (1999) Cell cycle-regulated attachment of the ubiquitin-related protein SUMO to the yeast septins. *J Cell Biol* **147**, 981–94.
19. Burke, D., Dawson, D. and Stearns, T. (2000) *Methods in Yeast Genetics*, Cold Spring Harbor Laboratory Press, Cold Spring Harbor, NY.

Chapter 17

Analysis of SUMOylation of Topoisomerase IIα with *Xenopus* Egg Extracts

Yoshiaki Azuma

Abstract

Posttranslational protein modification by the *S*mall *U*biquitin-like *MO*difiers (SUMO) is involved in many cellular functions including organization of nuclear structures and chromatin, transcriptional regulation, and nucleo-cytoplasmic transport. Both genetic and biochemical studies indicate that the SUMO modification pathway plays an important role in proper cell cycle control, especially in the normal progression of mitosis. DNA topoisomerase II has been shown to be modified by SUMO in budding yeast as well as in vertebrates. We have shown by biochemical analysis using the *Xenopus* egg extract (XEE) cell-free assay system that DNA topoisomerase IIα (Topo IIα) is modified by SUMO-2/3 on mitotic chromosomes in the early stages of mitosis. Inhibition of mitotic SUMOylation in the XEE assay system causes aberrant sister chromatid separation in anaphase and alters Topo IIα association with chromosomes.

Key words: Topoisomerase II, SUMO, *Xenopus*, egg extracts, chromosomes.

1. Introduction

Posttranslational modification by SUMO, *S*mall *U*biquitin-like *MO*difier, was discovered 10 years ago (1, 2). Since then it has become clear that SUMOylation is a major protein modification system with a broad impact on cellular functions. SUMO proteins and the mechanism of SUMOylation are highly conserved in eukaryotes. In vertebrates, there are multiple SUMO isoforms. SUMO-2 and SUMO-3 are closely related in their primary sequence (95% identical), whereas SUMO-1 is around 45% identical to either of the other two isoforms. All isoforms are around 50% identical to the SUMO homologue, Smt3, in budding yeast, which has a single SUMO gene in its genome (3). The

D.J. Clarke (ed.), *DNA Topoisomerases*, Methods in Molecular Biology 582,
DOI 10.1007/978-1-60761-340-4_17,

biochemistry of modification by SUMO, SUMOylation, is similar to ubiquitinylation. The conjugation process requires three sequential enzymes, E1, E2, and E3, and conjugation can be reversed by specific protease activity (1–3). Because of highly active deconjugation enzymes, SUMO proteases, studying SUMOylation under physiological conditions has been one of the challenging topics in this field (4, 5).

DNA topoisomerase II (Topo II) is an essential enzyme, required for cell proliferation, which regulates chromosomal structure (6). Genetic studies indicate that Topo II has an essential function in both chromosome condensation and segregation during mitosis (7, 8). This genetic evidence was further confirmed in the *Xenopus* egg extract (XEE) cell-free assay system, where only the α form of topoisomerase II (Topo IIα) is present (9). Immunodepletion of Topo IIα from XEEs completely inhibits the assembly of condensed chromosomes either from sperm chromatin (9) or from chicken erythrocyte nuclei (10). Inhibition of Topo IIα in XEEs with a specific inhibitor prevents remodeling and condensation of chromosomes derived from sperm nuclei and also prevents the proper function of the condensin complex, which participates in the assembly of condensed chromosomes (9, 11). Moreover, inhibition of Topo II in XEE using VP-16 at the metaphase–anaphase transition compromises sister chromatid separation (12). These findings indicate the importance of Topo IIα to various process of mitosis and emphasize the benefits of XEEs in the study of Topo IIα.

Findings that Topo II is modified by SUMO in budding yeast revealed a novel mechanism of Topo II regulation on mitotic chromosomes (13, 14). Similarly, we have identified Topo IIα as major SUMO-modified protein on mitotic chromosomes in XEE (15). SUMOylation of Topo II can be observed in mammalian cells when they are treated with Topo II inhibitors (16), and Topo II inhibitors enhance SUMO-2/3 modification of Topo IIα in mitotic mammalian cells (17).

Utilizing XEEs, we have demonstrated cell cycle-dependent SUMOylation of Topo IIα. Interestingly, SUMOylation of Topo IIα utilizes exclusively SUMO-2/3 under physiological conditions not SUMO-1. SUMO-1 modification of Topo IIα, however, can be observed after addition of exogenous SUMO-1 into XEE (15). This result suggests that there is a precise mechanism for selection of SUMO paralogues under physiological conditions and for temporal regulation during the cell cycle. XEEs are an excellent model system for studying SUMOylation because of their highly synchronized and manipulable cell cycle progression and the simplicity of biochemical fractionation of this material (18, 19). This article includes detailed protocols for the production of mitotic chromosomes in XEE and for the analysis of Topo II SUMOylation in this context.

2. Materials

2.1. Preparation of CSF Extracts from Xenopus Eggs

1. MMR: 100 mM NaCl, 2 mM KCl, 1 mM $MgSO_4$, 2 mM $CaCl_2$, 0.1 mM EDTA, 5 mM HEPES, pH 7.8. (Prepare 10X concentrated and store at room temperature.)
2. Pregnant mare serum gonadotropin (PMSG, EMD/Calbiochem): Dissolve in water at 200 units/ml, store at –20°C.
3. Human chorionic gonadotropin (HCG, Sigma-Aldrich): Dissolve in water at 1000 units/ml, store at 4°C.
4. Dejellying solution: 2% w/v cysteine, free base (EMD/Calbiochem), dissolve in water, and adjust to pH 7.8 with NaOH.
5. CSF-XB: 100 mM KCl, 0.1 mM $CaCl_2$, 2 mM $MgCl_2$, 5 mM EGTA, 50 mM sucrose, and 10 mM HEPES, adjust to pH 7.7 with KOH.
6. Protease inhibitor (LPC) solution: Dissolve a mixture of leupeptin, pepstatin, and chymostatin (all from EMD/Calbiochem) at a final concentration of 20 mg/ml each in dimethyl sulfoxide (DMSO, Sigma-Aldrich). Store at –20°C in aliquots of 30 µl/tube.
7. Cytochalasin B (CyB) solution: Dissolve cytochalasin B (EMD/Calbiochem) at 10 mg/ml in DMSO. Store at –20°C in aliquots of 30 µl/tube.
8. 50X Energy mixture: Dissolve in sterile water 375 mM phosphocreatine (Sigma-Aldrich), 50 mM ATP (Mg salt, Sigma-Aldrich), and 5 mM EGTA, pH 7.7. Adjust pH to ~7.0 and store at –80°C in aliquots of 100 µl/tube.
9. Calcium solution: 6 mM $CaCl_2$, 50 mM KCl, and 2 mM $MgCl_2$.

2.2. Preparation of Demembraned Sperm Nuclei

1. Buffer T: 15 mM PIPES, 15 mM NaCl, 80 mM KCl, 5 mM EDTA, 7 mM $MgCl_2$, and 200 mM sucrose. Adjust pH to 7.4 with KOH.
2. Demembrane buffer: Buffer-T containing 0.05% lysophosphatidyl choline (Sigma-Aldrich) and 20 mM maltose (Sigma-Aldrich).
3. Washing buffer: Buffer-T containing 3% BSA.
4. Haemocytometer.

2.3. Chromosome Assembly and Isolation

1. $CaCl_2$ solution: 6 mM $CaCl_2$, 50 mM KCl, and 2 mM $MgCl_2$.
2. Dilution buffer: 0.5X CSF-XB containing 18 mM β-glycerophosphate (Sigma-Aldrich), 0.25% (v/v) triton-X100

(Sigma-Aldrich), 1/2000 volume of LPC solution, 1/2000 volume of CyB solution, 0.4 μg/ml nocodazole (EMD/Calbiochem), and 0.2 μM okadaic acid.

3. Glycerol cushion: 0.5X CSF-XB containing 18 mM β-glycerophosphate (Sigma-Aldrich), 0.1% (v/v) triton-X100 (Sigma-Aldrich), and 30% (v/v) glycerol.
4. 2 ml conical bottomed microcentrifuge tubes (Corning).
5. Fix solution: 0.3 ml of 37% formaldehyde, 0.1 ml of 10X MMR, 0.6 ml 70% glycerol, 1 μg/ml Hoechst 33342 (EMD/Calbiochem).
6. Standard SDS-PAGE sample buffer (3X): 187 mM Tris–HCl, pH 6.8, 6% (w/v) SDS, 30% (v/v) glycerol, 0.01 mg bromophenol blue, 10% (v/v) 2-mercaptoethanol. A stock solution should be prepared without 2-mercaptoethanol and stored at room temperature.

2.4. Analysis of SUMOylation of Topoisomerase II

1. Gradient SDS-PAGE gel: 8–16% Tris–glycine gel (Invitrogen).
2. Standard SDS-PAGE running buffer (10X): 250 mM Tris, 1.92 M glycine, 1% (w/v) SDS. Store at room temperature.
3. PVDF membrane: Immobilon-P transfer membrane (Millipore).
4. Transfer buffer (20X): 1 M Tris, 750 mM glycine, 0.4% (w/v) SDS. Store at room temperature. Prepare 1X solution with 7.5% (v/v) methanol.
5. PBS-T: PBS containing 0.1% (v/v) Tween 20 (Sigma-Aldrich).
6. Blocking solution: 5% w/v skimmed milk powder in PBS-T.
7. Anti-Topo IIα/β monoclonal antibody (clone AK5).
8. Stripping buffer: 62.5 mM Tris–HCl, pH 6.8, 1% SDS.

3. Methods

3.1. Preparation of CSF Extracts from Xenopus Eggs

There are several established protocols for obtaining frog egg extracts that retain mitotic activity. The method described here preserves meiosis II arrest through preservation of *C*yto *S*tatic *F*actor (CSF) (18, 19). Extracts prepared in this manner are called CSF XEEs.

1. To induce oocyte maturation, the female frogs are primed by injecting 100 units of PMSG (0.5 ml/frog) at least 4 days before eggs are required. Primed frogs should be used within 2 weeks, or the quality of eggs will often become insufficient

for use. The day before the egg collection, each female should be injected with 500 units of HCG (0.5 ml/frog) and placed in an individual bucket that contains 2 l of MMR.

2. Fifteen hours after the HCG injection, eggs are recovered from each bucket into individual glass beakers, then washed once with MMR. Discard as much MMR as possible by decantation, then add dejellying solution to dissolve the jelly coat of the eggs. The completion of dejellying can be monitored by observing the disappearance of the space between the eggs. Discard the dejellying solution and briefly rinse the eggs once more with dejellying solution (*see* **Note 1**).
3. Quickly rinse the eggs by decanting twice with about 200 ml of MMR. During this rinse step, damaged and poor-quality eggs can be removed using a Pasteur pipet. Exchange the MMR for CSF-XB and carefully remove poor-quality eggs. Eggs that show clear separation of animal (dark colored) and vegetal (light colored) hemispheres of approximately equal size are usually of sufficient quality for XEE preparations. Enlarged, small, and abnormal colored eggs should be removed. Rinse the eggs by decanting three times more with CSF-XB (*see* **Note 2**).
4. Prepare a 14-ml round-bottom polypropylene tube with 1.5 ml of CSF-XB containing 7.5 µl each of LPC and CyB solution. Transfer eggs using a large bore transfer pipette. After removing excess buffer, centrifuge the tube at 170*g* for 30 s to pack the eggs. Again remove excess buffer and leave just enough buffer to protect the eggs from contact with air (*see* **Note 3**).
5. Centrifuge the packed eggs at 10,000*g* for 15 min at 16°C in a swinging bucket rotor (Beckman/Coulter JS13.1 or Sorval HB-6). After centrifugation, lysed eggs will be separated into three layers: lipids (bright yellow), crude cytoplasm (light brown or golden), and yolk (dark brown or gray) from top to bottom. There will be a thin layer of mitochondrial material between the cytoplasm and yolk, which is cloudier than the cytoplasm (*see* **Fig. 17.1**).
6. Extract the crude cytoplasmic fraction by withdrawing it from the side of the tube with a 16-G needle attached to a syringe. Withdrawing the cytoplasm too rapidly will cause contamination by either the lipid or the mitochondrial fractions, and those contaminations may compromise the quality of the XEE (*see* **Fig. 17.1**) (*see* **Note 4**).
7. Place the CSF extracts on ice. Add 1/2000 volume each of LPC and CyB solution to the extracts and 1/50 volume of energy mixture. Gently mix the extracts by taping the tube and keep it on ice.

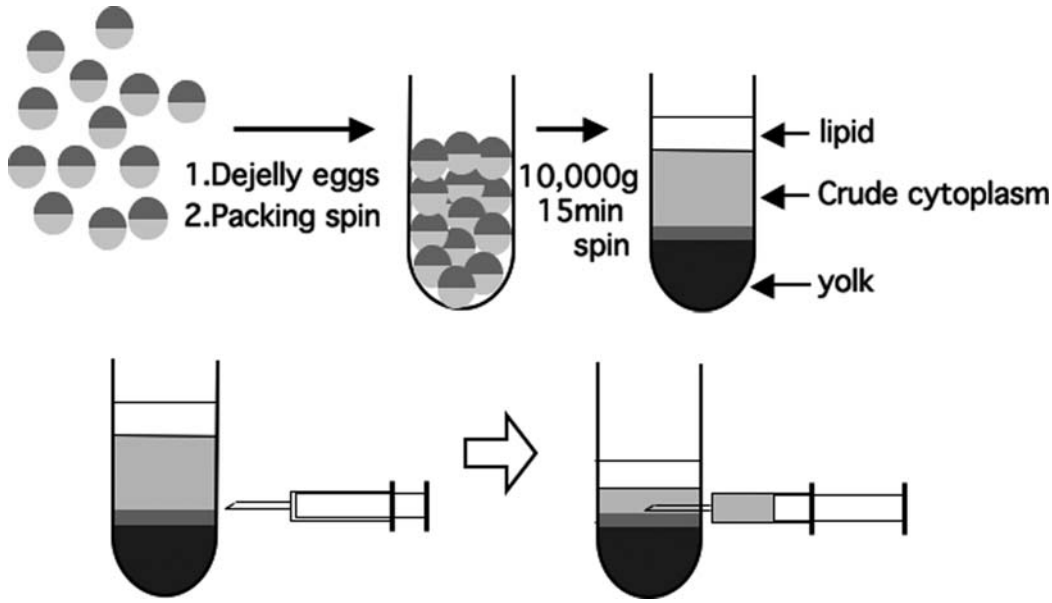

Fig. 17.1. ***Xenopus* egg extract (XEE) preparation**.

8. To obtain interphase extracts, take an aliquot of the CSF extract, and warm it up to room temperature. Add 1/10 volume of calcium solution to the CSF extracts and mix it rapidly but gently without forming bubbles. Incubate the extracts for 5–10 min at room temperature to complete the induction of interphase (*see* **Note 5**).

3.2. Preparation of Demembraned Sperm Nuclei

This protocol is designed to isolate a large number of sperm nuclei from more than six male frogs at one time. For small-scale preparation, reduce the amount of buffers accordingly. All the centrifugation should be done with a swinging bucket rotor at room temperature.

1. Anesthetize male frogs by injection of tricaine methanesulfonate (100 mg/kg) and kill by double pithing.
2. Dissect to obtain the testes, which are located behind the intestinal tract. Carefully remove the connective tissue and blood vessels around the testes (*see* **Note 6**).
3. Rinse the testes with buffer-T twice, and put the testes in round-bottom 2-ml microcentrifuge tubes containing 1 ml of buffer-T (four testes/tube). Mince the testes with forceps in the tubes.
4. Centrifuge at 150*g* for 10–20 s and collect the supernatant that contains sperm. Re-extract the sperm from the pellet with 0.5 ml of buffer-T and re-centrifuge to obtain a second supernatant.

5. Combine the first and the second supernatants, then sediment the sperm by centrifugation at 1350*g* for 2 min. A white pellet with a pink/red colored bottom will be obtained. Carefully separate the white pellet with a 1 ml pipetman and transfer to a 14 ml round-bottom tube containing 10 ml of buffer-T.
6. Centrifuge again at 1350*g* for 2 min to sediment the sperm, and resuspend the pellet with 10 ml of 0.2X buffer-T. Quickly mix and then centrifuge again at 1350*g* for 2 min (*see* **Note 7**).
7. Resuspend the pellet in 1 ml of buffer-T and add 3 ml of demembrane buffer. Quickly mix, then incubate at room temperature for 7 min. There will be a large chunk of precipitate formed during the incubation. At the end of the incubation, transfer the supernatant to a new tube containing 10 ml of a washing buffer, then mix the transferred supernatant quickly by inverting the tube.
8. Centrifuge the tube at 300*g* for 10 min to sediment the demembraned sperm nuclei. Resuspend the pellet in 10 ml of washing buffer and centrifuge again.
9. Resuspend the pellet in 1 ml of buffer-T, then estimate the concentration of sperm using a haemocytometer. Adjust the concentration to ~300,000 nuclei/ml with buffer-T, and aliquot 20 μl/tube. Snap freeze the sperm in liquid nitrogen and store at –80°C (*see* **Note 8**).

3.3. Assembly and Isolation of Chromosomes or Interphase Chromatin

SUMOylated Topo II from mitotic chromosomes can be observed as slow migrating isoforms on SDS-PAGE gels. So far, we have not detected SUMOylated isoforms of Topo II isolated from interphase chromatin. Therefore, the isolation of interphase chromatin is included as a negative control for analysis of Topo II SUMOylation. Another negative control that can be employed utilizes a dominant negative mutant of Ubc9, a SUMO E2 enzyme, that has the following mutations: C93S and L97S. Addition of this mutant protein to XEEs prevents Topo II SUMOylation (note that this method is not described in detail herein).

1. Put 100 μl of CSF extract or interphase extract into 2-ml round-bottom microcentrifuge tubes and add demembraned sperm nuclei to a final concentration of 3000–6000 nuclei/μl. Mix the extracts gently by tapping (*see* **Note 9**).
2. Incubate the extracts at room temperature and at 10–15 min intervals, take 1 μl of the reaction and mix with 4 μl of fixation solution on a slide glass to observe the DNA morphology with a fluorescence microscope. Usually, after 30–40 min of incubation, assembly of mitotic chromosomes or interphase nuclei will be complete (*see* **Note 10**).

3. Add four volumes of ice-cold dilution buffer to the reactions and mix rapidly by pipeting or inverting the tube.
4. Layer the diluted samples onto an ice-cold glycerol cushion in 2-ml conical-bottomed microcentrifuge tubes. Centrifuge with a swing bucket rotor at 10,000*g* for 5 min at 4°C.
5. Aspirate off the supernatant and resuspend the pellet in 500 µl of ice-cold glycerol cushion. Centrifuge again as above (step 4) then aspirate off the supernatant.
6. Add to the pellet 1X SDS-PAGE sample buffer (an equal volume to the original reaction). Mix by vortexing and heat the sample at ~100°C for 5 min. After heating, vortex the sample vigorously for 30 s and then reheat the sample for 5 min more. This process helps to disrupt DNA to make better separation in the SDS-PAGE gel. Centrifuge the boiled samples at 10,000*g* for 15 min at room temperature to pellet debris in the samples (*see* **Note 11**).

3.4. Analysis of SUMOylation of Topoisomerase II

To analyze the different molecular weight isoforms of Topo II and SUMOylated Topo II, we prefer to use a gradient SDS-PAGE gel. The gel electrophoresis and Western blotting conditions that are specific to this analysis are as follows:

1. Load 10–15 µl of the SDS-PAGE samples into each well of a pre-made gradient SDS-PAGE gel (8–16% or 4–20%).
2. Run the SDS-PAGE gel with 1X standard SDS-PAGE running buffer at 20–25 mA/gel for 2–3 h, until the bromophenol blue in the sample reaches the bottom of the gel.
3. Transfer the protein onto PVDF membrane with a semi-dry transfer apparatus and 1X transfer buffer at 45 mA/gel (8 × 7 cm gels) for 1.5 h.
4. Block the membrane with shaking in a blocking solution for 1 h at room temperature.
5. Probe the membrane with an anti-Topo IIα/β monoclonal antibody to detect *Xenopus* Topo IIα (*see* **Note 12**). The primary antibody should be diluted in blocking solution at 1/1000 and the membrane incubated with shaking overnight at 4°C.
6. Wash the membrane three times for 10 min each with shaking in PBS-T at room temperature.
7. Probe the membrane with the secondary antibody diluted in blocking solution at 1/2000–1/5000 with shaking for 1 h at room temperature.
8. Wash the membrane three times for 10 min each with shaking in PBS-T at room temperature.

9. Develop the membrane according to the secondary antibody conjugate that was employed (e.g., using ECL for a peroxidase-conjugated secondary antibody) and expose to X-ray film. A typical result of this analysis is shown in **Fig. 17.2**.

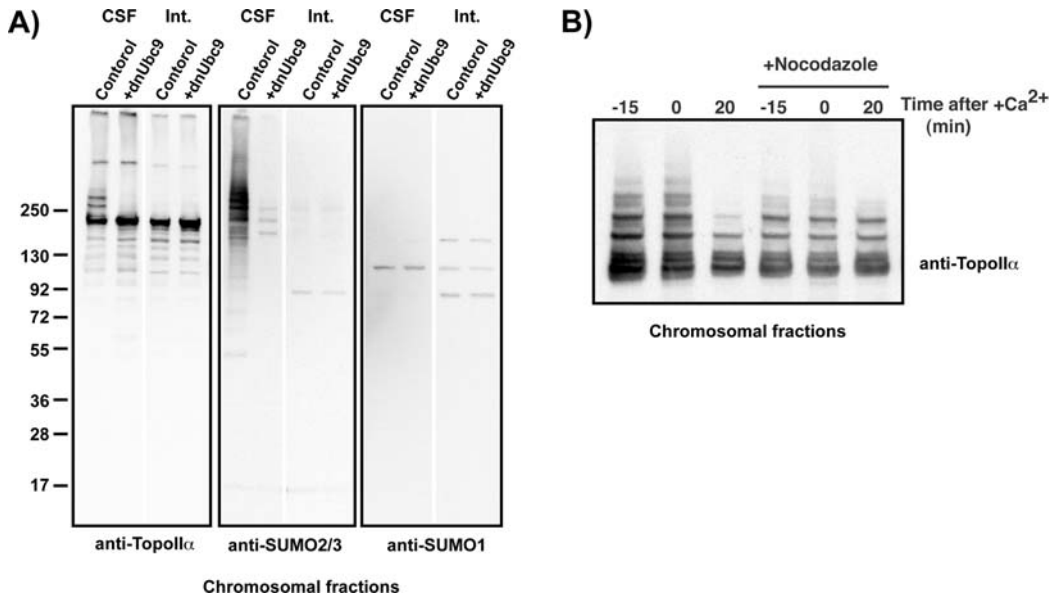

Fig. 17.2. **Detection of SUMOylated Topo IIα on mitotic chromosomes**. (**A**) Chromosomal fractions were isolated either from CSF (indicated as CSF) or interphase (indicated as Int.) egg extracts in the presence or absence of dnUbc9. The chromosomal fractions were analyzed by immunoblotting with the indicated antibodies. On mitotic chromosomes (CSF), Topo IIα shows molecular weight shifts, which corresponds to the protein detected with the anti-SUMO2/3 antibody. (**B**) CSF extracts were incubated with 8000 sperm nuclei/ml in the presence or absence of nocodazole. After 45 min of incubation (time 0), $CaCl_2$ was added to the reaction to drive the reactions into interphase. Chromosomal fractions were isolated at the indicated time points, and then isolated chromosomes were analyzed by immunoblotting with the anti-Topo II antibody. When the mitotic checkpoint was activated by the inclusion of nocodazole, this prevented exit from mitosis (20) and de-SUMOylation of Topo II induced by Ca^{2+}.

10. If the membrane needs to be stripped and re-probed with another antibody, strip the membrane by incubating it in stripping buffer at 55°C for 20 min. Next, wash the membrane briefly with water and then with PBS-T. Block the membrane with blocking buffer for 1 h and then proceed to the primary antibody step.

4. Notes

1. We use a 500–600 ml glass beaker for dejellying and washing the eggs. This size of beaker is large enough to mix the eggs gently and to observe the morphology of the eggs. Adjust the size of the beaker according to the volume of eggs you have.

2. Usually, low-quality eggs accumulate on the top and center of the eggs after you mix by rotating the beaker horizontally. If you observe more than 30% of the eggs are not of sufficient quality, they should not be used for XEE preparation.
3. Do not drop the eggs from the top of the tube. Place the tip of a transfer pipette in the buffer at the bottom and slowly put the eggs down into the buffer. Try not to put excess buffer in the tube with the eggs.
4. The color of the extracts will vary depending on the pigmentation of the eggs. Contamination by mitochondrial material will damage the extracts and make them no longer useful for cell cycle analysis. Use the appropriate size of syringe depending on the volume of the cytoplasmic fraction.
5. Mix $CaCl_2$ as quickly as possible. Mixing thoroughly is required to complete the release from CSF arrest.
6. Rolling the dissected testes on a paper towel is one of the easiest ways to remove extra tissue attached to the testes.
7. This wash step under hypotonic conditions is very effective when you are trying to isolate a large quantity of sperm from a large number of testes. After this wash step, all of the contaminating red blood cells will be disrupted and other contaminating somatic cells will tend to form an aggregate in the next step.
8. If you observed aggregated sperm, you can remove the aggregates by centrifuging the sperm at 150*g* for 10 s. The concentration of the sperm can be lower or higher depending on the application. For a morphological assay, a lower concentration of the stock sperm will be desired.
9. Assembled chromosomes tend to sink to the bottom of the tube. Using a round-bottom tube makes mixing the large volume of the reaction easier. When a larger reaction volume, more than 200 μl, is required, we use 5- or 14-ml round-bottom test tubes.
10. Condensed chromosomes and round nuclear morphology will be observed after 30 min of incubation with sperm [e.g., (11)].
11. Chromatin samples often separate poorly on SDS-PAGE gels. Occasionally, both Topo II and SUMO show smeary signals upon western blotting. We have found that high concentrations of salt, above 300 mM, and vigorous mixing by vortexing help to avoid such unclear separation on SDS-PAGE gels.
12. We are currently using both anti-SUMO-2/3 and anti-Topo IIα antibodies that have been generated in our laboratory. We tested several anti-Topo II antibodies (15), but some of them are not available currently. Our antibodies were made against the full-length SUMO-2/3 and the C-terminal fragment of Topo IIα.

Acknowledgments

I would like to thank to Mary Dasso for critical reading and her support. This work was supported by NIH/NCRR, CCET-COBRE (P20 RR015563), and is currently supported by NIH/NIGMS (GM080278).

References

1. Hay, R. T. (2005) SUMO: a history of modification. *Mol Cell* **18**, 1–12.
2. Johnson, E. S. (2004) Protein modification by sumo. *Annu Rev Biochem* **73**, 355–382.
3. Dasso, M. (2008) Emerging roles of the SUMO pathway in mitosis. *Cell Div* **3**, 5.
4. Mukhopadhyay, D. and Dasso, M. (2007) Modification in reverse: the SUMO proteases. *Trends Biochem Sci* **32**, 286–295.
5. Hay, R. T. (2007) SUMO-specific proteases: a twist in the tail. *Trends Cell Biol* **17**, 370–376.
6. Yanagida, M. (2005) Basic mechanism of eukaryotic chromosome segregation. *Philos Trans R Soc Lond B Biol Sci* **360**, 609–621.
7. Holm, C., Goto, T., Wang, J. C. and Botstein, D. (1985) DNA topoisomerase II is required at the time of mitosis in yeast. *Cell* **41**, 553–563.
8. Uemura, T. and Yanagida, M. (1984) Isolation of type I and II DNA topoisomerase mutants from fission yeast: single and double mutants show different phenotypes in cell growth and chromatin organization. *EMBO J* **3**, 1737–1744.
9. Hirano, T. and Mitchison, T. J. (1993) Topoisomerase II does not play a scaffolding role in the organization of mitotic chromosomes assembled in *Xenopus* egg extracts. *J Cell Biol* **120**, 601–612.
10. Adachi, Y., Luke, M. and Laemmli, U. K. (1991) Chromosome assembly in vitro: topoisomerase II is required for condensation. *Cell* **64**, 137–148.
11. Cuvier, O. and Hirano, T. (2003) A role of topoisomerase II in linking DNA replication to chromosome condensation. *J Cell Biol* **160**, 645–655.
12. Shamu, C. E. and Murray, A. W. (1992) Sister chromatid separation in frog egg extracts requires DNA topoisomerase II activity during anaphase. *J Cell Biol* **117**, 921–934.
13. Takahashi, Y., Yong-Gonzalez, V., Kikuchi, Y. and Strunnikov, A. (2006) SIZ1/SIZ2 control of chromosome transmission fidelity is mediated by the sumoylation of topoisomerase II. *Genetics* **172**, 783–794.
14. Bachant, J., Alcasabas, A., Blat, Y., Kleckner, N. and Elledge, S. J. (2002) The SUMO-1 isopeptidase Smt4 is linked to centromeric cohesion through SUMO-1 modification of DNA topoisomerase II. *Mol Cell* **9**, 1169–1182.
15. Azuma, Y., Arnaoutov, A. and Dasso, M. (2003) SUMO-2/3 regulates topoisomerase II in mitosis. *J Cell Biol* **163**, 477–487.
16. Mao, Y., Desai, S. D. and Liu, L. F. (2000) SUMO-1 conjugation to human DNA topoisomerase II isozymes. *J Biol Chem* **275**, 26066–26073.
17. Agostinho, M., Santos, V., Ferreira, F., Costa, R., Cardoso, J., Pinheiro, I., Rino, J., Jaffray, E., Hay, R. T. and Ferreira, J. (2008) Conjugation of human topoisomerase 2 alpha with small ubiquitin-like modifiers 2/3 in response to topoisomerase inhibitors: cell cycle stage and chromosome domain specificity. *Cancer Res* **68**, 2409–2418.
18. Desai, A., Murray, A., Mitchison, T. J. and Walczak, C. E. (1999) The use of *Xenopus* egg extracts to study mitotic spindle assembly and function in vitro. *Methods Cell Biol* **61**, 385–412.
19. Kornbluth, S., Yang, J. and Powers, M. (2001) Analysis of the cell cycle using *Xenopus* egg extracts. In Current Protocols in Cell Biology, K. M. Yamada, ed. (New York: John Wiley & Sons, Inc.), pp. 11.11.11–11.11.13.
20. Chen, R. H. and Murray, A. (1997) Characterization of spindle assembly checkpoint in *Xenopus* egg extracts. *Methods Enzymol* **283**, 572–584.

Chapter 18

The Dynamics of DNA Topoisomerase IIα in Living Cells

John R. Daum, Yin Yuan Mo, and Gary J. Gorbsky

Abstract

Here, we describe methods to prepare a mammalian expression plasmid encoding EGFP fused to the amino-terminus of human DNA topoisomerase IIα (Topo IIα) for use in studying the dynamics of Topo IIα in living cells. In previous studies, this plasmid was transfected into LLC-Pk cells, a porcine epithelial cell line that remains relatively flat during mitosis. After selection for stable integration, cells were cloned by serial dilution in microwells and used to grow a stable cell line expressing EGFP-Topo IIα; this cell line was termed LPk-GT2. Using photobleaching methods with conventional and patterned photobleaching, LPk-GT2 cells were used to demonstrate the rapid dynamics of Topo IIα exchange in both interphase nuclei and mitotic chromosomes. These rapid dynamics are dependent on enzyme activity since ICRF159, a catalytic inhibitor of Topo IIα, slows dynamics significantly. The methods utilized in these studies are described herein.

Key words: Nucleus, chromosome, kinetochore, mitosis, fluorescence, photobleaching, FRAP.

1. Introduction

DNA topoisomerase IIα (Topo IIα) is expressed primarily in actively dividing cells and shows dynamic changes at various stages of the cell cycle. In proliferating cells, both protein and message levels are low during the G1 phase and begin to rise during S phase, with a peak of protein expression during G2 and M phases (1–3). After mitosis, Topo IIα reconcentrates in the nuclei, and subsequently during G1 message levels decrease and the protein is degraded by the proteasome (1–5). In interphase cells, antibody labeling and expression of tagged forms of the protein show that the enzyme is nuclear with a high concentration in the nucleolus

D.J. Clarke (ed.), *DNA Topoisomerases*, Methods in Molecular Biology 582,
DOI 10.1007/978-1-60761-340-4_18,

(5–7). As the chromosomes condense during early mitosis, Topo IIα concentrates at the centromeres and along the axes of the chromosome arms (7–10).

This pattern of association with mitotic chromosomes and the persistence of Topo IIα in salt- and DNAse-treated chromosome fractions led to the idea that Topo IIα might form a stable mitotic chromosome scaffold (11). To test this notion, we and others (5, 6, 12) created cell lines that express Topo IIα fused to fluorescent proteins that were then used for photobleaching analyses. Surprisingly, Topo IIα showed rapid turnover in photobleaching experiments in both interphase nuclei and mitotic chromosomes. When inhibitors of topoisomerase II catalytic activity were applied to cells, Topo IIα became stably anchored on chromatin in both interphase and mitotic cells (10). These observations led to the conclusion that Topo IIα exhibits rapid exchange on chromatin that is dependent on enzyme activity. Further studies have implicated Topo IIα in a host of important roles for chromatin regulation in interphase and mitosis (13–17). The dynamic exchange of Topo IIα on chromatin is likely to be a key factor in these functions. Finally, several chemotherapeutic agents function through the activity of Topo IIα (18, 19).

Overexpression of Topo IIα in mammalian cells is toxic and induces apoptosis (20, 21). For this reason, establishment of cell lines stably expressing Topo IIα tagged with fluorescent proteins is dependent on spontaneous down regulation of the endogenous Topo IIα or by purposefully targeting endogenous gene expression (5, 12). Keeping in mind this caveat, the techniques described here will facilitate analysis of Topo IIα dynamics in living cells under various experimental conditions.

2. Materials

2.1. Construction of the EGFP-Topo IIα Plasmid

1. Reagents for molecular biology: restriction enzymes (*Kpn* I, *BamH* I, *Hind* III and *Sac* II; New England Biolabs); RNase-free DNase and Triazol reagent (Invitrogen); Gold Taq DNA polymerase (ABI); pCDNA3 plasmid (Invitrogen); pEGFP-C3 plasmid (Clontech).
2. Primers for PCR (Sigma-Genosis):
   a. N-terminus: IIa-B1 (sense), 5′-GGATCCGAAGTGTCACCATTGCAG and IIa-3.1 (antisense), 5′-GGTGGATCCAGCAATATCAT.
   b. C-terminus: IIa-C1A (sense), 5′-GTGACAGTGAAGAAGACAGCAG and IIa-C18.1 (antisense), 5′-GCGGCCGCGGTTAAAACAGATCATCTTCATC.

3. RGS-6xHis sequence: DNA encoding RGS-6xHis (Qiagen).
4. Primers to detect the exogenous Topo IIα:
   a. T1 (sense), 5′-GGTACCGATACCATGCGGGGTTCT.
   b. T2 (antisense) 5′-TAGCCATTTCGACCACCTGTCAC.

2.2. Transfection of LLC-Pk Cells and Selection of Stable Line

1. Culture medium for LLC-Pk cells: Dulbecco's modified Eagle's medium (DMEM; Gibco/Invitrogen) supplemented with 10% fetal bovine serum (Gibco/Invitrogen), 1X non-essential amino acids (Gibco/Invitrogen), 20 mM HEPES, and antibiotics (penicillin 100 U/l and streptomycin 100 μg/ml).
2. Transfection medium: Plasmid DNA for transfection prepared with lipofectamine plus according the manufacturer's directions in DMEM.
3. Selection medium: Complete culture medium containing 2 mg/ml G148.
4. Cloning plates: Corning 96-well tissue culture plates.

2.3. Imaging and Photomanipulation

1. Medium for cell culture on the microscope: If a stage incubator is used that allows a CO_2 atmosphere on the microscope stage, conventional CO_2-requiring culture medium can be used (*see* **Note 1**).
2. Microscope logistics and temperature control: Generally inverted research grade inverted microscopes are suitable for high-resolution imaging and photomanipulation of EGFP-Topo IIα. For LLC-Pk and other mammalian cells, the temperature of the stage must be maintained at or near 37°C. A number of approaches are possible. One solution is to employ a stage incubator. We have used stage insert heaters obtained from a variety of the microscope manufacturers. In addition we have used dedicated air curtain incubators such as the one provided by Nevtek (Model ASI 400). Surprisingly, a simple hair dryer mounted on a ring stand with a variable rheostat to control output works well to maintain stage temperature. An electronic thermometer with a small probe that can be taped to the stage is useful to assess temperature. Finally, since high resolution requires oil or water immersion objectives, it is essential to have either a stage incubator that heats the objective or to use a separate objective heater that will maintain temperature of the specimen just over the area being observed. We use the one manufactured by Biopetechs.
3. Preparation of glass coverslips for live cell microscopy: Because of the limited working distance of high resolution, high numerical aperture objectives, it is essential to culture cells on thin glass coverslips for imaging. We prepare 25 mm

round number 1.5 glass coverslips (usually one box of approximately 100 coverslips) dropping them one by one by hand into a solution of 95% ethanol in a glass petri dish. Dropping them one by one prevents them from sticking together. The coverslips are rinsed twice with fresh 95% ethanol. The ethanol is removed from the glass petri dish containing the coverslips; the lid is placed on the petri dish, and the dish is placed into a cold drying oven. The heat is then turned on, and the ethanol is allowed to evaporate for a few hours to overnight. The oven is then turned off and the petri dish is allowed to cool. The coverslips are now clean and sterile and ready to be used for cell culture.

4. Culture chambers for live cell microscopy: A variety of approaches and different types of microscope culture chamber systems have been developed. We use two approaches in our laboratory. We use commercial stainless steel chambers (Molecular Probes/Invitrogen) composed of two halves that screw together clamping a 25 mm coverslip on which cells are plated. The chambers are stored in 95% ethanol to maintain sterility. They are removed with tongs and allowed to dry in a tissue culture hood prior to use. A lower cost solution is to drill holes 18–20 mm in diameter in the bottom of a 35 mm plastic petri dish. Using a bead of silicone grease, a 25 mm glass coverslip is applied to the inside of the dish. The dish is sterilized by placing it upside down along with its lid on the surface of a UV light box for 10 min. If a high-resolution objective with a very shallow shoulder is used that bumps into the cut hole in the dish, the coverslips can be mounted with a grease ring on the outside of the chamber. These chambers should always be placed inside a larger plastic petri dish while in the incubator since they occasionally leak. A final issue is evaporation leading to hypertonicity of the medium in the observation. Our usual solution is to cover the medium with a thin layer of mineral oil that must be spread evenly. An alternative is to apply a large coverslip to the top of the chamber but an air space invites condensation on the top coverslip. With the steel chambers it is possible to fill the medium to the level of a shelf inside the chamber on which a 25 mm coverslip can be rested in contact with the medium surface.
5. Photobleaching apparatus: We use two different systems for photobleaching both produced by Photonics Instruments, the Micropoint dye laser system and the Mosaic digital diaphragm system.
   a. Micropoint dye laser system: This system uses a pulsed UV nitrogen laser to pump a small dye chamber that emits a visible wavelength beam. Different dyes provide different

wavelengths that can be adapted for different fluorophores. The primary dye we use is Courmarin 440, which produces light at 440 nm. This wavelength is sufficiently different from the normal excitation wavelength of GFP that a notch filter can be used to pass 440 nm light while still reflecting nearly all the excitation light from the mercury light source used for imaging. Attenuation elements on the system are empirically adjusted to allow photobleaching of EGFP in 3–10 pulses to be delivered at a repetition rate of 15–30 Hz.

b. Mosaic digital diaphragm system: This system uses a digital diaphragm to control the spread of light from an argon ion laser that emits at 495 nm. Minimum duration of the photobleaching pulse is empirically determined. For imaging with this system, we use a spinning disk confocal microscope coupled with a diode laser having an output of 473 nm. The difference between the two wavelengths allows design of the light path such that filter cubes in the microscope do not move in between photobleaching and observation.

6. Imaging systems: We use ORCA-ER cameras (Hamamatsu) and two imaging software packages: Metamorph from Molecular devices and Slidebook from Intelligent Imaging Innovations.

3. Methods

3.1. Construction of the EGFP-Topo IIα Plasmid

3.1.1. Construction of the His-Tagged Topo IIα Plasmid

1. To tag human Topo IIα, introduce the RGS-6xHis sequence at the *Kpn*I and *Bam*HI sites of pCDNA3 to make an N-terminal tag (pCDNA3-His). Ensure a Kozak consensus sequence is placed in front of the RGS-6xHis tag to improve translation.
2. To facilitate the subcloning of Topo IIαcDNA into pCDNA3-His, introduce a *Bam*HI site at the N-terminus of Topo IIαcDNA by PCR amplification, eliminating the first methionine (start codon) of Topo IIα. Similarly, introduce the restriction sites *Sac*II and *Not*I at the C-terminus after the stop codon.
3. Verify the sequences of the PCR products by DNA sequencing. The resultant plasmid is named pT14. It carries full-length Topo IIα cDNA in pCDNA3-His unidirectionally at the *Bam*HI and *Not*I sites without the start Topo IIα codon ATG.

3.1.2. Construction of EGFP-Tagged Topo IIα

1. Digest pT14 to completion with *Sac*II and digest partially with *Hind*III.
2. From the digest in step 1, gel purify the full-length Topo IIαcDNA plus RGS-6xHis region and ligate this in frame into pEGFP-C3 at the *Hind*III and *Sac*II sites (**Fig. 18.1**) (*see* Note 2).

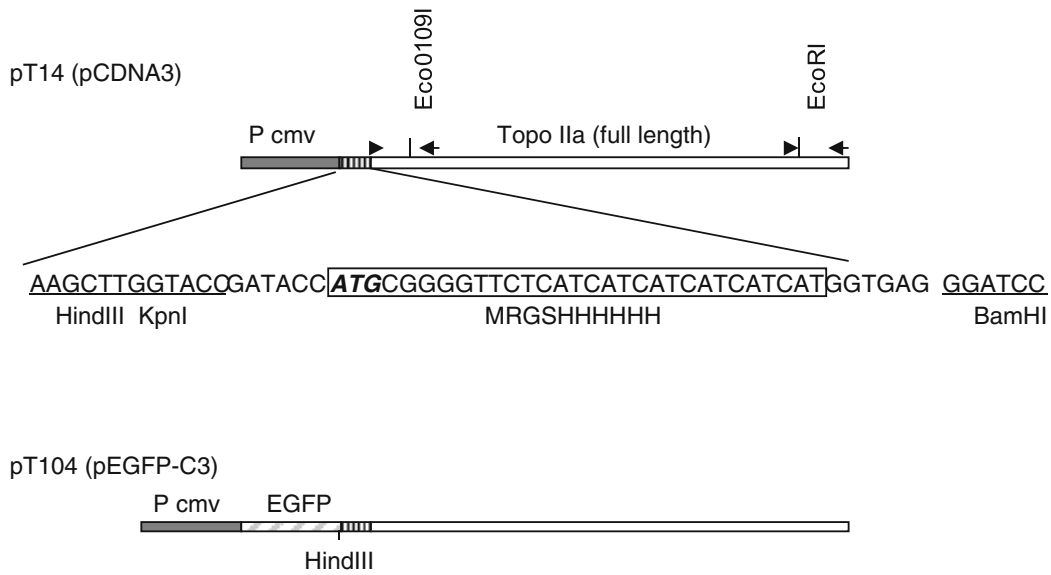

Fig. 18.1. **Production strategy used to generate pT104 plasmid containing EGFP-Topo IIα for transfection to produce GT2-LPk cells**. Primers used for amplifying the N- or C-terminal regions of Topo IIα by RT-PCR are shown as *arrows*. Restriction sites (*Eco* 0109I and *Eco*R I) are used for convenient cloning of PCR products. As indicated, both constructs use the same CMV promoter (Pcmv), but pT104 carries EGFP fused to Topo IIα. (Adapted from (24), © 2008 BioTechniques. Used by permission.)

3.2. Transfection of LLC-Pk Cells and Selection of a Stable Cell Line

1. Grow LLC-Pk cells in 35 mm dishes in culture medium for LLC-Pk cells until approximately 50% confluent.
2. To produce a stable cell line expressing EGFP-Topo IIα, transfect the LLC-Pk cells with the pT104 plasmid encoding EGFP-Topo IIα at 1 μg/ml using lipofectamine plus according to the manufacturer's instructions. Following 3 h in the transfection medium, add culture medium for LLC-Pk cells and culture the cells for 24 h.
3. Examine the cells by brief exposure to fluorescent light to assess the overall transfection efficiency. If the efficiency is 25% or greater, stable lines are selected.
4. To select for cell lines expressing stably integrated plasmid, transfer the cells to selection medium and after they have reached 80% confluence, passage them once into 100 mm tissue culture dishes and culture them for an additional 3 days in selection medium.

5. To isolate colonies, trypsinize the cells and plate at an average density of 1 cell/well in 96-well dishes (*see* **Note 3**).
6. To identify single cell colonies, observe the 96-well dishes with a tissue culture microscope and mark wells with single cells. Maintain these cultures until individual cells in the wells grow to confluence. Transfer the cells from each well to a well of a 12-well dish containing a 12-mm sterile circular coverslip covering a portion of the well. When the cells have populated the coverslip, remove the coverslip and assess the cells for expression and proper localization of EGFP-Topo IIα fluorescence (**Fig. 18.2**).
7. Grow to confluence the wells containing colonies with proper expression of EGFP-Topo IIα in interphase nuclei and mitotic chromosomes. FACS sort these cells to confirm and enrich EGFP-Topo IIα expressing cells and then transfer the sorted cells to larger dishes for expansion and freezing (*see* **Notes 4** and **5**).

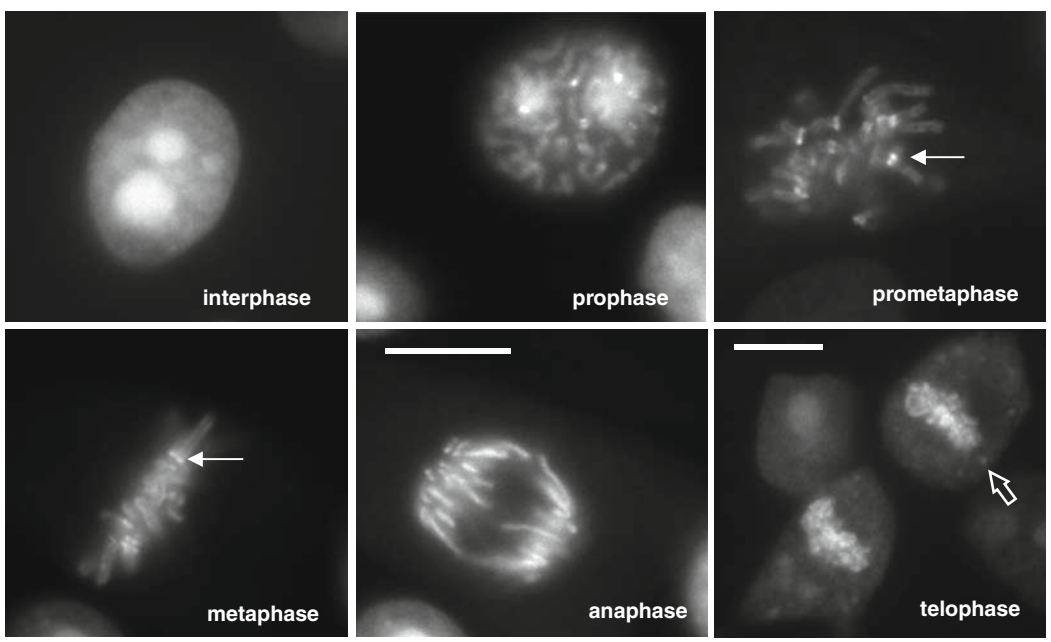

Fig. 18.2. **EGFP-Topo IIα localization in a panel of living GT2-LPK cells at various stages of mitosis**. EGFP-Topo IIα concentrates in the nucleus and particularly in the nucleoli of cells in interphase. It associates with chromosomes in prophase, becoming concentrated at kinetochores (*closed arrows*) and along chromosome arms in prometaphase and metaphase. During anaphase, the kinetochore concentration decreases but EGFP-Topo IIα remains and is associated with the chromosome arms. In late anaphase and telophase, EGFP-Topo IIα remains associated with the decondensing chromosomes. Some Topo IIα appears in the cytoplasm with a portion becoming concentrated in cytoplasmic foci (*open arrow*). Bars = 10 μm. (Adapted from (5), © Tavormina et al., 2002. Originally published in The Journal of Biology. doi:10.1083/jcb.200202053.)

3.3. Imaging and Photomanipulation

1. Observe the cells on a warm stage on an inverted microscope (e.g. Zeiss Axio Observer). When used with high numerical aperture water or oil immersion objectives, use an objective heater.
2. Image the cells by fluorescence, phase contrast, or DIC microscopy for targeting regions for photobleaching. To limit phototoxicity and photobleaching of EGFP, minimize the fluorescence exposures (*see* **Note 6**).
3. If using a nitrogen laser-pumped dye laser (Micropoint, Photonic Instruments), bleach by delivering three to eight pulses at a repetition rate of 30 Hz (*see* **Note 7**). Determine empirically the levels that cause photobleaching without cytotoxicity (**Fig. 18.3**).

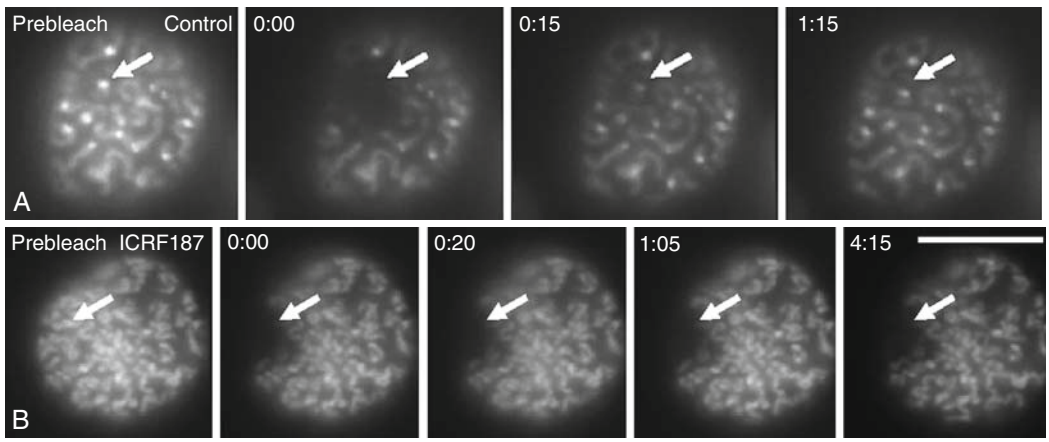

Fig. 18.3. **Recovery of EGFP-Topo IIα fluorescence on kinetochores and chromosome arms after photobleaching occurs rapidly and is slowed by catalytic inhibitors of Topo IIα enzyme activity**. (**A**) Targeting of kinetochores (*arrows*) and chromosome arms at prophase using point photobleaching with the Micropoint dye laser. (**B**) The topoisomerase II inhibitor ICRF187 shows a general reduction in the extent of chromosome condensation in prophase nuclei. ICRF187 treatment greatly slows recovery after photobleaching. Images include a prebleach image, one taken just after photobleaching (0 time) and those taken during recovery. Time is depicted as minutes:seconds after photobleaching. Bar = 10 μm. (Adapted from (5), © Tavormina et al., 2002. Originally published in The Journal of Biology. doi:10.1083/jcb.200202053.)

4. If using pattern photobleaching with the digital light processor-modulated system (Mosaic, Photonic Instruments), collect fluorescent images every 500 ms prior to and after the photobleaching pulse. Generate a photobleaching pattern template to target specific regions prior to data collection so that any delay during image acquisition due to the argon laser pulse is minimal. (The template can be drawn using a phase contrast or fluorescence image of the sample captured immediately before photobleaching.) The photobleaching pulse duration of the argon laser should be empirically determined, but generally ranges between 200 and 600 ms (**Fig. 18.4**).

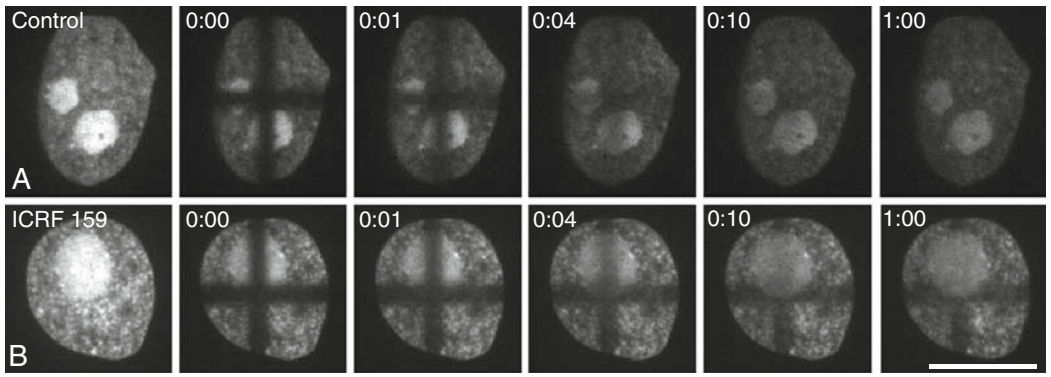

Fig. 18.4. **Recovery of EGFP-Topo IIα fluorescence in interphase nuclei using pattern photobleaching with the Mosaic argon laser system**. (**A**) Control cell nucleus shows rapid recovery of fluorescence after photobleaching. (**B**) The topoisomerase II inhibitor ICRF159 causes a change in Topo IIα distribution in interphase nuclei resulting in a more granular appearance and a relative decrease in concentration of Topo IIα in the nucleolus. ICRF159 greatly slows recovery of photobleaching in the nucleus although recovery is somewhat more rapid within the nucleolus even in the presence of the drug. Images include a prebleach image, one taken just after photobleaching (0 time) and those taken during recovery. Time is depicted as minutes:seconds after photobleaching. Bar = 10 μm.

3.4. Data Analysis

1. Metamorph and Slidebook software can be used for data collection and analysis. Use an area that includes but is larger than the target area for subtraction of local cytoplasmic background using the procedures described by Howell et al. (22) and according to the equation $F_S–F_{BG} = F_S–(F_L–F_S) \times A_S/(A_L–A_S)$, where F_S is the average fluorescence intensity within the target bleach zone, F_L is the average intensity in the larger background area, A_S is the area of the target bleach zone, and A_L is the area of the larger background zone. This generates the final intensity minus the background $F_S–F_{BG}$.
2. Normalize the acquisitions to adjust for the reduction of total cellular fluorescence due to photobleaching and image acquisition according to the procedures of Phair and Misteli (23) and using the equation $F_n = F_t \times T_0/F_0 \times T_t$, where F_n is the normalized fluorescence intensity in the bleach zone, F_t is the average intensity in the bleach zone at time point t, F_0 is the average intensity in the target bleach zone before photobleaching, T_t is the total cellular intensity at timepoint t, and T_0 is the total cellular intensity before photobleaching and long-term imaging. Integrated intensities of the target and background regions and their associated area measurements can be logged to Excel spreadsheets.
3. Carry out the analysis of photobleaching recovery half-times and percent recovery using the methodology described by Howell et al. (22) and using normalized relative intensity values. The equation $F_{inf}–F(t) = [F_{inf}–F(0)]e^{-kt}$ describes the perturbation-relaxation for fluorescence recovery after

photobleaching where F_{inf} is the normalized intensity of the photobleached area after maximum recovery and $F(0)$ is the normalized intensity at $t=0$ after photobleaching. Normalized relative fluorescence intensity values can be exported to GraphPad Prism software and the rate constant k then determined by nonlinear regression.

4. Calculate the half-time for recovery using $t_{1/2}=\ln 2/k$. The percent recovery is determined by the equation $F_{inf}–F(0)/F(p)–F(0)$, where $F(p)$ is the prebleach intensity at the target (**Fig. 18.5**).

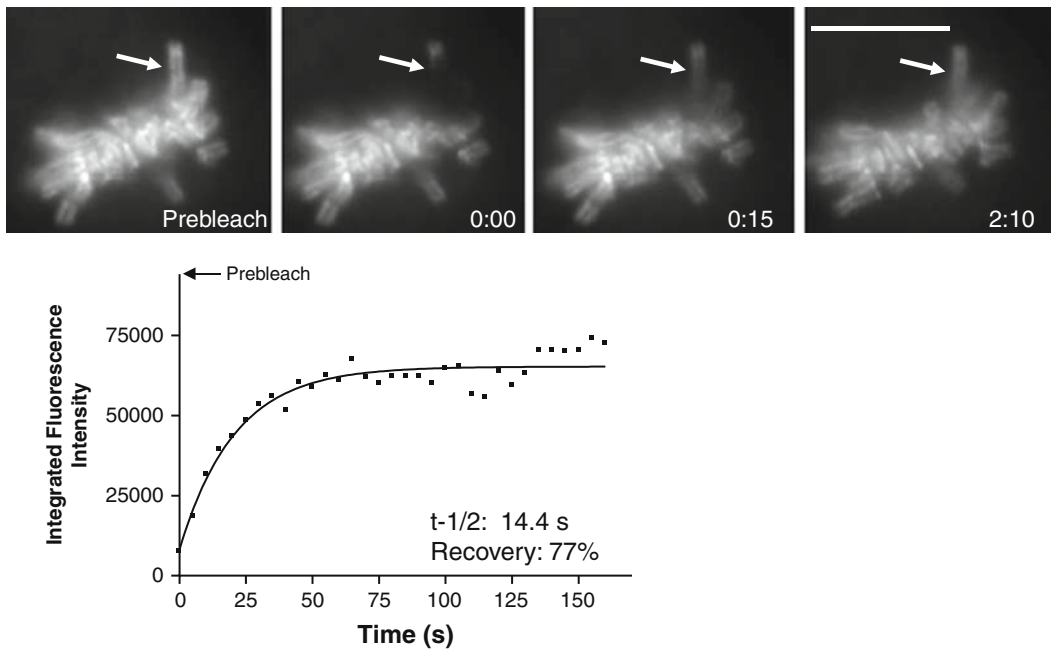

Fig. 18.5. **Data analysis of photobleaching and recovery of EGFP-Topo IIα in metaphase chromosome arm**. Images show a prebleach image and images taken at photobleaching and after for an isolated chromosome arm extending from the metaphase-arrayed chromosomes. The graph shows the fitting of corrected intensity measurements in the photobleached region to determine recovery half-times (*t*-1/2) and total degree of recovery (recovery). Bar = 10 μm. (Adapted from (5), © Tavormina et al., 2002. Originally published in The Journal of Biology. doi:10.1083/jcb.200202053.)

4. Notes

1. In most of our studies, this approach has not been available. Instead, we generally use a CO_2-independent medium, L-15 containing 10% FBS, and antibiotics.
2. Although this construct contains an internal start codon (ATG) from the 6xHis tag, the internal translational product will not be detected.

3. It is a good idea to freeze a portion of the remaining cells and to plate a portion of the cells in 100 mm dishes as a backup should the cloning be unsuccessful.
4. Because overexpression of Topo IIα is toxic, selection for EGFP-Topo IIα expression also selects for down regulation of endogenous Topo IIα expression.
5. A supplementary means for selection for lines expressing appropriate levels of EGFP-Topo IIα is fluorescence-activated cell sorting (FACS). FACS is also useful if cells are cultured for many passages, which sometimes leads to the development of non-expressing cells that retain G418-resistance.
6. It is advisable to target the regions of interest using phase-contrast microscopy and capture a prebleach fluorescence image immediately before photobleaching.
7. The laser should be attenuated to the appropriate level with neutral density filters.

Acknowledgments

Support was provided by the National Institutes of General Medical Sciences, from the Oklahoma Medical Research Foundation and from the McCasland Foundation. We thank Dr. Penny Tavormina for helpful suggestions.

References

1. Goswami, P. C., Roti Roti, J. L. and Hunt, C. R. (1996) The cell cycle-coupled expression of topoisomerase IIalpha during S phase is regulated by mRNA stability and is disrupted by heat shock or ionizing radiation. *Mol Cell Biol* **16**, 1500–1508.
2. Heck, M. M., Hittelman, W. N. and Earnshaw, W. C. (1988) Differential expression of DNA topoisomerases I and II during the eukaryotic cell cycle. *Proc Natl Acad Sci USA* **85**, 1086–1090.
3. Isaacs, R. J., Davies, S. L., Sandri, M. I., Redwood, C., Wells, N. J. and Hickson, I. D. (1998) Physiological regulation of eukaryotic topoisomerase II. *Biochim Biophys Acta* **1400**, 121–137.
4. Salmena, L., Lam, V., McPherson, J. P. and Goldenberg, G. J. (2001) Role of proteasomal degradation in the cell cycle-dependent regulation of DNA topoisomerase IIalpha expression. *Biochem Pharmacol* **61**, 795–802.
5. Tavormina, P. A., Come, M. G., Hudson, J. R., Mo, Y. Y., Beck, W. T. and Gorbsky, G. J. (2002) Rapid exchange of mammalian topoisomerase II alpha at kinetochores and chromosome arms in mitosis. *J Cell Biol* **158**, 23–29.
6. Christensen, M. O., Larsen, M. K., Barthelmes, H. U., Hock, R., Andersen, C. L., Kjeldsen, E., Knudsen, B. R., Westergaard, O., Boege, F. and Mielke, C. (2002) Dynamics of human DNA topoisomerases IIalpha and IIbeta in living cells. *J Cell Biol* **157**, 31–44.
7. Null, A. P., Hudson, J. and Gorbsky, G. J. (2002) Both alpha and beta isoforms of mammalian DNA topoisomerase II associate with chromosomes in mitosis. *Cell Growth Differ* **13**, 325–333.

8. Rattner, J. B., Hendzel, M. J., Furbee, C. S., Muller, M. T. and Bazett-Jones, D. P. (1996) Topoisomerase II alpha is associated with the mammalian centromere in a cell cycle- and species-specific manner and is required for proper centromere/kinetochore structure. *J Cell Biol* **134**, 1097–1107.
9. Sumner, A. T. (1996) The distribution of topoisomerase II on mammalian chromosomes. *Chromosome Res* **4**, 5–14.
10. Taagepera, S., Rao, P. N., Drake, F. H. and Gorbsky, G. J. (1993) DNA topoisomerase II alpha is the major chromosome protein recognized by the mitotic phosphoprotein antibody MPM-2. *Proc Natl Acad Sci USA* **90**, 8407–8411.
11. Earnshaw, W. C., Halligan, B., Cooke, C. A., Heck, M. M. and Liu, L. F. (1985) Topoisomerase II is a structural component of mitotic chromosome scaffolds. *J Cell Biol* **100**, 1706–1715.
12. Carpenter, A. J. and Porter, A. C. (2004) Construction, characterization, and complementation of a conditional-lethal DNA topoisomerase IIalpha mutant human cell line. *Mol Biol Cell* **15**, 5700–7511.
13. Coelho, P. A., Queiroz-Machado, J., Carmo, A. M., Moutinho-Pereira, S., Maiato, H. and Sunkel, C. E. (2008) Dual role of topoisomerase II in centromere resolution and aurora B activity. *PLoS Biol* **6**, e207.
14. Coelho, P. A., Queiroz-Machado, J. and Sunkel, C. E. (2003) Condensin-dependent localisation of topoisomerase II to an axial chromosomal structure is required for sister chromatid resolution during mitosis. *J Cell Sci* **116**, 4763–4776.
15. Jonstrup, A. T., Thomsen, T., Wang, Y., Knudsen, B. R., Koch, J. and Andersen, A. H. (2008) Hairpin structures formed by alpha satellite DNA of human centromeres are cleaved by human topoisomerase IIalpha. *Nucleic Acids Res* **36**, 6165–6174.
16. Takahashi, Y. and Strunnikov, A. (2008) In vivo modeling of polysumoylation uncovers targeting of topoisomerase II to the nucleolus via optimal level of SUMO modification. *Chromosoma* **117**, 189–198.
17. Warsi, T. H., Navarro, M. S. and Bachant, J. (2008) DNA topoisomerase II is a determinant of the tensile properties of yeast centromeric chromatin and the tension checkpoint. *Mol Biol Cell* **19**, 4421–4433.
18. McClendon, A. K. and Osheroff, N. (2007) DNA topoisomerase II, genotoxicity, and cancer. *Mutat Res* **623**, 83–97.
19. Montecucco, A. and Biamonti, G. (2007) Cellular response to etoposide treatment. *Cancer Lett* **252**, 9–18.
20. McPherson, J. P. and Goldenberg, G. J. (1998) Induction of apoptosis by deregulated expression of DNA topoisomerase IIalpha. *Cancer Res* **58**, 4519–4524.
21. Mo, Y. Y. and Beck, W. T. (1999) Association of human DNA topoisomerase IIalpha with mitotic chromosomes in mammalian cells is independent of its catalytic activity. *Exp Cell Res* **252**, 50–62.
22. Howell, B. J., Hoffman, D. B., Fang, G., Murray, A. W. and Salmon, E. D. (2000) Visualization of Mad2 dynamics at kinetochores, along spindle fibers, and at spindle poles in living cells. *J Cell Biol* **150**, 1233–1250.
23. Phair, R. D. and Misteli, T. (2000) High mobility of proteins in the mammalian cell nucleus. *Nature* **404**, 604–609.
24. Mo, Y. Y., Ameiss, K. A. and Beck, W. T. (1998) Overexpression of human DNA topoisomerase II alpha by fusion to enhanced green fluorescent protein. *Biotechniques* **25**, 1052–1057.

Chapter 19

Depletion and Mutation of Topoisomerase II in Animal Cells

Andrew C.G. Porter

Abstract

Eukaryotic type II topoisomerases (Topo II) are implicated in a wide range of cellular processes. Cells in which Topo II protein has been specifically depleted or mutated provide powerful systems for analysing the normal in vivo functions of Topo II proteins and for assessing their roles in various chemotherapy regimens. Summarised here are the ways in which Topo II has been depleted or mutated in animal cells and the type of information gleaned. The cell lines generated are tabulated and represent a useful resource for further in vivo studies of Topo II function, one that we expect to grow in size and utility in the coming years.

Key words: Topoisomerase II, depletion, siRNA, conditional knockout, inhibitors.

1. Introduction

The biochemical properties of the type II topoisomerases (Topo II) are well studied, but their exact roles in living cells remain less clear. One approach has been to study the effects of Topo II inhibitors on cell behaviour. This approach, which clearly overlaps with toxicological analyses of the many chemotherapeutic drugs that inhibit Topo II, has helped to implicate Topo II in a wide range of cellular processes, including DNA replication, repair and recombination, transcription, chromosome condensation, and chromosome segregation.

Two key limitations apply to such experiments, however, both relating to specificity. First, Topo II inhibitors do not generally distinguish between the α and β isoforms of Topo II, which have similar biochemical properties but different cellular roles (1). It is therefore difficult to use Topo II inhibitors to

D.J. Clarke (ed.), *DNA Topoisomerases*, Methods in Molecular Biology 582,
DOI 10.1007/978-1-60761-340-4_19,

study isoform-specific functions (although this situation may change with the development of highly isoform-specific Topo II inhibitors (2, 3)). Second, Topo II inhibitors do more than impair natural cellular Topo II functions; most importantly, they cause DNA damage, which, despite being central to their therapeutic activity, can greatly complicate the analysis of normal Topo II functions. DNA damage is most pronounced for the Topo II "poisons" that block Topo II after it has made a (normally transient) chromosomal double-strand break (DSB), but "catalytic" inhibitors also generate DNA damage, by mechanisms that remain unclear (4, 5). Furthermore, Topo II inhibitors may have cellular effects that are Topo II independent (6, 7). Topo II inhibitors can thus have both loss-of-function effects and dominant gain-of-function effects, and each of these may be Topo II dependent or Topo II independent, the former depending to widely varying degrees on the two Topo II isoforms.

With this background, genetic approaches to Topo II analysis are particularly important because they can be used for loss-of-function studies without the complications of dominant or non-specific effects and can be deployed in an isoform-specific manner.

There are three main uses for Topo II loss-of-function studies:

- To determine the normal in vivo roles of each Topo II isoform.
- To determine the contribution of each Topo II isoform to inhibitor toxicity.
- To analyse the role of particular Topo II domains or residues in a known in vivo function.

Considered here are four methods by which loss of Topo II function has been achieved in animal cells:

- Gene targeting (**Table 19.1**).
- Stable expression of shRNA (**Table 19.2**).
- Transient transfection with siRNA (**Table 19.3**).
- Isolation and characterisation of Topo II inhibitor-resistant cells (**Table 19.4**).

2. Stable Topo II Depletion/Mutation by Gene Targeting

Systems in which *TOPO II* genes have been modified by homologous recombination are summarised in **Table 19.1**. By making cells with precisely defined changes, gene targeting is arguably the most rigorous of the methods described here. This is offset, however, by the relatively large amount of work involved. Gene targeting in mouse embryonic stem (ES) cells has the advantage that

Table 19.1
Stable depletion of Topo II by gene targeting

Genotype	Cells	Species	Phenotype	Method/comment	References
β–/–	ES/mice	Mouse	–/– Mice die postnatally of respiratory failure and defective neural development	Standard ES cell/transgenic methodologies	(14)
β–/–	Embryo fibroblasts	Mouse	–/– Cells more resistant to Topo II poisons than +/+ controls	SV40 transformed from mice of ref (14)	(18)
β–/–	Embryo fibroblasts	Mouse	VP-16 induced γ-H2AX signal similar in –/– and +/– cells	Cells from mice of (14)	(19, 20)
β–/–	Nalm-6 (Pre-B)	Human	Increased sensitivity to NK314 but increased resistance to other poisons	Highly efficient HR. Also in Lig4–/– background	(3)
α–/–	ES/mice	Mouse	–/– Embryos block at 4- or 8-cell stage with aberrant chromosome segregation	Standard ES cell/transgenic methodologies	(13, 46)
α–/– + cDNA	HTETOP (fibrosarcoma)	Human	Conditional on addition of Tet: aberrant chromosome segregation, apoptosis, and polyploidy	Tet-repressible TOPO IIα cDNA introduced before gene targeting	(23, 31)
α+/–	ES cells	Mouse	+/– Cells have increased resistance to VP-16 and ICRF193	Standard ES methodologies	(27)
α+/–	DT40	Chicken	+/– Cells have increased resistance to VP-16 and ICRF193	Highly efficient HR	(12)
α+/Y165S	ES/Mice	Mouse	ES cells and mice are resistant to bisdioxopiperazines ICRF187 and ICRF193	Argues against Topo II-independent mechanisms of toxicity	(22)
α+/–	Nalm-6 (Pre-B)	Human	Increased resistance to NK314 and other Topo II poisons	Highly efficient HR. Also in Lig4–/– background	(3)

Table 19.2
Stable depletion of Topo II by expression of shRNA

Isoform	Cells	Species	Phenotype	Method/comment	References
β	PC12 (pheochromocytoma)	Rat	VP-16 induced γ-H2AX signal unchanged by Topo IIβ depletion	Clone PC12-I4 (Topo IIα) *vs* PC12-C4 (vector only) stably transfected with shRNA expressing lentivirus	(20)
β	NB4-MR2 (retinoic acid (RA)-resistant acute promyelocytic cells)	Human	Sensitivity to RA is restored, permitting granulocytic differentiation	Control KD also in parental RA-sensitive NB4 cells	(47)
α	Eu-Myc lymphoma cells	Mouse	shRNA expression gives growth advantage to cells in doxorubicin in vitro and in vivo	shRNA expressed from retroviral vector. Topo IIα depletion insufficient to prevent proliferation	(29)
α* or (α+β)*	DT40 (B cells)	Chicken	Aberrant chromosome segregation, apoptosis, and polyploidy on addition of Tet	shRNAs to Topo IIα (or to Topo IIα and Topo IIβ) expressed from stably transfected, Tet-repressible expression cassettes	(Johnson and Farr, personal communication)

* Conditional; RA, retinoic acid; KD, knockdown.

Table 19.3
Transient depletion of Topo II by delivery of siRNA

Isoform	Species	Cell type	Phenotype	References
α or α+β	Human	HeLa (cervical carcinoma)	Some lagging chromosomes after Topo IIα KD, but severe segregation defects after α+β KD	(30, 46)
β	Human	HTETOP	Topo IIβ depletion exacerbated the chromosome segregation defect caused by Topo IIα depletion	(31)
Single isoform	Fly	S2 (Drosophila embryo)	Chromosome segregation impaired, condensation mildly impaired. Kinetochore assembly normal. Abnormal arm congression. Poor resolution of metaphase chromosomes. Centromere nondisjunction, syntelic attachments. Mis-localisation and reduced activity of Aurora B kinase	(32–34)
α or β	Human	HeLa (cervical carcinoma)	Depletion of Topo IIα, but not Topo IIβ, increased resistance to NK314	(3)
α	Human	A431 (squamous carcinoma)	More resistant to poisons	(35)
α/β	Human	K562 (myelogenous leukaemia) U937 (histiocytic lymphoma)	Depletion of Topo IIβ (by 95% [K563] or 69% [U937]), but not Topo IIα (by 83%[K563] or 66% [U937]), increased melphalan-induced DNA crosslinks	(36)
α/β	Human	MCF-7 (breast cancer)	Depletion of Topo IIβ(by 70%) but not Topo IIα (by 42%), abrogates potentiation of Topo II poison-induced apoptosis by histone deacetylase inhibitors	(38)
α/β	Human	SK-N-SH (neuroblastoma) 1321N1 (astrocytoma)	Sensitivity to peroxide-mediated DNA damage is decreased by ~95% Topo IIα depletion but increased by ~95% Topo IIβ depletion	(37)

KD, knockdown.

Table 19.4
Depletion and/or mutation of Topo II in cells selected for resistance to Topo II inhibitors

Inhibitor	Topo IIα status	Topo IIβ status	Cell name (parental)	Sp	Cell type	References
Adriamycin	20-fold reduced protein (mRNA same); no promoter mutation	Normal mRNA and protein levels	MKN/ADR (MKN-45)	Hu	Stomach adenocarcinoma	(48)
Adriamycin	Reduced protein and activity. Fusion at nt 3494 to RAR gene	NR	P388/ADR/3 P388/ADR/7 (P388)	Mo	Leukemia	(42, 49)
Amsacrine	Arg486Lys	Protein undetectable; mRNA 10% normal (50)	HL-60/AMSA KBM-3/AMS (HL-60 and KBM-3)	Hu	Acute myleoid leukemia	(51–55)
Amsacrine	18 nt deletion (nt 344–361)	NR	ZRm1 (ZR-75B)	Hu	Breast cancer	(56)
Amsacrine	3 nt deletion (nt 641–643)	NR	MDA-AMSA6 (MDA-MB-231)	Hu	Breast cancer	(56)
Ellipticine	4–5 fold reduced; possible promoter mutation	Protein undetectable; truncated at aa 1710	DC-3F/9-OH-E (DC3F0)	Ha	Lung fibroblast	(57–60)
Etoposide	Homozygous NLS deletion (KSK, 1490–1492). SA mutation; alternative splicing	Normal MWt and amount of protein	H69-VP (NCI-H69)	Hu	Small cell lung cancer	(40, 61, 62)

Etoposide	5-fold lower protein, reduced MWt; cytoplasmic. Alst 109 aa missing +32 extra. 2 mRNAs: 6.2 (reduced) and 4.8 kb	Normal MWt and amount of protein	H209/V6 (H209)	Hu	Small cell lung	(39, 63–66)
Etoposide	C1959A (Ser654Arg) G4483A (Asp1496Asn)	NR	T47D-VP5 (T47D)	Hu	Breast cancer	(56)
Etoposide	615 nt in-frame deletion (nt 3193–3807) in one allele; predicted 140 kDa product not seen	NR	MDA-VP7 (MDA-MB-231)	Hu	Breast cancer	(56)
Etoposide	200 nt deletion (nt 4265–4464) in one allele; predicted 159 kDa product seen, mostly cytoplasmic	NR	T47D-VP1 (T47D)	Hu	Breast cancer	(56)
Etoposide	200 nt deletion + aa insertion (nt 4458–4459)	NR	MCF7-VP8 (MCF7)	Hu	Breast cancer	(56)
Etoposide	Lys797Asn; heterozygous	NR	CEM/VP-1 (CCRF-CEM)	Hu	T cell leukemia	(67)
Etoposide	Deletion of Ala429; gene amplification; WT poorly expressed	NR	FVP1b FVP3 (FEM-X)	Hu	Melanoma	(68, 69)
Etoposide*	Arg486Lys, Glu494Gly	NR	Primary bronchial cells	Hu	Small cell lung cancer	(70)
Etoposide	Protein reduced to 8%, 160 and 170 kDa forms	NR	H208/VP (NCI-H209)	Hu	SCLC	(71)
Etoposide	Protein and mRNA levels reduced to 30%	NR	FM3A/VP-2B (FM3A)	Mo	Mouse mammary carcinoma	(72)
Etoposide	Protein reduced to 20%	NR	T12-VP1 (T24)	Hu	Bladder cancer	(73)

(continued)

Table 19.4 (continued)

Inhibitor	Topo IIα status	Topo IIβ status	Cell name (parental)	Sp	Cell type	References
Etoposide	Protein reduced 5-fold; mRNA reduced 2.5-fold	mRNA reduced 3-fold	K/VP.5 K.VP.5-1 (K562)	Hu	Myeloid leukemia	(74–76)
Etoposide and camptothecin	Protein and mRNA reduced by 10- and 2-fold, respectively. One allele silent?	Protein/mRNA normal size and abundance	RERC (U937)	Hu	Monoblastic leukemia	(77)
Etoposide Teniposide	Arg493Gln Complemented by fly Topo IIα (41)	NR	VpmR-5 (CHO)	Ha	Ovary	(78)
Etoposide Teniposide*	Heterozygous deletions; mRNA of 2 and 4.8 kb and 160 kDa protein	NR	INER-37	Hu	Non-small cell lung cancer	(79)
Etoposide Teniposide	Transcription reduced to 20% due to increase sp3 expression	NR	KB/VP-2 KB/VM-4 (KB)	Hu	Epiderrmoid cancer	(73, 80)
Mitoxantrone	160 kDa; 108 C-term aa replaced by 13 novel aas. Less in nucleus	Protein absent; mRNA barely detectable	HL-60/MX2 (HL60)	Hu	Acute myleoid leukemia	(81–84)
Mitoxantrone	70% reduction. Regulatory mutation?	88% reduction. Regulatory mutation?	8226/MR20 (8226)	Hu	Myeloma	(85)
Teniposide	Arg449Gln and Pro802Ser. Both mutations confer resistance in yeast (43)	NR	CEM/VM-1 CEM/VM-1-5 (CCRF-CEM)	Hu	T cell leukemia	(43, 86–89)

ICRF-187	Increased protein (x5) and mRNA (x2)	Protein level unchanged	CEM/ICRF-8 CEM/ICRF-18 (CEM)	Hu	T cell leukemia	(90, 91)
ICRF-187	Arg162Gln; homozygous	Normal amount; drug sensitive	NYH/187-162 (NHY)	Hu	Small cell lung	(21, 92)
ICRF-187	Tyr165Ser; heterozygous; dominant. Confers resistance in mice	Normal amount; drug sensitive	NYH/187-165 (NHY)	Hu	Small cell lung	(21, 22, 92)
ICRF-159	Protein reduced by 50%. Tyr49Phe and deletion of aa309–313 (QQISF). Hu Y50F confers resistance in yeast	20% increase in protein	CHO/159-1 (CHO)	Ha	Ovary	(44)

* No drug selection required in culture; aa, amino acid; Ha, hamster; Hu, human; Mo, mouse; NR, not reported; Sp, species.

targeting is relatively efficient, that methods are particularly well established, and, of course, that ES cells can be used to generate genetically modified mice (8). The most efficient animal cell hosts for gene targeting, however, are certain B-cell lines such as chicken DT40 cells (9) and human Nalm-6 (10) or DG 75 (11) cells, and two of these have been used so far for Topo II studies (3, 12). Only one study in **Table 19.1** uses cells other than these, but with the right screening methods gene targeting of most cell lines is perfectly feasible, if somewhat more demanding due to lower efficiencies.

Homozygous *TOPO II* gene disruption in mice showed that Topo IIα (13), but not Topo IIβ (14), is essential for cell proliferation, although newborn *TOPO II*β–/– mice die of respiratory failure (14). Further analysis of *TOPO II*β–/– mice is being used to investigate the role of Topo IIβ during development and in the nervous system (15, 16). Mice in which *TOPO II*β disruption is restricted to skin cells have been used to show that the Topo IIβ isoform is mainly responsible for VP-16-induced carcinogenesis (17). Mouse embryo fibroblasts (MEFs) established from *TOPO II*β–/– mice have been used to show that the cytotoxicity of Topo II poisons is substantially Topo IIβ dependent (17–20). A human *TOPO II*β–/– Pre-B cell line has also been generated and used to explore the contribution of Topo IIβ to Topo II poisoning (3).

Because *TOPO II*α is an essential gene, conditional gene targeting is required to study the effects of homozygous *TOPO II*α disruption in adult cells, but this has not yet been described in mice. Non-lethal mutations can, however, be introduced by gene targeting, and there is one example of this in mice. Thus, a dominant *TOPO II*α point mutation known to confer cellular resistance to bisdioxopiperazine inhibitors (21) was introduced by gene targeting in ES cells to generate mice that were used to confirm that Topo IIα mediates toxicity of these inhibitors (22).

A conditional approach has been used in a human fibrosarcoma-derived cell line (HTETOP). These *TOPO II*α–/– cells express a tetracycline(Tet)-regulated *TOPO II*α cDNA, so that they are viable if Tet is absent from the growth medium (23). Addition of Tet results in >99.5% depletion of Topo IIα and complete loss of viability due to aberrant chromosome segregation leading to polyploidy and/or apoptosis. Chromosome condensation is largely unaffected. Depletion of Topo IIα in HTETOP can be used to investigate the contributions of Topo IIα to inhibitor-induced cell death (24) and to chromosome structure/function (25). Furthermore, because they can be rescued from Tet-sensitivity by transfection with Topo IIα expression plasmids, HTETOP cells provide a useful system for Topo IIα structure/function studies. Thus, for example, they have been used to address the role of specific Topo IIα phosphorylation sites (23) and the functional differences between the C-terminal regions of the two isoforms

(26). In the latter study it was noted that, if expressed at sufficiently high levels, Topo IIβ could rescue HTETOP cells from Tet-sensitivity. Because endogenous Topo IIβ expression does not rescue HTETOP from Tet-sensitivity, this result illustrates the importance of expressing Topo II at physiological levels in complementation experiments.

In the absence of conditional gene targeting, disruption of just a single *TOPO IIα* allele is still useful for studying the effects of reduced Topo IIα expression on Topo II inhibitor action (3, 12, 27).

3. Stable Topo II Depletion by shRNA Expression

There are relatively few reports of stable Topo II shRNA expression (**Table 19.2**). Although RNAi-mediated loss-of-function is usually incomplete, partial depletion can be useful in determining which isoforms mediate drug-induced responses. In rat PC12-I4 cells expressing Topo IIβ shRNA from a stably integrated lentiviral vector, partial Topo IIβ depletion did not appear to affect etoposide-induced γ-H2AX signal DSBs, suggesting that etoposide-induced DNA damage is primarily mediated by Topo IIα (20). Similar levels of Topo IIβ depletion in a human promyelocytic cell line resistant to retinoic acid (RA) restored RA sensitivity, implicating Topo IIα in the mechanism of RA resistance (47). An apparently more substantial depletion of Topo IIα in mouse lymphoma cells promoted proliferation in the presence of doxorubicin (Dox), compared with control cells, consistent with Topo IIα-mediated poisoning by Dox (29). In the absence of Dox, however, the Topo IIα-depleted cells proliferated normally. Thus, even relatively efficient Topo IIα depletion may be insufficient to study the essential role of Topo IIα, at least in some cell lines.

In a chicken B-cell line (DT40), however, stable conditional depletion of Topo IIα by expression of shRNA from a Tet-regulatable shRNA vector pSuperior (Oligoengine) was efficient enough to prevent proliferation, producing a phenotype similar to that seen in Topo IIα-depleted HTETOP cells (Johnson and Farr, personal communication). DT40 cells in which both isoforms are conditionally depleted in this way have also been made (Johnson and Farr, personal communication). Furthermore, these lines can be rescued from Tet-sensitivity by expression of Topo IIα using expression plasmids in which the shRNA target region has been silently mutated (Johnson and Farr, personal communication). These features, combined with the ease of gene targeting in

DT40 cells (9, 28), make these DT40 derivatives particularly attractive for analysing Topo II functions in a variety of genetic backgrounds.

4. Transient Topo II Depletion by siRNA Delivery

Unlike the other approaches summarised here, transient depletion does not generate cell lines for use in further experiments, but it is included because it is relatively quick and probably the best first option when a suitable stably depleted cell line is not available (**Table 19.3**). The main limitations compared with stable depletion are that depletion is achieved in <100% cells and that the effects of depletion cannot be studied for more than about 3–4 days. Transient depletion can nevertheless be used to address the roles of Topo II, even in cell proliferation. Notwithstanding the continued proliferation of lymphoma cells stably depleted of Topo IIα by shRNA expression (29), siRNA has been used successfully to impair Topo II-dependent chromosome segregation in HeLa cells. Thus, when Topo IIα was depleted to ~4% of normal levels in ~93% of cells transfected with Topo IIα siRNA, aberrant cytokinesis was observed in ~20% of the depleted cells 3 days after transfection (30). A similar proportion of Topo IIα-depleted HTETOP cells showed aberrant cytokinesis 3 days after addition of Tet and yet no cells survived this depletion (23), suggesting that chromosome segregation may have been lethally, if not always overtly, affected in most if not all of the siRNA-transfected HeLa cells. Nevertheless, when Topo IIβ siRNA was used to co-deplete Topo IIβ in Topo IIα-depleted HeLa cells (30) or HTETOP cells (31), a more pronounced chromosome segregation defect was observed. These results suggest that Topo IIβ can support the essential role of Topo IIα in chromosome segregation, even though Topo IIβ is dispensable and normally unable to support segregation in the absence of Topo IIα. Aberrant chromosome segregation associated with centromere defects was also noted in Drosophila S2 cells (32–34). In none of these studies was chromosome condensation severely affected.

In addition to these studies of chromosome dynamics, transient Topo II depletion by siRNA has been used to explore the contributions of Topo II to the toxic effects of Topo II inhibitors (3, 35) and other agents (36–38).

5. Isolation and Characterisation of Topo II Inhibitor-Resistant Cells

Many cell lines expressing reduced amounts and/or mutant forms of Topo II have been isolated, without the use of gene targeting or RNA interference, by selection for resistance to Topo II inhibitors (**Table 19.4**). The literature is extensive in this area and **Table 19.4** is unlikely to be exhaustive. Such cell lines have not only provided valuable evidence that Topo II is the key target for many cytotoxic drugs, but have also yielded important structural information, such as the location of nuclear localisation signals (NLS) [e.g. (39, 40)] and drug binding sites [e.g. (21, 22)]. It is also worth considering their use as hosts for further analyses of Topo II function in the light of the approaches summarised in **Tables 19.1**, **19.2**, and **19.3**.

The fact that all of the cells in **Table 19.4** have modifications to Topo IIα expression appears to indicate that this is the major isoform mediating drug sensitivity. This may, in part, reflect the fact that the tumour cell lines used are likely to overexpress Topo IIα. In many of these studies, however, the status of Topo IIβ was not investigated, and in 5 of the 12 cases where it was, Topo IIβ protein and/or mRNA levels were changed. Even if only a single Topo II isoform is mutated, multiple mutations affecting one or both alleles may be responsible for drug resistance, and mutations in other unrelated genes may also contribute to resistance. In some cases, transfection of an expression construct for wild-type Topo IIα has been shown to restore drug sensitivity [e.g. (41, 42)], providing valuable evidence that mutations in the endogenous Topo IIα gene confer resistance. Where DNA sequencing reveals more than one mutation, Topo II expression constructs that carry a single mutation can be made and tested for their ability to confer drug resistance in yeast (43, 44) or vertebrate cells (22).

While most of the cell lines listed in **Table 19.4** have not been subjected to exhaustive characterisations of this kind, they are included here as potential hosts for the analysis of Topo II function. In many cases, further characterisation will be required before proceeding, but this may be deemed worthwhile because either they carry a particular Topo II mutation of interest or provide a particular cell type of interest that is stably depleted of Topo II. The choice between this approach and working with cells engineered to have defined changes to Topo II expression, as described in previous sections (**Tables 19.1** and **19.2**), will depend on the particular requirements of any given experiment.

6. Related Methods

It is worth mentioning that cells naturally deplete Topo IIα when they stop dividing, and this fact can be exploited to distinguish between the roles of the two isoforms (20). Also, while this chapter focuses on animal cells, the ability to use yeast as a host for selecting mutant forms of animal Topo II is a powerful method (45) for identifying new Topo II mutations, at least those that confer drug resistance, that can then be characterised in animal hosts using the methods described here.

7. Summary and Conclusions

Summarised here are the approaches available to study Topo II function in vivo. As well as a wealth of information on Topo II function, such studies have provided a range of established cell lines that can be used for future studies (**Tables 19.1, 19.2**, and **19.4**). Cells deficient in either Topo IIα or Topo IIβ will continue to be useful for investigating the contribution of these proteins to the action of cytotoxic drugs. They will also help in continued efforts to characterise the different contributions of the two isoforms to fundamental cell biological processes, such as chromosome segregation and transcription, where much remains to be understood. Finally, the use of Topo II-depleted cells as hosts for expressing mutant forms of Topo II, and so establish structure–function relationships, is perhaps the area with the greatest potential. Such studies will build on the analysis of existing drug-resistant cell lines carrying known Topo II mutations, and allow detailed investigations of domains and residues involved, not just in drug resistance, but in all aspects of in vivo Topo II functions.

References

1. Austin, C. A. and Marsh, K. L. (1998) Eukaryotic DNA topoisomerase II beta. *Bioessays* **20**, 215–226.
2. Gao, H., Huang, K. C., Yamasaki, E. F., Chan, K. K., Chohan, L. and Snapka, R. M. (1999) XK469, a selective topoisomerase IIbeta poison. *Proceedings of the National Academy of Sciences of the United States of America* **96**, 12168–12173.
3. Toyoda, E., Kagaya, S., Cowell, I. G., Kurosawa, A., Kamoshita, K., Nishikawa, K., Iiizumi, S., Koyama, H., Austin, C. A. and Adachi, N. (2008) NK314, a topoisomerase II inhibitor that specifically targets the alpha isoform. *The Journal of Biological Chemistry* **283**, 23711–23720.
4. Jensen, L. H., Dejligbjerg, M., Hansen, L. T., Grauslund, M., Jensen, P. B. and Sehested, M. (2004) Characterisation of cytotoxicity and DNA damage induced by the topoisomerase II-directed bisdioxopiperazine anti-cancer agent ICRF-187 (dexrazoxane) in yeast and mammalian cells. *BMC Pharmacology* **4**, 31.

5. Oestergaard, V. H., Knudsen, B. R. and Andersen, A. H. (2004) Dissecting the cell-killing mechanism of the topoisomerase II-targeting drug ICRF-193. *The Journal of Biological Chemistry* **279**, 28100–28105.
6. Gewirtz, D. A. (1999) A critical evaluation of the mechanisms of action proposed for the antitumor effects of the anthracycline antibiotics adriamycin and daunorubicin. *Biochemical Pharmacology* **57**, 727–741.
7. Minotti, G., Menna, P., Salvatorelli, E., Cairo, G. and Gianni, L. (2004) Anthracyclines: molecular advances and pharmacologic developments in antitumor activity and cardiotoxicity. *Pharmacological Reviews* **56**, 185–229.
8. DeChiara, T. M. (2001) Gene targeting in ES cells. *Methods in Molecular Biology* (Clifton, NJ) **158**, 19–45.
9. Caldwell, R. B., Fiedler, P., Schoetz, U. and Buerstedde, J. M. (2007) Gene function analysis using the chicken B-cell line DT40. *Methods in Molecular Biology* (Clifton, NJ) **408**, 193–210.
10. Adachi, N., Kurosawa, A. and Koyama, H. (2008) Highly proficient gene targeting by homologous recombination in the human pre-B cell line Nalm-6. *Methods in Molecular Biology* (Clifton, NJ) **435**, 17–29.
11. Feederle, R., Delecluse, H. J., Rouault, J. P., Schepers, A. and Hammerschmidt, W. (2004) Efficient somatic gene targeting in the lymphoid human cell line DG75. *Gene* **343**, 91–97.
12. Adachi, N., Suzuki, H., Iiizumi, S. and Koyama, H. (2003) Hypersensitivity of nonhomologous DNA end-joining mutants to VP-16 and ICRF-193: implications for the repair of topoisomerase II-mediated DNA damage. *The Journal of Biological Chemistry* **278**, 35897–35902.
13. Akimitsu, N., Adachi, N., Hirai, H., Hossain, M. S., Hamamoto, H., Kobayashi, M., Aratani, Y., Koyama, H. and Sekimizu, K. (2003) Enforced cytokinesis without complete nuclear division in embryonic cells depleting the activity of DNA topoisomerase IIalpha. *Genes Cells* **8**, 393–402.
14. Yang, X., Li, W., Prescott, E. D., Burden, S. J. and Wang, J. C. (2000) DNA topoisomerase IIbeta and neural development. *Science* **287**, 131–134.
15. Lyu, Y. L., Lin, C. P., Azarova, A. M., Cai, L., Wang, J. C. and Liu, L. F. (2006) Role of topoisomerase IIbeta in the expression of developmentally regulated genes. *Molecular and Cellular Biology* **26**, 7929–7941.
16. Nur, E. K. A., Meiners, S., Ahmed, I., Azarova, A., Lin, C. P., Lyu, Y. L. and Liu, L. F. (2007) Role of DNA topoisomerase IIbeta in neurite outgrowth. *Brain Research* **1154**, 50–60.
17. Azarova, A. M., Lyu, Y. L., Lin, C. P., Tsai, Y. C., Lau, J. Y., Wang, J. C. and Liu, L. F. (2007) Roles of DNA topoisomerase II isozymes in chemotherapy and secondary malignancies. *Proceedings of the National Academy of Sciences of the United States of America* **104**, 11014–11019.
18. Errington, F., Willmore, E., Tilby, M. J., Li, L., Li, G., Li, W., Baguley, B. C. and Austin, C. A. (1999) Murine transgenic cells lacking DNA topoisomerase IIbeta are resistant to acridines and mitoxantrone: analysis of cytotoxicity and cleavable complex formation. *Molecular Pharmacology* **56**, 1309–1316.
19. Lyu, Y. L., Kerrigan, J. E., Lin, C. P., Azarova, A. M., Tsai, Y. C., Ban, Y. and Liu, L. F. (2007) Topoisomerase IIbeta mediated DNA double-strand breaks: implications in doxorubicin cardiotoxicity and prevention by dexrazoxane. *Cancer Research* **67**, 8839–8846.
20. Zhang, A., Lyu, Y. L., Lin, C. P., Zhou, N., Azarova, A. M., Wood, L. M. and Liu, L. F. (2006) A protease pathway for the repair of topoisomerase II-DNA covalent complexes. *The Journal of Biological Chemistry* **281**, 35997–36003.
21. Wessel, I., Jensen, L. H., Renodon-Corniere, A., Sorensen, T. K., Nitiss, J. L., Jensen, P. B. and Sehested, M. (2002) Human small cell lung cancer NYH cells resistant to the bisdioxopiperazine ICRF-187 exhibit a functional dominant Tyr165-Ser mutation in the Walker A ATP binding site of topoisomerase II alpha. *FEBS Letters* **520**, 161–166.
22. Grauslund, M., Thougaard, A. V., Fuchtbauer, A., Hofland, K. F., Hjorth, P. H., Jensen, P. B., Sehested, M., Fuchtbauer, E. M. and Jensen, L. H. (2007) A mouse model for studying the interaction of bisdioxopiperazines with topoisomerase IIalpha in vivo. *Molecular Pharmacology* **72**, 1003–1014.
23. Carpenter, A. J. and Porter, A. C. (2004) Construction, characterization, and complementation of a conditional-lethal DNA topoisomerase IIalpha mutant human cell line. *Molecular Biology of the Cell* **15**, 5700–5711.

24. Bridewell, D. J., Porter, A. C., Finlay, G. J. and Baguley, B. C. (2008) The role of topoisomerases and RNA transcription in the action of the antitumour benzonaphthyridine derivative SN 28049. *Cancer Chemotherapy and Pharmacology* **62**, 753–762.
25. Zhang, X. D., Goeres, J., Zhang, H., Yen, T. J., Porter, A. C. and Matunis, M. J. (2008) SUMO-2/3 modification and binding regulate the association of CENP-E with kinetochores and progression through mitosis. *Molecular Cell* **29**, 729–741.
26. Linka, R. M., Porter, A. C., Volkov, A., Mielke, C., Boege, F. and Christensen, M. O. (2007) C-terminal regions of topoisomerase IIalpha and IIbeta determine isoform-specific functioning of the enzymes in vivo. *Nucleic Acids Research* **35**, 3810–3822.
27. Kobayashi, M., Adachi, N., Aratani, Y., Kikuchi, A. and Koyama, H. (2001) Decreased topoisomerase IIalpha expression confers increased resistance to ICRF-193 as well as VP-16 in mouse embryonic stem cells. *Cancer Letters* **166**, 71–77.
28. Yamazoe, M., Sonoda, E., Hochegger, H. and Takeda, S. (2004) Reverse genetic studies of the DNA damage response in the chicken B lymphocyte line DT40. *DNA Repair* **3**, 1175–1185.
29. Burgess, D. J., Doles, J., Zender, L., Xue, W., Ma, B., McCombie, W. R., Hannon, G. J., Lowe, S. W. and Hemann, M. T. (2008) Topoisomerase levels determine chemotherapy response in vitro and in vivo. *Proceedings of the National Academy of Sciences of the United States of America* **105**, 9053–9058.
30. Sakaguchi, A. and Kikuchi, A. (2004) Functional compatibility between isoform alpha and beta of type II DNA topoisomerase. *Journal of Cell Science* **117**, 1047–1054.
31. Spence, J. M., Phua, H. H., Mills, W., Carpenter, A. J., Porter, A. C. and Farr, C. J. (2007) Depletion of topoisomerase IIalpha leads to shortening of the metaphase interkinetochore distance and abnormal persistence of PICH-coated anaphase threads. *Journal of Cell Science* **120**, 3952–3964.
32. Chang, C. J., Goulding, S., Earnshaw, W. C. and Carmena, M. (2003) RNAi analysis reveals an unexpected role for topoisomerase II in chromosome arm congression to a metaphase plate. *Journal of Cell Science* **116**, 4715–4726.
33. Coelho, P. A., Queiroz-Machado, J., Carmo, A. M., Moutinho-Pereira, S., Maiato, H. and Sunkel, C. E. (2008) Dual role of topoisomerase II in centromere resolution and aurora B activity. *PLoS Biology* **6**, e207.
34. Savvidou, E., Cobbe, N., Steffensen, S., Cotterill, S. and Heck, M. M. (2005) Drosophila CAP-D2 is required for condensin complex stability and resolution of sister chromatids. *Journal of Cell Science* **118**, 2529–2543.
35. Tsang, W. P., Kong, S. K. and Kwok, T. T. (2006) Epidermal growth factor induction of resistance to topoisomerase II toxins in human squamous carcinoma A431 cells. *Oncology Reports* **16**, 789–793.
36. Emmons, M., Boulware, D., Sullivan, D. M. and Hazlehurst, L. A. (2006) Topoisomerase II beta levels are a determinant of melphalan-induced DNA crosslinks and sensitivity to cell death. *Biochemical Pharmacology* **72**, 11–18.
37. Mandraju, R. K., Kannapiran, P. and Kondapi, A. K. (2008) Distinct roles of Topoisomerase II isoforms: DNA damage accelerating alpha, double strand break repair promoting beta. *Archives of Biochemistry and Biophysics* **470**, 27–34.
38. Marchion, D. C., Bicaku, E., Turner, J. G., Daud, A. I., Sullivan, D. M. and Munster, P. N. (2005) Synergistic interaction between histone deacetylase and topoisomerase II inhibitors is mediated through topoisomerase IIbeta. *Clinical Cancer Research* **11**, 8467–8475.
39. Feldhoff, P. W., Mirski, S. E., Cole, S. P. and Sullivan, D. M. (1994) Altered subcellular distribution of topoisomerase II alpha in a drug-resistant human small cell lung cancer cell line. *Cancer Research* **54**, 756–762.
40. Wessel, I., Jensen, P. B., Falck, J., Mirski, S. E., Cole, S. P. and Sehested, M. (1997) Loss of amino acids 1490Lys-Ser-Lys1492 in the COOH-terminal region of topoisomerase IIalpha in human small cell lung cancer cells selected for resistance to etoposide results in an extranuclear enzyme localization. *Cancer Research* **57**, 4451–4454.
41. Eder, J. P., Jr., Chan, V. T., Niemierko, E., Teicher, B. A. and Schnipper, L. E. (1993) Conditional expression of wild-type topoisomerase II complements a mutant enzyme in mammalian cells. *The Journal of Biological Chemistry* **268**, 13844–13849.
42. McPherson, J. P., Deffie, A. M., Jones, N. R., Brown, G. A., Deuchars, K. L. and Goldenberg, G. J. (1997) Selective sensitization of adriamycin-resistant P388 murine leukemia cells to antineoplastic agents following transfection with human DNA

topoisomerase II alpha. *Anticancer Research* **17**, 4243–4252.

43. Hsiung, Y., Jannatipour, M., Rose, A., McMahon, J., Duncan, D. and Nitiss, J. L. (1996) Functional expression of human topoisomerase II alpha in yeast: mutations at amino acids 450 or 803 of topoisomerase II alpha result in enzymes that can confer resistance to anti-topoisomerase II agents. *Cancer Research* **56**, 91–99.
44. Sehested, M., Wessel, I., Jensen, L. H., Holm, B., Oliveri, R. S., Kenwrick, S., Creighton, A. M., Nitiss, J. L. and Jensen, P. B. (1998) Chinese hamster ovary cells resistant to the topoisomerase II catalytic inhibitor ICRF-159: a Tyr49Phe mutation confers high-level resistance to bisdioxopiperazines. *Cancer Research* **58**, 1460–1468.
45. Leontiou, C., Lakey, J. H. and Austin, C. A. (2004) Mutation E522K in human DNA topoisomerase IIbeta confers resistance to methyl *N*-(4′-(9-acridinylamino)-phenyl) carbamate hydrochloride and methyl *N*-(4′-(9-acridinylamino)-3-methoxy-phenyl) methane sulfonamide but hypersensitivity to etoposide. *Molecular Pharmacology* **66**, 430–439.
46. Akimitsu, N., Kamura, K., Tone, S., Sakaguchi, A., Kikuchi, A., Hamamoto, H. and Sekimizu, K. (2003) Induction of apoptosis by depletion of DNA topoisomerase IIalpha in mammalian cells. *Biochemical and Biophysical Research Communications* **307**, 301–307.
47. McNamara, S., Wang, H., Hanna, N. and Miller, W. H., Jr. (2008) Topoisomerase IIbeta negatively modulates retinoic acid receptor alpha function: a novel mechanism of retinoic acid resistance. *Molecular and Cellular Biology* **28**, 2066–2077.
48. Son, Y. S., Suh, J. M., Ahn, S. H., Kim, J. C., Yi, J. Y., Hur, K. C., Hong, W. S., Muller, M. T. and Chung, I. K. (1998) Reduced activity of topoisomerase II in an Adriamycin-resistant human stomach-adenocarcinoma cell line. *Cancer Chemotherapy and Pharmacology* **41**, 353–360.
49. McPherson, J. P., Brown, G. A. and Goldenberg, G. J. (1993) Characterization of a DNA topoisomerase IIalpha gene rearrangement in adriamycin-resistant P388 leukemia: expression of a fusion messenger RNA transcript encoding topoisomerase IIalpha and the retinoic acid receptor alpha locus. *Cancer Research* **53**, 5885–5889.
50. Herzog, C. E., Holmes, K. A., Tuschong, L. M., Ganapathi, R. and Zwelling, L. A. (1998) Absence of topoisomerase IIbeta in an amsacrine-resistant human leukemia cell line with mutant topoisomerase IIalpha. *Cancer Research* **58**, 5298–5300.
51. Bakic, M., Beran, M., Andersson, B. S., Silberman, L., Estey, E. and Zwelling, L. A. (1986) The production of topoisomerase II-mediated DNA cleavage in human leukemia cells predicts their susceptibility to 4′-(9-acridinylamino)methanesulfon-m-anisidide (m-AMSA). *Biochemical and Biophysical Research Communications* **134**, 638–645.
52. Hinds, M., Deisseroth, K., Mayes, J., Altschuler, E., Jansen, R., Ledley, F. D. and Zwelling, L. A. (1991) Identification of a point mutation in the topoisomerase II gene from a human leukemia cell line containing an amsacrine-resistant form of topoisomerase II. *Cancer Research* **51**, 4729–4731.
53. Lee, M. S., Wang, J. C. and Beran, M. (1992) Two independent amsacrine-resistant human myeloid leukemia cell lines share an identical point mutation in the 170 kDa form of human topoisomerase II. *Journal of Molecular Biology* **223**, 837–843.
54. Mayes, J., Hinds, M., Soares, L., Altschuler, E., Kim, P. and Zwelling, L. A. (1993) Further characterization of an amsacrine-resistant line of HL-60 human leukemia cells and its topoisomerase II. Effects of ATP concentration, anion concentration, and the three-dimensional structure of the DNA target. *Biochemical Pharmacology* **46**, 699–707.
55. Odaimi, M., Andersson, B. S., McCredie, K. B. and Beran, M. (1986) Drug sensitivity and cross-resistance of the 4′-(9-acridinylamino)methanesulfon-m-anisidide-resistant subline of HL-60 human leukemia. *Cancer Research* **46**, 3330–3333.
56. Matsumoto, Y., Takano, H., Kunishio, K., Nagao, S. and Fojo, T. (2001) Incidence of mutation and deletion in topoisomerase II alpha mRNA of etoposide and mAMSA-resistant cell lines. *Japanese Journal of Cancer Research* **92**, 1133–1137.
57. Dereuddre, S., Delaporte, C. and Jacquemin-Sablon, A. (1997) Role of topoisomerase II beta in the resistance of 9-OH-ellipticine-resistant Chinese hamster fibroblasts to topoisomerase II inhibitors. *Cancer Research* **57**, 4301–4308.
58. Dereuddre, S., Frey, S., Delaporte, C. and Jacquemin-Sablon, A. (1995) Cloning and characterization of full-length cDNAs coding for the DNA topoisomerase II beta from Chinese hamster lung cells sensitive and resistant 9-OH-ellipticine. *Biochimica et Biophysica Acta* **1264**, 178–182.

59. Salles, B., Charcosset, J. Y. and Jacquemin-Sablon, A. (1982) Isolation and properties of Chinese hamster lung cells resistant to ellipticine derivatives. *Cancer Treatment Reports* **66**, 327–338.
60. Saxena, D., Yiu, G. K., Ni, X., Huang, K. C., Mantovani, R., Jacquemin-Sablon, A. G. and Ng, S. W. (2004) Characterization of promoter elements involved in the down-regulation of topoisomerase IIalpha expression in a drug-resistant cell line. *Gene* **342**, 145–155.
61. Grue, P., Grasser, A., Sehested, M., Jensen, P. B., Uhse, A., Straub, T., Ness, W. and Boege, F. (1998) Essential mitotic functions of DNA topoisomerase IIalpha are not adopted by topoisomerase IIbeta in human H69 cells. *The Journal of Biological Chemistry* **273**, 33660–33666.
62. Jensen, P. B., Christensen, I. J., Sehested, M., Hansen, H. H. and Vindelov, L. (1993) Differential cytotoxicity of 19 anticancer agents in wild type and etoposide resistant small cell lung cancer cell lines. *British Journal of Cancer* **67**, 311–320.
63. Mirski, S. E. and Cole, S. P. (1995) Cytoplasmic localization of a mutant M(r) 160,000 topoisomerase II alpha is associated with the loss of putative bipartite nuclear localization signals in a drug-resistant human lung cancer cell line. *Cancer Research* **55**, 2129–2134.
64. Mirski, S. E., Evans, C. D., Almquist, K. C., Slovak, M. L. and Cole, S. P. (1993) Altered topoisomerase II alpha in a drug-resistant small cell lung cancer cell line selected in VP-16. *Cancer Research* **53**, 4866–4873.
65. Mirski, S. E., Sparks, K. E., Yu, Q., Lang, A. J., Jain, N., Campling, B. G. and Cole, S. P. (2000) A truncated cytoplasmic topoisomerase IIalpha in a drug-resistant lung cancer cell line is encoded by a TOP2A allele with a partial deletion of exon 34. *International Journal of Cancer* **85**, 534–539.
66. Yu, Q., Mirski, S. E., Sparks, K. E. and Cole, S. P. (1997) Two COOH-terminal truncated cytoplasmic forms of topoisomerase II alpha in a VP-16-selected lung cancer cell line result from partial gene deletion and alternative splicing. *Biochemistry* **36**, 5868–5877.
67. Patel, S. and Fisher, L. M. (1993) Novel selection and genetic characterisation of an etoposide-resistant human leukaemic CCRF-CEM cell line. *British Journal of Cancer* **67**, 456–463.
68. Campain, J. A., Gottesman, M. M. and Pastan, I. (1994) A novel mutant topoisomerase II alpha present in VP-16-resistant human melanoma cell lines has a deletion of alanine 429. *Biochemistry* **33**, 11327–11332.
69. Campain, J. A., Slovak, M. L., Schoenlein, P. V., Popescu, N. C., Gottesman, M. M. and Pastan, I. (1995) Acquisition of multiple copies of a mutant topoisomerase IIalpha allele by chromosome 17 aneuploidy is associated with etoposide resistance in human melanoma cell lines. *Somatic Cell and Molecular Genetics* **21**, 451–471.
70. Kubo, A., Yoshikawa, A., Hirashima, T., Masuda, N., Takada, M., Takahara, J., Fukuoka, M. and Nakagawa, K. (1996) Point mutations of the topoisomerase IIalpha gene in patients with small cell lung cancer treated with etoposide. *Cancer Research* **56**, 1232–1236.
71. Jain, N., Lam, Y. M., Pym, J. and Campling, B. G. (1996) Mechanisms of resistance of human small cell lung cancer lines selected in VP-16 and cisplatin. *Cancer* **77**, 1797–1808.
72. Kawanami, K., Nakamura, T., Ono, M., Kusano, T., Okada, K., Kikuchi, A., Adachi, N., Kohno, K., Higashi, K. and Kuwano, M. (1996) Decreased DNA topoisomerase II alpha expression and cold-sensitive growth in a mouse mammary cancer cell line resistant to etoposide and doxorubicin. *Oncology Research* **8**, 197–206.
73. Takano, H., Ise, T., Nomoto, M., Kato, K., Murakami, T., Ohmori, H., Imamura, T., Nagatani, G., Okamoto, T., Ohta, R., Furukawa, M., Shibao, K., Izumi, H., Kuwano, M. and Kohno, K. (1999) Structural and functional analysis of the control region of the human DNA topoisomerase II alpha gene in drug-resistant cells. *Anti-Cancer Drug Design* **14**, 87–92.
74. Fattman, C. L., Allan, W. P., Hasinoff, B. B. and Yalowich, J. C. (1996) Collateral sensitivity to the bisdioxopiperazine dexrazoxane (ICRF-187) in etoposide (VP-16)-resistant human leukemia K562 cells. *Biochemical Pharmacology* **52**, 635–642.
75. Ritke, M. K., Roberts, D., Allan, W. P., Raymond, J., Bergoltz, V. V. and Yalowich, J. C. (1994) Altered stability of etoposide-induced topoisomerase II-DNA complexes in resistant human leukaemia K562 cells. *British Journal of Cancer* **69**, 687–697.
76. Ritke, M. K. and Yalowich, J. C. (1993) Altered gene expression in human leukemia K562 cells selected for resistance to etoposide. *Biochemical Pharmacology* **46**, 2007–2020.
77. Saleem, A., Ibrahim, N., Patel, M., Li, X. G., Gupta, E., Mendoza, J., Pantazis, P. and Rubin, E. H. (1997) Mechanisms of resistance in a human cell line exposed to

sequential topoisomerase poisoning. *Cancer Research* **57**, 5100–5106.

78. Chan, V. T., Ng, S. W., Eder, J. P. and Schnipper, L. E. (1993) Molecular cloning and identification of a point mutation in the topoisomerase II cDNA from an etoposide-resistant Chinese hamster ovary cell line. *The Journal of Biological Chemistry* **268**, 2160–2165.
79. de Lucio, B., Manuel, V. and Barrera-Rodriguez, R. (2005) Characterization of human NSCLC cell line with innate etoposide-resistance mediated by cytoplasmic localization of topoisomerase II alpha. *Cancer Science* **96**, 774–783.
80. Kubo, T., Kohno, K., Ohga, T., Taniguchi, K., Kawanami, K., Wada, M. and Kuwano, M. (1995) DNA topoisomerase II alpha gene expression under transcriptional control in etoposide/teniposide-resistant human cancer cells. *Cancer Research* **55**, 3860–3864.
81. Harker, W. G., Slade, D. L., Dalton, W. S., Meltzer, P. S. and Trent, J. M. (1989) Multidrug resistance in mitoxantrone-selected HL-60 leukemia cells in the absence of P-glycoprotein overexpression. *Cancer Research* **49**, 4542–4549.
82. Harker, W. G., Slade, D. L., Drake, F. H. and Parr, R. L. (1991) Mitoxantrone resistance in HL-60 leukemia cells: reduced nuclear topoisomerase II catalytic activity and drug-induced DNA cleavage in association with reduced expression of the topoisomerase II beta isoform. *Biochemistry* **30**, 9953–9961.
83. Harker, W. G., Slade, D. L., Parr, R. L., Feldhoff, P. W., Sullivan, D. M. and Holguin, M. H. (1995) Alterations in the topoisomerase II alpha gene, messenger RNA, and subcellular protein distribution as well as reduced expression of the DNA topoisomerase II beta enzyme in a mitoxantrone-resistant HL-60 human leukemia cell line. *Cancer Research* **55**, 1707–1716.
84. Harker, W. G., Slade, D. L., Parr, R. L. and Holguin, M. H. (1995) Selective use of an alternative stop codon and polyadenylation signal within intron sequences leads to a truncated topoisomerase II alpha messenger RNA and protein in human HL-60 leukemia cells selected for resistance to mitoxantrone. *Cancer Research* **55**, 4962–4971.
85. Hazlehurst, L. A., Foley, N. E., Gleason-Guzman, M. C., Hacker, M. P., Cress, A. E., Greenberger, L. W., De Jong, M. C. and Dalton, W. S. (1999) Multiple mechanisms confer drug resistance to mitoxantrone in the human 8226 myeloma cell line. *Cancer Research* **59**, 1021–1028.
86. Bugg, B. Y., Danks, M. K., Beck, W. T. and Suttle, D. P. (1991) Expression of a mutant DNA topoisomerase II in CCRF-CEM human leukemic cells selected for resistance to teniposide. *Proceedings of the National Academy of Sciences of the United States of America* **88**, 7654–7658.
87. Danks, M. K., Schmidt, C. A., Cirtain, M. C., Suttle, D. P. and Beck, W. T. (1988) Altered catalytic activity of and DNA cleavage by DNA topoisomerase II from human leukemic cells selected for resistance to VM-26. *Biochemistry* **27**, 8861–8869.
88. Danks, M. K., Warmoth, M. R., Friche, E., Granzen, B., Bugg, B. Y., Harker, W. G., Zwelling, L. A., Futscher, B. W., Suttle, D. P. and Beck, W. T. (1993) Single-strand conformational polymorphism analysis of the M(r) 170,000 isozyme of DNA topoisomerase II in human tumor cells. *Cancer Research* **53**, 1373–1379.
89. Mao, Y., Yu, C., Hsieh, T. S., Nitiss, J. L., Liu, A. A., Wang, H. and Liu, L. F. (1999) Mutations of human topoisomerase II alpha affecting multidrug resistance and sensitivity. *Biochemistry* **38**, 10793–10800.
90. Morgan, S. E. and Beck, W. T. (2001) Role of an inverted CCAAT element in human topoisomerase IIalpha gene expression in ICRF-187-sensitive and -resistant CEM leukemic cells. *Molecular Pharmacology* **59**, 203–211.
91. Morgan, S. E., Cadena, R. S., Raimondi, S. C. and Beck, W. T. (2000) Selection of human leukemic CEM cells for resistance to the DNA topoisomerase II catalytic inhibitor ICRF-187 results in increased levels of topoisomerase IIalpha and altered G(2)/M checkpoint and apoptotic responses. *Molecular Pharmacology* **57**, 296–307.
92. Wessel, I., Jensen, L. H., Jensen, P. B., Falck, J., Rose, A., Roerth, M., Nitiss, J. L. and Sehested, M. (1999) Human small cell lung cancer NYH cells selected for resistance to the bisdioxopiperazine topoisomerase II catalytic inhibitor ICRF-187 demonstrate a functional R162Q mutation in the Walker A consensus ATP binding domain of the alpha isoform. *Cancer Research* **59**, 3442–3450.

Note added in proof: "Johnson and Farr, personal communication" has recently been published. The reference is: Johnson, M., Phua, H. H., Bennett, S. C., Spence, J. M. and Farr, C. J. (2009) Studying vertebrate topoisomerase 2 function using a conditional knockdown system in DT40 cells. *Nucleic Acids Research.* [Epub ahead of print]

Subject Index

D.J. Clarke, (ed.), *DNA Topoisomerases*, Methods in Molecular Biology 582,
DOI 10.1007/978-1-60761-340-4, © Humana Press, a part of Springer Science+Business Media, LLC 2009

R

S

T

V

X